ANALYSIS OF TRANSCRIPTIONAL TARGETS OF SOX9 DURING EMBRYONIC HEART VALVE DEVELOPMENT REVEALS A CRITICAL NETWORK OF TRANSCRIPTION FACTORS

by

Victoria C. Garside

M.Sc., The University of Western Ontario, 2008

B.Sc., The University of Western Ontario, 2006

A THESIS SUBMITTED IN PARTIAL FULFILLMENT OF THE REQUIREMENTS FOR THE DEGREE OF

DOCTOR OF PHILOSOPHY

in

The Faculty of Graduate and Postdoctoral Studies

(Cell and Developmental Biology)

THE UNIVERSITY OF BRITISH COLUMBIA

(Vancouver)

November 2015

ABSTRACT

Cardiac malformations affect approximately 1% of human newborns and a large number of these are due to defects in the heart valves and septum. It has been suggested that cardiac valve diseases, which make up about one third of all cardiovascular defects, arise from underlying developmental malformations that occur during embryogenesis. Interestingly, the development of the heart valves (cardiac cushions) and tissues that form cartilage templates (such as the limb) share a number of key TFs, such as TWIST1, SOX9, and NFATC1 suggesting that they have similar transcriptional programs. It has been proposed that regulatory networks involved in cartilage formation, are also active during valve development and disease. The transcription factor SOX9 has an essential role in heart valve and cartilage formation and its loss leads to major congenital abnormalities in the embryo. Regardless of this critical role, little is known about how SOX9 regulates heart valve development or its transcriptional targets. Therefore, to identify transcriptional targets of SOX9 and elucidate the role of SOX9 in the developing valves, we have used ChIP-Seq on the E12.5 atrioventricular canal (heart valves) and limb buds. Comparisons of SOX9 DNA-binding regions among tissues revealed both context-dependent and context–independent SOX9 interacting regions. Context-independent SOX9 binding suggests that SOX9 may play a role in regulating proliferation-associated genes across many tissues. Generation of two endothelial specific *Sox9* mutants uncovers two potential roles for SOX9 in heart valve formation: first in the initial formation of valve mesenchyme and later in the survival and differentiation of valve mesenchyme. Analysis of tissue-specific SOX9-DNA binding regions with gene expression profiles from *Sox9* mutant heart valves indicates that SOX9 directly regulates a collection of transcription factors known to be important for heart development. Taken together, this study identified that SOX9 controls transcriptional

hierarchies involved in proliferation across tissues and heart valve differentiation. SOX9 transcriptional targets identified in this data could be used as predictive factors of heart valve disease, or as targets for new therapeutic strategies for disease and congenital defects.

PREFACE

The embryonic material for the SOX9 Chromatin Immunoprecipitation coupled with deep sequencing (ChIP-Seq) libraries on the Embryonic day (E) 12.5 atrioventricular canal (AVC) and E12.5 limb buds was collected by R. Cullum and the ChIPs were also performed by R.Cullum. Library construction, sequencing, and initial bioinformatics for peak generation were performed by the Michael Smith Genome Sciences Centre. SOX9 peak to gene associations were carried out by R. Cullum (Appendix IID, Appendix III). Genomic locations of SOX9 peaks and SOX9 motifs were assigned by bioinformatic analyses completed by R. Cullum (Figure 3-3C, D, Table 3-1). ChIP-qPCR validation of SOX9 ChIP-Seq peaks was executed by R. Cullum (Figure 6-1C, D). Z-scores for the SOX9 ChIP-Seq libraries were calculated by M. Bilenky (Appendix IA, B). The LacZ staining on *VE-Cre:LacZ* mouse E10.5 and E11.5 hearts was performed by ACY Chang (Figure 2-2B).

All animal protocols were approved by the UBC Animal Care and Ethics Committee (protocols: A12-0305 and A12-0297). The UBC Biosafety Committee approved the use of any biohazardous chemicals and material.

Portions of this thesis are modified from:
Victoria C. Garside, Alex C. Chang, Aly Karsan, and Pamela A. Hoodless (2013) Co-ordinating Notch, BMP, and TGF-β signaling during heart valve development. *Cellular and Molecular Life Sciences* **70**(16):2899-917.
Chapter 1 Introduction text and Figure 1-1 and 1-2.

Victoria C. Garside, Rebecca Cullum, Olivia Alder, Daphne Y. Lu, Ryan Vander Werff, Mikhail Bilenky, Yongjun Zhao, Steven J. M. Jones, Marco A. Marra, T. Michael Underhill, Pamela A. Hoodless (2015) SOX9 directly modulates the expression of key transcription factors required for heart valve development. **Submitted**.
Chapter 3,5,&6 including Figures 3-3, 5-2A, B, 5-8A, B, 6-1, 6-5A, B, and 6-6.

TABLE OF CONTENTS

LIST OF TABLES

LIST OF FIGURES

LIST OF ABBREVIATIONS

A- Atria
AV- Atrioventricular
AVC- Atrioventricular canal
BAV- Bicuspid aortic valve
BMP-Bone morphogenetic protein
BSA- Bovine serum albumin
CD- Campomelic Dysplasia
ChIP-Seq- Chromatin immunoprecipitation coupled with high-throughput sequencing
CPC- Cardiac progenitor cells
Cre- Cre recombinase
DABCO- 1,4-diazabicyclo[2.2.2]octane
DAPI- 4',6-Diamidino-2-Phenylindole, Dihydrochloride
Dll- Delta-like ligand
E- Embryonic day
ECM- Extracellular matrix
EMT- Epithelial-to-mesenchmyal transition
EndMT- Endothelial-to-mesenchymal transition
Epi- Epicardium
FDR- False discovery rate
FPKMs- Fragments per kilobase of exon per million reads
GO- Gene ontology
HF-SCs- Hair follicle stem cells
HMG- High mobility group
IF- Immunofluorescence
ISH- *In situ* hybridization
MSCs- Mesenchymal stem cells
MVP- Mitral valve prolappse
NC- Neural crest
NICD- Notch intracellular domain
OC- Ovarian cancer
OFT- Outflow tract
PBS-Phosphate buffered saline
PCR-Polymerase chain reaction
PFA- Paraformaldehyde
PHF- Primary heart field
pHH3- phospho histone H3
PWM- Positional weight matrix
qPCR- Quantitative PCR

RT-PCR- Reverse transcriptase PCR
TF- Transcription factor
TGFβ- Transforming growth factor beta
TSS- Transcriptional start site
TTS- Transcription termination site
SHF- Secondary heart field
SL- Semilunar
SOX9- SRY (sex determining region Y) related box 9
Sox9 cKO- *Sox9fl/fl;Tie2-Cre*
Sox9 mutant- *Sox9fl/fl;VE-Cre*
V- Ventricles
VC- Vertebral column
VE- Vascular endothelial cadherin
VEC- Valvular endocardial cells
VIC- Valvular interstitial cells
WT- Wildtype

ACKNOWLEDGEMENTS

Foremost, I would really like to thank my family especially my parents who always supported and encouraged me throughout my entire career both emotionally and financially. I would not be where I am if it was not for you! I would really like to thank my dad for opening my eyes to science at a young age and helping me think critically. Thank you to my mum who enlightened my creative side and always dared me to think outside the box. In addition, I would like to thank my husband Colin Prior for always being there for me through the good times and the bad times in research and in life. He always knows how to make me smile even when I find it hard to.

Next, I would like to thank my supervisor Dr. Pamela Hoodless for being an excellent supervisor and guiding me through the world of research. She taught me a lot about critical thinking, experimental design, and what is involved in pursuing an academic career. I am forever grateful for all of her help. Additonally, I would like to thank my fellow work collegues and lab mates. The lab environment has greatly enriched my scientific experience during my PhD. I would especially like to thank Rebecca Cullum and Olivia Alder for all of their help, advice and support during my PhD. I am thankful for all of the scientific discussions and collaborations that we have had over the years and they have really helped me to grow as a scientist and as a person. I am thankful for all of the help that the people of the Terry Fox Labs have given to me over the years and thank you to all of you that have made this a very fun experience as well. I would like to thank to my supervisory committee for their excellent advice and comments throughout my PhD. I am sure that our meetings and discussions have made me think much more critically about my research. A final thanks to everyone I have met and worked with along the way. Every little bit brought me here today.

DEDICATION

I would like to dedicate this dissertation to my family. I love you all very much.

CHAPTER ONE: Introduction

1.1 General introduction

Transcription factors (TFs) are essential for the precise coordination of lineage specification and differentiation, and ultimately the control of cell identity. Developing an understanding how TFs regulate and integrate many cellular processes during development has been a major focus of embryology. Recent advances in sequencing technologies have prompted the use chromatin immunoprecipitation coupled with deep sequencing (ChIP-Seq) to determine the DNA binding sites of TFs on a genome-wide level in numerous tissues. With the discovery of technologies like ChIP-Seq and/or transcriptome analysis (RNA-Seq) researchers are one step closer to uncovering the regulatory networks that govern the cellular processes in embryonic development. However with each technological advance forward in the field, the complexity of these relationships and networks deepens. Transcriptional networks play a major role in guiding the correct development of the embryonic heart valves and many TFs are essential to this process during development. Aberrant expression of TFs has been linked to a number of congenital heart valve defects and adult heart valve diseases and therefore, a more complete picture of how these TFs function during normal heart valve development and adult valve maintenance would be highly valuable for the innovation of novel therapeutics and establishment of additional biomarkers of disease.

1.2 Heart valve formation

1.2.1 Embryonic development of the heart valves

The heart is one of the first organs to form and function within the developing embryo (1). It delivers sufficient oxygen and nutrients throughout and establishes proper blood flow in the

fetus. The first step of heart formation is specification of cardiac progenitor cells (CPCs), which takes place prior to their ingression through the primitive streak during gastrulation (embryonic day (E) 6-7.0 in mouse). Subsequently, CPCs undergo an epithelial-to-mesenchymal transition (EMT) and migrate out from the primitive streak to create the left and right heart fields (E7.5). The heart fields will move laterally and fuse on the midline of the anterior side of the embryo. Fusion of the two heart fields forms the cardiac crescent at E8.0 (reviewed in (2)). The differentiation of the cells within the cardiac crescent produces the endocardial and myocardial progenitor cells and together they make up the primary heart field (PHF). The PHF will give rise to the left ventricle, atrioventricular canal (AVC), parts of the right ventricle and atria. The secondary heart field (SHF), a secondary population of progenitor cells originating from the splanchnic mesoderm which are located anterior to the PHF, will contribute to parts of the right ventricle and atria and the outflow tract (OFT). The two arms of the cardiac crescent fuse along the embryonic midline forming the linear heart tube (E8.5) (2). The linear heart tube consists of a monolayer of endothelium and several layers of myocardium at E9.0 (Figure 1-1) and loops rightward to form the chambers of the heart. The process of rightward looping brings the chambers into their final positions in the mature heart. Two constrictions appear in the looped heart, the AVC, between the atria and ventricle, and the OFT, between the ventricle and great arteries (Figure 1-1) and these regions will eventually form the mature valves and contribute to the septa of the heart (additional information on early heart formation in (2-4)).

The septum divides the heart into four functional chambers and valves function to ensure uni-directional blood flow. During heart valve development, the AVC and the OFT will form four sets of heart valves: two sets of atrioventricular (AV) valves and two sets of

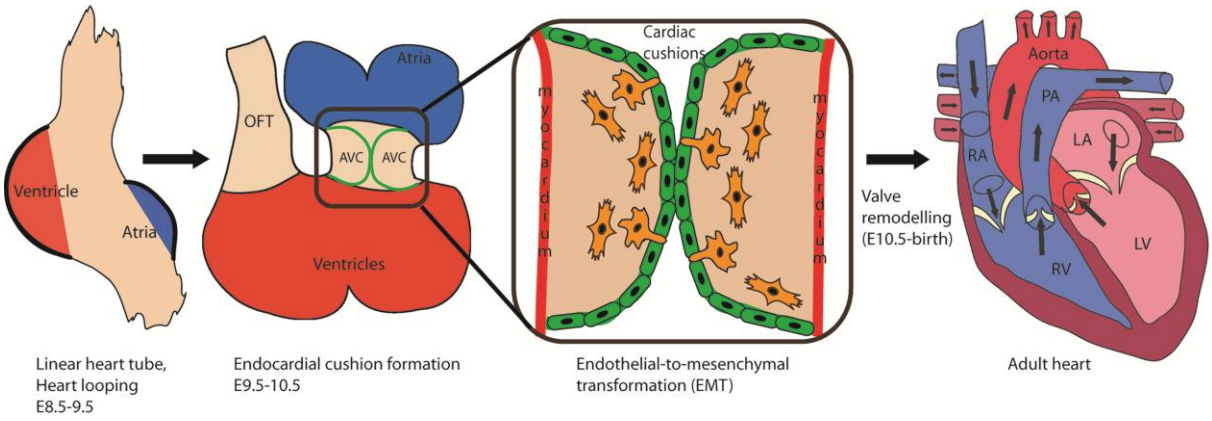

Figure 1-1 Mouse heart valve development. Valve development begins at E9.5 as the atrioventricular canal (AVC) endocardial cells undergo endothelial-to-mesenchymal transformation (EMT) to create the valve mesenchyme. Following EMT, the valve mesenchyme undergoes remodeling and differentiation to generate the adult heart valve leaflets. Cells depicted in green are endocardial cells, and cells in orange are valve mesenchyme. AVC – atrioventricular canal, RA – right atria, LA – left atria, RV – right ventricle, LV – left ventricle, PA – pulmonary artery.

semilunar (SL) valves, respectively. The AV valves are made up of the mitral valve, which regulates blood flow from left atrium to left ventricle; and the tricuspid valve, which prevents blood backflow between right atrium and right ventricle. The two SL valves are the aortic valve, which regulates blood flow from the left ventricle into the aorta; and the pulmonary valve, which regulates blood flow between the right ventricle and pulmonary artery (5).

Heart valve formation is initiated through locally increased production of cardiac jelly in the AVC and OFT. The cardiac jelly is comprised of extracellular matrix (ECM) secreted by the myocardium into the interstitial space between the endocardium and myocardium and creates swellings known as the cardiac cushions. Although the cushions are initially acellular, endocardial cells overlying the cushion undergo EMT (also referred to as EndMT (endothelial-to-mesenchymal transition)) to indicate the endothelial origin of the cells) to form mesenchymal cells (6). In the mouse, EMT begins at approximately E9.5 in the AVC and E10.5 in the OFT (Figure 1-1). During EMT, endocardial cells lose cell-cell junctions and cell polarity, transition into mesenchymal cells, and acquire a migratory phenotype (7). The mesenchymal cells invade the ECM and populate the cardiac cushions (8,9). The OFT, which will form the SL valves, develops similarly with the exception that neural crest cells migrate and contribute to the OFT cardiac cushions (reviewed in (10)).

Following invasion of the mesenchyme into the cardiac cushion, these cells will proliferate, differentiate and remodel to form thin delicate valve leaflets and septal structures of the mature heart (11,12). The cardiac cushions form the valves and septa through two major steps: remodelling and maturation (E10.5-adult), and elongation (E14.5-adult). Valve remodelling can be divided into a number of overlapping steps: proliferation and expansion of mesenchyme cells (E10.5-E12.5), differentiation of mesenchyme cells (E12.5-E16.5), and valve

condensation and maturation (E15.5-adult) (11,13-15). To date, the majority of research in the field has concentrated on the initial stages of the EMT process since AVC explant cultures allows for robust measurement of EMT (7). In contrast, our understanding of valve differentiation, maturation and condensation are currently lacking. This may be due to the absence of an established culture model system to examine the later stages of valve development.

1.2.2 Composition of the adult heart valve

The adult heart valve leaflets are highly organized structures composed of three stratified layers: the atrialis in AV valves or ventricularis in SL valves, spongiosa and fibrosa which are mainly composed of elastin, proteoglycans, and collagens, respectively (12). In AV valves, the fibrosa layer is located on the ventricular side of the valve whereas in SL valves, it is located away from the ventricle. The fibrosa layer maintains strength and integrity of the valve (16). The atrialis and ventricularis face the blood flow and provide the flexibility of valve (17). The spongiosa, the middle layer of the valve, acts as a sponge and allows for valve compression to absorb the pressures from blood flow. The heart valve leaflets are enclosed in a sheath of valvular endocardial cells (VECs) with valvular interstitial cells (VICs) dispersed throughout the valve leaflet. VICs are descendants of the mesenchymal cells found in the cardiac cushions during embryogenesis. Lineage tracing studies in mice using *Tie2*, which is expressed in endocardial cells prior to EMT, shows that the bulk of cells present in the valves after birth are derived from endocardium with the exception of the AV parietal leaflets (18-20). It was shown that epicardial-derived cells start to migrate into the lateral AV cushions at E12.5 and selectively contribute to parietal leaflets of the mouse AV valves (20). VICs play an important role in maintaining proper

valve homeostasis but can be aberrantly activated during valve disease (21). More recent research is now focused on how VICs are generated during development, how they maintain adult homeostasis, and how they become activated during disease progression.

A number of studies have suggested that crucial developmental signalling pathways, involved in normal embryonic valve formation, such as transforming growth factor beta (TGFβ), bone morphogenetic protein (BMP), and Notch, are also activated during heart valve disease (3,22). Thus, advancing our understanding of how these signalling pathways function and interact during heart valve development will provide key insights into mechanisms of adult heart valve disease.

1.2.3 Major signalling events during heart valve development

Many signalling pathways are implicated in the formation of the cardiac valves however three critical signalling pathways are required for early specification and initiation of EMT in the cardiac cushions. To create the appropriate environment for EMT in the cushions, BMPs from the myocardium signal to the overlying endocardium. For the initiation of EMT, Notch signalling is also required and together with BMP and TGFβ signalling pathways as they synergize to transform the endothelial cells into mesenchyme and promote mesenchymal cell invasiveness. Together, these three crucial signalling pathways create the cardiac cushions and populate them with mesenchyme cells, setting off the cascade of events required to form mature heart valves and septa.

BMPs and TGFβs are part of the TGFβ superfamily. This family comprises over 30 ligands that can be categorized into several subgroups: activins/inhibins, nodals, BMPs, growth and differentiation factors, Müllerian inhibiting substance and TGFβs. To activate signalling, the

ligands bind to a tetrameric, transmembrane receptor complex that contains two type I and two type II receptors. In mammals, there are five distinct type II receptors and seven type I receptors, which form specific combinations that dictate ligand binding specificity. The receptors will phosphorylate and activate an intracellular canonical signalling pathway that is mediated by receptor-regulated Smad proteins (R-Smads). Following phosphorylation, R-Smads interact with the binding partner, Smad4, and move into the nucleus where they interact with DNA-binding proteins to regulate transcription of TGFβ superfamily responsive genes (23,24) (Figure 1-2A).

There are two major phases where BMP signalling is essential for valve formation. First, BMP signalling sets up a permissive environment that allows endocardium to become activated, and secondly, together with both Notch and TGFβ signalling promotes EMT and mesenchyme invasion. Together, these two roles of BMP signalling ensure mesenchyme growth, survival, and eventually leading to valve remodelling. The majority of the mouse models for BMP signalling result in defects during early cardiac cushion formation (reviewed in (22)), and therefore, the essential role of BMP signalling in the early stages of cardiac cushion formation are well documented. However, due to early lethality in mouse models the role of the BMP signalling molecules during valve remodelling, differentiation, and adult homeostasis is less understood. Emerging data suggests that BMP signalling may be abnormally activated during valve disease. To corroborate this, BMP2 is increased in calcified regions in diseased valve leaflets (25,26) and there are higher levels of BMP signalling in fibrosa endothelium of human diseased aortic valves (27). This suggests that BMP signalling may be involved in the process of calcification during adult valve disease and that there may be additional roles for BMP signalling in the later stages

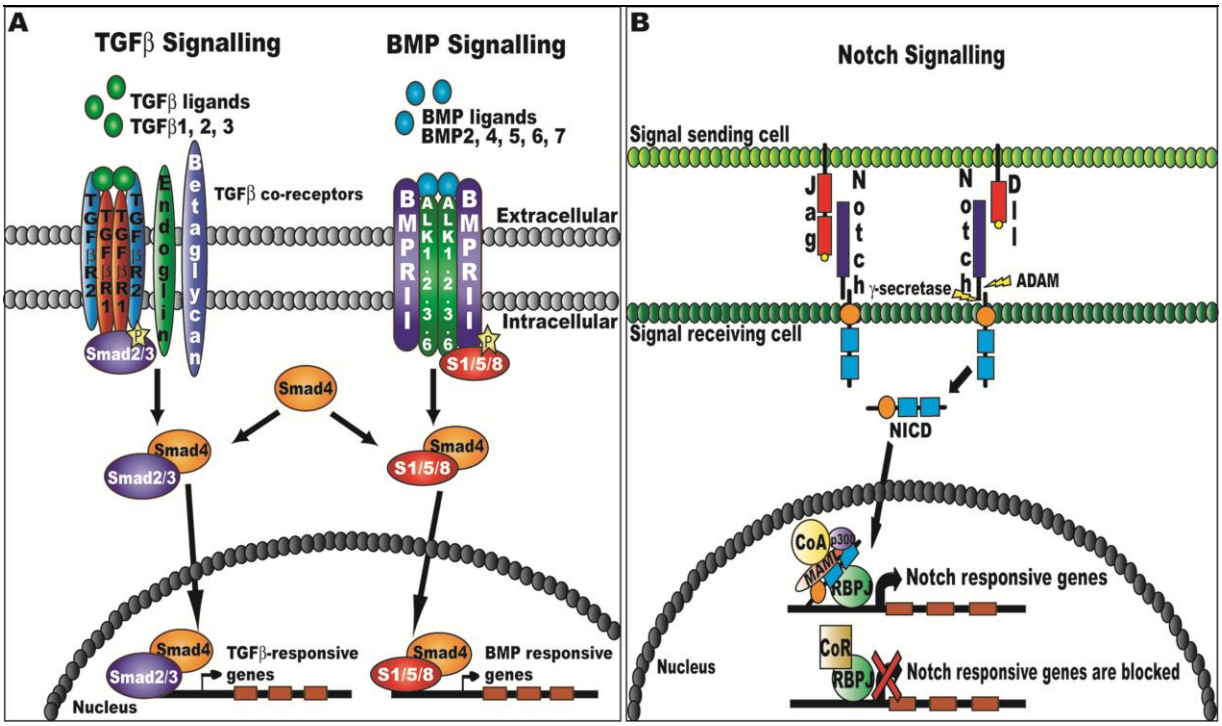

Figure 1-2 Major signalling pathways during heart valve development. **A.** TGFβ superfamily signalling. TGFβ signalling initiates as aTGFβ ligand binds to the heterodimeric receptor (containing twoTGF βR1 and twoTGF βR2) leading to activation of SMAD2/3. SMAD2/3 then binds to its co-factor SMAD4 and enters the nucleus to activate TGFβ responsive genes. BMP signaling functions similarly where a BMP ligand binds to the receptor (BMPRII/ALK2/3/6) and activates SMAD1/5/8. SMAD1/5/8 binds to SMAD4 and moves to the nucleus to activate BMP responsive genes **B.** Notch signalling pathway begins as a signal sending cell expressing Jag binds to Notch on a signal receiving cells which leads to a cleavage event that releases Notch intracellular domain (NICD). Following this, NICD moves to the nucleus and together with its co-factors activates Notch responsive genes.

of embryonic valve formation and in adult valve maintenance.

TGFβ signalling plays an essential role in the initial promotion and cessation of EMT, and in cushion mesenchyme proliferation and differentiation during heart valve development. Tissue-specific knockout mouse models suggest that the TGFβ receptors have very diverse yet specific roles dependent on the tissue and time point in which they are expressed (reviewed in (22)). This makes it difficult to determine the exact role of TGFβ signalling molecules in developing heart valves. Moreover, early lethality of many of the mouse models precludes our understanding of the potential roles of these signalling components in later stages of valve remodelling and differentiation. The use of inducible knockout systems will be highly valuable in teasing out the exact roles of TGFβ signalling components during heart development.

Furthermore, TGFβ signalling has a significant role in maintaining adult heart health by regulating cardiac fibrosis and hypertrophy after injury and in hypertension (23,28). In a normal adult valve, VICs, the main cellular component, are quiescent and maintain the integrity of the valve leaflet. Following injury, TGFβ signalling activates VICs (29), sustains VIC activation and regulates *in vitro* valve repair via activated VICs (30). Persistent activation of VICs can alter the mechanical properties of the valve through changes in ECM composition and thus increasing susceptibility to disease. TGFβ signalling has been associated with a number of valve diseases (31-33) and suggests that aberrant activation/inhibition of this pathway during embryonic development may increase the probability of valve disease later in life. To aid in the discovery and design of new potential therapeutics for congenital heart defects and valve disease additional studies are required examining the role of TGFβ signalling in later stages of heart valve development and adult VIC activation.

Notch signalling is involved in numerous developmental events and processes including formation of the heart valves. Notch signalling is an essential driver of EMT and its components are widely expressed throughout heart valve development (22). Activation of Notch requires the binding of a transmembrane Notch ligand on a signalling cell to a transmembrane Notch receptor on a signal-receiving cell. In mammals, there are four Notch receptors, Notch 1-4, and five Notch ligands, Delta-like (Dll) 1, 3, 4 and Jagged (Jag) 1, 2. Activation of Notch signalling has three major steps: ligand binding, release of the Notch intracellular domain (NICD) via two proteolytic cleavages of the Notch receptor, and finally translocation of NICD into the nucleus to function as a transcription factor along with its binding partners RBPJ and MAML (Figure 1-2B).

To examine the functions of Notch signalling during valve development, transgenic mouse models have been generated for downstream, intracellular effectors, such as NICD, RBPJ and MAML. Of note, not all of these Notch intracellular effectors are specific to only Notch signalling. The loss of Notch intracellular effectors can lead to a complete block in Notch signalling, while overexpression of NICD leads to constitutive activation of Notch signalling. This allows examination of effects in the presence or absence of Notch signalling. Gain of function experiments with constitutive endocardial Notch activation using NICD leads to the activation of a mesenchymal gene program in the ventricular endocardium and ventricular explants have the ability to undergo a non-invasive EMT and upon addition of BMP2, ventricular explants can undergo a full invasive EMT (34). This data indicates that Notch signalling plays an important role in endocardial patterning of the AVC and chambers of the heart and that BMP2 has a role in inducing invasive EMT. However, constitutive activation of NICD may not recapitulate normal *in vivo* activities of Notch signalling and it should be noted

that some phenoptypes may be an artifact. Conversely, absence of RBPJ causes a loss of cushion mesenchyme in valve regions, EMT defects, and collapsed endocardium in the developing heart (35). Overall, the data suggests that Notch activation and signalling via RBPJ is essential for the endothelial cell lineage and EMT in the cardiac cushions. Mouse Notch receptor knockout studies reveal that Notch1 is essential for cardiac valve formation. Notch ligand mutant mice do not show abnormalities in cardiac valves, suggesting that redundancy may play a role for Notch ligands during valve formation. Additionally, the loss of Notch target genes has further emphasized the significance of Notch signalling during cardiac development. A number of the complete and endothelial specific mouse knockout studies for Notch signalling result in embryonic lethality at E10.5 (reviewed in (22)) and suggests that Notch signalling has a critical role in early phases of cardiac valve formation following EMT. However, the roles of Notch signalling in later valve development and in the adult valve disease are not fully understood. Notch signalling has also been implicated in adult heart valve calcification (36) and valve diseases share many similarities with cartilage and bone formation in the developing limbs (37,38).

1.3 Embryonic limb development and shared features of limb and heart valve formation

1.3.1 Development of the cartilage template in the developing limb

The development of the bones of the vertebrate skeleton is derived through two different processes: intramembranous ossification, which forms flat bones; and endochondral ossification, which forms long bones (39). Endochondral ossification requires the formation of a cartilage template prior to bone formation whereas intramembranous ossification does not form a cartilage template and forms directly from mesenchymal condensations (reviewed in (40)). During the

process of endochondral ossification, the undifferentiated mesenchyme cells will migrate into regions that are fated to become bone. These cells will become packed in this locale (without proliferating) triggering condensation, which signifies the start of cartilage formation. Undifferentiated mesenchyme secretes a primitive ECM enriched with collagen type I, tenascin, hylauronan, and fibronectin (41) but as condensation commences, the mesenchyme in the core differentiate and alter the composition of the ECM. To date, little is known about what drives the process of mesenchymal condensation, however, it is known that BMPs are critical for the formation of chondrogenic condensations (39). The differentiated mesenchyme in the core of the condensation develop into chondrocytes (cartilage cells) and secrete ECM rich in collagen type II, IX, and XI, aggrecan and link protein (41). Chondrocytes start proliferating, then undergo further differentiation, and turn into hypertrophic chondrocytes. During this time, these cells reduce production of collagen type II and start to secrete collagen type X (41). Hypertrophic chondrocytes enlarge, terminally differentiate, and exit cell cycle to become terminally differentiated chondrocytes. Simultaneously, blood vessels start to invade the cartilage template and bring in the osteoblast cells (bone forming cells). Following this, the terminally differentiated chondrocytes undergo apoptosis to allow the osteoblasts to fill this area and replace cartilage with bone (reviewed in (42)). Any alterations in the process of endochondral ossification lead to major abnormalities of the skeleton such as achondroplasia and osteochondrosis.

1.3.2 Functional similarities between the developing heart valves and limbs

The composition of the developing limb cartilage is similar to that of developing heart valves, where both tissues are largely composed of highly organized ECM and mesenchymal cells that

undergo proliferation, condensation and remodeling to form heart valves or limb buds. Moreover, heart valve and tissues that form cartilage templates (such as the limb) share a number of key TFs, such as TWIST1, SOX9, and NFATC1 (43) suggesting that their transcriptional programs are comparable (37,38,44). Furthermore, heart valves and tissues made up of cartilage have functionally similar tissue composition in that they both differentiate from SOX9 positive mesenchyme and produce comparable ECM structures. To support the similarity seen in the transcriptional programs of developing heart and limbs, loss of the transcription factor, SOX9, prior to mesenchymal condensation during limb formation leads to agenesis of the cartilage and bone (45) and loss of SOX9 in the heart valve endothelium results in major abnormalities in the heart valves cauding embryonic death (46). This suggests that SOX9 is essential for heart valve and limb development and that SOX9 plays a key role in their formation, differentiation and organization.

1.4 The role of the sex determining region Y (SRY) box 9 (SOX9) during embryonic development

Signalling pathways play a crucial role during development and initiate a cascade of events that can lead to the activation of TFs that coordinate gene expression. The SRY (sex determining region Y) box (SOX) TFs play a key role in the formation of numerous organs during development and receive signals from many signalling pathways such as TGFβ, BMP and Notch.

1.4.1 SOX transcription factors

The SOX TF family is subdivided into groups (A-H) based on their sequence similarity in the high mobility group (HMG) domain that is required for DNA binding (reviewed in (47)). The

SOXA subgroup only has one member, SRY, while the SOXB group is further divided into SOXB1 containing SOX1, 2, and 3 and SOXB2 containing SOX14 and SOX21. The SOXC subgroup contains SOX4, 11, and 12 and the SOXD group is comprised of SOX5, 6, and 13. SOXE includes SOX8, 9, 10 and SOXF has SOX7, 17, 18. Lastly, SOXG and SOXH only have one member each, SOX15 and SOX30 respectively. SOXs have been shown to bind to the DNA sequence ATTGTT or similar motifs via the HMG domain (reviewed in (47)) and it has been suggested that the HMG domain's interaction with the DNA itself can result in DNA bending. This DNA bending capability may be another regulatory role for SOX factors during development although this exact function remains to be shown *in vivo*.

SOX factors require the binding of other additional co-factor TFs on the nearby DNA and form TF complexes to efficiently regulate their target genes (47). Of note, the SOXD subgroup contains a coiled-coil dimerization domain that allows these factors to bind with other SOXD proteins. The SOXE TFs consist of a self-dimerization domain that could aid in the formation of these TF complexes with itself and other partner proteins. In addition, different SOX subgroups can work together to form TF complexes to regulate their target genes. For example, during chondrogenesis SOX9 can dimerize with itself to regulate genes (*Col2a1*) but it also works together with SOXD factors, SOX5 and SOX6, as a SOX trio to regulate chondogenic genes like *Aggrecan* (48). During successive developmental events, several SOX TFs along with their binding partners are known to bind and regulate their future co-factors. Two examples of these types of interactions are found during melanocyte development. For example, SOX10 binds together with PAX3 to activate the *Mitf* gene, following this activation MITF then binds with SOX10 to activate other melanocyte-specific genes (49,50). The next example illustrates when a SOX factor activates another SOX factor and then both SOX factors work together to regulate

additional downstream genes. In sex determination, SRY and its binding partner SF1 activate SOX9. Following that, SRY and SOX9 make a co-factor complex that regulates the *Amh* gene which is essential for male gonad development (51). Additionally, SOX proteins within the same subgroup often have similar functions and are expressed in the same developing tissues, although exact expression patterns of each individual SOX factor can vary within the tissue (47). For example, all of the SOXE TFs have roles involved in neural crest cell development and SOXF factors have important functions in the developing vasculature (47). This suggests that there may be some level of redundancy between SOX factors within a subgroup. However this is not always the case, as it has been demonstrated that one member of a SOX factor subgroup may be more critical than the others for a specific developmental process or function (reviewed in (47)).

1.4.2 The many roles of SOX9 during development

The SOXE TFs have important roles in gene regulation during the development of numerous organ systems, in sex determination, and in the neural crest (reviewed in (47,51,52). In particular, SOX9 plays a critical role in the development of testis, pancreas, limb, heart, intestine, liver, and many others (reviewed in (53)). In humans, mutations in the SOX9 locus that generate haploinsufficency cause a disorder called campomelic dysplasia (CD) which includes skeletal abnormalities, sex reversal, and in some cases heart defects (54) for further details on CD see Section 1.6). Loss of one allele of *Sox9* in mice is lethal at perinatal stages and mutant embryos have defects such as cleft palate and bending and hypoplasia of cartilage-derived skeletal structures resembling the phenotype of CD in humans. To bypass this, *Sox9* and its functions during development have been examined using the Cre/Lox system to delete specifically within different subsets of cells. It has been described that SOX9 has three general

roles during development: proliferation of progenitor cells, EMT, and in ECM differentiation including ECM organization and deposition (53).

1.4.3 The role of SOX9 in proliferation, EMT, and ECM

The role of SOX9 in progenitor cell proliferation has been described in the developing pancreas where SOX9 is expressed in all early pancreatic epithelial cells and is subsequently down regulated upon commitment (reviewed in (53)). Pancreata from CD patients are hypoplastic, consistent with a potential role in proliferation (55). Mouse studies where SOX9 was specifically deleted in the developing pancreas also produced severe hypoplasticity (56), confirming the importance of SOX9 in the maintenance of pancreatic progenitor fate and proliferation. Intriguingly, numerous SOX9 mutant organs are hypoplastic and have defects in proliferation (46,57-59) and yet to date, no direct SOX9 target genes involved in regulating proliferation or cell cycle have been identified in any of these systems. The direct relationship between SOX9 and proliferation has been somewhat tenuous but several studies have attempted to draw a more mechanistic link between the two. For instance, in rat mesenchymal stem cells (MSCs), a stable knockdown of SOX9 caused reduced proliferation, increased levels of cyclin D1 and p21, delayed S-phase progression, and increased stability of the cyclin D1 protein (60). This suggests that SOX9 plays an essential role in the progression of cell cycle through S-phase via degradation of cyclin D1 in rat MSC. Not only does SOX9 have a role in proliferation in progenitor/stem cells but it has been shown to have important functions in stem cell maintenance (61,62). In adult hair follicle stem cells, genes bound by SOX9 are required to maintain stemness via secreted factors in the niche (62) and regulate chromatin dynamics at super enhancers (63).

Moreover, altered levels of SOX9 have been associated with many cancers (53,64), and altered SOX9 levels are linked to poor prognosis, increased proliferation and invasiveness in many cancers. In breast cancer, SOX9 is associated with more aggressive cancer subtypes (65) and in colorectal cancer, SOX9 promotes tumour growth and progression (64). The majority of studies demonstrating a link between SOX9 and proliferation have suggested that SOX9 positively affects proliferation. On the contrary, SOX9 has also been shown to have a suppressive role on proliferation in the intestinal epithelium and SOX9 deficient crypts have increased levels of proliferation (66). These differences in the proliferative role of SOX9 in the intestinal epithelium may be due todifferences in expression levels in different subsets of cells within the crypts. Overall, this shows that SOX9 is an extremely context-dependent TF and therefore this complexity must be taken into account when trying to understand the function of SOX9 in a given tissue. Overall, SOX9 plays a critical but context-specific role in maintaining appropriate levels of proliferation and sustaining cell cycle progression during development, in stem/progenitor cells, and in cancer.

SOX9 has also been implicated in the process of EMT in neural crest (NC) cells (reviewed in (53)). During development, NC cells undergo EMT and migrate out from the dorsal neural tube to populate multiple regions within the embryo. NC cells contribute to a diverse number of tissues such as the cartilage, skin and the heart. Premigratory and migratory NC cells express SOX9 and loss of function studies demonstrate that SOX9 is important for neural crest cell formation (53). SOX9 has been shown to activate transcription factors like *Snai2* and together they can induce EMT (67). Several other SOX9-expressing cells undergo EMT-like processes such as astrocytes, pancreatic progenitors, cartilage, and cardiac valves and further support the notion that SOX9 may be important for the process of EMT during development. The process of

EMT is central to cancer metastasis and SOX9 may be playing an important role in driving cell invasiveness via EMT.

The regulation of ECM organization and differentiation in chondrogenesis is one of the well known functions of SOX9 (68). SOX9 is highly expressed as the condensing mesenchyme is becoming committed to chondroprogenitors and the expression of SOX9 is not down regulated until they become terminally differentiated chondrocytes (68). The ECM environment is constantly changing during cartilage formation and SOX9 contributes to this process by regulating genes like the collagens (*Col2a1*, *Col9a1*, *Col11a2*, *Col27a1*) and key matrix proteins (Aggrecan, Matrilin-1 and COMP) in chondrocytes (53). The composition of the ECM is also important for the formation of the developing heart valves where SOX9 is highly expressed in the valve mesenchyme (following EMT) throughout their development and suggests that SOX9 has a necessary role in regulating ECM components during valve formation.

1.5 SOX9 is essential for the development of the heart valves and limb.

SOX9 has been shown to have a crucial role during heart valve development (46,69). SOX9 is highly expressed in the developing mouse endocardial cushions (E9.5-E16.5) within the mesenchyme cells (69-71) and in the remodelling and maturing heart valve leaflets (E16.5-after birth)(46,72). *Sox9* null embryos could be generated by conditionally deleting one allele of *Sox9* in oocytes (using *Zona pellucid 3 (Zp3)-Cre*) and one allele in spermatids (using *Protamine 1 (Prm1)-Cre*) followed by crossing these mice together to obtain completely null embryos (69). Embryos that completely lack *Sox9* die at E11.5-12 due to congestive heart failure and have severely hypoplastic endocardial cushions and authors suggest that SOX9 may play a role in the proliferation and differentiation of the endocardial cushions during EMT (69). Using a *LacZ*

reporter mouse to examine *Sox9* expression, Akiyama *et al*. found that *Sox9* turns on in newly transformed mesenchymal cells that have migrated into the cardiac cushion (69) and it has been shown that its expression is directly downstream of Notch signaling in endothelial cells transduced with NICD (73). Endothelial *Sox9* deletion using the *Tie2-Cre* driver strain (which is a receptor tyrosine kinase that is expressed in all endothelial cells and its descendents including the valve mesenchyme) with the *Sox9 flox* mouse was embryonic lethal just prior to E14.5 with hypoplastic endocardial cushions, reduced mesenchymal cell proliferation and alterations in ECM composition (46). These data indicate that SOX9 expression is turned on in the mesenchyme (the valve precursor cells) and is involved in proliferation of these cells during early valve formation. Additionally, SOX9 has been demonstrated to have an essential role in late heart valve formation, where the loss of SOX9 using *Col2a1-Cre,* which deletes *Sox9* in the fibrosa layer of the valve, causes abnormal ECM patterning, loss of cartilage-associated proteins and thickened valve leaflets (46). These findings demonstrate that SOX9 has multiple roles during cardiac valve formation, initially during the expansion of the valve precursors and later for the proper expression and distribution of the ECM in the valve leaflets.

The loss of one allele of *Sox9* in mice using *Col2a1-Cre* promotes calcification of the heart valve leaflets, increased matrix remodelling and inflammation of the heart valves suggesting that SOX9 may also play a role in heart valve disease (46,72). In addition, SOX9 has been associated with valve calcification in human aortic valve disease (36,74,75) and in mouse valve disease models (76,77). Therefore, understanding the role of SOX9 and its downstream target genes during heart valve development may give us better insights into the progression of cardiac valve disease and may lead to the development of novel therapeutics.

SOX9 is essential for chondrogenesis (78) and is highly expressed in mesenchmyal condensations, maintained in differentiated chondrocytes but is eventually silenced at terminal differentiation in hypertrophic chondrocytes in order for proper bone formation to occur (68). SOX9 is known to bind to the DNA sequence WWCAAWG in promoters and enhancers of cartilage-specific genes (79-84) and can bind and regulate DNA as monomers and dimers (85,86). The loss of SOX9 before mesenchymal condensation (using *Prx1-Cre*) in the developing limb buds leads to cartilage agenesis and subsequent bone formation although patterning of the limb axes remains intact (45). The loss of SOX9 prior to mesenchmyal condensations produces an expanded apoptotic domain in the limb and indicates a potential role for SOX9 in suppression of apoptosis. In addition, SOX5 and SOX6 (known transcriptional targets and co-factors of SOX9 in the limb) expression was lost in the mutant limbs (45). Furthermore, deletion of SOX9 after mesenchymal condensation formation (using *Col2a1-Cre*, which allows the initial formation of chondrocytes) leads to chondrodysplasia. Cells failed to fully differentiate into chondrocytes, and had decreased proliferation resulting in abnormal joint formation (45). SOX9 limb mutant mouse models demonstrate that SOX9 is essential for the formation of cartilage and subsequent development of bone in the developing limb buds.

Surprisingly, there are only a few genes known to be directly transcriptionally regulated by SOX9 and most of these "target" genes have been identified in the developing limb. Some of the identified cartilage-specific targets of SOX9 are *Col2a1*, *Col9a1*, *Col11a2*, *Acan*, *Hapln1* (CLP), *Comp*, and *Mia1* (Cd-rap) (79-84,87,88) with *Col2a1* being the most well characterized to date. Although a few genes have been speculated to be SOX9 targets in the developing heart valves, none have been shown to be direct. One study demonstrated that SOX9 represses *Spp1* in maturing heart valves and chondrocytes to inhibit matrix mineralization (89). Moreover, SOX9

knockdown in primary valve explants lead to an increase in *Spp1* transcripts and a decrease in *Col2a1* and *Hapln1* (cartilage-associated genes) whereas an over-expression of SOX9 leads to the inverse. This suggests that *Spp1* expression is required for matrix mineralization following the loss of SOX9 in primary heart valve explants (89). This may indicate why the loss of SOX9 can lead to calcification as seen in mice with heterozygous loss of SOX9 using *Col2a1-Cre*. In summary, SOX9 plays an essential role in the formation of the heart valves and limb buds and identification of the global downstream transcriptional targets of SOX9 during heart valve and limb development will provide a better understanding of the exact role of SOX9 during the expansion, differentiation, remodelling and maturation of the valves and limbs and in congenital defects and disease.

1.6 Campomelic dysplasia

Campomelic dysplasia (CD) is characterized by the bowing of long bones, facial abnormalities, pelvic and vertebral defects, hypoplastic scapulae, clubbed feet, absence of a set of rib bones, and sex determination defects (54). Overall, CD is usually lethal but there is a small subset of patients that survive. Acampomelic CD, a variant of CD is also due to mutations in the SOX9 locus and has all of the same clinical phenotypes except the bowing of the long bones. Interestingly, mild versions of CD tend to be associated with rearrangements within the chromatin, potentially disrupting regulatory elements, rather than alterations in the *Sox9* coding region (85). This indicates that mild forms of CD are likely due a decreased dosage of SOX9 during development. A mutation that disrupts the dimerization domain of SOX9 was identified in a CD patient that did not have sex reversal and suggests that the dimerization capability of SOX9 is necessary for chondrogenesis and not for sex determination (85). Furthermore, loss of

one allele of *Sox9* in mice results in perinatal lethality with defects resembling the phenotype of CD (90). The mouse model of CD indicates that dosage of SOX9 is critical at two major steps during cartilage formation: mesenchymal condensation and the transition of differentiated chondrocytes to hypertrophic chondrocytes (90). Since SOX9 takes a central role in multiple abnormalities found in CD these mice can be used as a model to understand how the loss of one TF affects the formation numerous organs during development.

1.7 Congenital heart defects and heart valve disease

1.7.1 Congenital heart valve abnormalities

Congenital abnormalities of the heart can affect 1-5% of human newborns and approximately a third of these cardiac defects are due to heart valve malformations (91,92). The most prevalent heart valve malformations are bicuspid aortic valve (BAV), in which patients exhibit two aortic valve cusps instead of three; and mitral valve prolapse (MVP), in which patients suffer from floppy mitral valve leaflets that can slip past their normal position into the left atrium. Reports on the prevalence of congenital heart defects vary widely (ie. 1-5% of newborns) since BAV and MVP are not usually included. BAV affects 2% of the general population but the consequences are rarely seen until adulthood (91,92) whereas MVP affects up to 5% of the general population but is rarely detected in newborns as symptoms are frequently not severe (91). However, these congenital anomalies can lead to an increased pressure on the heart and predispose these patients to valve disease later in life. Tetralogy of Fallot, hypoplastic left heart syndrome, and Ebstein's anomaly are other examples of congenital heart defects that include heart valve and septal abnormalities. There are a number of syndromes that also include heart valve and septal defects such as Williams, Marfan, Trisomy 21, Alagille, Turner, and Noonan syndrome (92).

1.7.2 Adult heart valve disease

According to the World Health Organization, cardiovascular diseases are the number one cause of death worldwide; in 2008 approximately 17.3 million people died from cardiovascular disease, which accounts for 30% of global deaths. In the US, approximately 3-5% of cardiovascular deaths are due to valve disease (93). Adult valve disease can become evident as stenosis, a narrowing of the valve opening resulting in less blood flow; or as regurgitation, an incomplete closure of the valve causes backflow of blood in the heart. If valve disease goes undiagnosed it can lead to secondary effects, such as improper ventricular function and eventually heart failure. Initial stages of heart valve disease involve activation of VICs, which leads to abnormal ECM deposition and disorganization. There are two types of ECM changes that can occur in the heart valves during valve disease: myxomatous disease involves increased deposition of proteoglycans, loss of collagen, and destruction of elastin fibrils leading to "floppy" valves and regurgitation, while fibrotic disease involves degradation of proteoglycans along with increased levels of collagen and elastin fibre fragmentation resulting in stiffening of the valve leaflets known as valve stenosis (11,94,95). Valve fibrosis can often progress further, leading to valve calcification (3). Accumulation of calcium in the valve causes them to stiffen, which impacts the valve's ability to open and close and can eventually lead to heart failure. To date, little is known about the progression of valve calcification, myxomatous and fibrotic valve disease.

Many cases of valve disease in adults involve pre-existing defects in the heart valves and suggest that abnormalities that occur during embryonic valve development may lead to susceptibility to valve disease later in life (3,96-99). The literature suggests that key pathways and factors regulating valve development are also implicated in valve disease and congenital

heart defects (37,74). Unfortunately, there are limited options for treatment of valve disease and the current treatment option is valve replacement using either mechanical or prosthetic valves (100); however, a major fault with replacement surgery is that additional surgeries are often required. Consequently, the search for alternate treatments of heart valve disease drives the need for further investigation of heart valve development and disease and their underlying biology.

1.7.3 The involvement of SOX9 and signaling pathways in heart valve disease

Sox9 expression has been shown to be up-regulated in human myxomatous mitral valve disease (31,76). *Scleraxis* mutant mouse AV valves displayed characteristics of human valve disease and it was found that both SOX9 and ECM proteins were up-regulated in the mutant valves (101). Heart valves from mice with a mutation in *Col1a2* (Osteogenesis imperfecta murine mice) share a number of characteristics with myxomatous valve disease including increased expression of *Sox9* (77). In addition, SOX9 has been linked to human aortic valve stenosis and pediatric and adult aortic valve disease (74,75). In mouse, heterozygous loss of *Sox9* using a flox allele with *Col2a1-Cre* resulted in thickened heart valve leaflets and deposits of calcium on the valves similar to the calcification seen in heart valve disease (46,72). Generally, the literature suggests that the loss of SOX9 in the heart valves results in calcification, however in human and mouse diseased aortic valves, SOX9 was found to be up-regulated along with RUNX2, a known osteogenic marker that is indicative of calcification (75,77). To date, up-regulation of *Sox9* has been implicated in both myxomatous and calcific valve diseases which have very different disease processes and reveals conflicting roles for SOX9 in the progression heart valve disease and consequently additional studies are required to tease out the role of SOX9 in valve disease.

Signalling pathways also play a key role in the progression of heart valve disease. For example, Notch has been implicated in valve calcification, a common form of heart valve disease (36), and mutations in *NOTCH1* have been linked with familial, non-syndromic, autosomal-dominant calcific aortic valve disease (CAVD) and associated with BAV (102). To further support a role for Notch signalling during valve disease, heterozygous *Notch* or *Rbpj* mice have a higher risk of developing calcification of the aortic valve (103,104). Inhibition of Notch in rat aortic valve interstitial cells causes a significant decrease in SOX9 (already known to be involved in aortic valve calcification) and cartilage-associated factors (36). Using an *in vitro* valve calcification model, loss of Notch lead to high levels of calcification and conversely, increased levels of Notch signalling reduced calcification (36). Of note, the addition of SOX9 could rescue the accelerated calcification triggered by the loss of Notch (36) and demonstrates that Notch signalling may be regulating SOX9 in VICs. This data suggests that the loss of both Notch and SOX9 in the cardiac valves could lead to adult valve disease and subsequent calcification of the valves. Therefore, understanding the role of Notch signalling and the role of SOX9 during valve formation may provide key insights into their involvement during valve disease.

1.8 Hypothesis and aims of this study

My hypothesis is that SOX9 regulates the same critical genes in both heart and limb development and by identifying unique and shared SOX9 target genes I will provide novel insights into similarities and differences between valve and limb regulatory networks and will determine genes essential for heart valve formation. To explore the *in vivo* functional role of SOX9 in valve and limb development, I have analyzed and characterized the transcriptional

targets of SOX9 identified by chromatin immunoprecipitation coupled with deep sequencing (ChIP-Seq) on E12.5 mouse embryonic AVC and limb. Briefly, ChIP-Seq is a technique that will identify TF DNA binding sites on a genomic level within a given tissue (105,106). The ChIP pulls down (enriches) DNA sequences that SOX9 antibodies bind to and these are sequenced and mapped back to the genome. Regions of the genome that are enriched with DNA sequences are called 'peaks' and these represent SOX9 DNA binding regions within the genome. This method allows for the identification of *in vivo* transcriptional targets of SOX9 in developing valve and limb on a genome wide level.

To identify the critical of role of SOX9 in the heart valves, I have generated and characterized the phenotype of a novel endothelial specific (*Vascular Endothelial cadherin* (*VE*) *Cre* crossed with the *Sox9 flox* mice) SOX9 mutant mouse and the previously described endothelial specific SOX9 mutant mouse (*Tie2-Cre* crossed with the *Sox9 flox* mice). After the proper characterization of the SOX9 mutant mice, I examined gene expression alterations in the absence of SOX9 by comparing WT and SOX9 mutant heart valves using RNA-Seq. To determine the critical targets of SOX9, I have employed various bioinformatic analyses to compare the SOX9 ChIP-Seq libraries to the RNA-Seq libraries generated from WT and SOX9 mutant heart valves. Lastly, I have selected several candidate genes from the list of genes discovered by comparing ChIP-Seq and RNA-Seq libraries based on differential expression and gene function for further examination in the developing valves. Collectively, this work will help to elucidate novel and key factors involved in the regulatory networks required for heart valve formation, and improve our understanding of heart development and heart-related disease processes.

CHAPTER TWO: Material and methods

2.1 Mice strains and tissue dissection

All animal protocols were approved by the Animal Care Committee at the University of British Columbia. C57BL/6J mice were used for all ChIP-Seq libraries. ICR outbred mice were used for ChIP-qPCR validation. To generate *Sox9fl/fl* (WT) and *Sox9fl/fl;VE-Cre* or *Sox9fl/fl;Tie2-Cre/+* (*Sox9* cKO) embryos, *Sox9fl/fl* female mice were crossed with *VE-Cre*/*Tie2-Cre* male mice to generate *Sox9fl/+;VE/Tie2-Cre* male mice and then these males were mated with *Sox9fl/fl* female mice. All mice were backcrossed more than seven generations. *Sox9fl/fl* (*B6.129S7-Sox9tm2Crm/J*) and *Tie2-Cre (B6.Cg-Tg(Tek-cre) 12Flv/J)* mice were obtained from Jackson Laboratories (Sacramento, USA). The *VE-Cre* mice were a kind gift from the Karsan lab. The *Sox9fl* allele was genotyped using primers specific to the flox region and *VE*/*Tie2-Cre* was detected using primers specific to *Cre recombinase* (Table 2-1). Embryos from timed matings were considered embryonic day (E) 0.5 at noon of the day a vaginal plug was observed. For the SOX9 ChIP-Seq libraries, the atrioventricular canal (AVC) and limb buds were manually dissected in cold phosphate buffered saline (PBS) using forceps and a dissecting microscope. Whole hearts and heart regions including the AVC, atria, ventricles, and outflow tract were manually dissected from *Sox9fl/fl* and *Sox9fl/fl;VE-Cre* or *Sox9fl/fl;Tie2-Cre/+* embryos for immunofluorescence, qPCR, *in situ* hybridization and/or RNA-Seq libraries. Littermates were used for experiments comparing WT and *Sox9* cKO and at the least an n of 3 was used for all experiments. *Sox9fl/fl*, *Sox9fl/fl;VE-Cre* and *Sox9fl/+;Tie2-Cre* mice were maintained on a C57BL6 background.

Table 2-1 Primer sequences

Primers for Genotyping		
Name	**Forward 5'to 3'**	**Reverse 5' to 3'**
Sox9fl/fl	AGACTCTGGGCAAGCTCTGG	GTCATATTCACGCCCCCATT
Cre	CGTACTGACGGTGGGAGAAT	CCCGGCAAAACAGGTAGTTA
Primers for qRT-PCR		
Name	**Forward 5'to 3'**	**Reverse 5' to 3'**
Sox9	CAGCAAGAACAAGCCACACGTCAA	TTGTGCAGATGCGGGTACTGGTCT
Fgfr2	TAGTCATGGCTGAAGCAGTGGGAA	TCTGATACCAGATCAGACAGGTCC
Trp53	ACAAGAAGTCACAGCACATGACGG	TTCCTTCCACCCGGATAAGATGCT
Akt2	GGAGGTCATGGAGCATAGATTC	AAGTACCTTGTGTCCACTTCTG
Prkaca	ATGTAGCTGGTGGCGAGATGTTCT	TGAGAAGATTCTCGGGCTTCAGGT
Cdkn1b	AAACTCTGAGGACCGGCATTTGGT	TCTTCTGTTCTGTTGGCCCT
Rfwd3	AAAGTGCCATCTTCCAAAGCCCAG	AGGTGGCCAGATAGCTGTTCTGAT
Junb	CTTTAAAGAGGAACCGCAGACCGT	TTTGATGCGCTCCTGGTCTTCCAT
Hdac2	TACAACAGATCGCGTGATGACCGT	TCCCTTTCCAGCACCAATATCCCT
Sox4	GCCCGACTTCACCTTCTTT	AAGGACAGCGACAAGATTCC
Mecom/Evi1	TCCTCCTCATCCAACAACACCTCA	ATCCGCAATTTCATCGGGAACAGC
Pitx2	GGAAGCCACTTTCCAGAGAA	CGGCGATTCTTGAACCAAAC
Hand2	CACCAGATACATCGCCTACCTCAT	GGTCTTCTTGATCTCCGCCTTGAA
Nfia	GTCACAAACACCAATAGCTGC	AGACTTGAGGCGCTTTGTAG
Vim	GACCTTGAACGGAAAGTGGA	AGCCACGCTTTCATACTGCT
Cdh2	AGGGTGGACGTCATTGTAGC	CTGTTGGGGTCTGTCAGGAT
Cdh1	ACGACACAGCCAATGGACCAAGAT	TCGGGCATATACTCCTGCAGTGTT
Cdh5	ACCGAGAGAAACAGGCTGAA	AGACGGGGAAGTTGTCATTG
Postn	TGTGTATCGGACGGCTATCT	CTCTGCTGGTTGGATGATTTCT
Eln	CTCATCCATCCATCCATCCATC	GACAGGTGAACCAGGTTGATAG
Fbn1	ATGAATGCAACCAGGCTCCCAAAC	AGCTCCTTCCATCCTCTTGCAGAA
Mgp	ACCCTGTGCTACGAATCTCACGAA	TGTTGATCTCGTAGGCAGGCTTGT
β-actin	CCAGAGCAAGAGAGGTATCCTGAC	CATTGTAGAAGGTGTGGTGCCAG

Primers for luciferase vector cloning		
Name	**Forward 5'to 3'**	**Reverse 5' to 3'**
Mecom	CAGAAGGTTCTAGAAGCAAGGCAC	CCCAGGTATCCAGTACAAAGTAAATTATCA
Prkaca	TGTCTCCGCCAATCGACGGCTT	TGCTTCCCGCGTCTCTCT
Rfwd3	AGAAGAAGCAGGGAGCAGCCTCA	CCTGAGATTAAAGGCGTGAGCCAT
Trp53	ACTAGCGGTGCTAGCCAGAAGTAT	ACGATGTCTGGTGCGCGATAAGAA
Junb	AGAAACAGGCTAGGGAAAGAGAGC	TTCCTGTGCCCTAATATGGGTGCT
Nfia	TGCAAACGATGAGGGTACTGGACT	CCGTCCAGCTCCAGTGAATAATGGAA
Fgfr2	TCTCTGCCCTTTGTCCTTTG	TCTGTGTGCTTCCATGTTCC
Cby1/Fam227a	CATTTTTAACACAACAAAGC	GCCTGCAGCTTTCTGCAAGG
Wasf1/Cdc40	TCATCTTCCCTCATTCCCGAGCC	ACCCGCGCCTGCAGCAGGGGGA
Primers for site directed mutagenesis		
Name	**Forward 5'to 3'**	**Reverse 5' to 3'**
Hdac2 1st M	GGGGCTAAAGTCCGCTTGTGCGCACCTCCG	GCGGACTTTAGCCCCGCGCTCAGAGACCCG
Hdac2 2nd M	GGGGCTAAAGTCCGCCGGTGCGCACCTCCG	GCGGACTTTAGCCCCTTGCTCAGAGACCCG
Hdac2 DM	GGGGCTAAAGTCCGCCGGTGCGCACCTCCG	GCGGACTTTAGCCCCGCGCTCAGAGACCCG
Flanking Primers	CGAGCTCTAGACTGCCCGGGATTCG	GGCTAGCGACGGCCGGTGCTGCAGC
Primers for Taqman qRT-PCR		
Name	**Company, Catalog #**	
Sox9	ABI, Mm00448840_m1	
Gapdh	ABI, Mm99999915_g1	
Lef1	ABI, Mm00550265_m1	
Twist1	ABI, Mm00442036_m1	
Tbx20	ABI, Mm00451515_m1	
Ccnd1	IDT, Mm.PT.58.28503828	
Primers for ChIP-qPCR		
Cops5	AAACACTTCCTTAGGGTTGGCTCG	CTCGCAGTTCACACGAACGGATTT
Eed	GGGAGGAAAGAGAAGTCACCT	TAACTCGAAGTTGTTCTCCCGAGC
Fos	ATCTCCGAATCCTACACGCGGAA	CCGTCTTGGCATACATCTTTCACC
Hdac1	TGGGCCTGTACCAAAGTCCG	TGTGAAGCGGGCTGCAGAGTTTA
Hdac2	AACCAGTGCGCGTAAGACCGA	TTCTACGGGTAGTCACACACAGTC
Primers for ChIP-qPCR		
Name	**Forward 5'to 3'**	**Reverse 5' to 3'**
Junb	CCAGCTACAGACGCTTCTAGTCAT	AGGCTTATTAGTCGCCGATGGTTG

Primers for ChIP-qPCR		
Name	**Forward 5'to 3'**	**Reverse 5' to 3'**
Srpk2	GCTACAACACAAACACGAAATGCT	GGACAAATCAAATAGAAGCAGCCAGGG
Timp2	CCATTCACGTGCCGCTGAATCATTTG	TGGCTTCTTGGCATAGAAACTGCG
Ctgf	TAAGCATGCACTGCTCACTCCAGA	AAACACATGGCAGCTCCCTAAAGC
Mecom/Evil	TGTCCAGGGCATGCTTCTGACTAA	CTGGCTGCTAAACCTGCTTACACA
Fgfr2	ACCTCTGTGCGACGCAGGAAATAA	TGGCAGGAGACACGGAACTAAACA
Id3	TTCCCACACATTCGCCATCAAAGC	CCACAACAGATTAAAGACCAGGAGGG
Trp53	GCAGGAGCATTTCCGGTTTCTTGT	TCCTCAAACCACAGAACCAGCCTA
Prkaca	TCACTCATCCAGGAGCCTATGGT	ATTGGTTCAGGCCTCCCTGACTGA
Rfwd3	ACGGCGACCAATCTCTTCTCTTCT	CTCGCCCAGAAATGTATCAAAGGC
Cul4a	TACTGGTTAATGGTGATGTGCGCC	AACCAACGTGCAGAGGTTACCGT
Fgf11	GGGACTCCCTAACTGTCGT	AACAGGGAAATCGGCAGAGAGCAA
Col2a1	AGAGCTGTGAATCGGGCTCTGTAT	AGGCTGTGCATTGTGGGAGA
Apoc3	CGTGAAAAGCATGGGCAAATC	AGGGATAAAACTGAGCAGGC
Hnf1	CATGAGGCCTGCACTTGCAA	GGGAAATTCTCCAAGGTTCA
Tat	GAGTCAGGCTTCAAATCTCTGGTC	GGGAAATTCTCCAAGGTTCA
Wasf1	AAAGTGCGGATCGGGCAATACC	AGAATGAGCATCCACCCACTTACC
Wasf2	AAGTTCATAGGCTCGGCCTGTTCT	ACAGGGAAAGACCTCGGCTAACAT

2.2 Immunofluorescence, cell counts, *in situ* hybridization and H&E staining

Hearts were fixed in 4% paraformaldehyde (PFA, Sigma) overnight and were subjected to a sucrose gradient (15%, 30%, 65%) prior to embedding. Hearts were embedded in TissueTek O.C.T. (Sakura) in cryomolds and were cryosectioned using the Leica CM3050S cryostat at 6-8μm thickness. For *in situ* hybridization (ISH) slides were sectioned at 10 μm thickness. Slides were maintained at -80˚C until immunostaining. Following removal of slides from the -80˚C freezer, slides were dried for 10 minutes at room temperature. Borders were drawn around sections with a wax pen (Diagnostic Biosystems) and were re-fixed with 4% PFA for 10-20 minutes at room temperature. Slides were washed with 1X PBS three times for 5 minutes each. A blocking solution of 5% Bovine Serum Albumin (BSA, Roche) with 0.1% Triton X-100 (Sigma) diluted in PBS was added to the sections for 1 hour at room temperature. Primary antibodies were diluted in blocking solution (see antibody dilutions in Table 2-2) and placed into a humidified chamber overnight at 4˚C. The following day, the primary antibody was removed and washed with 1XPBS three times for 5 minutes at room temperature. Secondary antibodies were diluted in blocking solution at 1:500 (see Table 2-2 for secondary antibodies) and incubated for one hour at room temperature. Sections were washed with 1X PBS three times for 5 minutes each. 4',6-Diamidino-2-Phenylindole, Dihydrochloride (DAPI, 1 μg/mL, Sigma) was added to the last PBS wash for 10 minutes at room temperature to label nuclei. DAPI was washed off with PBS. Slides were mounted with 50-100 μL of 20 mg/mL DABCO (1,4-diazabicyclo[2.2.2]octane, Sigma) and coverslips were added and sealed with nail polish for visualization. Images were captured with OpenLab v5.0 (PerkinElmer) on a Zeiss Axioplan 2 compound microscope or TCS SP5 Leica confocal microscope with the Leica Application suite software. For immunofluorescence images, cell counts for SOX9 positive nuclei or phospho

Table 2-2 Antibodies for immunostaining

Primary antibodies			
NAME	**HOST SPECIES**	**COMPANY & CATALOG**	**DILUTION**
SOX9	rabbit	Millipore	1/600
PHOSPHO HISTONE H3 (PHH3)	rabbit	AbCam	1/100
CYCLIND1	mouse	Santa Cruz	1/100
EVI1	rabbit	Santa Cruz	1/100
PERIOSTIN	rabbit	Abnova	1/100
CD31	rat	BD Biosciences	1/100
Desmin	Mouse	Medicorp	1/100
Secondary antibodies			
NAME	**HOST SPECIES**	**COMPANY & CATALOG**	**DILUTION**
ALEXA FLUOR 488	rabbit	ThermoFisher Scientific,	1/500
ALEXA FLUOR 594	rabbit	ThermoFisher Scientific,	1/500
ALEXA FLUOR 488	mouse	ThermoFisher Scientific,	1/500
ALEXA FLUOR 594	mouse	ThermoFisher Scientific,	1/500

histone H3 (pHH3) positive nuclei in the AVC and/or the eipcardium (epi) were performed on three to five sections and averaged between at least three WTs and three *Sox9* cKOs hearts (N=3) using ImageJ software or by manually counting. ISH was performed as described previously(107). Hemotoxylin and Eosin (H&E) staining (Sigma) was performed according to the manufacturer's protocols.

2.3 RNA isolation

Atrioventricular canals (AVCs), atria, ventricles and outflow tracts (OFT) from ICR or C57BL6 or single AVCs, atria, ventricles and OFT (generated from crossing *Sox9fl/fl* females and *Sox9fl/+;Tie2-Cre* or *Sox9fl/+;VE-Cre* male mice) were dissected out from the heart of embryos. Tissues from ICR and C57BL6 were pooled together and for *Sox9/Cre* crosses only single tissues were used for RNA isolation. Tissues were directly placed into Trizol (ThermoFisher Scientific). For tissues from *Sox9/Cre* crosses, the samples were stored at -80˚C until embryos were genotyped (See section 2.7). RNA was isolated with Trizol using the manufacturer's protocol. Briefly, tissues were homogenized in Trizol and incubated for 5 minutes at room temperature. Chloroform (EMD Biosciences) was added at 1/5 the volume of Trizol and vigorously agitated for 20 seconds. Samples were ccentrifuged at high speed (>13000rpm) for 10 minutes at 4˚C. The aqueous layer was taken and RNA was precipitated with an equal volume of isopropanol (EMD Biosciences). Samples were centrifuged down at high speed (>13000 rpm) at 4˚C to collect precipitates for at least 10 minutes. Isopropanol was removed and pellets were washed with 70% ethanol (EMD Biosciences). The ethanol was removed and samples were air dried for 10 minutes at room temperature. Pellets were re-suspended in RNase and DNAse free water (ThermoFisher Scientific). The quality of the RNA was assessed using the Nanodrop 1000

(RNA with approximately OD260/280= 1.8-2.0, OD260/230= 2.0-2.2 was considered good quality) and RNA was stored at -80˚C.

2.4 RT-PCR, qRT-PCR, and ChIP-qPCR

RT-PCR was performed as previously described (108) with a several modifications. cDNA was synthesized using the Transcriptor First Strand cDNA Synthesis Kit (Roche) and HIFI Taq polymerase (ThermoFisher Scientific) was used for RT-PCR and for initial steps of cloning. qPCR was performed with FastStart Universal SYBR Master (sRox, Roche) according to the manufacturer's protocol on the ABI 7900HT Fast Real-Time PCR System. Conditions for qPCR were as described (109). Primers used in RT-PCR, qRT-PCR and ChIP-qPCR are found in Table 2-2. Relative quantification was used for qRT-PCR. Housekeeping genes were used as endogenous controls for all Taqman assays (*Gapdh*) and qRT-PCR (*Actb*). For single heart part specific qRT-PCR analysis on AVC, ventricles and atria, mouse *Sox9, Lef1, Twist1, Tbx20* and *Gapdh* Taqman primers and probes (ThermoFisher Scientific) were used on WT and *Sox9* cKO embryonic heart parts. For ChIP-qPCR, fold enrichment was calculated by 2^(Ct difference between SOX9 and IgG ChIP). Regions tested for enrichment in ChIP-qPCR were within SOX9 peak regions (see Table 2-1 for primer sequences. If multiple peaks were present in heart or limb for shared target genes then the most likely candidate was chosen based on Positional Weight Matrix (PWM) score and proximity to the gene.

2.5 Chromatin immunoprecipitation coupled with high-throughput sequencing (ChIP-Seq)

Three independent ChIPs generated from pooled embryos were combined for SOX9 ChIP-Seq libraries (total: 164 E12.5 AVCs and 39 E12.5 limb buds). For a simplistic illustration of the

ChIP-Seq protocol see Figure 2-1). For the ChIP, tissues were homogenized in 1% formaldehyde and incubated at room temperature for 10 minutes. Samples were incubated with 0.125 M glycine at room temperature for 5 minutes. Following pelleting and washing, samples were re-suspended in 5 volumes of ChIP cell lysis buffer (10 mM Tris–Cl, pH 8.0, 10 mM NaCl, 3 mM MgCl2, 0.5% NP-40) with a protease inhibitor cocktail (Roche). Cells were re-homogenized and put on ice for 5 min. Cells were pelleted again and re-suspended in 3 volumes of ChIP nuclear lysis buffer (1% SDS, 5 mM EDTA, 50 mM Tris–Cl, pH 8.1) containing a protease inhibitor cocktail (Roche). For sonication (Sonicator 3000, Misonix), samples were placed in an ice water bath and sonicated for 20 cycles of 30 seconds on, 40 seconds off. Sonicated chromatin was diluted with ChIP dilution buffer (to 250 μL, 0.01% SDS, 1.1% Triton X-100, 167 mM NaCl, 16.7 mM Tris–Cl, pH 8.1). 3μg of rabbit polyclonal anti-mouse SOX9 antibody (Millipore AB5535) or negative control of 3μg of rabbit polyclonal IgG antibody (Santa Cruz) was added to samples and incubated overnight while rocking at 4˚C. Simultaneously, Protein A/G beads (ThermoFisher Scientific) were blocked with 1 mg/mL BSA and 0.1 mg/mL herring sperm DNA in ChIP dilution buffer overnight. The following day, samples were incubated with blocked Protein A/G beads for four hours rocking at 4˚C. Beads were precipitated and washed with several buffers. The washes are as follows: low salt buffer (0.1% SDS, 1% Triton X-100, 2 mM EDTA, 20 mM Tris–Cl, pH 8.1, 150 mM NaCl), high salt buffer (low salt buffer with 500 mM NaCl), lithium chloride buffer (0.25 M LiCl, 1% NP-40, 1% deoxycholate, 1 mM EDTA, 10 mM Tris–Cl, pH 8.1) and two final washes with TE buffer. For the elution of the bead complexes 125 μL elution buffer (1% SDS, 0.1 M NHCO3) was added and samples were rotated at room temperature for 15 minutes, twice. Proteinase K with RNAse A (ThermoFisher Scientific) and 0.192 M NaCl (reverse crosslinking) were added to samples and incubated

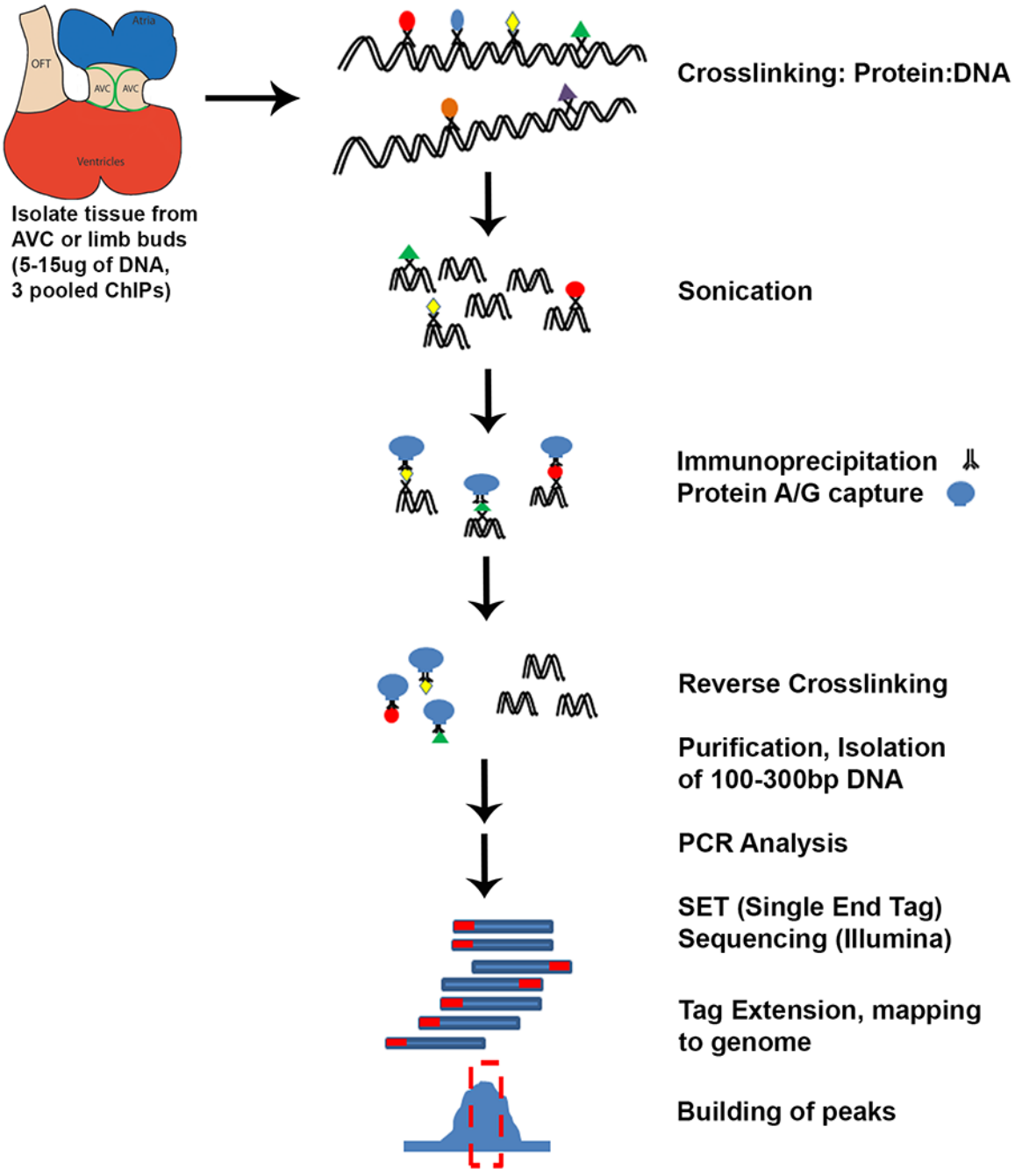

Figure 2-1 Generation of SOX9 ChIP-Seq libraries from E12.5 AVC and E12.5 limb buds. Approximately 5-15ug of total DNA was collected from the E12.5 AVC and limb buds. Tissues were homogeneized and subjected to crosslinking (protein:DNA). Crosslinked protein:DNA was sonicated and immunoprecipitated using the SOX9 antibody. Protein:DNA complexes (shown in different colours:red, green, yellow) were reverse crosslinked and DNA was isolated. DNA was sent for sequencing and bioinformatic analyses were performed to determine SOX9 peaks.

at 65˚C overnight. Purification of DNA was performed with two rounds of phenol-chloroform extraction and ethanol precipitation. Samples were spun down and pellets were re-suspended in 50 µL dH2O. A sample of genomic DNA was extracted as input for sequencing. Limb ChIP was performed alongside the heart ChIP to confirm enrichment of known target genes via ChIP-qPCR.

ChIP DNA was sent to the Genome Sciences Centre (Vancouver, BC) for library generation. DNA was purified using 8-12% PAGE to isolate 100-300 bp fragments for short read (50 bp) sequencing on an Illumina Genome Analyzer 2 as described previously (110). The Burrows-Wheeler Aligner (111) aligned reads to the mouse genome (mm9) and unmapped reads were removed. FindPeaks3.1 (112) created virtual fragments by directionally extending uniquely mapped reads to a constant length (200 bp). Virtual fragments were profiled across the genome to identify regions of enrichment or "peaks". A False Discovery Rate (FDR) was applied to threshold ChIP-Seq data as described (113) and false positives were limited using sequenced control data (input DNA). For each ChIP-Seq peak that passed the FDR ~0.01 threshold, we found the maximal coverage of the control sample in the region +/-300bp. A local z-score was calculated between the peak height and control coverage and peaks below the threshold were filtered out. Peaks that passed filtering, z-score, peak height, FDR based peak height cut-offs and did not overlap with control peaks (height over 30) were retained for analysis. Peak edges were refined by using a percentage of the maximum peak height to determine the peak edge cut off point. For each dataset, different criteria were used due to differences in sequencing depth and background noise. For screenshots and visual comparisons, we used unthresholded big wig or bed files. The data has been deposited to the GEO database (GSE73225).

2.6 Bioinformatic analysis of ChIP-Seq

Wig and BED files generated by FindPeaks3.1 were analyzed using tools in UCSC Genome browser (114) (http://genome.ucsc.edu/), Galaxy (115) (http://main.g2.bx.psu.edu/), and Cistrome (116) (http://cistrome.dfci.harvard.edu/).

SOX9 bound regions (peaks) were associated with genes through a "yes-no" process that ensured transcriptional start site (TSS) proximity was weighted prior to distance from either end of a gene (Appendix IID). This mapping system ensured that most peaks were only associated with one gene. The distribution of SOX9 peaks was analyzed by dividing the genome into categories: greater than 10 kb from a TSS; distal promoter (5-10 kb from a TSS); proximal promoter (less than 5 kb from a TSS); at a TSS (+/-100 bp); within the first 1 kb of a gene, within the first 1-5 kb of a gene; mid-gene (greater than 5 kb from either end of a gene); within the last 5 kb of a gene; at a transcription termination site (TTS); within 5 kb of the 3' end of a gene; and greater than 5 kb from the 3' end of a gene. SOX9 peaks were assigned to one of these regions using Cistrome. Cistrome's SeqPos tool (116) and Screen Motif tool were used for motif analysis of SOX9 peaks. PWMs for the SOX monomer and dimer motifs were generated by SeqPos. PWMs used in Screen Motif were based on highest enrichment, p-value and top z-score.

Gene Ontology (GO) analysis was performed using GOrilla (117). Lists were ranked using p-value and top categories were filtered for redundancy. Co-factor analysis on SOX9 peaks was performed using oPOSSUM (http://opossum.cisreg.ca/oPOSSUM3/) (118).

2.7 Genotyping *Sox9* mutant embryos

Sox9 mutant/cKO crosses were setup as mentioned above (for further information see Figure 2-2). Genomic DNA was collected from mouse ear punches or embryonic tissue (limb and hind

torso) and extracted using the KAPA mouse genotyping kit (Kapa Biosystems) according to the manufacturer's protocol. For the PCR reaction, 0.5 µL (for embryonic tissue) or 1.5 µL (for ear punches) was used as template for the genotyping PCR reaction. HIFI Taq polymerase (ThermoFisher Scientific) was used for the PCR reaction according to the manufacturer's protocol. The conditions used for the *Sox9fl/fl* PCR are: one step of 94˚C for 3 minutes, followed by 94˚C for 30 seconds, 60˚C for 30 seconds, 72˚C for 30 seconds repeated for 35 cycles and one final extension step of 72˚C for 2 minutes. The PCR program for *Cre* primers is similar with the exception of the 35 cycles which have 94˚C for 30 seconds, 55˚C for 1 minute, and 72˚C for 1 minute. The expected sizes of the bands for the *Sox9fl/fl* primers for WT were 250 base pairs (bp), heterozygous 300 bp and 250 bp and mutant 300bp. See genotyping primers Table 2-1.

2.8 RNA-Seq and bioinformatic analysis

RNA from single AVCs for each genotype (WT and *Sox9* cKO hearts) were used to synthesize cDNA (see RT-PCR method section) for Taqman assays to confirm efficient loss of *Sox9* in the *Sox9* cKO (*VE/Tie2-Cre*) AVCs. For the RNA-Seq libraries: RNA from two or three littermate AVCs with enrichment (WT, *Sox9fl/fl*) or loss (*Sox9* cKO) of *Sox9* in the AVC were pooled together. Pooled AVC RNA samples were further purified by GeneJet clean up and concentration micro kit (ThermoFisher Scientific). RNA quality was assessed on the BioAnalyzer (Agilent Technologies) and all samples had scores over 8.7 with a required passing score of 7. Duplicate RNA-Seq libraries for each genotype were generated and sequenced using Illumina Mi-Seq. Sequence reads were aligned with the Tophat2 tool (119) on Galaxy using the mouse reference genome mm9 (NCBI build 37) to generate BAM files. Aligned data from all

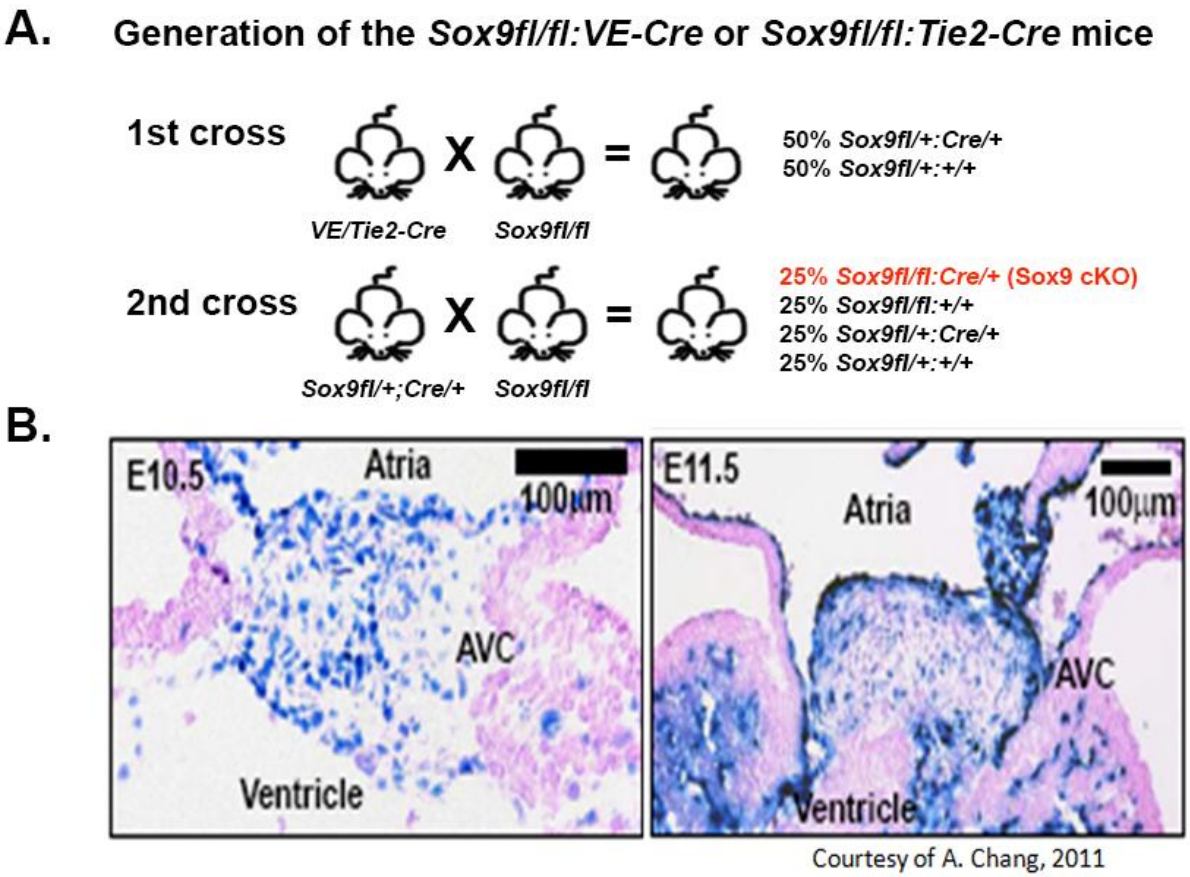

Figure 2-2 Generation of the *Sox9fl/fl;VE-Cre* and/or *Sox9fl/fl;Tie2-Cre* mice. A. The crosses needed to generate *Sox9* mutant mice. **B.** Lineage tracing with the *VE-cadherin*-tTA (VEtTA) strain (a gift from L. Benjamin, Harvard Medical School) crossed with TetOS-lacZ (a gift from D. Dumont, Samuel Lunenfeld Research Institute) illustrating the cell types in the E10.5 and E11.5 heart that *VE* will delete in. These images are shown with permission from Dr. A. Chang during his time at Dr. Aly Karsan's laboratory (unpublished).

four libraries were analyzed and Fragments per Kilobase of exon per Million reads (FPKMs) were calculated using Cufflinks (120). Differential expression between WT and *Sox9* cKO RNA-Seq libraries was determined using Cuffdiff (120). Gene FPKMs from Cufflinks were an average of the duplicate libraries for each genotype and only included genes represented in both duplicate libraries. Separate from Cuffdiff outputs, fold change was determined between WT and *Sox9* cKO gene FPKMs to assess differential expression. For genes to be included for downstream analyses several criteria needed to be met: greater than or equal to 1 FPKM in either WT or *Sox9* cKO and greater than or equal to 1.5 fold change between *Sox9* cKO and WT AVC gene expression. Cistrome and Galaxy were used to determine differentially expressed genes that were associated with SOX9 peaks.

GO analysis was performed using GOrilla (117). Mouse genes from RNA-Seq were used as background. Lists were ranked using p-value and top categories were filtered for redundancy. Ingenuity Pathway Analysis (Qiagen) biofunctions was used for GO analysis on SOX9 target genes overlapping in all libraries and to generate an interaction network of the biofunctions: transcription, cardiogenesis, and abnormal morphology of the heart on down-regulated SOX9 targets in the heart. Heat maps of gene expression data was generated using TM4 meV.

2.9 Cell culture, transfection, cloning and luciferase assays

Cells were maintained in an incubator at 37˚C with 20% oxygen and 5% carbon dioxide. HEK 293T cells were maintained in normal growth medium (DMEM (Stemcell) + 10%FBS + Penstrep, ThermoFisher Scientific). Growth medium for the cells was changed every two to three days. HEK 293T cells were transfected at 60-70% confluency using polyethylenimine (PEI, Polysciences Inc) following a published protocol(121). Luciferase assays were performed

two days following transfection using the Dual-Luciferase Reporter Assay System (Promega). SOX9 peak regions of interest were cloned into pGL3 vector with a minimal promoter (E1B) or pGL4b promoter-less vector to test luciferase activity for individual enhancers/promoters in the presence or absence of SOX9 (pcDNA3-SOX9 over-expression vector).

2.10 Site directed mutagenesis

Primers were designed to mutate the putative SOX9 dimer site in the SOX9 peak associated with the *Hdac2* promoter region. The first SOX9 site the CAA portion was mutated to ACC and the second site of TGG to GGT similar to other studies to generate mutant constructs. Smaller fragments with homologous regions were generated and melted together. See primers in Table 2-1. The PCR conditions used to generate mutant sequences were 94˚C for 3 minutes for one cycle, 94˚C for 30 seconds, 60˚C for 30 seconds, and 72˚C for 1 minute for all for 10 cycles. There was a 20 minute hold at room temperature to allow for the addition of flanking primers followed by 35 cycles of 94˚C for 30 seconds, 60˚C for 30 seconds, and 72˚C for 1 minute. There was one extension cycle of 72˚C for 10 minutes. HIFI Taq was used to maintain high fidelity and decrease random mutation. Mutant sequences were cloned into the pGL4b vector and sent for sequencing to confirm the mutations in the SOX9 dimer site. Mutant vectors were used in luciferase assays to assess the effect on the activity of SOX9.

CHAPTER THREE: Identification and characterization of SOX9 binding sites in the developing heart valve and limb genome.

The goal of this analysis was to determine where SOX9 binds within the genome of the E12.5 AVC and limb buds to identify potential transcriptional targets of SOX9 and ultimately understand the function (through its gene targets) of SOX9 within these tissues. To do this, ChIP-Seq was performed on E12.5 AVC (primitive heart valves) and limb buds with an antibody that recognizes the SOX9 protein. This analysis identified the genomic locations of SOX9 binding in these two tissues and based on the genomic location of SOX9 bound regions, we determined the potential SOX9 target genes. SOX9 bound regions and transcriptional targets were compared among different tissues to determine tissue-specific and context-independent functions of SOX9. Furthermore, bioinformatic analyses of SOX9 bound regions can reveal tissue-specific co-factors of SOX9. However, this analysis is entirely dependent of the specificity of the SOX9 antibody and therefore I decided first to characterize SOX9 expression using this antibody during heart valve development using this antibody.

3.1 *Sox9* mRNA and protein is enriched in the mouse heart valves throughout development

At E12.5, SOX9 has been reported to be widely expressed in mesenchyme throughout the developing mouse heart valves (69) and condensing mesenchyme in the developing limb (122). To confirm the enrichment of *Sox9* mRNA in the developing heart valves, qRT-PCR and *in situ* hybridization were used (Figure 3-1). *Sox9* mRNA levels were enriched in the AVC region at E10.5, E12.5, and E14.5 from 3-12 fold over the atria (Figure 3-1 part A-C). *Sox9* mRNA levels were also enriched in the OFT region at E10.5 and E12.5 which will form the aortic and

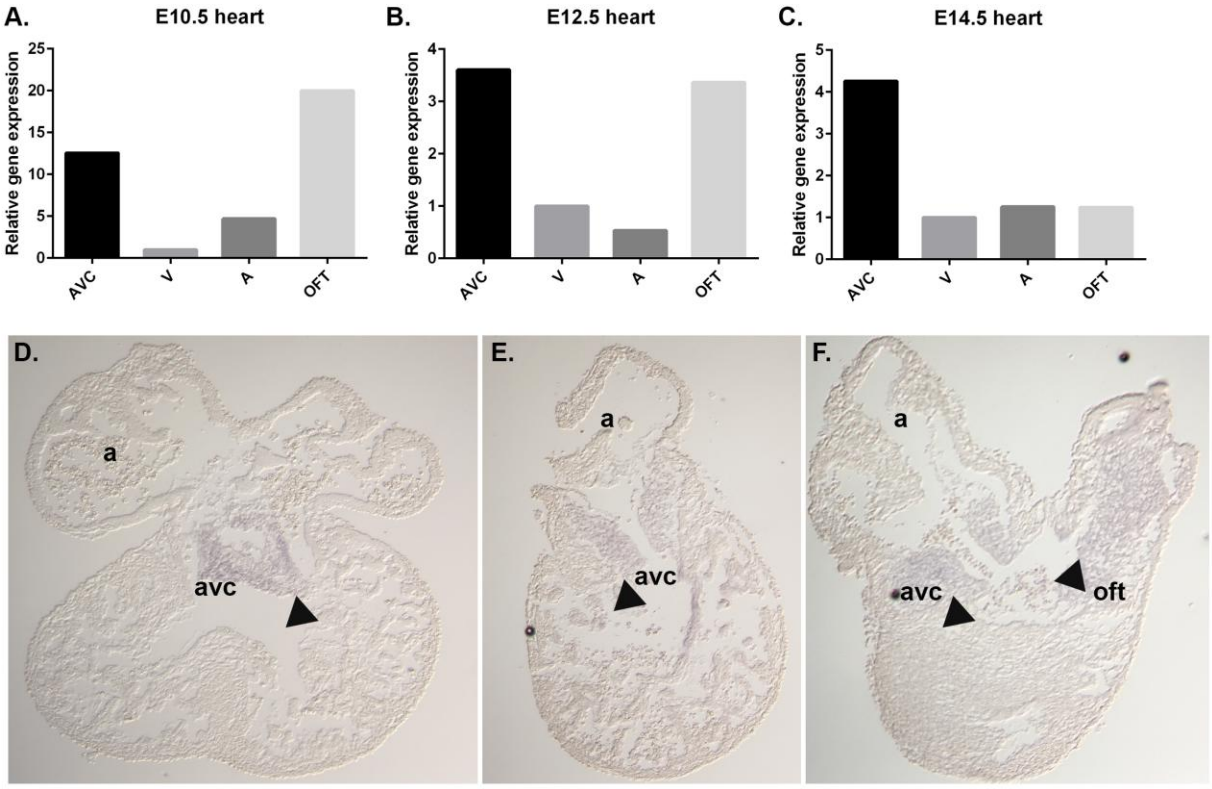

Figure 3-1 *Sox9* mRNA is enriched in the developing heart valves. A-C. A representative qRT-PCR for *Sox9* on E10.5 (**A.**), E12.5 (**B.**) and E14.5 (**C.**) valves (AVC), ventricles (V), atria (A), and outflow tract (OFT) relative to β-actin. **D-F.** Whole mount *in situ* hybridization with a probe specific for *Sox9* on E12.5 hearts. **D-E.** Highlight valve (AVC) specific expression in cross-section (**D.**) and saggital section (**E.**) **F.** Shows both AVC and OFT *Sox9* expression in the cardiac cushions.

pulmonary valves (Figure 3-1A, B). Similar to the qRT-PCR results, *Sox9* transcripts were found in the valve forming regions of the E12.5 heart by *in situ* hybridization (Figure 3-1D). Since mRNA transcripts and protein levels do not necessarily correlate, I wanted to examine SOX9 protein levels in the embryo. To ensure that the SOX9 antibody (Millipore, AB5535) binding was specific to locations in the embryo known to express SOX9 protein, immunofluorescence was performed on E12.5 whole embryo sections (Appendix IA, B, E) and E10.5 heart sections (Appendix IC, D, F). In the E12.5 embryo SOX9 protein was found in locations previously demonstrated to express SOX9 such as the limb buds (arrowhead Supplemental Figure 1 part A) and somites. SOX9 protein was highly expressed in the E10.5 heart valves as expected (Appendix I).

To determine how SOX9 protein is expressed throughout heart valve development, embryonic hearts from E9.5 (when the valves first form via EMT) through to E16.5 (during remodeling and differentiation stages) were examined using immunofluorescence (Figure 3-2). SOX9 protein was found to be enriched in the heart valves at all stages examined. Overall, this data suggests that SOX9 plays an important role in heart valve development during initial valve formation, remodeling and differentiation. SOX9 was also expressed in another subset of cells within the developing heart called the epicardium (Figure 3-2, see arrowheads). The epicardial progenitor cells are a thin layer of cells found on the outside of the heart (E10.5-E14.5) and a subset of these cells will undergo an EMT at around E14.5 and invade the myocardium to give eventually give rise to the coronary vasculature and aid in myocardial growth (reviewed in (123)). However, epicaridal progenitor cells are not derived from endocardial EMT (124) like the AV valves.

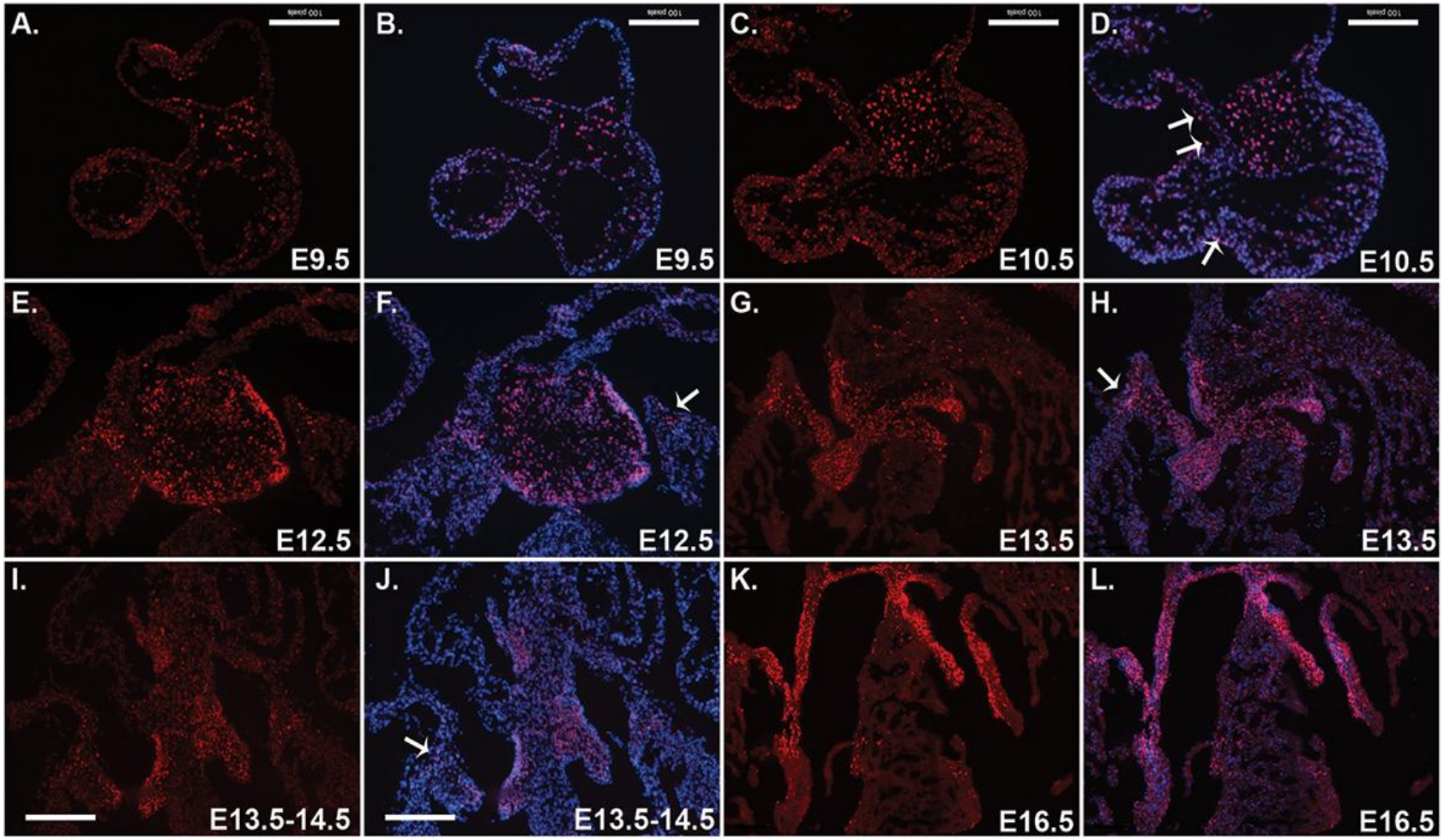

Figure 3-2 SOX9 protein is enriched in the heart valves during heart development. Immunofluorescence on embryonic hearts at E9.5 (A, B), E10.5 (C, D), E12.5 (E, F), E13.5 (G, H), E13.5-14.5 (I, J), and E16.5 (K, L) with an antibody specific to SOX9 (red). Panels A, C, E, G, I, and K illustrate SOX9 staining only and panels B, D, F, H, J, L show the merged image of SOX9 and DAPI (blue). For later stage hearts the image is focused in on the AV valve region of the heart.

3.2 SOX9 directly binds thousands of DNA regions in the developing heart and limb

One way to determine the function of a TF is to analyze the genes that this TF controls in a given context. Therefore to investigate the role of SOX9 in heart valve development, genome-wide profiles of SOX9 DNA-binding sites were generated for E12.5 heart valves (AVC) and limb buds using ChIP-Seq. The SOX9 genome-wide profiles for the E12.5 limb buds were generated to illustrate the similarities of the SOX9 initiated transcriptional programs in the developing heart valves and limbs. It has been suggested that developing valves and limbs share many similarities to one another and SOX9, and its transcriptional target genes, have been most well characterized in the developing limb. Thus, the limb provides a method of validating the SOX9 ChIP-Seq data by detecting previously identified SOX9 transcriptional target genes and an excellent tool to identify similarities between heart valve and limb SOX9-initiated transcriptional programs. Embryonic tissues were manually dissected out of the E12.5 embryo. Limb buds were pinched off the embryo. The E12.5 hearts were taken out of the embryo and further dissected to obtain only the AVC region by removing the ventricles, atria and OFT. A total of 164 E12.5 AVCs and 39 E12.5 limb buds were pooled in separate groups and used for three independent SOX9 (Millipore AB5535) ChIPs. The SOX9 antibody used for immunofluorescence analysis was also used for ChIP. Dissections and ChIPs were performed by R. Cullum in the Hoodless lab. The DNA from the three ChIPs was sent to the Genome Sciences Center for sequencing. Sequenced reads for each library were mapped to the mouse genome (mm9, NCBI build 37) and SOX9 peaks (regions of the genome where SOX9 is binding) were identified using a false discovery rate (FDR) of 0.01 followed by subtraction of an input DNA control. A local z-score was calculated between SOX9 peak height and control coverage for each library and SOX9 peaks below the threshold were filtered out (Appendix IIA, B). Peaks that passed filtering, z-

score, FDR based peak height cut-offs and did not overlap with control peaks were retained for analysis. This identified a total of 2607 and 9092 SOX9 peaks in the E12.5 AVC and limb, respectively (Figure 3-3A, Appendix III). To validate the specificity of the SOX9 peaks in the limb, SOX9 binding was confirmed at the exact same regions as previously identified to be regulated by SOX9 in *Col2a1*, *Acan*, and *Col11a2* (79,80,82) target genes (Appendix IIC).

To determine the degree of similarity in SOX9 binding between the AVC and limb, ChIP-Seq libraries were compared using a Venn diagram and identified 782 SOX9 peaks that were shared (29.8% of E12.5 AVC peaks) (Figure 3-3A). This data supports that there are similarities between the SOX9 initiated transcriptional programs in the valves and limb. Although there are similarities between the libraries, there were 1825 and 8310 unique SOX9 peaks in the E12.5 AVC and limb, respectively and indicate that SOX9 also has many tissue-specific binding sites. The increased number of unique SOX9 peaks in the limb is likely due to the heterogeneity of the limb buds at this time point and may reflect the diverse transcriptional programs in each different type of chondorcyte. To determine the potential target genes of SOX9, SOX9 peaks for each library were associated with genes through a "yes-no" process that ensured transcriptional start site (TSS) proximity was weighted prior to distance from either end of a gene (Appendix ID). This mapping system ensured that most peaks were only associated with one gene. From peak-to-gene associations, 2453 and 5750 potential gene targets of SOX9 were identified in the E12.5 AVC and limb respectively. Notably, 1605 genes were targeted by SOX9 in both tissues; this was more than double the shared SOX9 binding sites (Figure 3-3B) and suggests SOX9 targets similar genes in the valves and limb by using tissue-specific regulatory elements.

To determine how many SOX9 peaks contain a consensus SOX motif, *de novo* motif analysis was performed on SOX9 peaks with SeqPos (116). SeqPos is a program that identifies

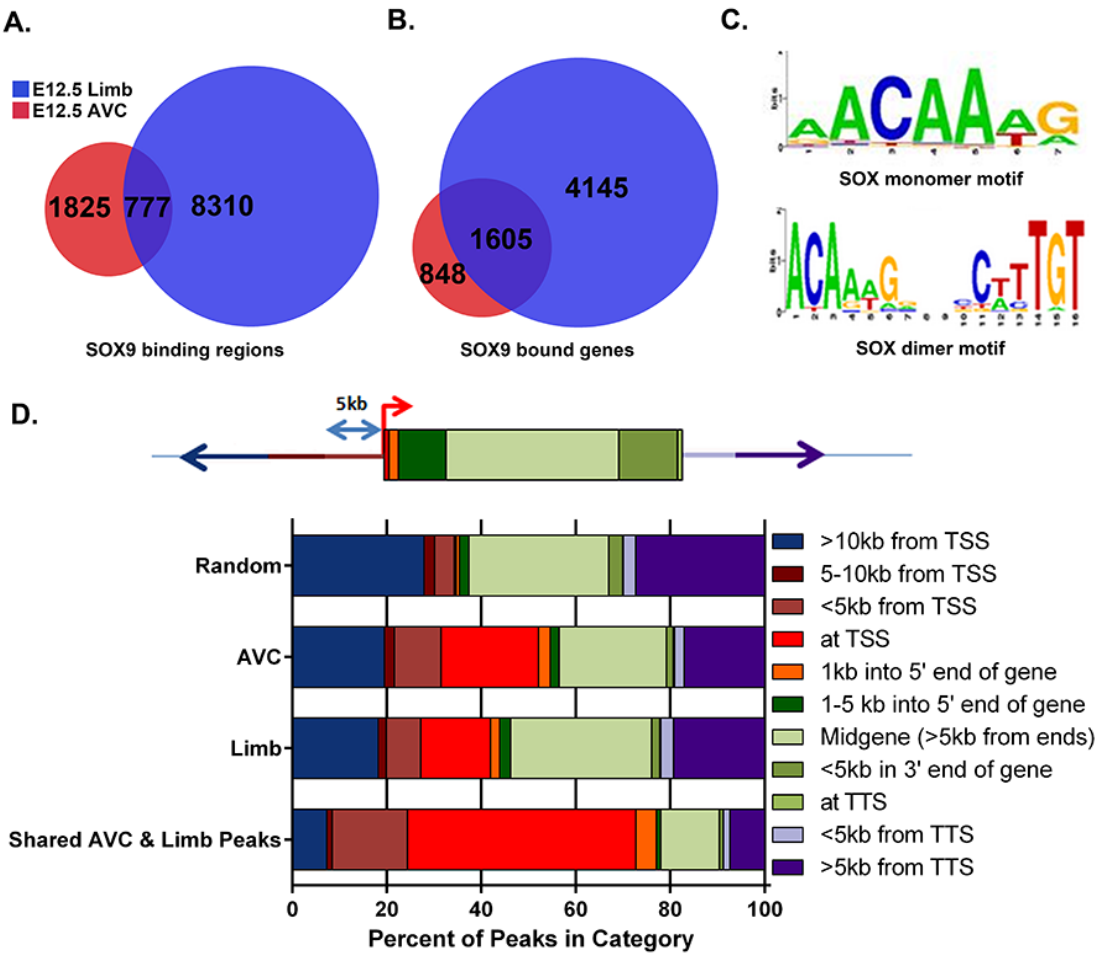

Figure 3-3 Comparison of SOX9-initiated transcriptional programs in developing limb and heart and genomic peak locations. A. Venn diagram of peaks and **B**. targeted gene overlap between the E12.5 valve (AVC) and limb ChIP-Seq libraries. Note: SOX9 peaks overlap and SOX9 target gene overlap are completely separate from one another. ie. 782 peaks do not correspond to 1605 genes in the Venn diagram overlap. **C**. Positional weight models for the SOX monomer and dimer binding sites as identified from the ChIP-Seq data. Letter height indicates importance of the base for SOX9 binding. **D.** Distribution of SOX9 peaks across the genome in E12.5 AVC, E12.5 limb and shared binding sites in both tissues.

TF DNA binding motifs found in the SOX9 peak DNA sequences. This analysis generated both a SOX monomer (aACAAa/tg/t) and a SOX dimer (ACAaaGnnnnt/at/cTGT) position weight matrix (PWM) that is similar to the SOX9 JASPAR motif (Figure 3-3C). Of note, several other SOX monomer motifs were also identified in the SOX9 peaks but for simplicity the top ranked SOX motif based on highest enrichment, p-value and top z-score is shown. In sex determination, SOX9 is known to bind as a monomer to a single DNA binding site in the regulatory regions of Steroidogenic Factor 1 and Anti-Müllerian Hormone, whereas proteins required for chondrogenesis, like Collagens XI and IX, feature a SOX9 homodimer binding motif (85). To establish how many SOX9 peaks contain a SOX monomer and/or dimer site, all SOX9 peaks were scanned with Screen Motif using the top SeqPos PWMs for the monomer and dimer motif. Approximately, 77% of SOX9 limb peaks and 58% of SOX9 E12.5 AVC peaks contained at least one monomer or dimer motif (Table 3-1). The SOX dimer sequence was identified in 34% of SOX9 limb peaks compared to 13.5% of SOX9 AVC peaks, suggesting that SOX9 primarily binds as a monomer in E12.5 heart valves. Consensus SOX binding motifs are highly degenerate and thus this analysis may not capture all versions of the SOX9 binding motifs.

3.3 SOX9 binds active promoter regions within the genome

To determine where SOX9 binds within the genome in relation to genes, SOX9 peaks were associated to putative target genes by dividing the genome into categories (Appendix IID & Methods). Approximately 22% and 31% of SOX9 binding sites in the limb and AVC, respectively, were found either directly over the TSS or in the 5kb upstream promoter regions. Furthermore, 64% of the overlapping SOX9 peaks in the AVC and limb were bound to the

Table 3-1: SOX9 monomer and dimer binding sites under the SOX9 peaks in heart and limb

Library	# Peaks	Monomer sites	Peaks with sites	Dimer Sites	Peaks with sites	Peaks with either monomer or dimer
E12.5 AVC SOX9	2607	2589	1409 (54.0%)	386	353 (13.5%)	1516 (58.2%)
E12.5 Limb SOX9	9092	10095	5678 (62.5%)	3491	3118 (34.3%)	6975 (76.7%)
Random Average 10 of 2607	2607	1917 +/- 56	1101 +/- 20 (42.2 +/- 0.76%)	131 +/- 10	123 +/- 8 (4.71 +/- 0.29%)	1147 +/- 39 (44.02 +/-1.50%)
Random Average 10 of 9092	9092	6793 +/- 117	3852 +/- 50 (42.38 +/-0.55%)	493 +/- 33	459 +/-30 (5.05 +/- 0.33%)	3946 +/- 42 (43.43% +/-0.46%)
Shared peaks	777	957	498 (64.1%)	175	155 (19.9%)	510 (65.6%)

Statistics on SOX9 motifs						
SOX9 motifs	**Peaks w sites**	**peaks w/o sites**	**expected w/ sites**	**expected w/o sites**	**two-tailed p-value**	**Chi-squared**
AVC monomer	1409	1198	1101	1506	<0.0001	149.152
AVC dimer	353	2254	123	2484	<0.0001	451.378
Limb monomer	5678	3414	3852	5240	<0.0001	1501.908
Limb dimer	3118	5974	459	8633	<0.0001	16222.645

TSS/5kb upstream regions (Figure 3-3D) and this suggests that SOX9 binding is biased to sites at or near promoter regions. Interestingly, the genes associated with overlapping SOX9 peaks in AVC and limb were enriched by Gene Ontology (GO) analysis for genes associated with metabolic processes and cell cycle regulation (Figure 3-4A, Appendix IV). Several examples of overlapping SOX9 peaks in the AVC and limb that are associated with cell cycle and proliferation and chromatin modifier genes such as *Trp53* (p53), *Junb*, *Rfwd3*, *Hdac1/2*, and *Eed* are shown using the UCSC genome browser (Figure 3-5). A role for SOX9 in proliferation has been suggested on numerous occasions since many tissue-specific SOX9 mutant mice have decreased cell numbers and hypoplastic organ structures (46,57-59). To determine the underlying functions of SOX9 target genes in the AVC and limb only, GO analysis was performed on E12.5 AVC SOX9 peaks and E12.5 limb SOX9 peaks (Figure 3-4B, C, Appendix V). In the AVC, SOX9 target genes were enriched for functions like adhesion, transcription, motility, WNT and TGFβ signaling and heart development (Figure 3-4B). SOX9 limb specific targets were involved in processes like mesenchyme development, chondrocyte differentiation, WNT and BMP signaling, and limb development (Figure 3-4C, Appendix VI). Interestingly, GO analysis on limb target genes also highlighted functions implicated in heart valve morphogenesis, EMT, and endocardial cushion development (Figure 3-4C, Appendix VI) and further support that the AVC and limb SOX9 transcriptional programs share many similarities.

3.4 Identification of potential co-factors of SOX9

3.4.1 DNA motif analysis identifies numerous potential co-factors of SOX9

Given that many SOX factors require the binding of additional co-factor TFs on the nearby DNA to efficiently regulate their target genes (47), SOX9 peak DNA sequences were analyzed

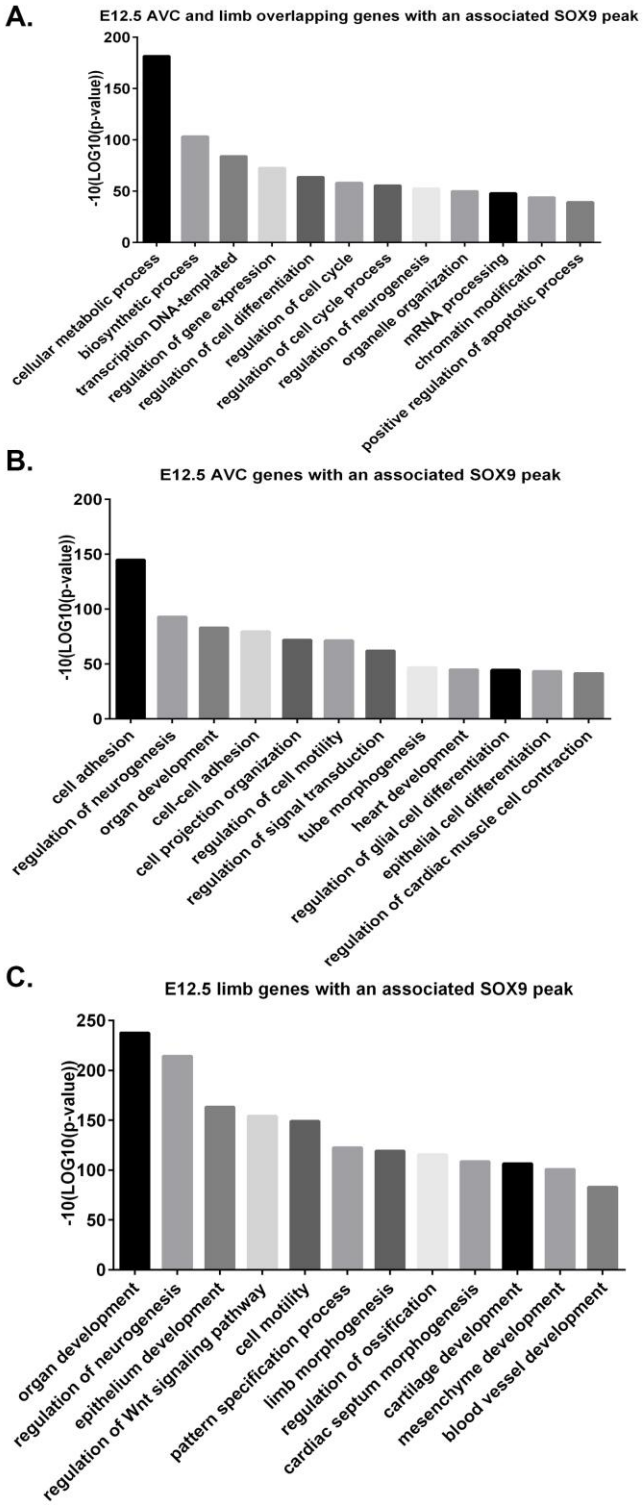

Figure 3-4 GO analysis reveals tissue specific functions for genes associated with SOX9 binding sites. GO analysis on the shared E12.5 AVC and limb (**A.**), AVC (**B**.), and limb (**C.**) target genes associated with SOX9 peaks.

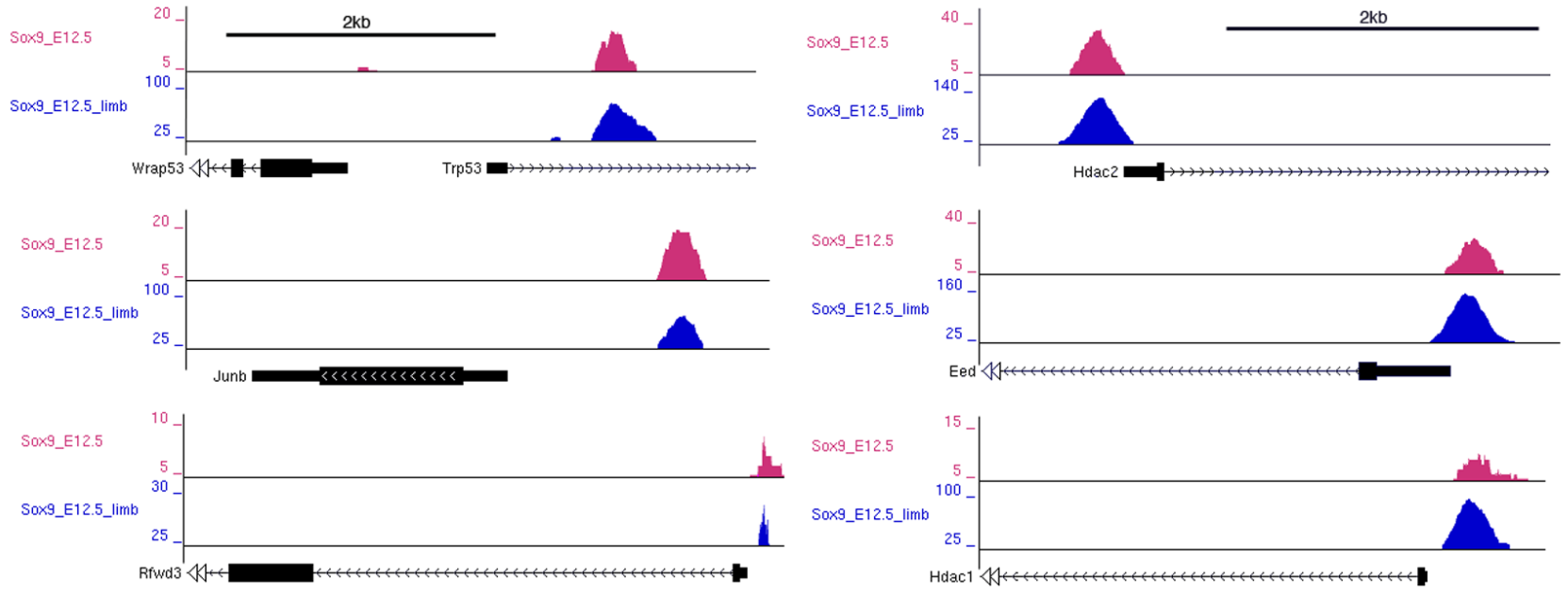

Figure 3-5 UCSC genome browser screen shots of shared SOX9 binding locations in the developing heart and limb that are associated with cell proliferation/cell cycle and chromatin modifier genes. From top left down: *Trp53*, *Junb*, and *Rfwd3*. From top right down: *Hdac2*, *Eed*, and *Hdac1*. The top library is the E12.5 AVC SOX9 ChIP-Seq (pink) and the bottom library is the E12.5 limb SOX9 ChIP-Seq (blue). Below the libraries is the gene structure.

for potential co-factor binding motifs using an online program called oPOSSUM (http://opossum.cisreg.ca/oPOSSUM3/) (118) (Figure 3-6, Appendices VII, VIII, IX). oPOSSUM uses a background set of DNA sequences of equivalent peak sizes and G:C content as the SOX9 peaks (generated by another tool in oPOSSUM) and searches the DNA sequences found under the SOX9 peaks for enriched TF DNA binding motifs. Based on a number of criteria, such as the number of TF motif sites found in SOX9 peaks versus background etc, were taken into account and TF motifs were ranked by z-score. The top co-factor binding site found in the AVC, limb and shared SOX9 binding regions is NFY which is known to bind at promoters to the DNA sequence 5' CCAAT 3' and regulate transcription. It is not surprising to find a promoter biased TF like NFY to be enriched in the SOX9 binding regions since we have already demonstrated that SOX9 binding is biased to promoter regions (Figure 3-3D). The SOX9 motif was enriched in all three sets as expected (Figure 3-6) and durther supports that SOX9 was bound to these regions. Additional SOX motifs were also identified such as SOX17 and SOX5. Many of the TF motifs identified are shared between libraries however the level of enrichment within SOX9 peak DNA sequences varies (Appendix VII, VIII, IX). Interestingly, the Arnt:Ahr binding motif was within the top five enriched motifs for each dataset (Figure 3-6) and suggests that HIF1a (where ARNT is a subunit) and SOX9 potentially regulate hypoxic genes together. However, additional experiments would be required to demonstrate this relationship.

Another way to examine the targets of SOX9 and to identify potential co-factors of SOX9 is to compare AVC and limb SOX9 ChIP-Seq libraries to other publicly available ChIP-Seq libraries. To look at the gene targets of SOX9 in other SOX9 expressing cell populations, SOX9 AVC and limb ChIP-Seq libraries were compared to SOX9 ChIP-Seq on hair follicle stem cells

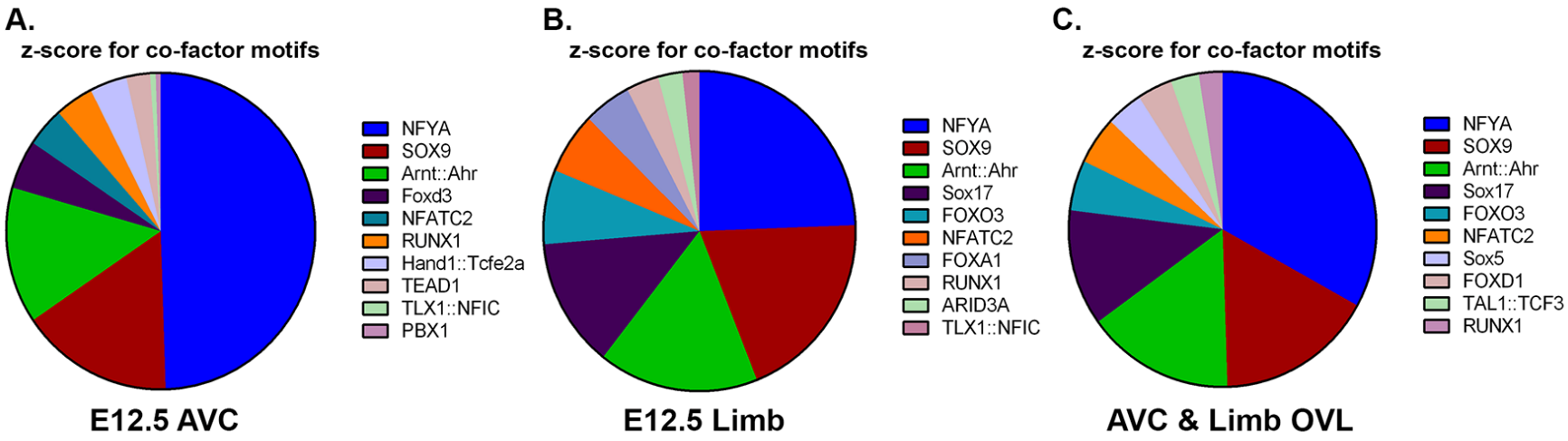

Figure 3-6 SOX9 peaks are enriched for numerous potential co-factor binding sites. Co-factor analysis using oPOSSUM (http://opossum.cisreg.ca/oPOSSUM3/) on SOX9 E12.5 AVC (**A.**), limb (**B.**) and shared (**C.**) SOX9 peaks.

(HFSCs) (62) and on the vertebral column (VC) (125) using a Venn diagram. This identified overlapping and non-overlapping SOX9 peaks (and their respective gene targets) indicative of common and tissue specific functions in different cell types for SOX9 (Figure 3-6A-B). The degree of overlap between the HFSCs SOX9 peaks and SOX9 AVC and limb peaks was fairly high considering the diversity of these cell types from one another and identifies potential common functions between these tissues (Figure 3-7A). An additional reason for the higher degree of similarity between these SOX9 ChIP-Seq libraries could be due to the use of the same SOX9 antibody (Millipore, AB5535) for the ChIP. Surprisingly, the overlap between the SOX9 VC peaks and that AVC and limb was much lower than expected given that the VC cells should have a more comparable function to the AVC and limb (Figure 3-7B). However, this study used a different SOX9 antibody (R&D Systems AF3075) and this may account for lower degree of overlap between libraries or that these cells types do not share similarity in function. A third study published SOX9 ChIP-Seq on rib chondrocytes (129) and would be ideal to compare the SOX9 AVC and limb peaks with but unfortunately the ChIP-Seq data was not fully released. These comparisons highlight the extremely context dependent role of SOX9 within different tissues and further supports that SOX9's regulation of its target genes is likely to be dependent on the binding of specific co-factors in different tissues.

3.4.2 Comparison of SOX9 ChIP-Seq with published ChIP-Seq data sets reveals new insights into potential co-factors of SOX9

Different SOX factors are known to work together to regulate their target genes. SOX4 is expressed highly in the developing heart valves at a level as high as SOX9 (based on RNA-Seq data from the lab/data not shown) and known to be important for valve development (130).

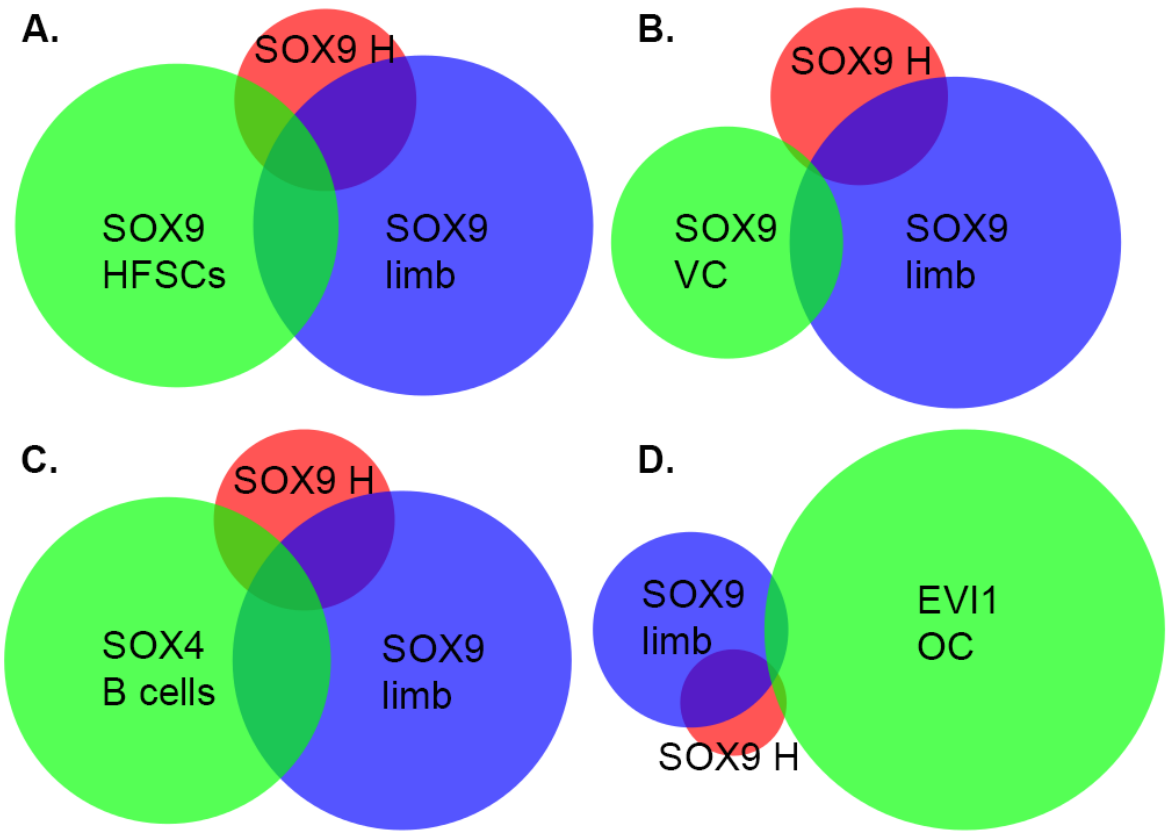

Figure 3-7 Comparison of SOX9 peaks the AVC and limb with other TF ChIP-Seq libraries using Venn diagrams: SOX9 on hair follicle stem cells (HF-SCs(126)) and SOX9 on the vertebral column (VC) (125) **(A, B),** and other potential co-factor TFs: SOX4 on B cells (127) and EVI1 on ovarian cancer cells (OC) (128) **(C, D)**. SOX9 H represents the SOX9 AVC ChIP-Seq library.

Therefore, it could be possible that SOX9 and SOX4 function together as co-factors to regulate valve-specific genes. The only publicly available SOX4 ChIP-Seq data set was generated on B-cells, and therefore SOX9 AVC and limb peaks were compared this SOX4 ChIP-Seq data set (127) (Figure 3-7C). Although it is not a functionally relevant cell type almost 1000 peaks were shared between the libraries (Figure 3-7C) similar to the SOX9 HFSC overlap suggesting that there are common binding regions for SOX4 and SOX9. This data supports the notion that SOX9 and SOX4 may work together as co-factors in the developing heart valve.

Another transcription factor of interest was EVI1 (*Mecom*) since the EVI1 motif was identified by oPOSSUM in the SOX9 peaks. In the oPOSSUM analysis, the EVI1 motif was not found in a high number of SOX9 peaks and therefore was not highly enriched in this analysis (Appendices VII, VIII, IX). However, identifying the EVI1 motif was still intriguing as it has been shown to have a role in heart valve development (131). Currently, the only EVI1 ChIP-Seq data set available was performed on human ovarian cancer cells (OC) (128). Although the EVI1 ChIP-Seq was performed on an unrelated cell type, a follow up study by the same group that generated the ChIP-Seq demonstrated that a number of targets of EVI1 identified in OC cells were implicated in congenital heart defects (131). Upon comparison of SOX9 and EVI1 binding regions, the overlap identified by the Venn diagram was not very high (Figure 3-7D) and this may be due the highly dissimilar cellular contexts of the ChIP-Seq libraries. Additional co-factor analysis on SOX9 peaks in the E12.5 AVC using SeqPos revealed 431 target genes with EVI1 motifs that have interesting implications in heart valve development. Overall, this suggests that SOX4 and EVI1 may function as potential co-factors together with SOX9 to regulate different subsets of genes during heart valve development.

In the interest of identifying potential co-factors of SOX9 in a relevant cellular context SOX9 AVC and limb peaks were also compared to TWIST1 and SMAD3 AVC ChIP-Seq libraries that were readily available in the lab (Appendix X). TWIST1 and SMAD3 were not identified as potential co-factors of SOX9 by oPOSSUM but this may be due to the short highly degenerate nature of TWIST1 and SMAD3 binding motifs. Previous work suggests that SMAD3 associates with SOX9, recruits P300 and activates SOX9-dependent transcription in chondrocytes (132,133). Several hundred peaks overlap between SOX9 and SMAD3 and this supports that there may be some type of cooperation together in the developing heart valves similar to chondrocytes. Further analysis of co-targeted SOX9 and SMAD3 target genes would necessary to determine the nature of their relationship in gene regulation. Interestingly, TWIST1 is targeted by SOX9 in the AVC data set and it is known that SOX factors often regulate their co-factors. Comparison of the TWIST1 and SOX9 AVC ChIP-Seq libraries demonstrates that the degree of overlap between the TWIST1 and SOX9 AVC peaks was very low (Appendix X) and indicates that they likely do not function as co-factors. To support this, previous work in chondrocytes suggests that TWIST1 functions to suppress cartilage formation by directly inhibiting SOX9 during chondrogenesis (134,135). However, there may be a feedback relationship between TWIST1 and SOX9 in the heart valves. Future studies will be directed at understanding the critical co-factors of SOX9 and how they regulate their target genes during heart valve and limb development.

CHAPTER FOUR: Characterization of the *Sox9fl/fl;VE-Cre* mice

To gain a better understanding of which transcriptional targets of SOX9 are critical for heart valve development, I wanted to generate a mouse line with an endothelial-specific deletion of *Sox9* (specifically deleting SOX9 in the AVC). Subsequently, I wanted to use this endothelial-specific *Sox9* mutant to analyze the transcriptional changes in the AVC following the loss of SOX9 with the ultimate goal of comparing altered genes identified in the SOX9 mutant with the transcriptional target genes identified in the AVC. These comparisions would help to narrow down the potential SOX9 transcriptional targets that are essential to heart valve development.

4.1 SOX9 negative AV mesenchyme cells are absent in *Sox9* mutant valves

To generate an endothelial-specific *Sox9* mutant, I obtained the genetically modified *Sox9fl/fl* mouse from Jax Laboratories (USA) and crossed to the *Vascular Endothelial cadherin (VE) Cre* mouse (a kind gift from Dr. Aly Karsan). In this system, the presence of *Cre recombinase* (*Cre*) in the endothelium will induce the excision of a portion of the *Sox9* coding region by binding flox sites contained in the mutant flox allele. *Sox9* will be deleted by *VE-Cre* in the AVC endocardium and in subsequent AVC mesenchymal cells of heart valves as early as E9.5. Although *Tie2-Cre* is the most-commonly used mouse line for deletion in endothelium and an endothelial-specific knockout of *Sox9* using *Tie2-Cre* has already been generated (46). The *VE-Cre* mouse line was chosen since it has been shown to be more specific to the endothelium than *Tie2-Cre* (136) and was readily available in house. To generate *Sox9flox/flox;VE-Cre* mice, it is important that the female is *Sox9fl/fl* without *Cre* to generate *Sox9* mutants embryos as it has been shown that in some cases *Cre* can be inappropriately activated in the mother causing

excision in all progeny (137). Inappropriate excision of *Sox9* by *Cre* in the developing embryos could lead to abnormalities that are not dependent on the genotype of the embryo. Of note, the *VE-Cre* mouse was made in house by the Karsan lab and is not the commercially available mouse. Dr. A. Chang (during his time in the Karsan lab) evaluated the efficiency of *VE* as a promoter by crossing the *VE-cadherin*-tTA (VEtTA) strain (a gift from L. Benjamin, Harvard Medical School) with *TetOS-lacZ* mouse (a gift from D. Dumont, Samuel Lunenfeld Research Institute) and performing LacZ staining on E10.5 and E11.5 hearts following removal of doxycycline the previous day (see Figure 2-2, with permission granted by Dr. A Chang). When doxycycline is removed it will activate β-galasctosidase and allows it to be expressed. Therefore, any cell that has *VE* will express β-galasctosidase and can be visualized by LacZ staining, which turns cells blue. LacZ staining indicates that there is efficient recombination using the *VE* promoter in the E10.5 and E11.5 AVC mesenchyme cells however some unmarked cells were still present. Although it was not the exact same *VE-Cre* mouse, it demonstrates that *VE* as promoter can drive efficient recombination within the developing heart valves. However, it is essential to test *Cre* efficiency in every mouse line as there can be variability in efficiency between lines.

To evaluate the efficiency of *Sox9* deletion in *Sox9fl/fl;VE-Cre/+* heart valves, embryonic hearts were collected at E9.5, E10.5 and E12.5 and examined using immunofluorescence with an antibody specific for SOX9 (Figure 4-1). As a note, the SOX9 antibody used for immunofluorescence is exactly the same one used for ChIP-Seq experiments. Very little differences between *Sox9fl/fl;+/+* (WT) and *Sox9fl/fl;VE-Cre/+* (*Sox9* mutant) were detected at E9.5 and E10.5 (Figure 4-1A-H). At E12.5, *Sox9* mutant AVC cushions were reduced in size

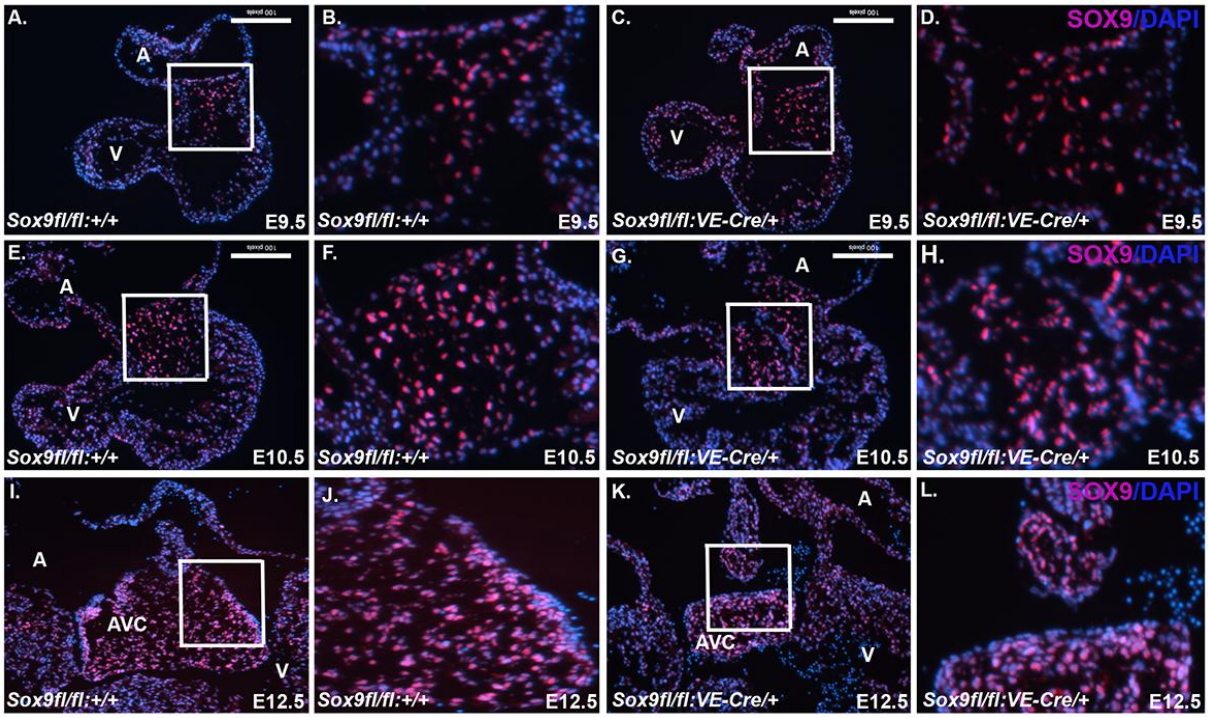

Figure 4-1 SOX9 is not lost in the developing heart valves of the *Sox9fl/fl;VE-Cre* mice despite valve abnormalities. Immunofluorescence for SOX9 on WT (**A, B, E, F, I, J,** *Sox9fl/fl;+/+)* and *Sox9* cKO (**C, D, G, H, K, L,** *Sox9fl/fl;VE-Cre)* on E9.5 (**A-D**), E10.5 (**E-H**) and E12.5 (**I-L**) hearts.The AVC is highlighted by the white box and magnified in the following panel.

when compared to WT (Figure 4-1I-L). Additionally, the atrial septum of the *Sox9* mutant had not fused with the AVC whereas the WT septum had already fused (Figure 4-1I-L). At all of the embryonic stages examined SOX9 negative mesenchyme could not be detected suggesting that either *Sox9* was not being deleted properly or that *Sox9* negative mesenchymal cells are lost. Cell counts showed 50% fewer SOX9 positive cells in E12.5 *Sox9fl/fl;VE-Cre/+* AVC cushions compared to WT confirming the reduced number in overall SOX9 positive cells (Figure 4-2A) Since the *Sox9* mutant AVC is smaller in size, the numbers of SOX9 positive cells were compared to DAPI (marks nuclei) positive cells to adjust for decrease cell numbers and demonstrated that *Sox9* mutant AVCs had 28% less SOX9 positive cells over DAPI (Figure 4-2B).

To confirm that *Sox9* transcript was also still present in the *Sox9* mutant valves, I examined the *Sox9* transcript levels in the AVC relative to other regions of the heart using qRT-PCR on WT, double heterozygous (*Sox9fl/+;VEC/+)* and *Sox9* mutant AVC, atria (A) and ventricles (V) using primers specific to the flox region of *Sox9* (Figure 4-2C). *Sox9* mRNA levels are enriched in the WT AVC relative to other regions of the heart. Thus for this analysis, WT atria was set to 1 to show *Sox9* enrichment in the AVC. As expected *Sox9* was 9 fold higher in the WT AVC compared to the WT atria (Figure 4-2C). The double heterozygous and *Sox9* mutant AVCs also had highly enriched levels of *Sox9* transcript (Figure 4-2C). This data indicates that *Sox9* mRNA was not significantly reduced in the *Sox9* mutant AVC. The increased levels of *Sox9* in the double heterozygous and *Sox9* mutant atria are likely due to AVC or epicardial contamination that occurred during manual dissections. However, it could indicate that *Sox9* transcript levels have reduced enrichment in the double heterozygous and *Sox9* mutant AVC (Figure 4-2C) although immunofluorescence data does not support this.

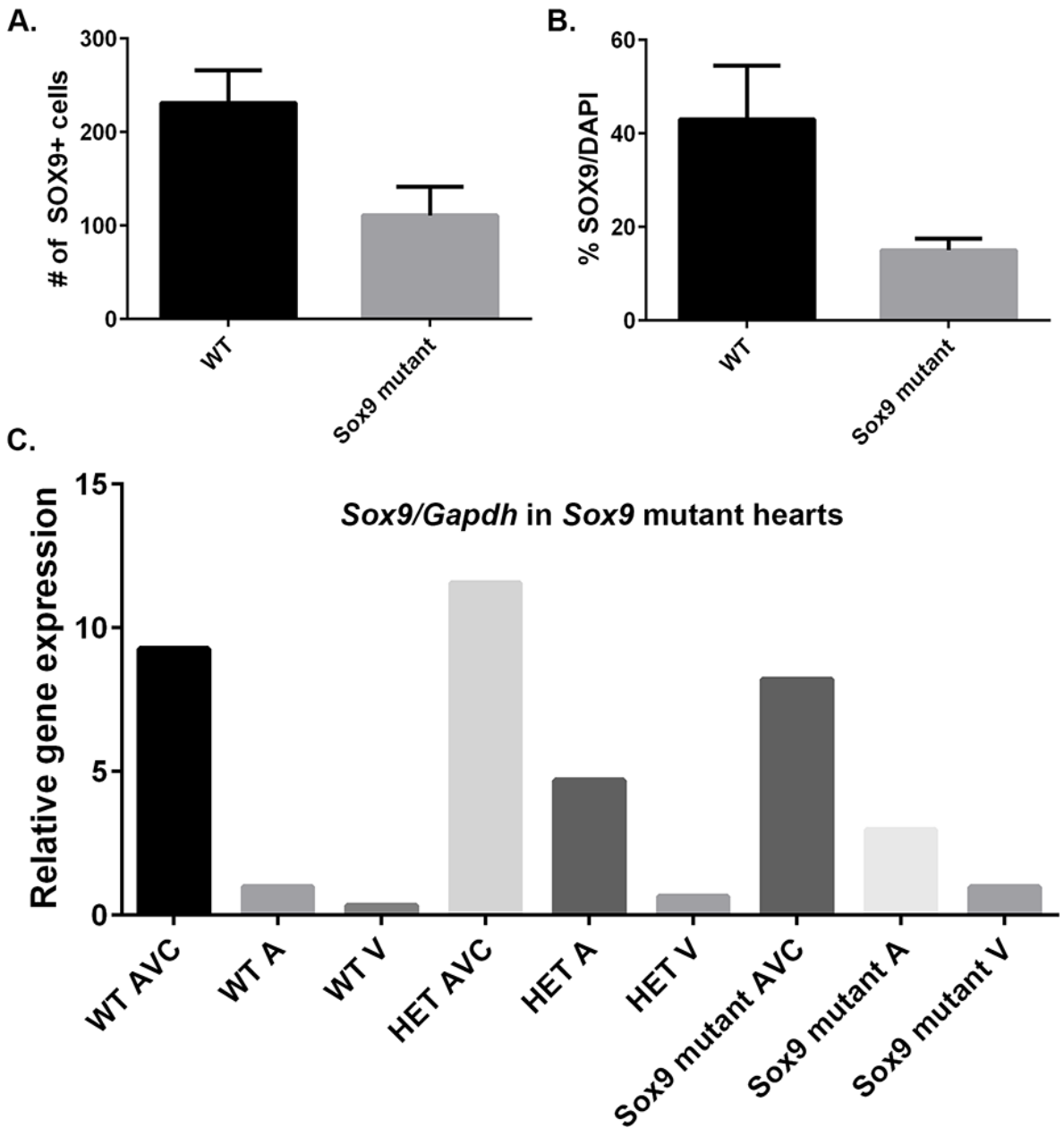

Figure 4-2 *Sox9fl/fl;VE-Cre* mice have reduced numbers of SOX9+ valve cells and decreased total valve cell numbers. Cell counts of SOX9+ cells (**A.**) and SOX9+ cells relative to DAPI (**B.**) on WT (*Sox9fl/fl;+/+*) and *Sox9* mutant (*Sox9fl/fl;VE-Cre*) valves. **C.** A representative Taqman qRT-PCR for *Sox9* relative to *Gapdh* on AVC (valves), A (atria), V (ventricles) for WT, Heterozygous (*Sox9fl/+;VE-Cre*) and *Sox9* mutant hearts.

It is intriguing that SOX9 negative mesenchyme cells could not be identified in *Sox9* mutant AVCs and there are a number of possible reasons for this phenomenon. One potential explanation for the absence of SOX9 negative cells in the AVC could be that other SOX9 positive mesenchymal cells are migrating into the mutant AVC to assist recovery from the loss of the normal AVC mesenchyme cells. In the developing heart there are several other SOX9 positive populations of cells such as the mesenchymal caps of the atrial septum and ventricular septum and the epicardial cells. Of note, the neural crest cells that migrate into the OFT valves are also SOX9 positive. Immunofluorescence for SOX9 on the WT E12.5 heart easily identified the other SOX9 positive cell populations of the septal caps and epicardium (Figure 4-3, arrowheads). Another potential explanantion for the lack of SOX9 negative mesenchyme may be due to the inefficiency of the *VE-Cre* system and future work should be focussed on performing lineage tracing with this mouse line.

4.2 SOX9 is maintained at later stages of heart valve development in *Sox9* mutants

SOX9 protein has been demonstrated to be a long lived protein in limb development (138). For example, it has been shown that SOX9 protein is maintained in hypertrophic chondrocytes even though there is no *Sox9* transcript in these cells. SOX9 protein is lost once cells become terminally differentiated chondrocytes (138). To determine if SOX9 protein is eventually lost in the *Sox9* mutant heart valves, later stages (E13.5 and E16.5) of heart valve development were examined (Figure 4-4). In E13.5 and E16.5 hearts SOX9 protein was still present in the AV valves but there were noticeable changes in the valve phenotype at E16.5 such as changes in size and structure in valve leaflets. This data indicates that *Sox9* deletion by *VE-Cre* is having an effect on the heart valve development (Figure 4-4E-H). However in the majority of cases the

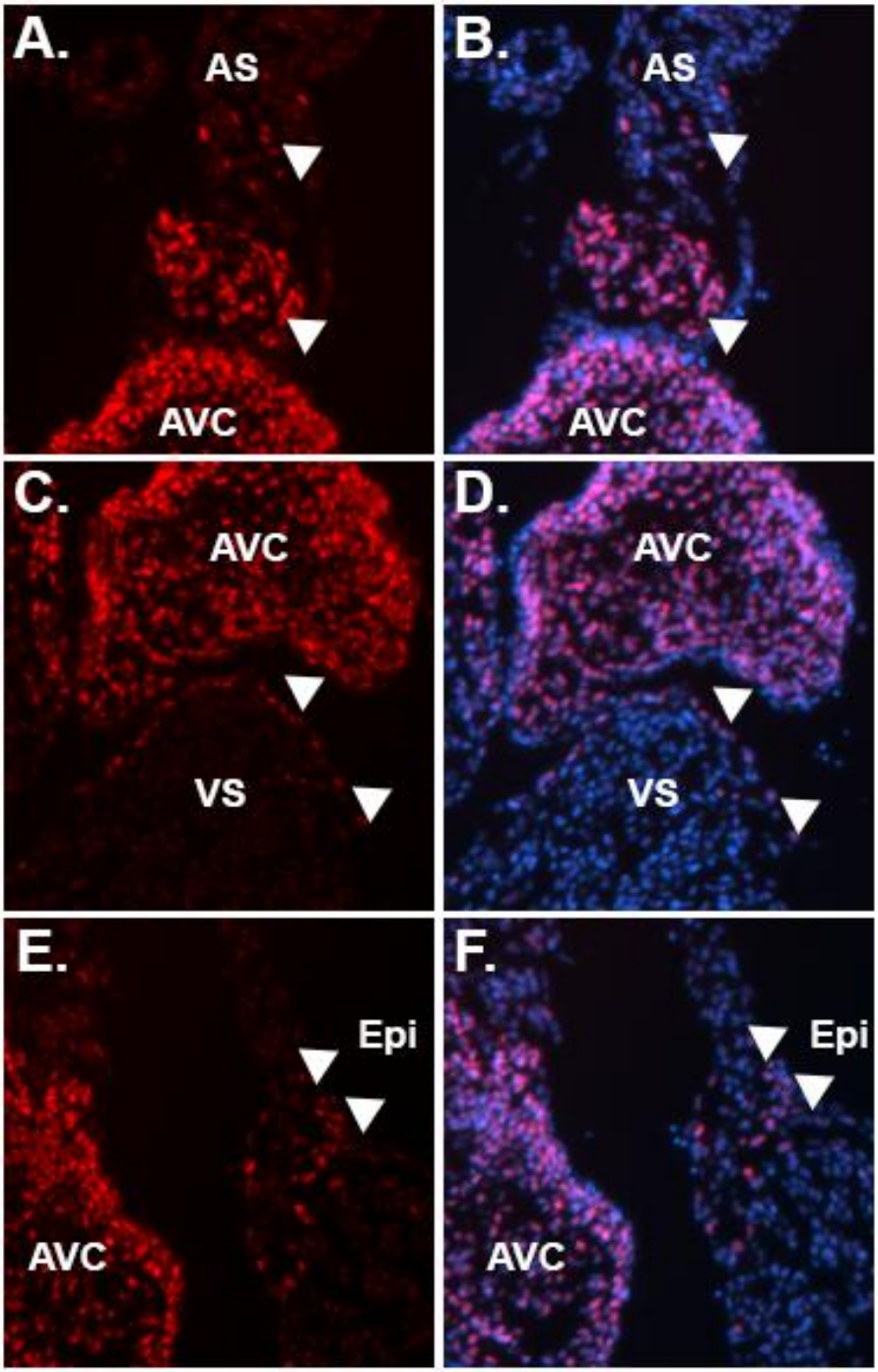

Figure 4-3 Additional sources of SOX9+ mesenchyme found in the developing heart at E12.5. **(A, B)** The mesenchymal cap of the atrial septum (AS), **(C,D)** the mesenchymal cells on the surface of the ventricular septum (VS), and **(E,F)** the epicardial layer on the outside of the heart. SOX9 is labelled in red and DAPI in blue.

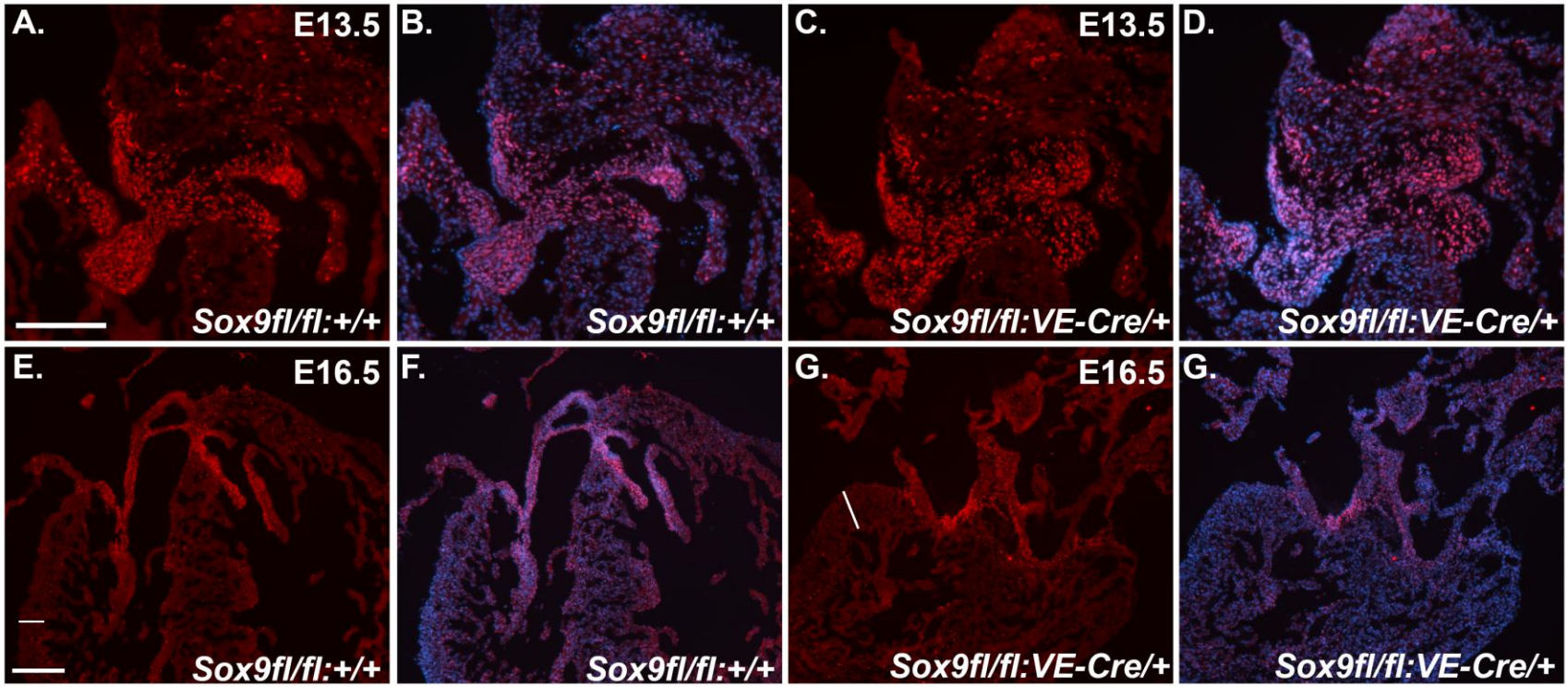

Figure 4-4 SOX9 positive cells can still be detected at later stages of valve development in *Sox9fl/fl;VE-Cre* mice. The majority of *Sox9fl/fl;VE-Cre* mice are not embryonic lethal. Immunofluorescence for SOX9 on WT (**A, B, E, F)** and *Sox9* cKO (**C, D, G, H**) hearts at E13.5(**A-D**) and E16.5 (**E-H**).

valve phenotype was not severe enough to be embryonic lethal and *Sox9* mutant mice survive well into adulthood (Table 4-1). In addition to the valve phenotype, the myocardium of the ventricles appear to be thickened in the *Sox9* mutants compared to WT. To see if the observed phenotypes were transient in the E16.5 *Sox9* mutant hearts, *Sox9* mutant mice were taken at birth to examine their hearts for physical differences (Figure 4-5). Similar to the E16.5 hearts, there was increased thickness in the ventricular myocardium and decreased chamber size in the *Sox9* mutant hearts compared to WT (Figure 4-5, arrowheads). Additionally, the *Sox9* mutant ventricular myocardium looks more compact with less open spaces within the heart and less trabeculated than its WT counterparts. Interestingly, the phenotype in the ventricular myocardium of *Sox9* mutant hearts is similar to cardiac hypertrophy. Cardiac hypertrophy can occur in patients with hypertension or heart valve stenosis and these conditions lead to a thickening of the ventricular myocardium and reduced ventricular chamber size (reviewed in (139)). It is possible that the increased ventricular myocardial thickness in *Sox9* mutant hearts could be indicative of cardiac hypertrophy due to improper heart valve function.

4.3 Adult *Sox9* mutants have slightly thickened valves leaflets

Since the ventricular phenotypes in the *Sox9* mutants at birth were similar to hypertrophy, mice were aged until approximately to one year and taken for histological analyses to examine the heart. Hematoxylin and Eosin staining of the adult *Sox9* mutant AV heart valves reveals *Sox9* mutants have a slight thickening at the base of the leaflets (Figure 4-6, arrows). Although this thickening is slight, even minor changes in valve structure and composition can lead to the improper function of the heart valves, such as floppy valves that regurgitate or stiff valves that

Table 4-1 Genotypes from *Sox9fl/fl;*+/+ and *Sox9fl/+;VE-Cre/*+ mouse crosses to generate SOX9 mutant embryos

Time point	WT (*Sox9fl/+;*+/+ & *Sox9fl/fl;*+/+)	HET (*Sox9fl/+;VE-Cre/*+)	SOX9 cKO (*Sox9fl/fl;VE-Cre/*+)	# of litters
E9.5	4	3	2	1
E10.5	5	1	3	1
E12.5	19	6	10	4
E13.5	5	1	2	1
E16.5	2	1	4	1
Adult	42	24	13	14

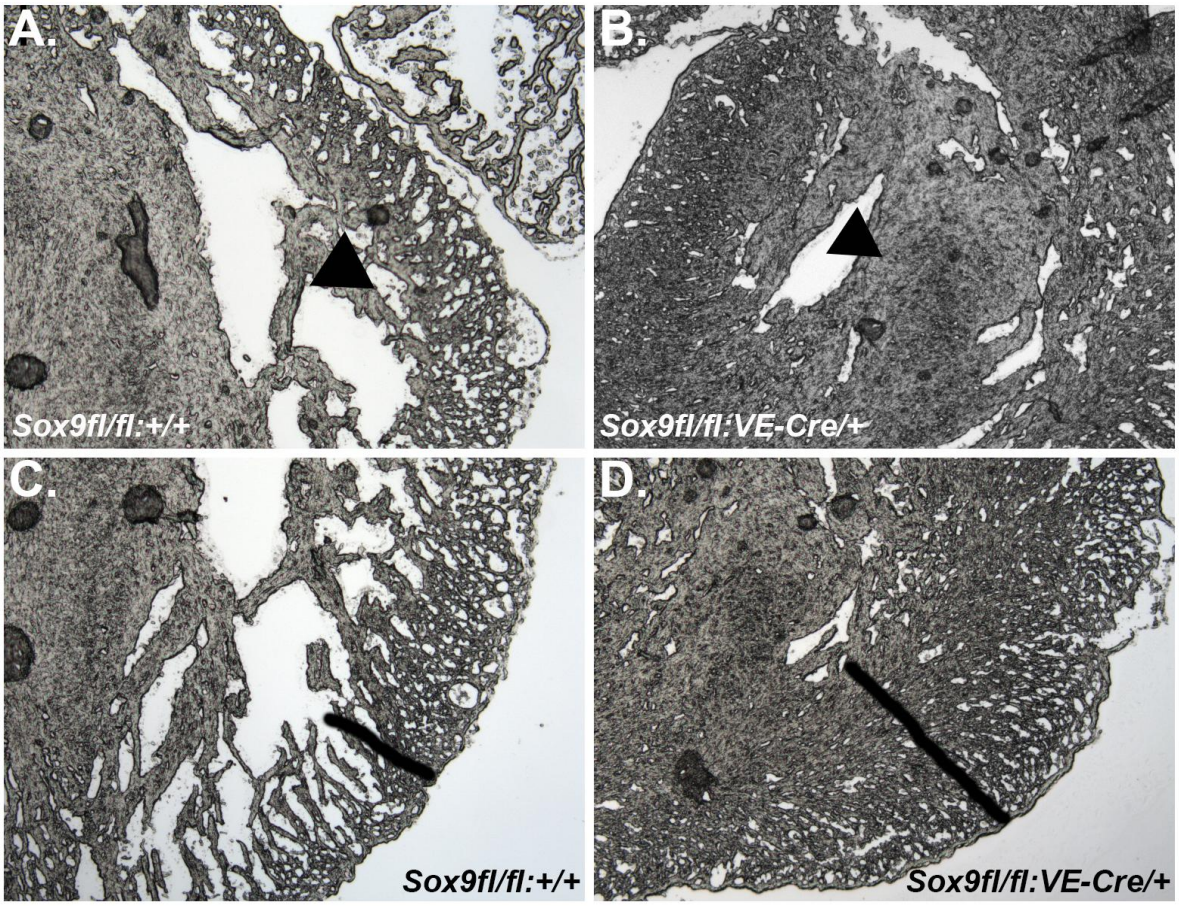

Figure 4-5 Ventricular abnormalities in the *Sox9fl/fl;VE-Cre* postnatal mice hearts when compared to WT (*Sox9fl/fl;*+/+). **(A, B)** Highlights the differences in chamber size in *Sox9fl/fl;VE-Cre* versus WT (arrowheads). **(C, D)** Highlights differences in ventricular thickness between *Sox9fl/fl;VE-Cre/+* and WT (line). N=2.

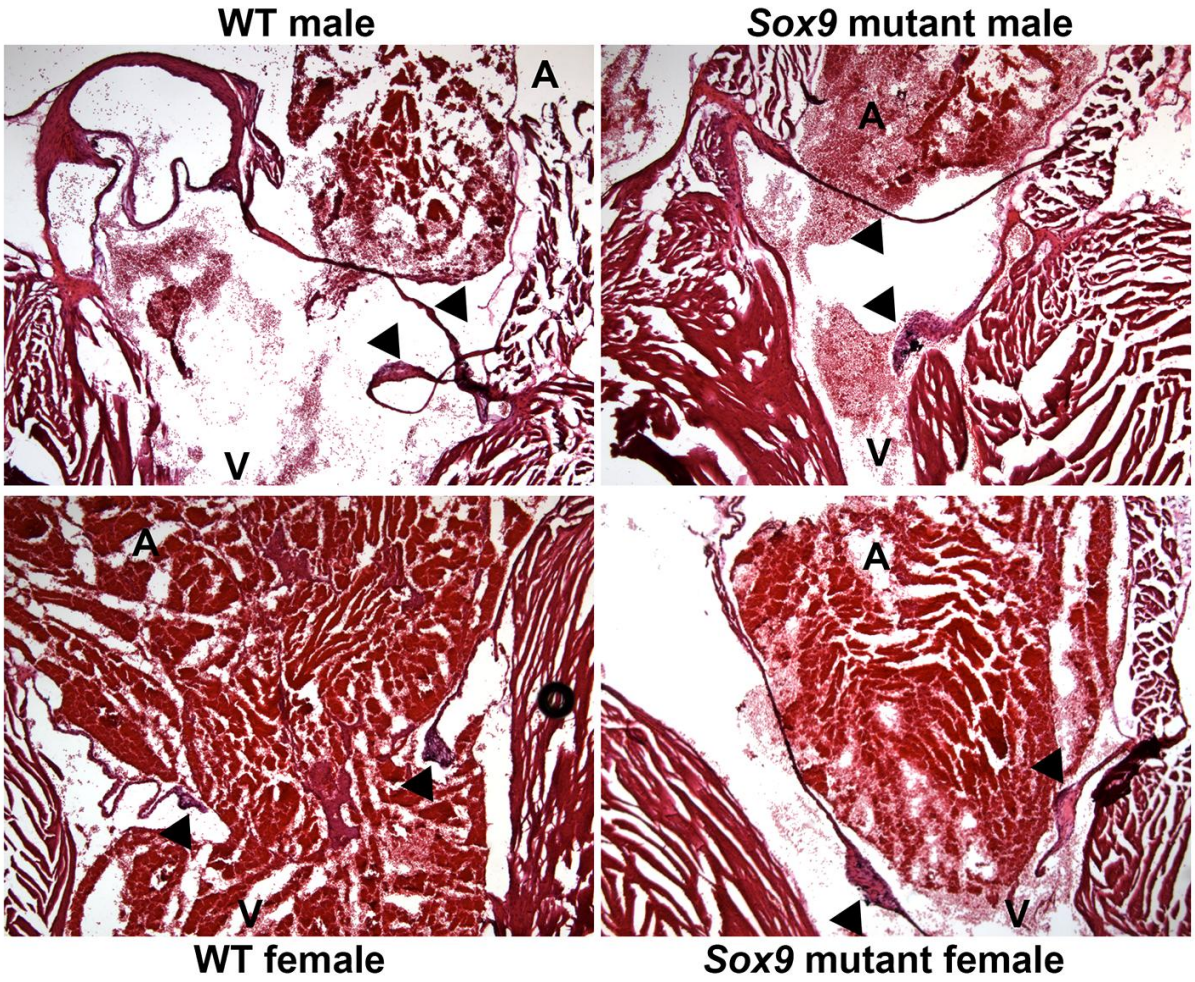

Figure 4-6 Hematoxylin and Eosin staining of 10 month old adult WT and *Sox9fl/fl;VE-Cre* AV heart valves. Arrows indicate AV heart valves. A=atria, V=ventricles. N=2.

cause stenosis. Currently, this analysis was performed on two sets of hearts that gives an n of 2 for each genotype and to obtain a significant difference in valve thickness further animals will need to be examined. Additional mice are being aged to one year for analysis. Surprisingly, there were no overt differences in the ventricular myocardium thickness or in the architecture of the ventricular myocardium of the adult *Sox9* mutant hearts examined to date. However when the hearts were taken for dissection, the *Sox9* mutant female heart was noticeably bigger in size compared to her WT littermate (data not shown). Hypertrophic hearts often have an increase in total size of the heart and it is possible that there are increases in myocardial thickness not seen in the images taken of the *Sox9* mutant female heart. Further analyses are required to establish if there are similar changes in the *Sox9* mutant adult ventricular myocardium as seen in the postnatal mutant hearts. Overall, *Sox9* mutant hearts have a very mild phenotype on heart valve development and may be a useful model to study heart valve disease. However, it will be necessary to determine if *Sox9* mutant mice are susceptible to or already valve disease by testing heart function and blood flow as well as additional staining procedures to examine differences in heart valve composition and structure.

CHAPTER FIVE: Characterization and analysis of the *Sox9fl/fl;Tie2-Cre* mice

Given that the *Sox9fl/fl;VE-Cre* mutant mice had no detectable SOX9 negative mesenchyme in the AVC it was not an efficient system to examine the differences in SOX9 transcriptional changes upon loss of *Sox9*. Since our goal is to parse out critical targets of SOX9 in the developing heart by comparing the transcriptional changes identified between WT and *Sox9*-deficient heart valves to the SOX9 AVC ChIP-Seq data, it was necessary to find another system to delete SOX9 in the embryonic heart valves. Previous work by Lincoln *et al* had shown that endothelial-specific deletion of *Sox9* using *Tie2-Cre* where both endothelial cells and mesenchymal cells of the AVC cushions fail to express SOX9 are embryonic lethal (46). *Tie2-Cre* has been previously shown to specifically label epithelial cells and not cardiomyocytes, epicardium or distal OFT mesenchyme, however it does have some non-specific labeling in mesoderm (124,140). *Sox9fl/fl;Tie2-Cre* mice die during embryogenesis as a result of heart valve defects including hypoplastic cardiac cushions, reduced mesenchyme proliferation and altered ECM composition (46). Therefore, I decided to take advantage of this previously published mouse model with the intent of analyzing transcriptional changes that occur upon loss of *Sox9* in the developing valves. In order to reduce confusion between mutant mouse models *Sox9fl/fl;Tie2-Cre* mice will always be referred to as the *Sox9* cKO whereas the *Sox9fl/fl;VE-Cre* mice will be called *Sox9* mutants.

5.1 SOX9 negative mesenchyme was detected as early as E10.5 in the AVC

To ensure efficient deletion of *Sox9* by *Tie2-Cre* and to determine if SOX9 negative mesenchyme can be detected in the AVC, immunofluorescence using an antibody specific for

SOX9 was performed on *Sox9fl/fl* (WT) and *Sox9fl/fl;Tie2-Cre* (*Sox9* cKO) hearts starting at E9.5 (Figure 5-1). At E9.5, SOX9 was still detected in AVC mesenchyme of the *Sox9* cKO (Figure 5-1 C, D) but by E10.5 and E11.5 SOX9 negative AVC mesenchyme was identified in *Sox9* cKO valves (Figure 5-1 G, H, K, L, arrowheads). However, some SOX9 positive mesenchyme cells were observed in the E11.5 AVC (Figure 5-1, asterisk) suggesting that *Sox9* deletion by *Tie2-Cre* was not complete. No overt morphological differences between the E9.5 and E10.5 WT and *Sox9* cKO hearts were observed but there was a slight decrease in AVC size between WT and *Sox9* cKO by E11.5 (Figure 5-1).

Since we wanted to match the embryonic time point chosen for SOX9 E12.5 AVC ChIP-Seq to the transcriptome analysis of *Sox9*-deficient valves, I wanted to fully characterize the E12.5 *Sox9* cKO AVC prior to library generation (Figure 5-2). Immunofluorescence for SOX9 coupled with confocal microscopy revealed that the E12.5 *Sox9* cKO valves were significantly reduced in size and overall SOX9 positive mesenchyme in the AVC was also reduced when compared to WT (Figure 5-2A, B). *Sox9* cKO hearts had several additional defects including decreased thickness of the ventricular myocardium and delayed septal fusion with the AVC (Figure 5-2A). Illustrating the specificity of *Sox9* deletion in the *Tie2-Cre* lineage, SOX9 expression was lost in the AVC, whereas the epicardial cells that descend from a separate lineage still express SOX9 (Figure 5-2A, B). To confirm the decreased numbers of SOX9 positive mesenchyme cells in the AVC of the *Sox9* cKO hearts, the total numbers of SOX9 positive mesenchyme cells were counted in the AVC for WT and *Sox9* cKO (Figure 5-2C). *Sox9* cKO valves had approximately 65% less SOX9 positive cells than the WT (Figure 5-2C). Due to the extreme compaction of the nuclei in the *Sox9* cKO AVC (Figure5-2A, B), DAPI nuclei counts could not be performed since it was extremely difficult to separate nuclei apart in the

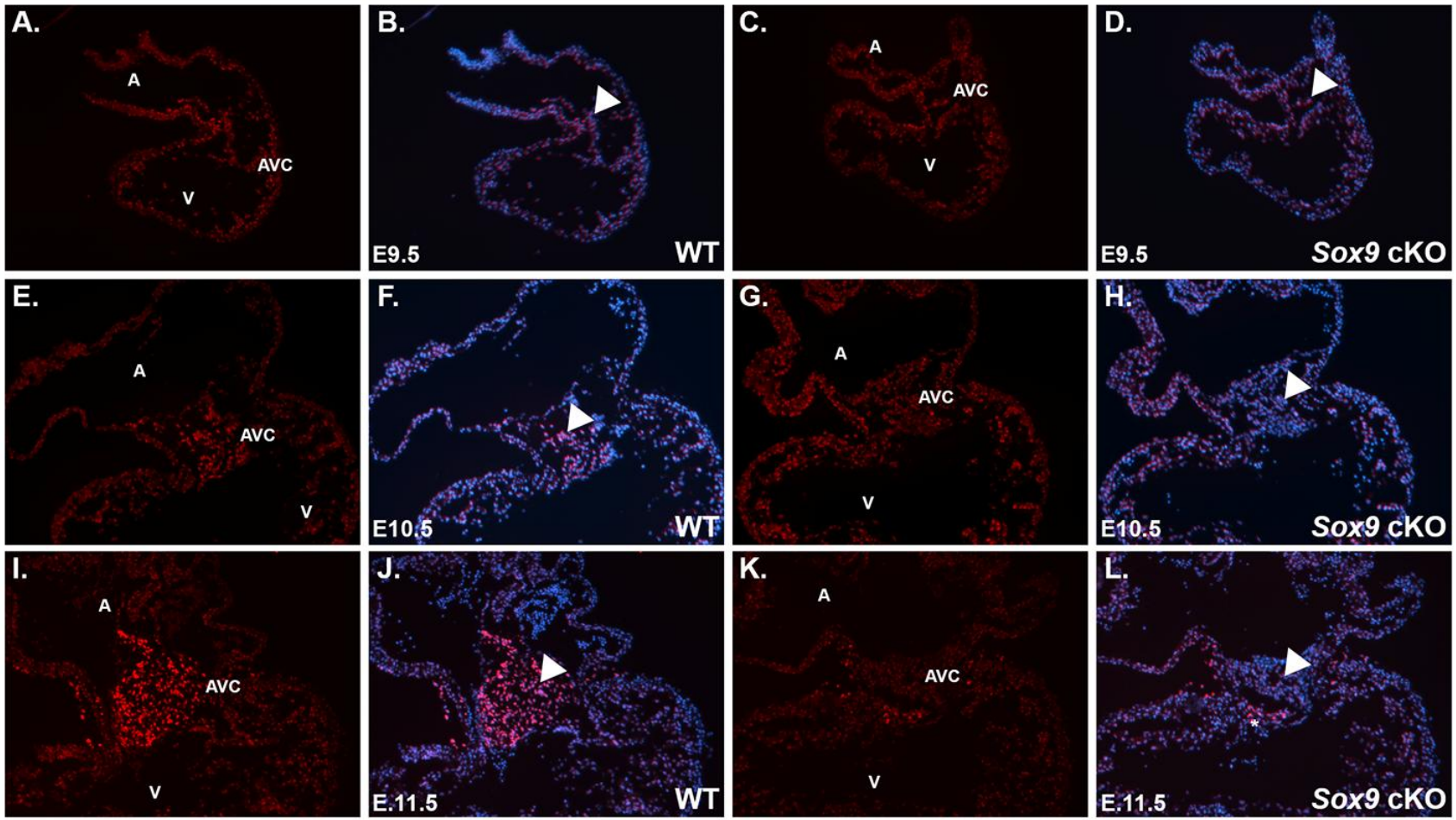

Figure 5-1 SOX9 deletion occurs in the *Sox9fl/fl;Tie2-Cre* heart valves as early as E10.5 in the mouse. Immunofluoresence on the WT (A, B, E, F, I, J) and *Sox9* cKO (C, D, G, H, K, L) hearts for SOX9 at E9.5 (A-D), E10.5 (E-H), and E11.5 (I-L). Panels A, C, E, G, I, K are SOX9 (red) staining only. Panels B, D, F, H, J, L are merged images with SOX9 (red) and DAPI (blue) staining. Images were captured on a Zeiss Axioplan 2 microscope.

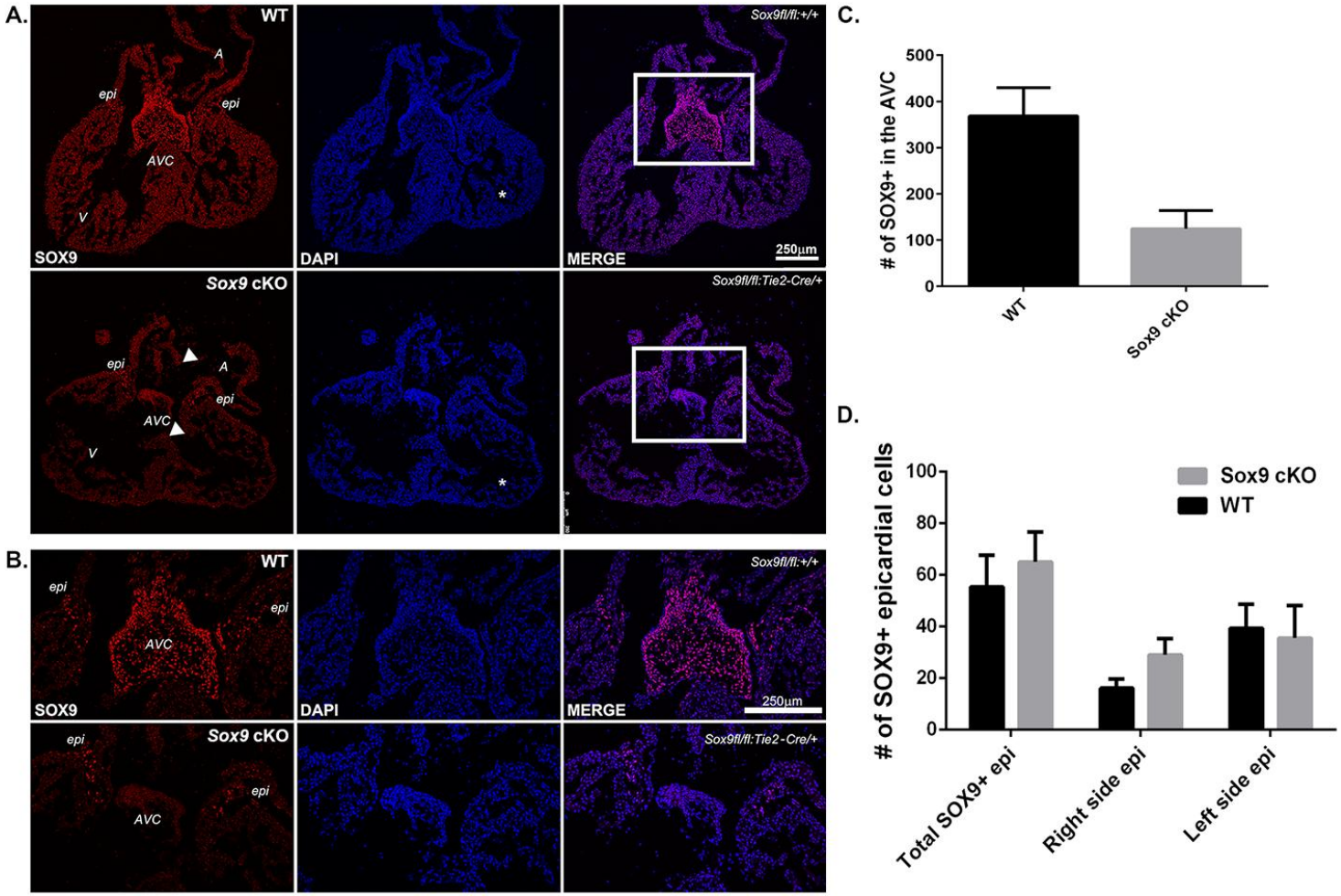

Figure 5-2 The loss of SOX9 in the *Sox9fl/fl;Tie2-Cre* E12.5 heart valves leads to major valve abnormalities and reduced valve cell numbers. A. Immunofluorescence for SOX9 on E12.5 WT (top panel) and *Sox9* cKO (bottom panel) hearts**. B.** An inset of part A highlighting the valve region of the heart. Average valve cell counts (**C.**) and epicardial cell counts at the AV junction (**D.**) on WT and *Sox9* cKO hearts.

Sox9 cKO AVC. There appeared to be more epicardial cells in the AVC region of the *Sox9* cKO than in WT based on immunofluorescence for SOX9 and suggests that eipcardial cells could be migrating into the *Sox9* cKO AVC or that these cells are not migrating out over the surface of the heart as they should be at this time point. However, epicardial lineage tracing would be necessary to confirm that epicardial cells are present within the AVC. To examine changes in epicardial cell numbers in the *Sox9* cKO AVC, SOX9 positive cells were counted on each side of the heart and totaled up (Figure 5-2D). Overall, there were no significant differences but there was a slight trend towards an increase in total epicardial cell numbers in the *Sox9* cKO AVC region particularly on the right side of the heart (Figure 5-2D). This may indicate that there is a slight delay in epicardial cell migration on the right side of the heart of the *Sox9* cKO however further studies are required to show this more definitively.

5.2 Deletion of *Sox9* was variable in the *Sox9* cKO heart valves

As expected from the Lincoln *et al* study, deletion of *Sox9* by *Tie2-Cre* leads to death in the majority of embryos by or just after E13.5 due to severely hypoplastic and malformed AV valves (Figure 5-3, Table 5-1). The *Sox9* cKO valves are severely reduced in size compared to WT and the blood begins pooling and clotting within the chambers of the heart (Figure 5-3). Of note, the efficiency of *Sox9* deletion in the AVC by *Tie2-Cre* is variable. Immunofluorescence for SOX9 was performed on three separate *Sox9* cKO hearts to demonstrate the variability of *Sox9* deletion by *Tie2-Cre* (Figure 5-4). Some *Sox9* cKO valves had 90-95% *Sox9* deletion (Figure 5-4A, B), others had 45-50% *Sox9* deletion (Figure 5-4C, D) and some even had only 10-15% *Sox9* deletion (Figure 5-4E, F). This illustrates that complete deletion of *Sox9* was not always achieved in the *Sox9* cKO AVC and therefore demonstrates a major caveat in pooling

Table 5-1 Genotypes from *Sox9fl/fl;*+/+ and *Sox9fl/+;Tie2-Cre/*+ mouse crosses suggest that *Sox9* cKO embryos die after E13.5.

Time point	WT (*Sox9fl/+;+/+* & *Sox9fl/fl;+/+*)	HET (*Sox9fl/+;Tie2-Cre/+*)	SOX9 cKO (*Sox9fl/fl;Tie2-Cre/+*)	# of litters
E9.5	6	2	2	1
E10.5	5	2	1	1
E11.5	1	3	3	1
E12.5	96	65	55	30
E13.5	7	6	2	2
E16.5	5	1	0	1
Adult	19	14	1*	7

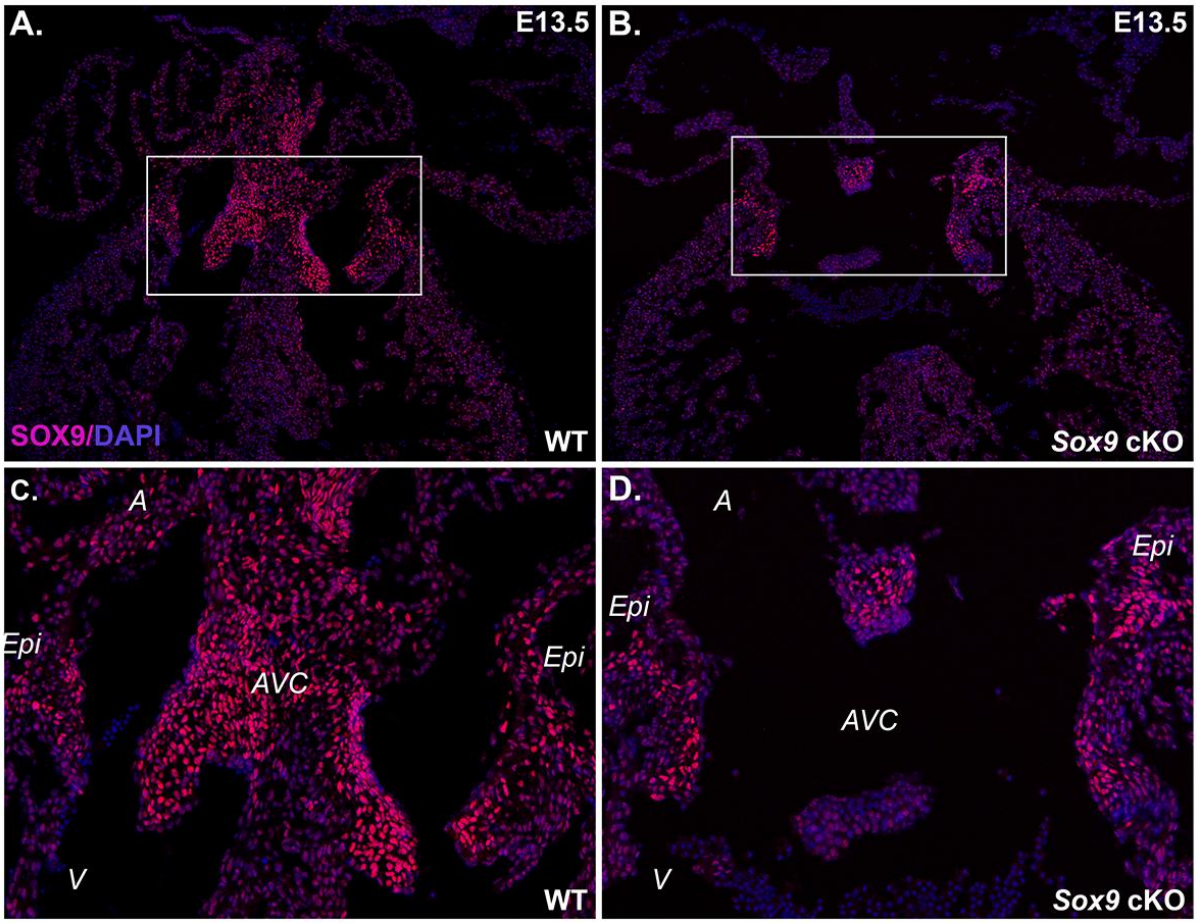

Figure 5-3 The absence of SOX9 in the *Sox9fl/fl;Tie2-Cre* heart valves is embryonic lethal between E13.5-14.5. Immunofluorescence for SOX9 on E12.5 WT (**A, C**) and *Sox9* cKO (**B, D**) hearts. Panels C and D are an inset of A and B highlighting the valve region of the heart.

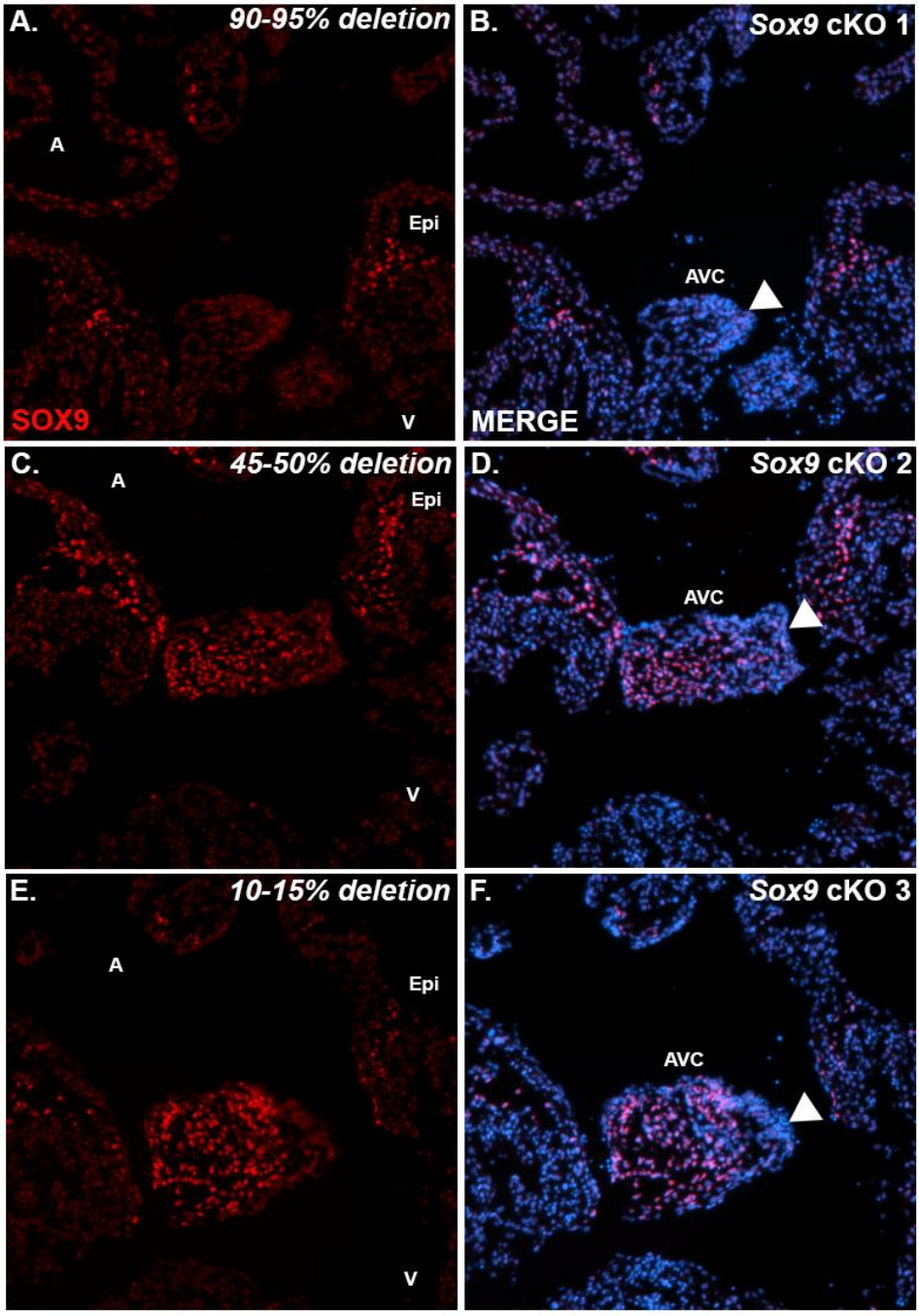

Figure 5-4 *Sox9* deletion by *Tie2-Cre* is extremely variable in the *Sox9* cKO heart valves. Immunofluorescence for SOX9 on three different E12.5 *Sox9* cKO hearts illustrating 90-95% deletion (**A, B**), 45-50% deletion (**C, D**) and 10-15% deletion (**E, F**). Panels A, C and E are SOX9 staining only (red) and panels B, D, and F are the merged images with DAPI (blue).

Sox9 cKO hearts for any type of future analysis. This variability in *Sox9* deletion was further confirmed at the transcript level using Taqman assays for *Sox9* relative to *Gapdh* on WT and *Sox9* cKO AVCs with more or less deletion of *Sox9*, compared to atria and ventricles for each genotype (Figure 5-5). Atria were set to 1 for each genotype to demonstrate the lack of *Sox9* enrichment in the *Sox9* cKO AVC compared to WT. This method could be used to identify *Sox9* cKO AVCs with more or less efficient deletion of *Sox9* and separate them out for future analyses.

5.3 Proliferation defects in the *Sox9* cKO valves

Similar to Lincoln *et al*.(46), a decrease in proliferation was observed in *Sox9* cKO AVCs when compared to WT using immunofluorescence with an antibody specific to phospho histone H3 (pHH3, a marker of mitosis) (Figure 5-6). Interestingly, numerous SOX9 conditional mutants have defects in proliferation and decreased cell numbers in the mutant tissue (46,57-59). Additionally, in rat mesenchymal stem cells, knockdown of SOX9 caused reduced proliferation and increased levels and stability of cyclin D1 (60). Consequently, cyclin D1 protein was investigated in the WT and *Sox9* cKO valves by immunofluorescence (Figure 5-7A). Similar to rat mesenchymal stem cells, cyclin D1 protein was maintained in the cytoplasm in a subset of the *Sox9* cKO AVC mesenchyme (Figure 5-7A, arrows). Several cyclin D1 positive cells were also observed in the WT (Figure 5-7A, arrows) however fewer cells were detected and not found in a specific pattern as seen in the *Sox9* cKO AVC. *Ccdn1* (cyclin D1) transcript levels were measured between WT and *Sox9* cKO AVC using Taqman assays (Figure 5-7B). Surprisingly, *Ccdn1* mRNA levels were slightly reduced in the *Sox9* cKO AVC when compared to WT although the levels were not significant (Figure 5-7B). Although cyclin D1 was not a direct

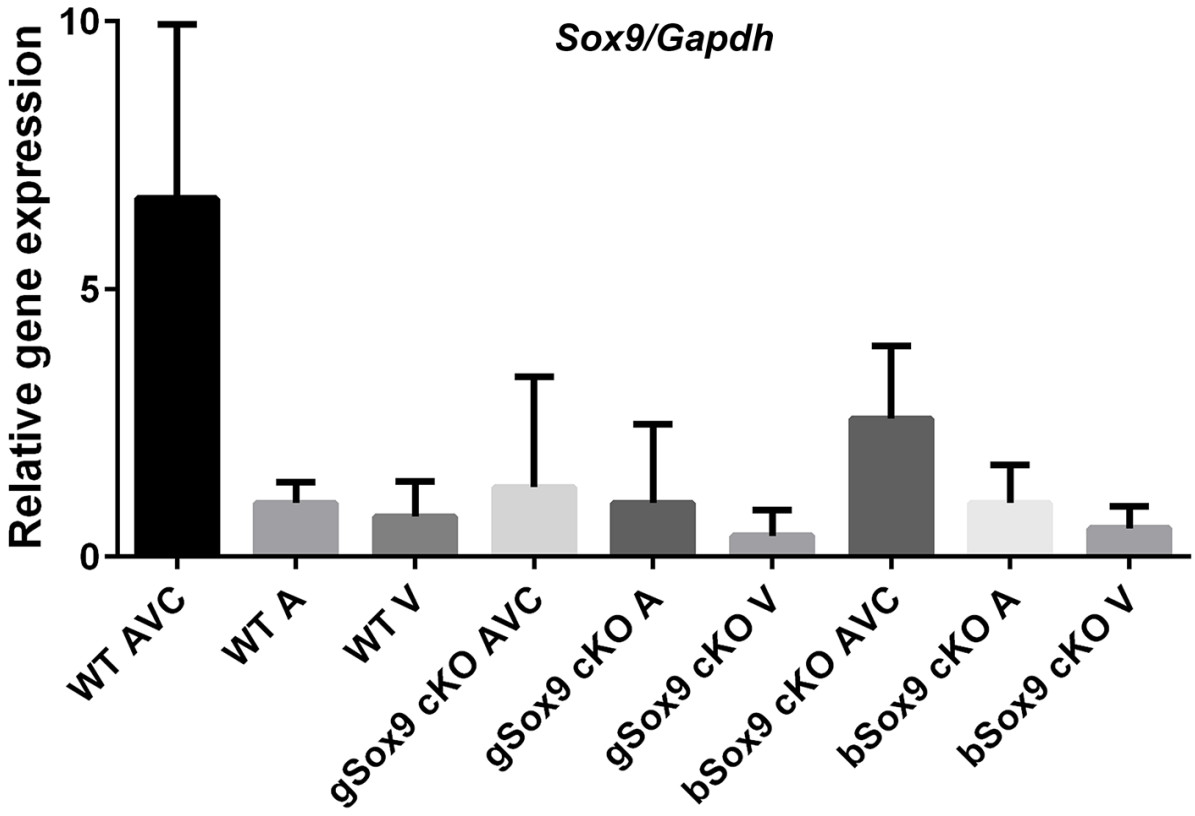

Figure 5-5 Verification of *Sox9* deletion, by *Tie2-Cre*, in the *Sox9* cKO heart valves. *Sox9* cKOs were grouped by the level of *Sox9* deletion (more complete deletion (g) versus incomplete deletion (b)). Taqman assays for *Sox9* and *Gapdh* were used for this analysis. Atria were set to 1 to determine the level of SOX9 enrichment (WT) or loss (*Sox9* cKO). An N of 12 or greater for AVC and A and an n of 8 for the ventricles (V).

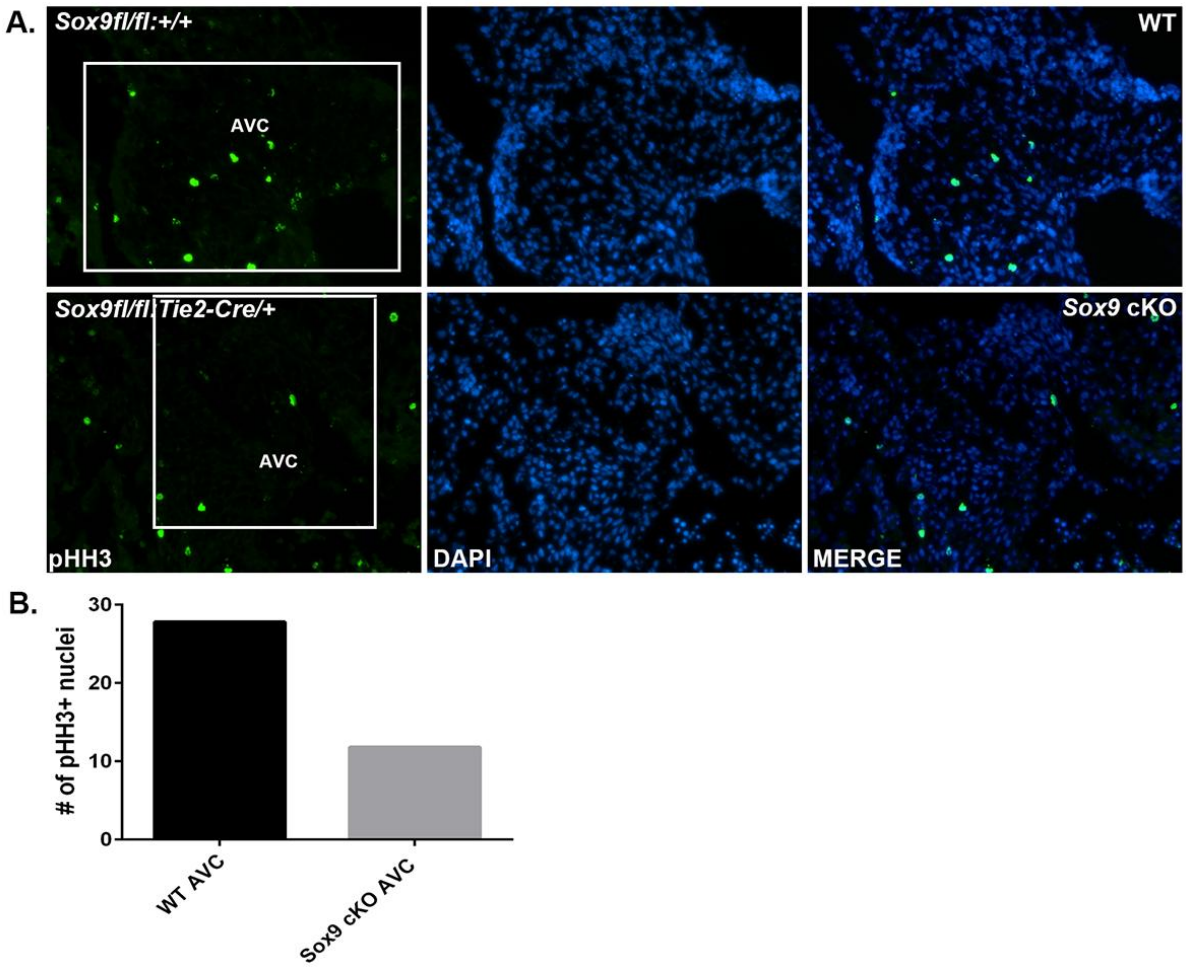

Figure 5-6 Proliferation is reduced in the *Sox9* cKO valves compared to WT. A. Immunofluorescence on WT (top panels) and *Sox9* cKO (bottom panels) hearts for phospho histone H3 (a marker of mitosis, green). **B**. Counts of pHH3 positive cells on WT and *Sox9* cKO valve regions that are highlighted by a boxed in region in part A.

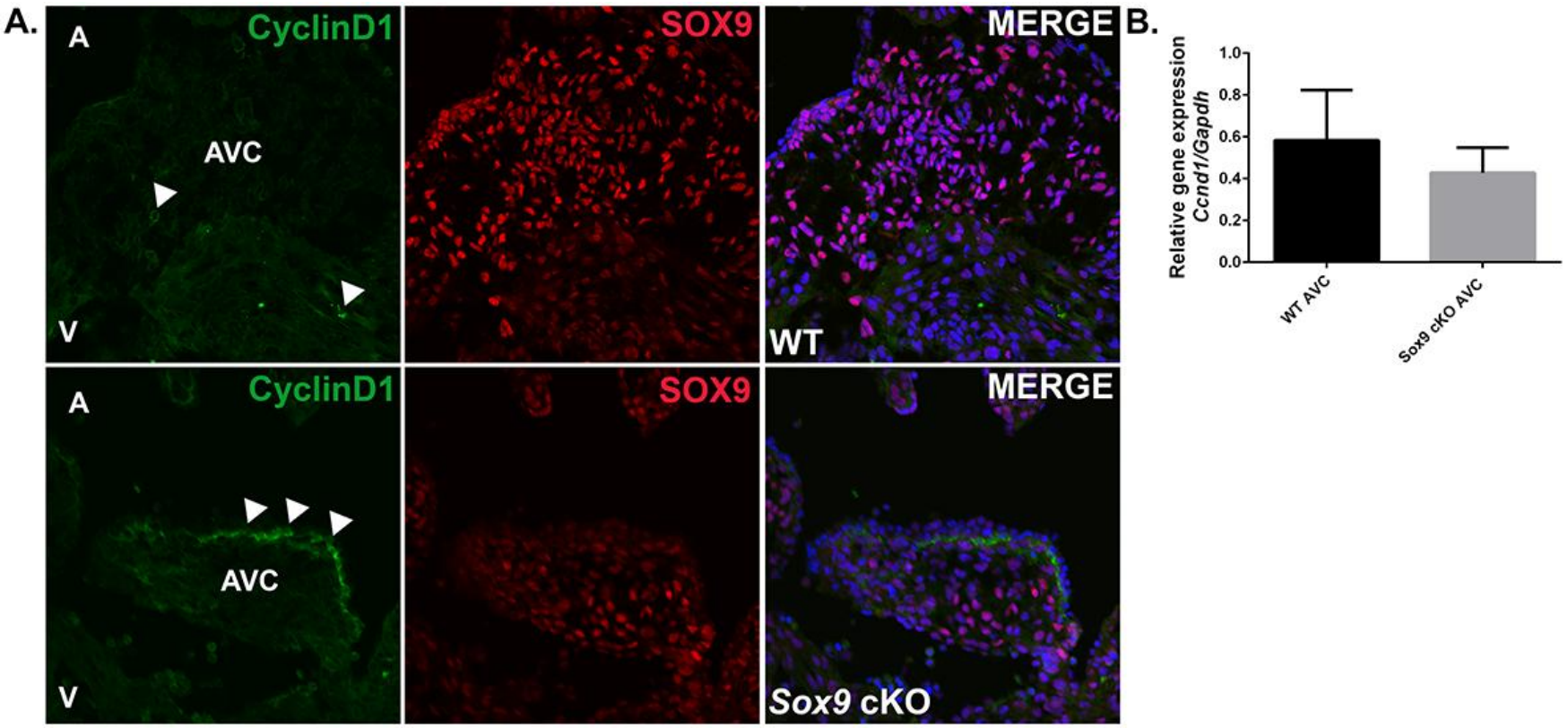

Figure 5-7 Cyclin D1 immunostaining suggests that SOX9 is required to exit S phase during cell cycle. A. Immunofluorescence for cyclin D1 on WT (top panel, n=2) and *Sox9* cKO (bottom panel, n=3) E12.5 hearts sections. Arrows indicate cells with cyclin D1 staining. Representative images taken on a confocal microscope. **B.** Taqman qRT-PCR assays on WT and *Sox9* cKO for cyclin D1 (*Ccnd1*) relative to *Gapdh.* WT levels are set to 1. N= 5 or greater.

target of SOX9 in the AVC by ChIP-Seq analysis this data suggests that SOX9 may target other factors that are involved in regulating cyclin D1 at the protein level to maintain its stability such as the F-box and WD repeat domain containing proteins that degrade cyclinD1 (141).

5.4 Global transcriptional alterations in the *Sox9* cKO heart valves

To identify critical gene targets of SOX9 that may be responsible for the valve abnormalities resulting in embryonic death in the *Sox9* cKO, the transcriptome of the E12.5 AVC was compared in the presence (WT) and absence of *Sox9* (*Sox9* cKO). Since the efficiency of *Sox9* deletion in the AVC by *Tie2-Cre* is variable, RNA was isolated from individual AVCs from E12.5 WT and *Sox9* cKO and qRT-PCR verified the loss of *Sox9* for each sample. RNA-Seq libraries were generated with RNA from 2-3 AVCs pooled for WT and confirmed *Sox9* cKO and performed in duplicate for each genotype (Figure 5-8A). Differential expression between WT and *Sox9* cKO RNA-Seq libraries was determined using Cuffdiff (120) and fold change was calculated between WT and *Sox9* cKO gene FPKMs. Gene FPKMs from Cufflinks were an average of the duplicate libraries for each genotype. This analysis identified 657 genes that were at least 1.5 fold down-regulated in the E12.5 *Sox9* cKO AVC and 352 genes that were at least 1.5 fold up-regulated in the E12.5 *Sox9* cKO AVC (Appendix XI). Interestingly, down-regulated genes in the *Sox9* cKO AVC are involved in cartilage and heart valve development, and EMT based on GO analysis (Figure 5-8B). While up-regulated genes in the *Sox9* cKO AVC included functions like response to hypoxia and stress and regulation of cardiac muscle hypertrophy (Figure 5-8C).

To rule out a general reduction in AVC expressed genes due to the reduced size of the

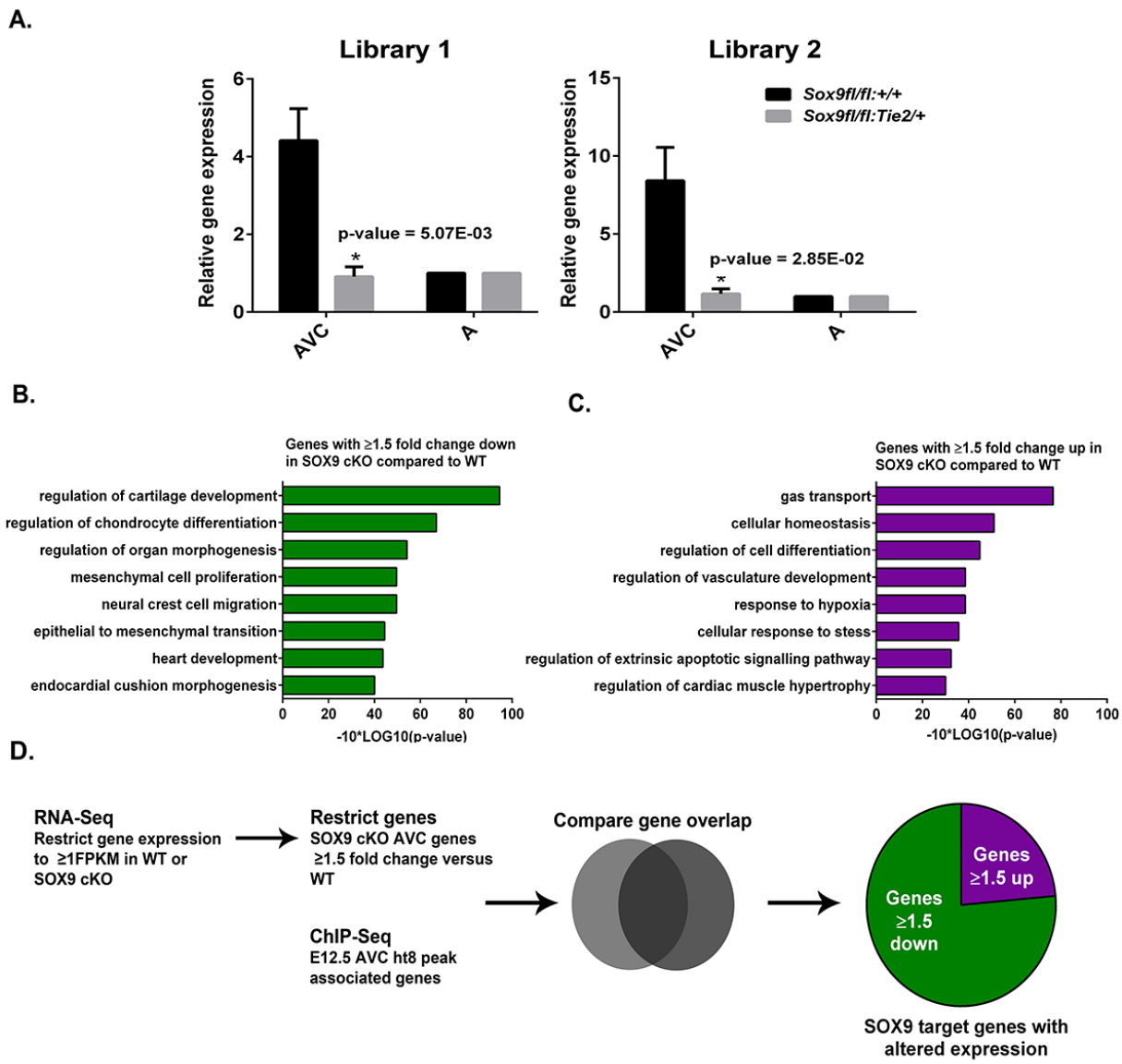

Figure 5-8 Comparison of differential transcripts in the *Sox9* cKO AVC identified by RNA-Seq and SOX9 ChIP-Seq reveals a key subset of genes important for heart valve formation. A. Taqman assays for Sox9 relative to Gapdh for each library on the WT and *Sox9* cKO AVC and atria. Significance is determined using Student's T-test. N=3 for each genotype in each library. GO analysis on genes reduced **(B.)** or increased **(C.)** by greater than 1.5 fold change in the Sox9 cKO versus WT valves. **D.** The workflow for comparing RNA-Seq data with the ChIP-Seq data to identify critical SOX9 targets required for valve formation.

Sox9 cKO AVC cushion, differentially expressed transcripts identified in the *Sox9* cKO AVC were compared to a previously generated list of 206 AV-enriched genes identified in mouse heart (142). I found that 59% of AV-enriched genes have no change or changes less than 1.5 fold between WT and *Sox9* cKO. This suggests that the reduced expression of a subset of AV-enriched genes in the *Sox9* cKO valves is likely due to the specific loss of SOX9 and not from the decreased valve size (Figure 5-9A). To illustrate this, subsets of AV-enriched genes that have no change in expression in WT versus *Sox9* cKO AVC are shown (Figure 5-9B). Additionally, to demonstrate that housekeeping genes were not heavily changed by *Sox9* deletion in the AVC, housekeeping gene expression levels from the RNA-Seq libraries are shown (Figure 5-9C, D).

To further investigate genes that are critical to heart valve development and are regulated by SOX9, genes with altered expression in *Sox9* cKO AVCs were associated with gene targets of SOX9 in the E12.5 AVC using Cistrome (116) (Figure 5-8D). This analysis identified 139 genes that are both SOX9 gene targets in the E12.5 AVC and have altered expression (greater than 1.5 fold change) in *Sox9* cKO AVC. Of the 139 identified genes, approximately three quarters were down-regulated and one quarter were up-regulated (Figure 5-8D, Table 5-2, Appendix XII, XIII). To illustrate the overall gene expression changes of SOX9 targets with a 1.5 fold change (or greater) in expression level heat maps were generated for the down and up-regulated genes (Figure 5-10). Overall, this data suggests that SOX9 likely fine tunes gene expression levels rather than acting as an on/off switch as many traditional transcription factors. On the other hand, SOX9 may have another unknown role other than regulating transcriptional activity of its target genes.

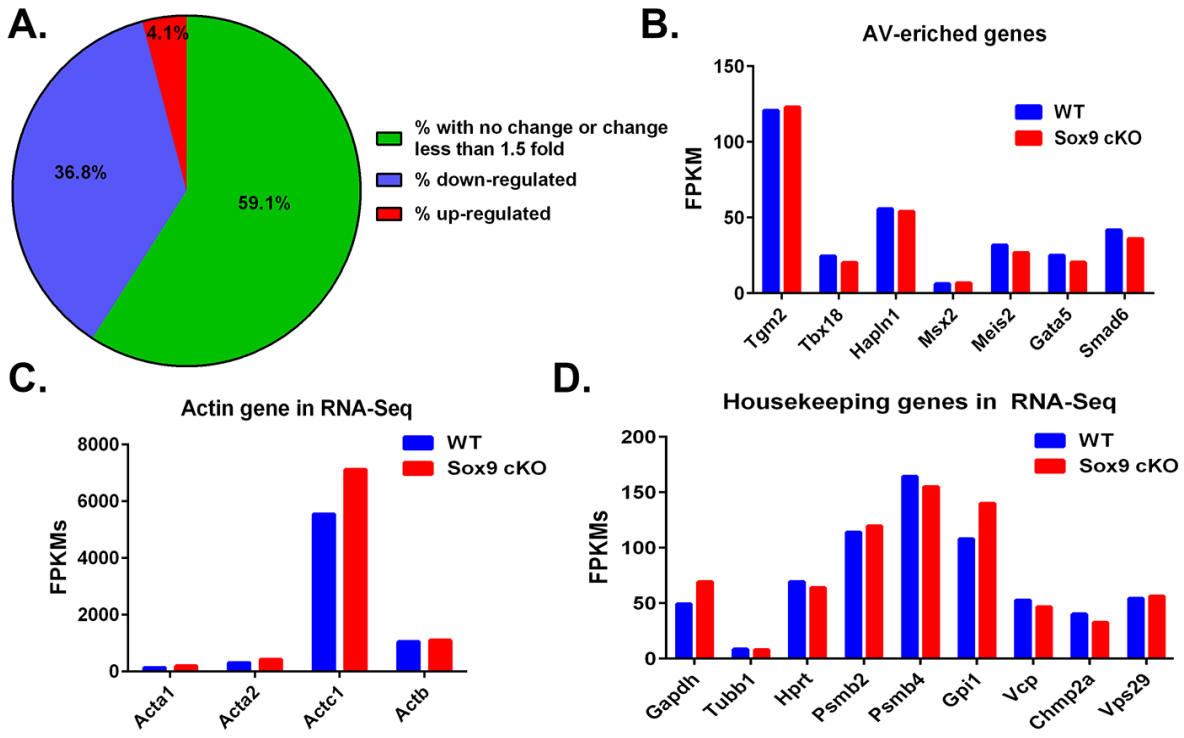

Figure 5-9 SOX9 selectively targets a subset of AV-enriched genes in the AVC. A. A pie chart of the AV enriched genes identified in the Delaughter paper separated by genes that are up and downregulated and with no change **B**. Selected AV-enriched genes that show no change in *Sox9* cKO valves. Actin **(C.)** and housekeeping genes **(D.)** expression levels between WT and *Sox9* cKO illustrating no or little change in expression.

Table 5-2 The top ten SOX9 targets with altered gene expression in the *Sox9* cKO

Genes with ≥1.5 fold change down in the Sox9 cKO with restrictions (≥ 1FPKM in either WT or Sox9 cKO) that have a SOX9 peak						
Gene symbol	**Full Gene Name**	**Gene ID**	**WT FPKM**	**cKO FPKM**	**p-value from Cuffdiff**	**Fold change down in cKO**
Btn1a1	butyrophilin, subfamily 1, member A1	NM_013483	6.92	0.29	0.0001	18.197
Prelp	proline/arginine-rich end leucine-rich repeat protein	NM_054077	3.97	0.32	0.0002	9.701
Tnrc6b	trinucleotide repeat containing 6B	NM_144812	66.09	13.91	0.0004	4.724
Ctnna2	catenin (cadherin-associated protein), alpha 2	NM_001109764	3.30	0.56	0.0006	5.141
Col6a6	collagen, type VI, alpha 6	NM_001102607	4.10	1.19	0.0010	3.246
Ntn4	netrin 4	NM_021320	9.84	3.24	0.0026	2.975
Pitx2	paired-like homeodomain 2	NM_001042504	19.54	7.02	0.0028	2.758
Twist1	twist family bHLH transcription factor 1	NM_011658	37.16	13.38	0.0035	2.765
Fgfr2	fibroblast growth factor receptor 2	NM_010207	19.88	7.65	0.0035	2.577
Clmp/ 9030425E11Rik	CXADR-like membrane protein	NM_133733	17.83	7.00	0.0058	2.527
Genes with ≥1.5 fold change up in the Sox9 cKO with restrictions (≥ 1FPKM in WT or Sox9 cKO) that have a SOX9 peak						
Gene symbol	**Full Gene Name**	**Gene ID**	**WT FPKM**	**cKO FPKM**	**p-value from Cuffdiff**	**Fold change up in cKO**
Bhlhe40	Basic Helix-Loop-Helix Family, Member E40	NM_011498	12.17	56.04	5.00E-05	4.575
Fos	FBJ murine osteosarcoma viral oncogene homolog	NM_010234	2.45	13.97	0.0002	5.522
Dusp4	Dual specificity phosphatase 4	NM_176933	9.16	22.42	0.0072	2.431

Gene symbol	Full Gene Name	Gene ID	WT FPKM	cKO FPKM	p-value from Cuffdiff	Fold change up in cKO
Stc1	Stanniocalcin 1	NM_009285	4.32	9.66	0.0227	2.206
Ddit3	DNA-damage-inducible transcript 3	NM_001290183	11.93	72.50	0.0461	6.036
Nrg1	Neuregulin 1	NM_178591	2.98	6.50	0.0466	2.140
Junb	Jun B proto-oncogene	NM_008416	2.40	5.41	0.0510	2.201
Fhdc1	FH2 domain containing 1	NM_001033301	1.06	2.05	0.0801	1.859
Gramd1b	GRAM domain containing 1B	NM_172768	10.72	18.23	0.1035	1.694
Gm14005	Gm14005 predicted gene 14005	NR_028589	1.07	3.18	0.1101	2.803

Figure 5-10 *Sox9* cKO valves have major changes in gene expression when compared to WT valves. A heat map generated using meV of the expression changes occurring between WT and *Sox9* cKO valves.

CHAPTER SIX: SOX9 has functions involved in regulation of proliferation, transcriptional networks, and ECM formation during heart valve development

To determine the context-independent functions of SOX9, regions of DNA bound by SOX9 were compared amoung different tissues using publicly available data sets. Identification of regions that are commonly bound by SOX9 in multiple tissues suggests that these are potential context-independent transcriptional targets of SOX9. Consequently, the group of genes associated with commonly bound regions may represent a general function(s) of SOX9 across tissues. Furthermore, to identify tissue-specific (context-dependent) functions of SOX9 in the developing heart valves, genes associated with SOX9 bound regions in the AVC were compared with genes that have altered expression in the *Sox9* cKO AVC. This analysis will help to reveal the specific roles of SOX9 in the developing heart valves.

6.1 SOX9 occupies regulatory regions of genes associated with proliferation

As previously mentioned, *Sox9* conditional mutant mice in different organ systems often have defects in proliferation and it seems that regulation of proliferation associated genes may be a common role for SOX9 across tissues. Although it is known that *Sox9* mutants have proliferation defects, to date no direct transcriptional targets have been associated with this role in proliferation. To further delineate common functions of SOX9, SOX9 peaks in the AVC and limb were compared with a publicly available SOX9 ChIP-Seq dataset that was generated in HF-SCs (62). A Venn diagram of the three SOX9 ChIP-Seq libraries demonstrated that SOX9 bound at 293 identical genomic locations in all three libraries (Figure 6-1A), suggesting that SOX9 has common targets in AVC, limb and HF-SCs. GO analysis using the biofunctions category

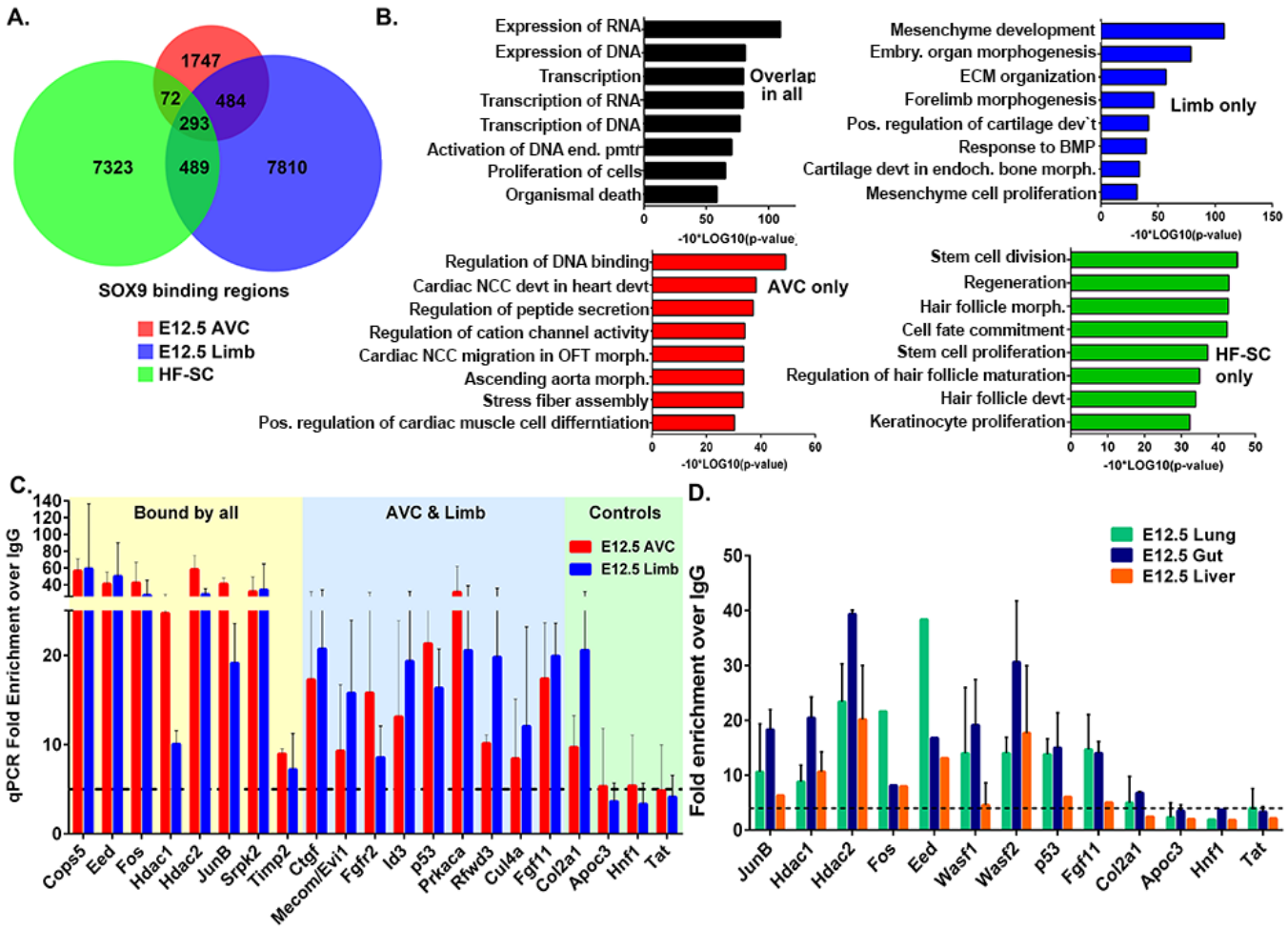

Figure 6-1 Common SOX9 targets among developing tissues provide evidence for a role in proliferation. A. Venn diagram of SOX9 peaks in E12.5 AVC, E12.5 limb, and hair follicle stem cells (HF-SCs). **B.** The top 8 terms from GO analysis on SOX9 target genes overlapping in all and unique GO terms for each tissue. **C.** ChIP-qPCR (n=3) on SOX9 target genes bound in all associated with proliferation for SOX9 binding in the E12.5 AVC and limb or **D.** E12.5 lung, gut and liver (n=3 for *Wasf1/2*, *Hdac1/2*, n=2 for *Junb*, *p53*, *Fgf11*,*Col2a1*, *Apoc*, *Tat*, n=1 for *Fos* and *Eed*). *Apoc3*, *Hnf1*, *Tat* are negative controls regions not bound by SOX9.

(Ingenuity) on the 293 common SOX9 peaks associated with target genes featured proliferation of cells as one of the top GO categories (Figure 6-1B, Table 6-1). In fact, 106 of the overlapping SOX9 target genes are included the in "proliferation of cells" GO category (Figure 6-2). Several examples of genes associated with “proliferation of cells” that were bound by SOX9 in all three libraries include *Junb*, *Cops5*, *Fosl1*, *Fosl2* and *Fos*. Of note, several genes involved in cell proliferation had SOX9 binding sites in heart valve and limb only, such as *Trp53* and *Fgfr2*. To validate the genes identified by the SOX9 ChIP-Seq libraries, ChIP-qPCR was performed on E12.5 AVC and limb to confirm that shared binding sites were occupied by SOX9 (Figure 6-1C). For the first time, it has been demonstrated that SOX9 occupies the regulatory regions of genes that are associated with proliferation and that this binding was shared among different cell types suggesting that these sites are context independent.

Given that SOX9 is required for the development of many organs and is known to be involved in progenitor proliferation (53), we anticipated that shared SOX9 binding sites regulating proliferation genes would also be occupied by SOX9 in other SOX9-expressing tissues. ChIP-qPCR for SOX9 examining the regulatory regions of proliferative genes was performed on the E12.5 lung, gut, and liver (Figure 6-1D). The ChIP-qPCR demonstrated that many of the proliferation associated shared binding regions were also occupied by SOX9 (Figure 6-1D) and suggests that SOX9 may have a common role in the regulation of cell proliferation across developing tissues.

6.2 Context-independent SOX9 binding regions in the AVC, limb, and HF-SCs

To identify context independent activities of SOX9, GO analysis was performed on genes targeted by SOX9 from non-overlapping SOX9 peaks from each of the AVC, limb, and HF-SC

Table 6-1 The top 15 biofunctions identified by IPA on the genes with overlapping SOX9 peaks in the AVC, limb, and HF-SCs

Diseases or Functions Annotation	p-Value	# of Molecules	minus 10*(LOG10 (p-value))
expression of RNA	1.12E-11	81	109.5078
expression of DNA	7.56E-09	61	81.21478
transcription	1.03E-08	68	79.87163
transcription of RNA	1.11E-08	67	79.54677
transcription of DNA	2.03E-08	58	76.92504
activation of DNA endogenous promoter	9.22E-08	46	70.35269
proliferation of cells	2.89E-07	106	65.39102
organismal death	1.42E-06	84	58.47712
infection by RNA virus	1.43E-05	37	48.44664
proliferation of tumor cell lines	2.33E-05	52	46.32644
Viral Infection	2.43E-05	56	46.14394
cell transformation	3.17E-05	19	44.98941
HIV infection	4.79E-05	31	43.19664

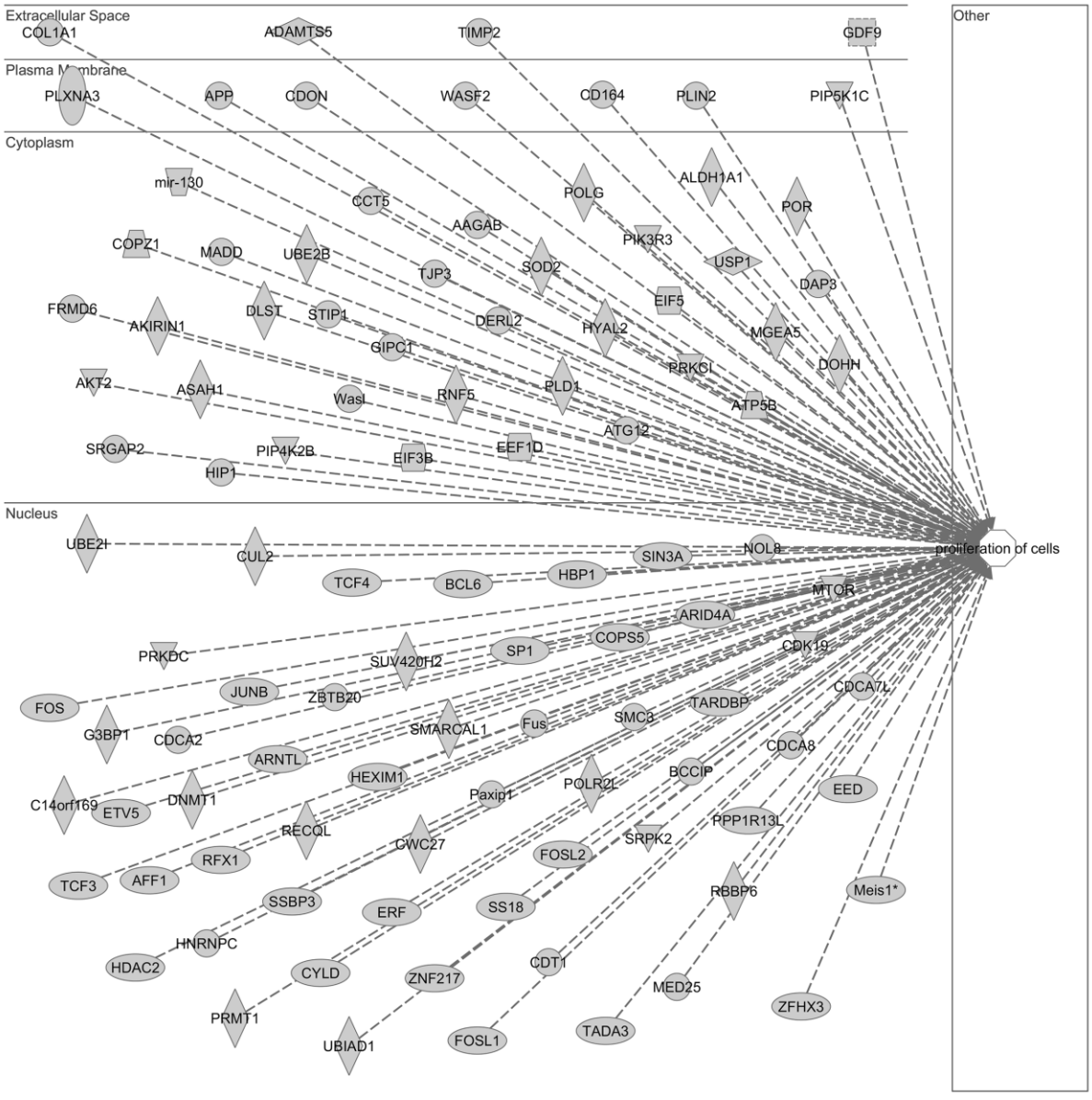

Figure 6-2 SOX9 targets genes involved in proliferation of cells. Ingenuity Pathway Analysis using biofunctions on genes targeted by SOX9 in all three ChIP-Seq libraries (E12.5 AVC, E12.5 limb, HF-SCs) that are associated with proliferation of cells (106 genes). Genes are subdivided by their gene products location within the cell or outside the cell.

libraries. Redundant terms were filtered out between categories (Figure 6-1B). HF-SC-specific SOX9 targets contained unique GO terms like stem cell division; hair follicle morphogenesis and cell fate commitment (Figure 6-1B) as previously reported. Limb-specific SOX9 targets revealed unique GO terms implicated in mesenchyme development, ECM organization and forelimb morphogenesis (Figure 6-1B). SOX9 AVC-specific target genes identified unique GO categories involved in DNA binding, cardiac neural crest cells (NCC) development, and ascending aorta morphogenesis (Figure 6-1B). Identifying genes involved in cardiac NCC in the AVC specific GO categories supports the model that many genes are shared in AVC and OFT development, such as *Twist1*, *Hand2*, and *Pitx2*. Overall, the genes associated with tissue-specific SOX9 bound regions strongly reflect the unique characteristics of each tissue and indicate that SOX9 plays important and context specific roles in different tissues which are linked with tissue identity.

6.3 Proliferation associated target genes are both activated and repressed by SOX9

Currently, little is known about how SOX9 regulates its target genes. *Col2a1* is the most well characterized SOX9 target gene and its regulation by SOX9 is very complex (reviewed in (132)). Overall, SOX9 has been shown to be a transcriptional activator but recent evidence suggests that it can also act as a repressor. SOX9 can bind to gene regulatory regions as a monomer, in sex determination, or as a dimer during chondrogenesis (85,86). Furthermore, the SOX9 DNA binding site tends to be variable and degenerate with a consensus site of WWCAAWG. Given that the understanding of SOX9's transcriptional regulation of its target genes is lacking, I examined SOX9 peak regions of a set of proliferation associated target genes (*Hdac2*, *Prkaca*, *Rfwd3*, *Trp53*, and *Junb*) to identify whether SOX9 acts as an activator or repressor on these

target genes and to determine the exact SOX9 DNA binding site. Target genes of interest were selected based on the GO category of proliferation of cells or regulation of cell cycle identified from common targets of SOX9. Although SOX9 targets have been identified by ChIP-Seq analysis, it is not known whether these sites are functional and whether it is activating or repressing the target gene.

Unfortunately, relevant cell lines for the heart valve and limb buds are limited and primary cultures or explants derived from these tissues are not easily transfectable. Therefore, HEK 293T cells were selected as they are easily transfectable and ideal for over-expression studies. To examine how SOX9 regulates select target genes, luciferase assays, a measurement of transcriptional activity, were coupled with and without SOX9 (via pDNA3-SOX9) over-expression in HEK 293T cells (Figure 6-3A). All of the SOX9 bound regions associated with *Hdac2*, *Prkaca*, *Rfwd3*, *Trp53,* and *Junb* were located at promoter regions. The average size of the SOX9 peak size for the selected targets was 200-300 base pairs. Reporter vectors were generated by cloning in the overlapping SOX9 peak regions (see primers in Table 2-1) identified in the AVC and limb SOX9 ChIP-Seq libraries into the pGL4b (promoter-less) luciferase vector. Titrations for SOX9 over-expression were performed on the pGL4-*Hdac2* promoter vector and the optimal SOX9 concentration was determined to be 0.1 μg per well in a 24 well plate (data not shown). In the presence of SOX9, the *Hdac2*, *Prkaca*, *Rfwd3,* and *Trp53* regulatory regions were activated by SOX9 by at least 1.5-1.7 fold whereas SOX9 inhibited *Junb* by 1.7 fold (Figure 6-3A).

Interestingly, the SOX9 peak region associated with the *Hdac2* promoter contains a potential SOX9 dimer site. To determine if the dimer site in the *Hdac2* promoter is in fact the SOX9 binding site and secondly if SOX9 is binding as a dimer, I mutated the SOX9 dimer site in

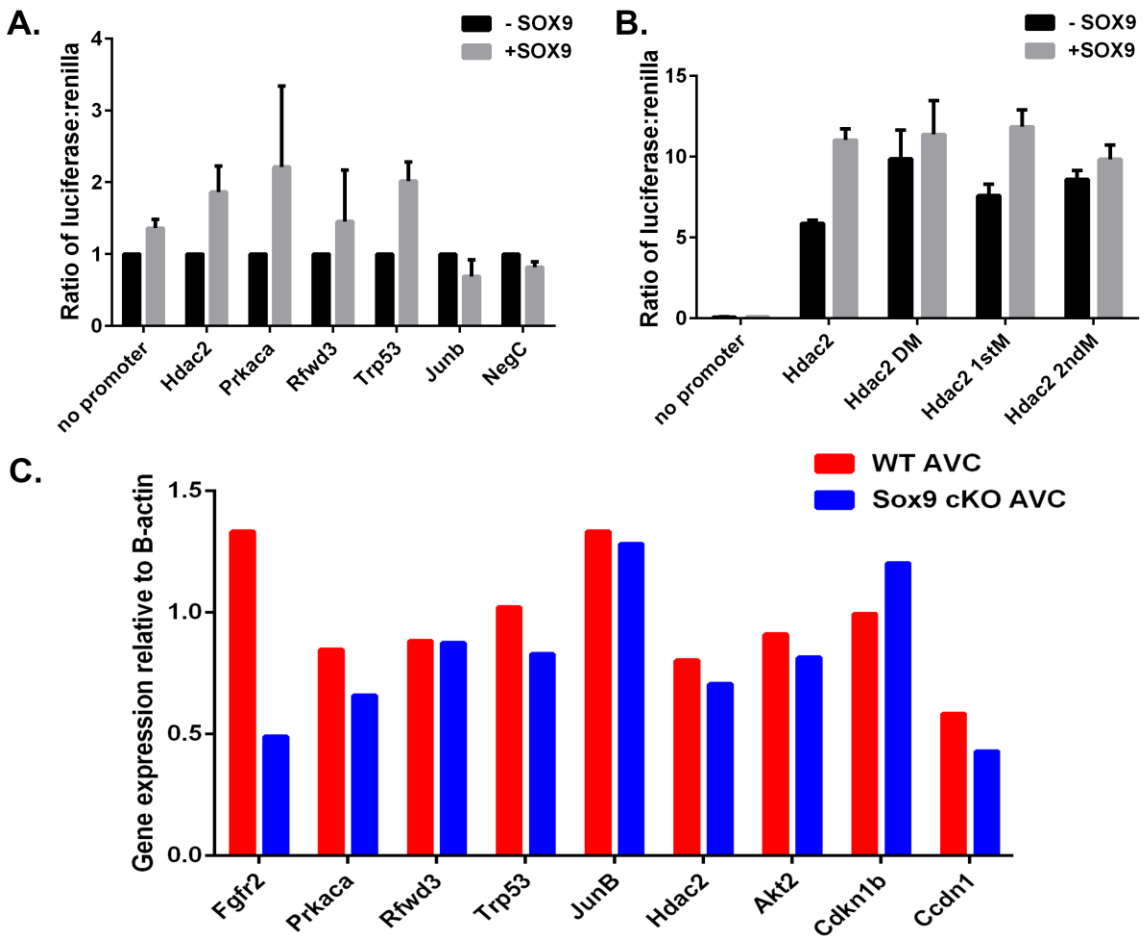

Figure 6-3 SOX9 regulates genes associated with cycle and proliferation. A. Luciferase assays on SOX9 binding regions (promoter bound) of cell cycle associated genes in HEK 293T cells with /without overexpression of SOX9. **B.** Site directed mutagenesis coupled with luciferase assays in HEK293T with/without overexpression of SOX9 of the SOX9 dimer site within the SOX9 peak located in the *Hdac2* promoter region. 1st M indicates mutation of the first SOX9 site in the dimer. 2nd M indicates mutation of the second SOX9 site in the SOX9 dimer and DM indicates the mutation of both SOX9 sites in the dimer. **C.** A representative qRT-PCR for cell cycle and proliferation associated genes on WT and *Sox9* cKO heart valves. β-actin was used as a control for qRT-PCR. *Ccdn1* is not a SOX9 target gene.

the *Hdac2* promoter using site directed mutagenesis and generated three luciferase constructs. The first construct contained mutations in both SOX9 sites (double mutant, DM), the second contained a mutation in the first SOX9 site (1st site mutant, 1st M) and the last contained a mutation in the second SOX9 site (2nd site mutant, 2nd M). Based on previous literature, the CAA portion of the SOX9 consensus site (WWCAAWG) was mutated to ACC using primers containing the mutated sequence (Table 2-1). Using these vectors in luciferase assays, the induction of the *Hdac2* promoter by SOX9 over-expression was eliminated upon mutation of both SOX9 sites (Figure 6-3B). Additionally, based on single site mutations of SOX9 sites in the *Hdac2* promoter it appeared that the second site in the SOX9 dimer was the more critical SOX9 binding site for activation of *Hdac2* (Figure 6-3B). Since the SOX9 DNA binding motif is highly degenerate, identifying the exact binding motifs of SOX9 will help to clarify the exact positions required for SOX9 binding and may aid in the discovery of additional SOX9 binding sites in other organ systems.

To further substantiate SOX9's role in activation or inhibition of its target genes, I examined the expression level changes that occur following the loss of SOX9 *in vivo*. RNA isolated from the WT and *Sox9* cKO AVC was used for qRT-PCR to examine the expression levels of the genes identified by GO to impact proliferation: *Hdac2, Prkaca, Rfwd3, Trp53, Junb, Fgfr2, Akt2, Cdkn1b,* and *Ccdn1* (Figure 6-3C). Overall, no significant changes in the expression of proliferation associated genes were observed between WT and *Sox9* cKO AVCs with the exception of *Fgfr2*. However, a trend towards a decrease for *Hdac2, Prkaca*, *Rfwd3,* and *Trp53* mRNA expression levels was noted (Figure 6-3C). The SOX9 bound regions for *Hdac2, Prkaca*, *Rfwd3,* and *Trp53* were activated by SOX9 (Figure 6-3A) in the luciferase assays except for *Fgfr 2*(data not shown) and matched the slight decreased in transcript levels in the RNA-Seq.

qRT-PCR revealed that *Akt2* and *Junb* had no change in mRNA expression levels between WT and *Sox9* cKO whereas *Cdkn1b* (also known as p27, a cell cycle inhibitor) had increased expression in the *Sox9* cKO AVC (Figure 6-3C). Generally, the changes in transcript expression levels between WT and *Sox9* cKO AVCs in the RNA-Seq and qRT-PCR matched for the SOX9 target genes associated with cell cycle/proliferation. However, there were a few exceptions such as *Junb* which was up-regulated in the *Sox9* cKO AVC RNA-Seq library and *Cdkn1b* which had no change in expression level in the RNA-Seq (Appendix XI). Although no drastic changes were observed in gene expression of the proliferation associated genes between WT and *Sox9* cKO AVC, it could be that even small to moderate changes in cell cycle and proliferation could have detrimental effects on organ formation during development.

6.4 SOX9 targets a network of TFs known to be involved in heart development

Given that a major goal of this study was to discover SOX9 target genes that are critical for heart valve formation, up- and down-regulated SOX9 target genes identified by ChIP-Seq and RNA-Seq analysis were further analyzed by Ingenuity Pathway Analysis (IPA, Qiagen) for GO terms and functions specific to heart development. IPA highlighted enrichment in functions associated with transcription, cardiogenesis, and abnormal heart morphogenesis (Table 6-2). IPA was used to generate a relationship network between these three GO terms to determine if there were any commonalities between them (Figure 6-4). Lines indicate the type of relationship between the gene and GO term. For example, loss of *Pitx2* (green colour of the molecule=loss, red=increase) leads to an activation of abnormal morphology of the heart (orange line) and inhibition of transcription and cardiogenesis (blue line) (Figure 6-4). Yellow lines indicate that data supports both activation and inhibition relationships for the gene and GO term. Notable TFs associated

Table 6-2 The top 20 biofunctions identified by IPA on SOX9 target genes with differential expression in the *Sox9* cKO AVC.

Diseases or Functions Annotation	p-Value	Activation z-score	# Molecules
morphology of digestive system	3.00E-10	1.398	22
perinatal death	1.11E-09	2.453	22
abnormal morphology of skull	4.26E-09		13
expression of DNA	4.33E-09	-0.484	33
abnormal morphology of digestive system	4.51E-09	1.169	20
transcription of DNA	5.15E-09	-0.223	32
neonatal death	5.66E-09	1.997	18
organismal death	1.77E-08	3.71	45
cell death	2.37E-08	0.846	51
activation of DNA endogenous promoter	2.85E-08	-0.487	26
seizures	3.16E-08	0.308	16
morphology of head	3.29E-08	1.499	24
apoptosis	4.02E-08	1.548	43
seizure disorder	4.44E-08	-0.047	17
abnormal morphology of head	5.89E-08	2.219	23
tooth development	1.10E-07		8
morphology of body cavity	1.18E-07	1.513	27
cardiogenesis	1.43E-07		14
differentiation of connective tissue	1.51E-07	0.486	18
abnormal morphology of heart	1.73E-07		15

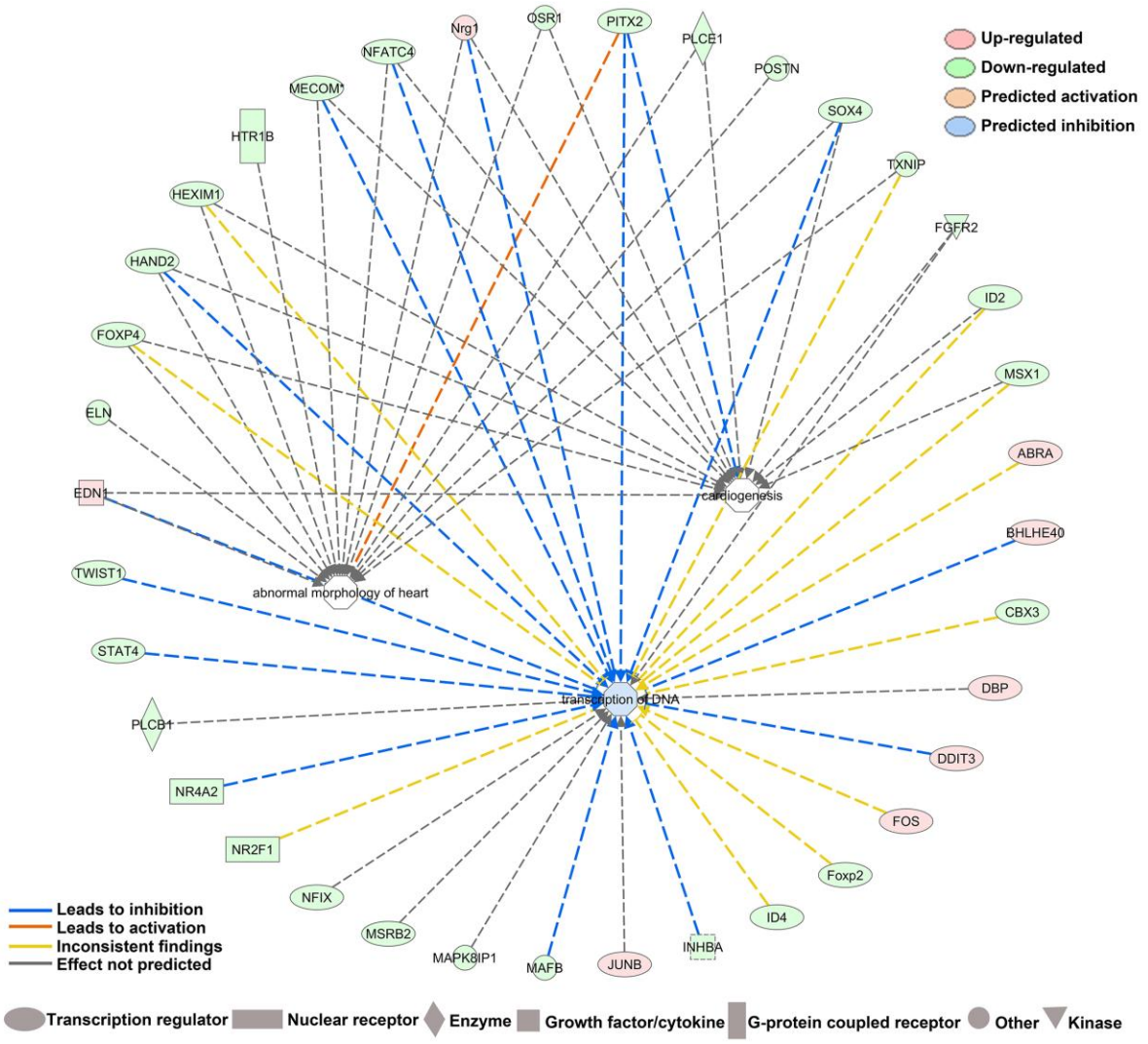

Figure 6-4 SOX9 ChIP-Seq and differential transcripts in the *Sox9* cKO AVC comparison reveals critical transcriptional networks involved in valve formation. A network of transcription, cardiogenesis and abnormal heart morphology biofunctions identified by Ingenuity. Lines indicate the type of relationship between the gene and GO term. Ie. Loss of *Pitx2* leads to an activation of abnormal morphology of the heart and inhibition of transcription and cardiogenesis. Yellow lines indicate that there is data support both activation and inhibition. Libraries performed in duplicate from pooled valves.

with heart development that are down-regulated in the *Sox9* cKO AVC and are SOX9 targets in the AVC include *Sox4, Hand2, Twist1*, *Foxp4, Mecom,* and *Pitx2*. Interestingly, almost 20% of the top differentially expressed genes that are targeted by SOX9 are transcription factors and suggests that SOX9 may be regulating a network of transcription factors to drive heart valve development. In addition, several ECM components known to be important for heart valve formation such as *Periostin* and *Elastin* were reduced (Figure 6-4, Appendix XII). Up-regulated genes that were SOX9 targets also contain several TFs, for example, *Bhlhe40*, *Ddit3*, and *Junb* (Figure 6-4, Appendix XIII). Thus, indicating that SOX9 can likely act as both a transcriptional activator and repressor of critical factors based on ChIP-Seq and RNA-Seq analysis.

Our data indicates that SOX9 activates a network of critical TFs and ECM components that may have crucial functions that are required during heart valve development. To confirm that SOX9 acts as a transcriptional activator of the TFs, *Mecom* and *Nfia*, luciferase assays coupled with SOX9 over-expression were employed as described above (Figure 6-5A). SOX9 activated the *Mecom* and *Nfia* enhancers by 2.44 and 2.17 fold respectively (Figure 6-5A). This data supports that direct binding of SOX9 activates transcription of important TFs during heart valve development. Since SOX9 lies upstream of a group of known TFs involved in heart development, I determined whether the TFs, *Sox4*, *Mecom, Twist1*, *Pitx2, Hand2,* and *Nfia* transcript levels were reduced in the *Sox9* cKO AVC by qRT-PCR (Figure 6-5B). Of note, *Sox4*, *Mecom*, *Twist1*, *Lef1* and *Tbx20* levels were significantly reduced in the *Sox9* cKO AVC (Student's T-test between WT and *Sox9* cKO levels for each transcript, $p>0.05$). Two additional SOX9 targeted TFs important in heart valve development, *Lef1* and *Tbx20*, were also reduced in *Sox9* cKO AVC but were below the 1.5 fold change cut-off used for the RNA-Seq analysis (Figure 6-5B). In all cases, expression of these TFs were reduced in *Sox9* cKO AVCs compared

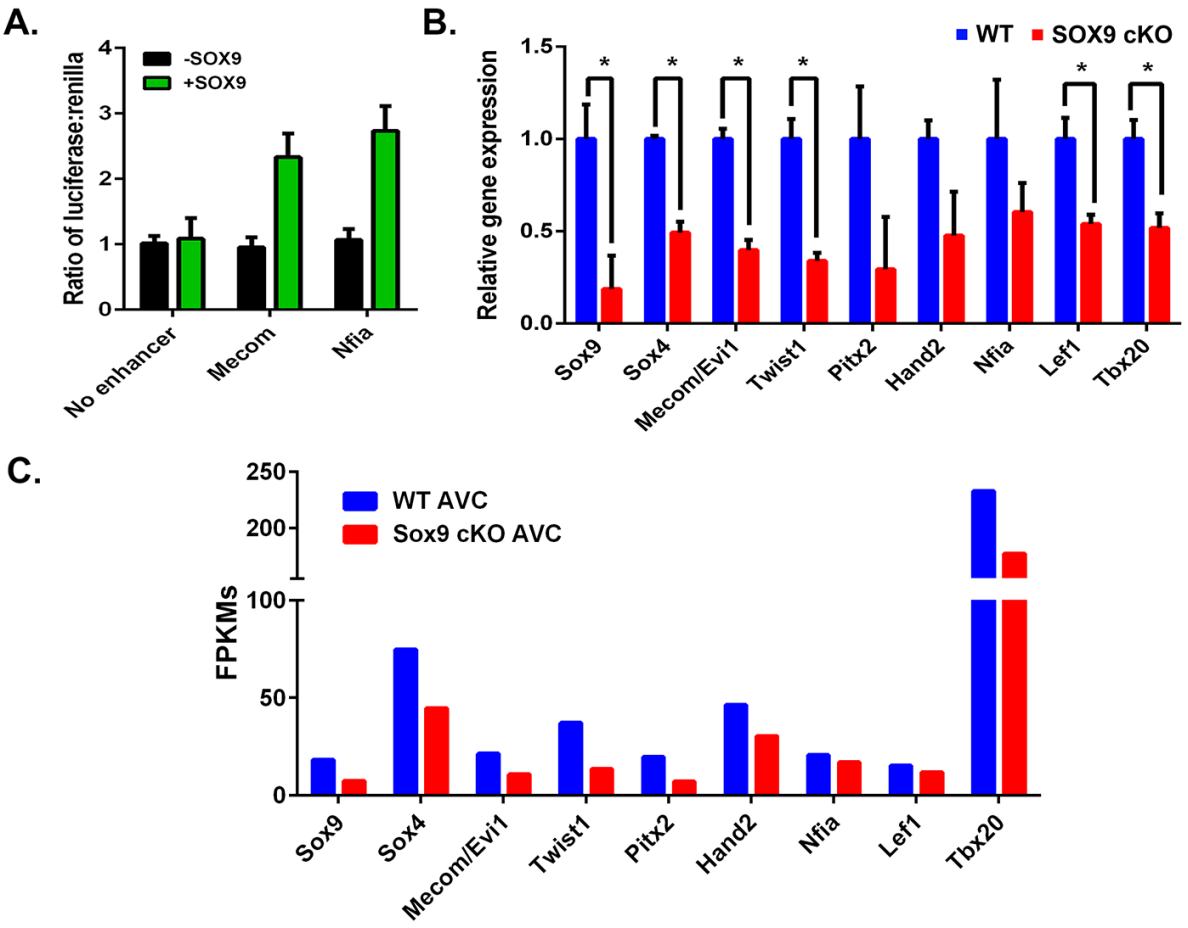

Figure 6-5 *Sox9* activates transcription factors that are known to be essential for heart valve development. A. Luciferase assays for SOX9 enhancer sites associated with the transcription factors *Mecom* and *Nfia* on HEK293T with SOX9 overexpression. N=3. **B.** qRT-PCR for *Sox9* and selected target TFs on WT and SOX9 cKO AVCs. *Sox9*, *Twist1*, *Lef1*, *Tbx20* have an n of 8 or greater and *Sox4*, *Mecom/Evi1*, *Pitx2*, *Hand2*, and *Nfia* have an n of 3 or greater. **C.** FPKMs from the RNA-Seq analysis on WT and Sox9 cKO heart valves illustrating similar expression patterns to those identified in the qRT-PCR. *significance by a two tailed Student's T-test.

to WT. Alterations in transcript levels identified by qRT-PCR correlated to the expression changes seen in the RNA-Seq libraries on WT and *Sox9* cKO AVC (Figure 6-5C).

To verify that loss of SOX9 in heart valves causes downstream effects that disrupt valve development, we focused on the known and essential TF, *Twist1*. Quantitative RT-PCR confirmed that the *Twist1* transcript is reduced at E12.5 and also at an earlier time point (E10.5) in the *Sox9* cKO AVC (Figure 6-6A, B). Using *in situ* hybridization, *Twist1* mRNA was specifically expressed in the valve mesenchyme in the E12.5 AVC and was reduced to about half of the WT levels in the SOX9 mutant valves (Figure 6-6C). This was similar to the level of reduction in *Twist1* mRNA seen in mutant valves at E12.5 via qRT-PCR (Figure 6-6B). This data suggests that SOX9 may fine tune the levels of *Twist1* in the developing heart valves. *Mecom/*Evi1was another TF of interest, as generation of a hypomorphic allele of *Mecom/Evi1* demonstrated that it has an important role in OFT valve formation (131). *Mecom/Evi1* is expressed in AVC but no role in AVC valve development was described. Quantitative RT-PCR for *Mecom/Evi1* confirmed that the transcript is enriched in the AVC (Figure 6-7A). Since I had already confirmed that the *Mecom/Evi1* transcript was reduced in the *Sox9* cKO valves, I decided to examine the protein levels of EVI1 using immunofluorescence with an antibody specific to EVI1 in the developing WT heart valves from E12.5-E14.5 (Figure 6-7B). EVI1 protein was specifically expressed in regions of the valve mesenchyme that was condensing at E12.5 and remained expressed there until E14.5 (Figure 6-7B, arrowheads). Of note, EVI1 protein was reduced in the *Sox9* cKO hearts except within regions where SOX9 had escaped *Cre* excision based on the location in serial sections (Figure 6-7C, asterisk). This data demonstrates that SOX9 directly regulates *Mecom/Evi1,* and that EVI1 is reduced in the absence of SOX9.

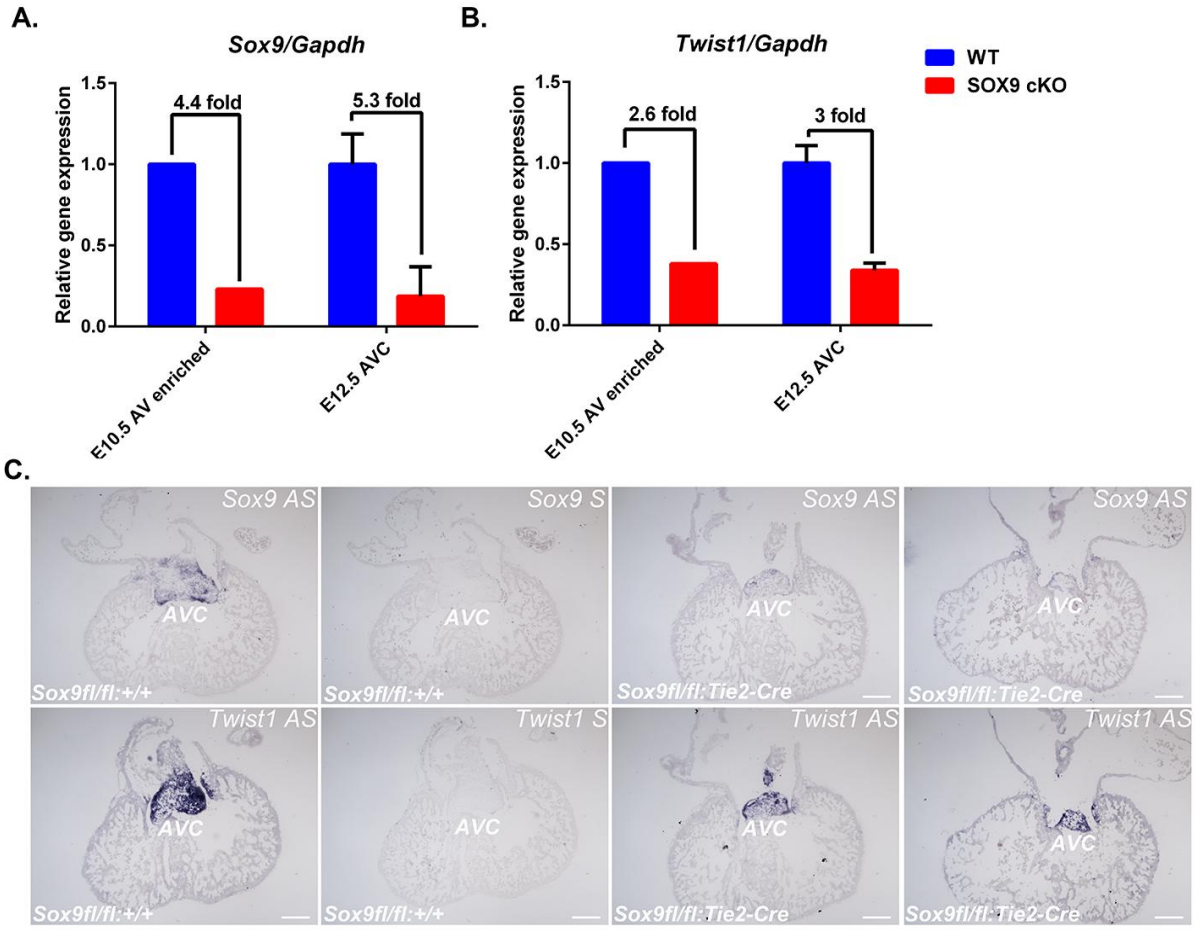

Figure 6-6 The critical EMT regulator *Twist1* is reduced in the *Sox9* cKO heart valves. Taqman assays for **A.** *Sox9* and **B.** *Twist1* relative to *Gapdh* on E10.5 (n=2) and E12.5 (n>6) *Sox9fl/fl* (WT) and *Sox9fl/fl;Tie2-Cre* (*Sox9* cKO) AV-enriched regions. **C.** *In situ* hybridization for *Sox9* and *Twist1* on WT (*Sox9fl/fl;*+/+) and *Sox9* cKO (*Sox9fl/fl;Tie2-Cre/*+) hearts. AS=antisense DIG-labelled probe. S=sense DIG-labelled probe. N=3.

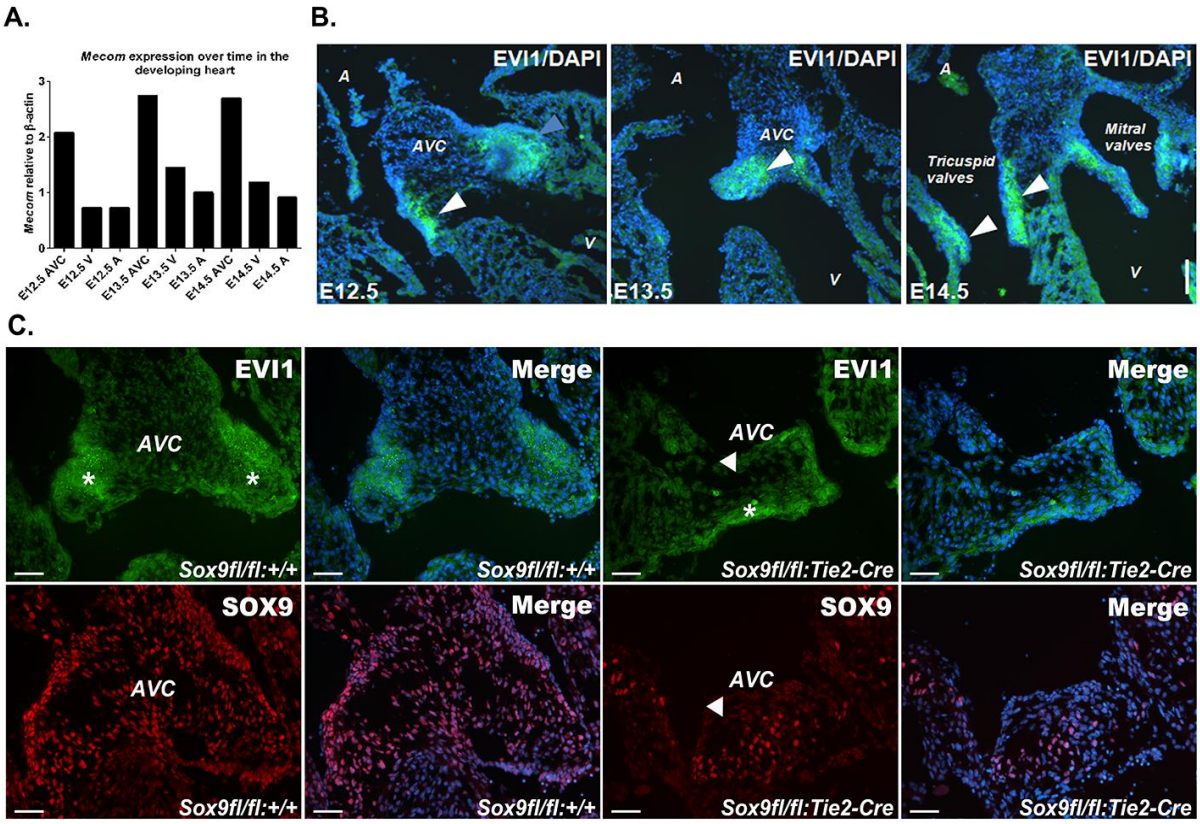

Figure 6-7 EVI1 is enriched in the AVC specifically in condensing mesenchyme and reduced upon deletion of *Sox9*. A. A representative qRT-PCR on WT E12.5-E14.5 AVC, ventricle (V), and atria (A) for *Mecom/Evi1* transcript illustrates AVC enrichment over both V and A during embryonic valve development. **B.** Immunofluorescence (IF) for EVI1 (green) on E12.5-E14.5 hearts. DAPI (blue) was used to stain nuclei. Arrowheads indicate EVI1 expression in the condensed mesenchyme of the heart valves. **C.** IF for EVI1 on E12.5 WT and *Sox9* cKO hearts. *EVI1 positive regions. Arrowhead =SOX9 negative and EVI1 negative regions.

6.5 Additional known roles for SOX9 in EMT and ECM organization

SOX9 has been shown to induce EMT along with the help of other factors in cell types such as the neural crest (67) and since the embryonic heart valves require EMT to populate them with mesenchyme, I decided to analyze EMT markers in the WT and *Sox9* cKO heart valves. As a first step, qRT-PCR was performed on E12.5 AVC from WT and *Sox9* cKO for the epithelial markers, *Cdh1* (E-cadherin) and *Cdh5* (VE-cadherin) and mesenchymal markers, *Vim* (Vimentin) and *Cdh2* (N-cadherin) (Figure 6-8A). There were no significant differences in epithelial or mesenchymal markers mRNA expression levels between WT and *Sox9* cKO AVC. N-cadherin mRNA levels via qRT-PCR had a slight decrease, however when examining the transcript levels in the WT and *Sox9* cKO RNA-Seq libraries there were no differences in any of the markers (Figure 6-8B). The E-cadherin transcript was below the level of detection in the RNA-Seq libraries and consequently was not included (Figure 6-8B). Although the transcript levels did not change between WT and *Sox9* cKO valves, it is possible that epithelial and mesechymal markers could be changing at the protein level. To examine epithelial markers at the protein level, immunofluorescence was performed for CD31 (Pecam1, epithelial marker, BD Biosciences) on E10.5 WT and *Sox9* cKO hearts (Figure 6-8C). Overall, epithelial markers were not changed at the transcript or protein level in the *Sox9* cKO AVCs and suggest that SOX9 was not essential for maintaining the expression these markers in the heart valves. This was not entirely surprising as SOX9 negative mesenchyme was found in *Sox9* cKO valves and suggests that SOX9 is not essential for the initial stages of EMT or for the epithelium.

Another critical function of SOX9 in the limb is in ECM generation and organization and the ECM is very important for heart valve development, and therefore I decided to investigate if there are any differences in ECM molecules in the *Sox9* cKO hearts. Quantitative RT-PCR for

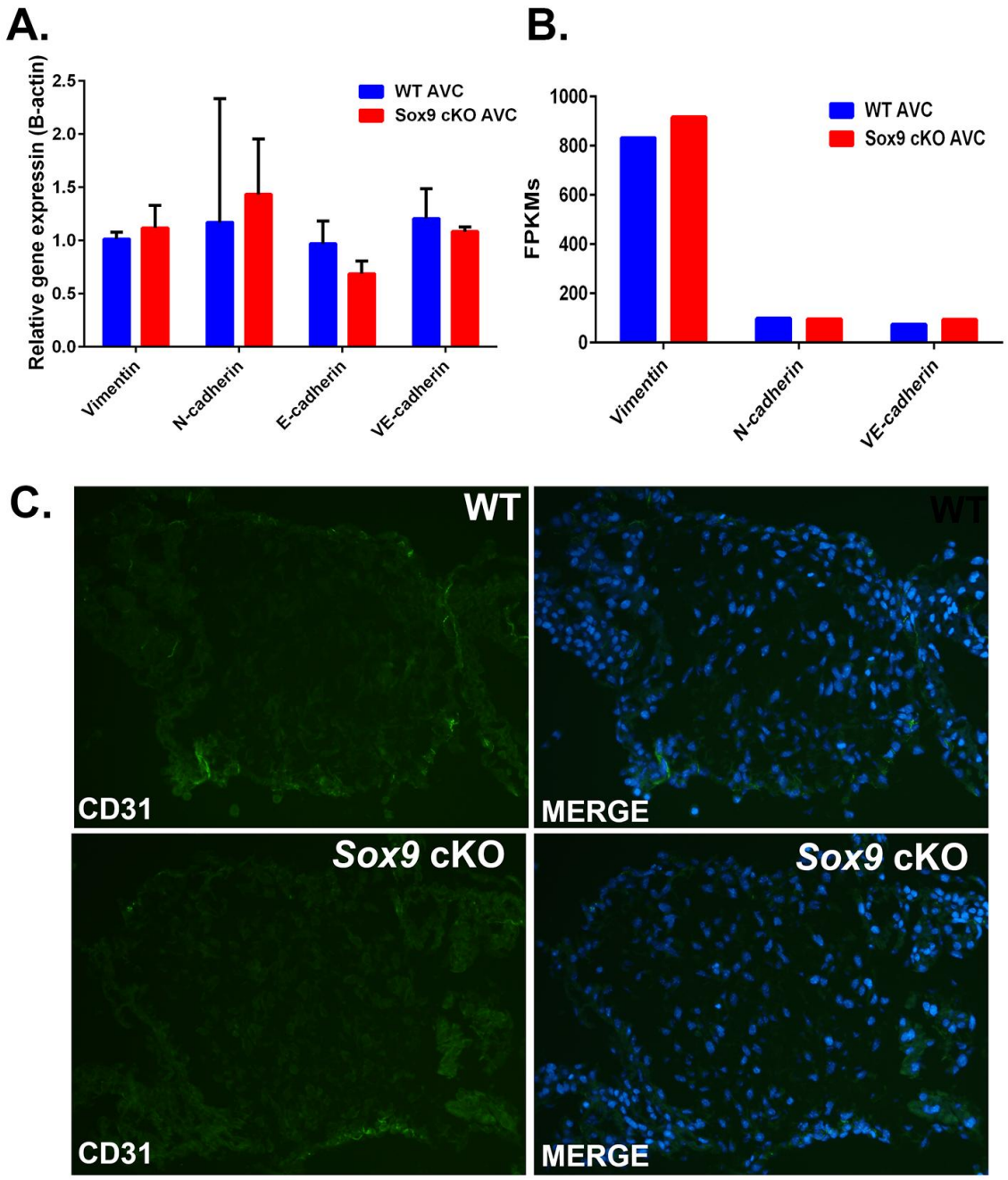

Figure 6-8 EMT markers are unaffected by the loss of *Sox9* in the developing heart valves. **A.** qRT-PCR on WT and *Sox9* cKO E12.5 heart valves for *Vimentin, N-cadherin, E-cadherin and Vascular endothelial cadherin* transcripts. β-actin was used as a control. N=3. **B.** FPKMs from the RNA-Seq analysis on WT and *Sox9* cKO heart valves illustrating similar expression patterns to those identified in the qRT-PCR. **C.** Immunofluorescence for CD31 (green) on E12.5 WT and *Sox9* cKO hearts. DAPI (blue) was used to stain nuclei.

Postn (Periostin), *Eln* (Elastin), *Fbn1* (Fibrillin 1), and *Mgp* (Matrix Gla Protien) on WT and *Sox9* cKO AVC revealed that ECM molecules were reduced in the *Sox9* cKO valves with the exception of *Fbn1* (Figure 6-9A). These alterations in transcript levels of the selected ECM molecules matched the RNA-Seq libraries expression levels perfectly (Figure 6-9B). Additionally, the RNA-Seq libraries on WT and *Sox9* cKO AVC demonstrated that *Col9a1*, *Col9a3*, *Prelp*, *Col6a6*, *Mfap4*, *Matn4*, etc. were also greater than 1.5 fold down-regulated in *Sox9* cKO valves when compared to WT (Appendix XI). Immunofluorescence was performed for PERIOSTIN on WT and *Sox9* cKO hearts to determine if the protein level was also reduced in the *Sox9* cKO AVC (Figure 6-9C). PERIOSTIN levels did not appear to be reduced in the *Sox9* cKO AVC and seemed to be up-regulated compared to overall valve area (Figure 6-9C). Additional studies are required in order to determine the exact role of SOX9 in the regulation of ECM molecules as many of these molecules are carefully controlled at the protein level as well. Overall, the data suggests that SOX9 plays a role in regulating the transcript level of key ECM genes during heart valve development.

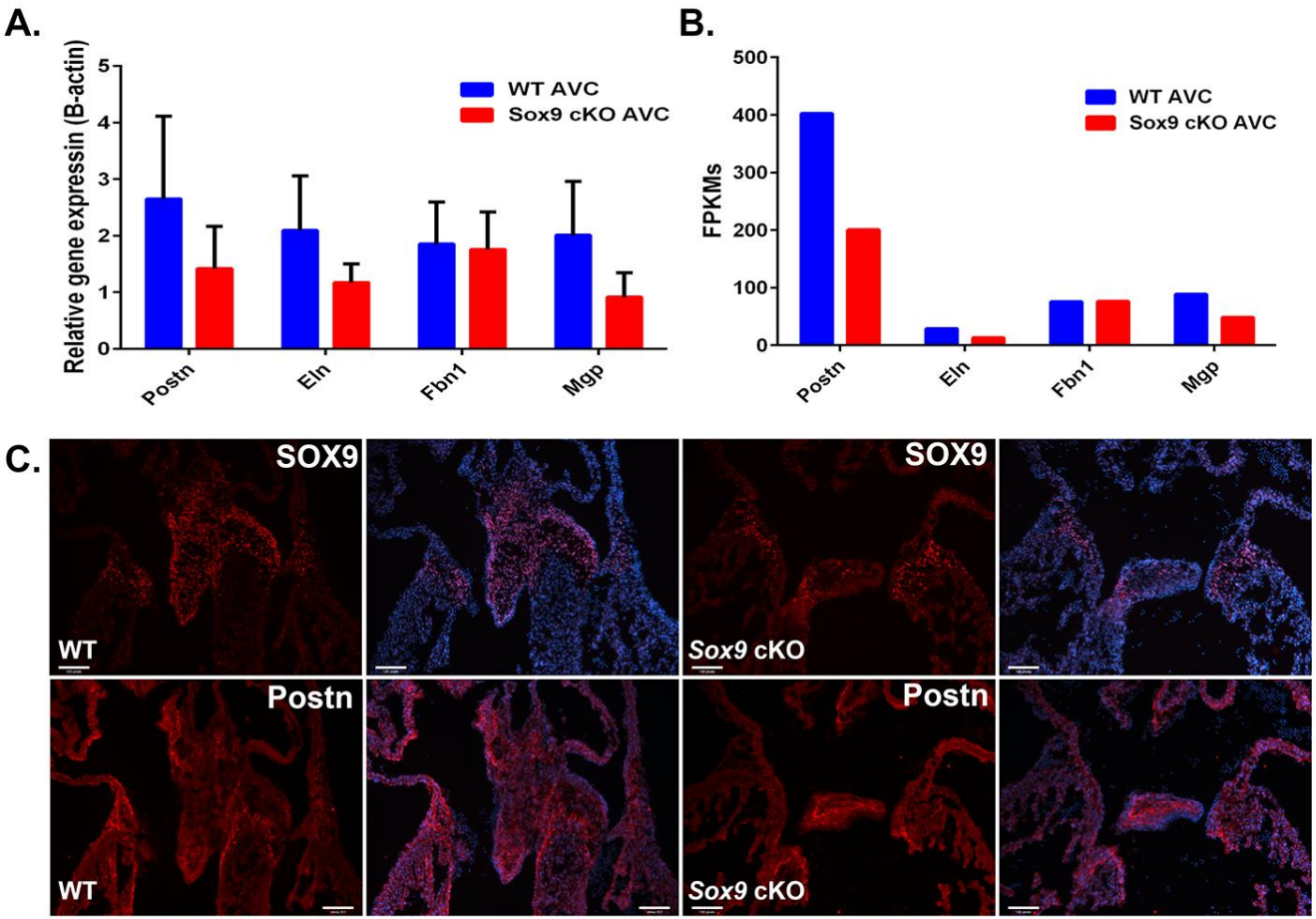

Figure 6-9 ECM molecules mRNA levels are reduced in the *Sox9* cKO heart valves. A. qRT-PCR on WT and *Sox9* cKO E12.5 heart valves for *Periostin (Postn), Elastin (Eln), Fibrillin 1 (Fbn1)* and *Matrix Gla protein (Mgp)* transcripts. β-actin was used as a control. N=3. **B.** FPKMs from the RNA-Seq analysis on WT and *Sox9* cKO heart valves illustrating similar expression patterns to those identified in the qRT-PCR. **C.** Immunofluorescence (IF) for PERIOSTIN and SOX9 on E12.5 WT and *Sox9* cKO hearts. DAPI (blue) was used to stain nuclei.

CHAPTER SEVEN: Discussion

7.1 Thesis overview

Taken together, we have shown that shared SOX9 binding sites identifies a common function of SOX9 in regulating proliferation in a diverse number of tissues; SOX9 binding was biased toward promoter regions, SOX9 tissue-specific binding sites with transcriptome data from tissues lacking SOX9 supports discovery of critical SOX9 targets; and SOX9 activates a core network of TFs required for heart valve development.

In this thesis, I have investigated the global SOX9 binding sites in the E12.5 heart valves and limb and found that the transcriptional programs initiated by SOX9 in the developing heart valves and limb share numerous similarities in SOX9 binding locations and downstream target genes. Analysis of SOX9 binding in the valves and limb also revealed that SOX9 preferentially binds at or near promoters, can bind as both monomers and dimers, and that SOX9 binding regions contain motifs for numerous potential co-factors such as HIF1α, FOXs, and RUNX proteins. Generation of two endothelial specific conditional *Sox9* knockout mouse models using *VE-Cre* and *Tie2-Cre* crossed with *Sox9fl/fl* revealed two potentially different roles for SOX9 during heart valve development. The *VE-Cre* crossed with *Sox9fl/fl* suggests a role for SOX9 in the early stages of EMT and generation of mesenchyme while *Tie2-Cre* crossed with *Sox9fl/fl* indicates a role for SOX9 in maintenance of the mesenchyme and mesenchyme differentiation. Analysis of the *Sox9fl/fl;Tie2-Cre* (*Sox9* cKO) mutant valves demonstrated that *Sox9* mutants have reduced AVC cushion size, proliferation defects and defects were ultimately embryonic lethal. Analysis of shared SOX9 binding sites among different tissues revealed a role for SOX9 in proliferation. Furthermore, transcriptome analysis on WT and *Sox9* cKO valves compared

with SOX9 transcriptional targets in the heart valve highlighted critical roles for SOX9 in the regulation of heart valve specific transcription factor networks and ECM molecules. Overall, I have identified critical characteristics of SOX9 binding and identified its transcriptional targets, identified roles for SOX9 in proliferation, transcription factor network regulation and maintenance of the ECM in the developing heart valves.

7.2 SOX9 occupies the promoter and upstream regulatory regions associated with thousands of target genes including its future co-factors

SOX9 is known to be essential for heart valve development as the loss of SOX9 specifically in the valves is embryonic lethal (46). Even though SOX9 has a critical role in the heart valves, the protein expression pattern has not been well characterized throughout the literature with the majority of studies focussed on the early stages of valve formation. For this reason, I analyzed SOX9 protein expression throughout embryonic valve development (E9.5-E16.5) using immunofluorescence. SOX9 was highly enriched in cardiac cushions and the entire AV valve regions at all stages examined and suggests that SOX9 likely has multiple roles in heart valve formation as the AV valves are undergoing diverse cellular processes including proliferation, differentiation and remodeling during this time. Immunofluorescence for SOX9 on the WT and *Sox9* cKO hearts also helped to support the specificity of the SOX9 antibody for the SOX9 ChIP-Seq libraries. In addition, SOX9 was found specifically in the limb, lung, and somites in the E12.5 whole embryo using immunofluorescence as expected from previous publications.

To gain a better understanding of the role of a specific transcription factor, one can examine its downstream transcriptional targets. To analyze SOX9 binding in the embryonic heart valves and limb, two genome-wide SOX9 ChIP-Seq libraries on the E12.5 AVC and limb were

generated. To our knowledge, we are the first group to perform ChIP-Seq for SOX9 on the embryonic heart valves and limb buds. To date, studies that have performed ChIP-Seq on mouse embryonic tissues are limited (143-145). Only three groups within the last year has analyzed SOX9 binding sites using ChIP-Seq on HF-SCs (126), on the vertebral column (125), and on postnatal rib chondrocytes (129). Of note, the data was not released for the rib chondrocyte study. Additionally, in the last month, two other studies have published global SOX9 binding sites in a chondrocyte cell line (146) and in postnatal rib chondrocytes (147) using the same SOX9 antibody. Global analysis of SOX9 binding in similar but different developing tissues has revealed novel common- (context-independent) and tissue-specific (context-dependent) mechanisms of gene regulation.

For the first time, we have identified over 2400 novel SOX9 target genes in the mouse embryonic heart valves. In addition to the handful of known SOX9 target genes in the limb, we have identified 5700 SOX9 target genes during chondrogenesis. The SOX9 ChIP-Seq limb library has identified *Col2a1*, *Col9a1*, *Col11a2*, *Acan*, *Hapln1* (CLP), *Comp*, and *Mia1* (Cd-rap) (79-84,87,88), known cartilage-specific targets of SOX9, and thus verifies that the SOX9 ChIP-Seq libraries are of high-quality and highly specific for SOX9 binding. Interestingly, SOX9 targets a number of its known co-factors during chondrogenesis, including *Sox5*, *Sox6*, *Barx2*, and *Zfp219* (48,148,149), and suggests that SOX9 has the ability to enhance its own specificity to its cartilage-specific target genes. In the limb, SOX9 may regulate factors that are known to control its own expression. For instance, in the limb SOX9 ChIP-Seq data, SOX9 targets *Bmpr1b* and *Notch1* which have been shown to have a role in the regulation SOX9 expression during chondrogenesis (150,151).

A number of novel characteristics about SOX9 DNA-binding behavior within the genome were discovered in the developing heart and limb. For example, SOX9 binding sites are widely distributed throughout the genome but are biased to promoter regions of its target genes particularly when a SOX9 binding site is shared in multiple tissues. Additionally, this work demonstrated that SOX9 preferentially binds as monomers in the heart valves and that the SOX9 dimer motifs were more prevalent in the limb than the AVC. Dimer motifs were expected to be more abundant in the limb as dimer sites have been previously reported for chondrogenic genes required for limb development (86). Although a SOX9 dimer motif has been described in chondrogenic genes, we are the first to present a positional weight matrix for the SOX9 dimer motif in the developing limb and heart valves.

Several studies have suggested that heart valve development shares many similarities with cartilage and bone formation in the developing limb (37,38). Comparisons of the SOX9 DNA bound regions (peaks) in the AVC and limb by using Venn diagrams revealed that 782 SOX9 binding sites directly overlap in the AVC and limb and supports that these developmental programs are similar. Furthermore, when SOX9 DNA binding regions are assigned to genes and these target genes were compared between the AVC and limb using a Venn diagram, there were 1605 target genes shared between the two tissues, further highlighting the similarities in these two tissues. SOX9 DNA binding regions that directly overlap in the AVC and limb suggests a common (context independent) function in these two tissues. GO analysis on the genes in the AVC and limb with directly overlapping DNA bound regions identified numerous metabolic functions, transcription, and regulation of cell cycle and further supports the notion of context-independent functions of SOX9. Regulation of cell cycle was of particular interest as these two tissues are rapidly growing during development and several genes found in this category include

Trp53 (p53), *Junb*, *Rfwd3*, *Hdac1/2* and *Eed*. Based on the higher number of commonly targeted genes versus shared SOX9 binding sites in the valves and limbs, SOX9 likely has tissue-specific binding sites for the heart valves and limb for the same target genes. GO analysis on the AVC and limb libraries revealed many context dependent functions such as regulation of WNT signaling, atrioventricular valve development, and atrial septum morphogenesis in the AVC and mesenchyme development, chondrocyte differentiation, and connective tissue development in the limb.

SOX transcription factors are known to bind in complexes with other SOXs or other transcription factors in order to efficiently regulate their target genes (47). To get an idea of the potential co-factors of SOX9, the DNA sequences under SOX9 peaks were analyzed using oPOSSUM to search for enriched transcription factor motifs. For AVC, limb, or shared SOX9 peaks the top motifs by z-score that were found in all three analyses were motifs for NFYA, SOX9 and ARNT. It was reassuring to have SOX9 as one of the top enriched motifs as these are SOX9 DNA binding sites identified by ChIP-Seq. Enrichment of the NFYA motif is expected since SOX9 binding is biased to the TSS/promoter regions and NFY is known to bind to promoters to activate transcription (reviewed in (152)). Interestingly, the ARNT motif was enriched in SOX9 DNA binding regions for all three analyses. HIF1 is a heterodimer made up of an oxygen regulated α subunit and a β subunit called ARNT (153). Both hypoxia and HIF1a are known to play a role in the development of the limb buds and heart valves (154,155). The inactivation of HIF1a in limb bud mesenchyme leads to decreased levels of SOX9 and HIF1a can bind to the SOX9 promoter, suggesting SOX9 is directly regulated by HIF1a (154). It is possible that HIF1a activates SOX9 and then together they regulate genes involved in hypoxia. Many of the motifs identified in the SOX9 DNA binding regions were found in all three libraries

however the degree of enrichment of these motifs changes. Other motifs of note were the other SOX, FOX, RUNX, and NFI factors. Further analyses will be aimed at understanding the relationship between these co-factors and SOX9 and their co-targeted genes.

Analysis of transcription factors using ChIP-Seq is becoming more prevalent. This data can be used to compare with the SOX9 ChIP-Seq data sets as a way to identify common functions for SOX9 or to identify co-factors and their downstream co-targeted genes. To examine common functions for SOX9 among different cell types, I compared our SOX9 ChIP-Seq data sets with two publicly available ChIP-Seq data sets for SOX9 on HF-SCs (126) and the E12.5 vertebral column (125). Comparison of SOX9 DNA binding regions in the AVC and limb with the HF-SCs revealed a high level of similarity between these cells, which was more than expected based on the functions of these different cell types. This may indicate that SOX9 positive mesenchyme progenitor cells in the AVC and limb have stem cell-like functions during development. Of note, the SOX9 antibody (Millipore, AB5535) used for ChIP-Seq on HF-SCs was the same antibody used for the SOX9 ChIP-Seq on the E12.5 AVC and limb. The E12.5 vertebral column undergoes endochondral ossification of the cartilage template comparable to the development of the embryonic limb. Due to this, it was expected that the SOX9 limb DNA binding sites would share a higher degree of overlap. However, SOX9 DNA binding sites in the HF-SCs and the limb had more overlap than SOX9 DNA binding sites in the E12.5 vertebral column and limb. On the other hand, the vertebral column study used a different SOX9 antibody (R&D Systems AF3075), which may account for the lower degree of overlap between libraries or it may be that vertebral column cells have a very different SOX9-initiated transcriptional program from the limb. Comparisons of SOX9 ChIP-Seq data sets in different cell types

highlight the extremely context dependent role of SOX9 and supports that regulation of SOX9 and of its target genes is likely dependent on the binding of its co-factors in different tissues.

In the embryonic limb SOX9 and SOX5/6 are known to work together to regulate chondrogenic genes like *Aggrecan* as the SOX trio (48) and therefore I compared our SOX9 ChIP-Seq data to SOX4 ChIP-Seq data as it is expressed in the developing heart valves (130) and SOXC factors such as SOX4 are also known to be important in limb development (156). The only SOX4 ChIP-Seq data available used B-cells as a source of tissue (127). Remarkably, the degree of overlap between the SOX9 DNA binding sites in the AVC and limb and SOX4 DNA binding in B cells was as high as the comparisons with SOX9 HF-SC DNA binding sites. This data suggests that SOX9 and SOX4 could be functioning together to regulate their targets and may have similar roles as they are bound in same regions of the genome even within different cell types. If the SOX4 ChIP-Seq was performed on a more relevant cell type, the degree of overlap between SOX9 and SOX4 DNA binding sites would likely be higher. Since SOX4 is a direct target of SOX9, the ability of SOX4 to act as a co-factor of SOX9 would likely be dependent on SOX9-mediated activation of SOX4 and consequently SOX4 and SOX9 may work together on genes necessary for later stages of heart valve development.

An EVI1 (*Mecom*) motif was identified by oPOSSUM as a potential co-factor of SOX9 and has been shown to have a role in heart valve development (131). The only publicly available EVI1 ChIP-Seq data set was on human OC cells (128). The comparison of SOX9 and EVI1 DNA binding sites did not show a high degree of overlap between these tissues. However, a follow up study from the same group that generated the EVI1 ChIP-Seq, demonstrated that genes known to be implicated in congenital heart defects were targets of EVI1 in OC cells (131). SOX9 peaks that contain EVI1 motif suggest that SOX9 and EVI1 may function together to

regulate valve-specific genes during heart valve development. Overall, this analysis suggests that SOX4 and EVI1 may function as co-factors together with SOX9 to regulate different subsets of genes during development. Future studies will be directed at understanding the critical co-factors of SOX9 and how they regulate their target genes together during heart valve and limb development.

7.3 SOX9 negative mesenchyme was absent in the *Sox9fl/fl;VEC* heart valves

The *Sox9* mutant (*Sox9fl/fl;VEC*) was generated to determine how SOX9 transcriptional target genes are affected by the loss of SOX9 in the developing heart valves. To my surprise, no SOX9 negative mesenchyme cells could be identified in the developing heart valves at any of the time points that were examined. Initially one would assume that the *VE-Cre* deletion was inefficient and was not deleting in the AVC mesenchyme cells, however the *Sox9* mutants had significantly smaller cardiac cushions suggesting that *Cre* was in fact deleting in at least some portion of the cells. Although SOX9 should be deleted as early as E9.5 in the AVC, SOX9 has been shown to be a long lived protein and perhaps explaining the presence of SOX9 positive mesenchyme in *Sox9* mutants. Additionally, examination of *Sox9* transcript levels in the *Sox9* mutant AVCs revealed that *Sox9* transcript levels were not significantly affected when compared to WT.

So, why are the *Sox9* mutant valves so much smaller than the WT? One possibility is that when *Sox9* is deleted by *VE-Cre* in the endothelium, the cells undergo apoptosis immediately and never become mesenchyme and as a result fewer mesenchymal cells are migrating into the AVC. SOX9 positive mesenchyme present in the *Sox9* mutant AVCs could be due to cells escaping complete *VE-Cre* deletion and proliferating. In order to completely delete *Sox9* both alleles have to be deleted and it is possible that *Cre* is only efficiently deleting one allele. Due to

the lower numbers of mesenchymal cells in the valves, the cushion size was reduced compared to WT. However, data from other SOX9 mutant mice suggests it is possible to detect apoptotic SOX9 negative cells. For example, when *Sox9* was deleted in the limb, they found that apoptotic domains were expanded in SOX9 mutants within a specific zone of chondrocytes (45). On the other hand, deletion of *Sox9* in the heart valves using another epithelial-specific *Cre* (*Tie2-Cre*) did not identify any differences in the levels of apoptosis between WT and *Sox9* mutants but rather they found decreased levels of proliferation in cells with *Sox9* deletion (46,69). We also observed this in our work on the *Sox9* cKO using *Tie2-Cre*. Although apoptosis of SOX9 negative cells may not be a likely explanation for the defect seen in the *Sox9fl/fl;VEC* mutant valves as these studies examined the entire AVC cushions. It may be that increased apoptosis only occurs in the AV endocardium or specific regions of the AVC ie. proliferating versus differentiating mesenchyme. It is difficult to distinguish these regions within the AVC as there are currently no known markers for proliferating and differentiating zones of the valves.

Another possibility for the less severe phenotype and presence of SOX9 positive mesenchyme in the *Sox9* mutants is that there may be contribution of SOX9 positive cells from other mesenchymal cell sources in the heart such as the epicardium and the mesenchymal caps on the atrial and ventricular septums. These different cell types could migrate into the AVC region as a result of the mutant heart being under stress from insufficient blood circulation and increased pressure/demand on the heart. One famous example of other cell types migrating into the heart from other regions of the embryo is in OFT development where the neural crest cells migrate into the OFT and give rise parts of the valves and great arteries (157). The contribution of SOX9 positive mesenchyme from the septal mesenchymal caps to *Sox9* mutant valves is less likely as the mesenchymal caps of the septums are derived through EMT (124) and would be

affected by the deletion of *Sox9* by *VE-Cre*. The involvement of the epicardial cells migrating into the *Sox9* mutant valve region is much more likely as epicardial cells are derived from a completely separate lineage (158,159) and would not be affected by *VE-Cre.* Epicardial cells have already been shown to migrate in the AV valve region in WT valves as another group demonstrated by lineage tracing that they contribute to the parietal leaflet of the AV valves at later stages of heart valve development (160). However, further studies using lineage tracing would be required to demonstrate whether epicardial cells can migrate into *Sox9* mutant AV valves. Another alternative is that the *VE-Cre* is less efficient at driving recombination than *Tie2-Cre* and to rule out this possibility further experiments must be performed.

Although SOX9 protein is maintained during later stages of heart valve development in the *Sox9* mutant valves, it appears that the hearts were undergoing some forms of stress due to the decreased valve mesenchyme cell numbers. In postnatal *Sox9* mutant heart valves, the chamber size was decreased and ventricular thickness appeared to be greatly increased. The increased ventricular thickness may be indicative of cardiac hypertrophy and therefore increased and prolonged stress in the *Sox9* mutant hearts when compared to WT. The cardiac hypertrophy seen in the postnatal *Sox9* mutant myocardium might suggest that the *Sox9* mutant valves are not functioning properly and leading to the increased stress on the heart. Given that and the fact that *Sox9* mutants survived to adulthood, I wanted to see if older adult *Sox9* mutants of approximately one year show signs of heart valve disease such as altered structure/composition of the ECM of the adult heart valves, calcification, or increased thickness of the developing heart valves. Hematoxylin and eosin staining on the adult *Sox9* mutant valves demonstrated that the mutant valves had a slight thickening at the base of the valves and may be indicative of floppy valves that can lead to regurgitation of blood flow. However, the differences in valve thickness

were minimal and animal numbers were not high enough to provide significance. Further analysis of adult *Sox9* mutant valves is required to determine if there is any indication of valve disease. Surprisingly, the adult *Sox9* mutant ventricular myocardium did not show the overtly increased thickness as seen in the postnatal *Sox9* mutant hearts. It is possible that *Sox9* mutant mice that survive up to a year may not develop cardiac hypertrophy and *Sox9* mutant mice that do develop signs of cardiac hypertrophy may not survive until this time point. In addition, the variation seen in adult *Sox9* mutant hearts could also be due to inefficient deletion by *VE-Cre* or the variability in timing of Cre deletion. Further analysis of the *Sox9* mutant mice is required to determine if there are any signs of heart valve disease or if these mice develop a way to recover from the loss of SOX9 positive mesenchyme during heart valve development.

7.4 Confirmation that *Sox9* cKO (*Sox9fl/f;Tie2-Cre*) valves have decreased size and proliferation that leads to major heart defects and embryonic death

Given that the *Sox9* mutants derived from *VE-Cre* deletion did not result in *Sox9* negative mesenchymal cells in the AVC, I decided to look into other options for *Sox9* deletion in the valves. Previous work demonstrated that *Sox9* deletion using *Tie2-Cre* leads to embryonic lethality between E11.5-14.5 with hypoplastic cardiac cushions, decreased mesenchyme proliferation and altered ECM (46). A similar phenotype was observed in this study and I noted several additional phenotypes not mentioned by the previous work such as a delay in septation and decreased myocardial thickness in the *Sox9* cKO. The delay in septation may occur due to the decreased AVC cushion size and therefore making it more difficult for septal fusion with the AVC. Alternatively, since *Tie2-Cre* deletes SOX9 in the mesenchymal cap of the atrial septum as it is derived through EMT (124), the migration/growth of the septum guided by the

mesenchymal cap towards the AVC cushions could be affected. The size of the atrial mesenchymal cap was greatly reduced in size and almost absent in some *Sox9* cKO hearts while their WT counterparts' septums had already fused. Further analyses would be required to determine the exact cause of the delayed septation in *Sox9* cKO hearts.

The decreased myocardial thickness was a bit perplexing as SOX9 is not expressed in the myocardium. The epicardial population surrounding the myocardium express SOX9 which is not affected by *Tie2-Cre* deletion and these cells do not migrate into the myocardium until later stages of heart development to form the coronary vasculature, smooth muscle cells, and cardiac fibroblasts (124). Since there are no cells within the myocardium that would be affected by *Tie2-Cre* deletion, it would be more likely that the thinning of the myocardial walls may be a defect secondary to valve abnormalities that lead to increased stress or pressure on the heart due insufficient regulation of blood flow. Overall, the data supports that SOX9 is a critical regulator of heart valve formation as found previously by the Yutzey laboratory. To understand the septal and myocardial defect, further studies of the embryonic *Sox9* cKO hearts using echocardiography to determine how the hearts chambers and valves are functioning and to detect areas of damage or Doppler ultrasound to examine blood flow.

Unlike the *VE-Cre*, the *Sox9* cKO heart valves generated using *Tie2-Cre* has SOX9 negative mesenchyme that can be easily detected. Although both *VE-Cre* and *Tie2-Cre* are presumably both endothelial specific *Cre* driver strains, they have very different outcomes in the heart where *Sox9fl/fl;VE-Cre* (*Sox9* mutants) are not embryonic lethal and survive to adulthood with smaller valves that contain SOX9 positive mesenchyme whereas the *Sox9fl/fl;Tie2-Cre* (*Sox9* cKO) are embryonic lethal with SOX9 negative mesenchyme in the heart valves. However, *Sox9* deletion by *VE-Cre* also suggests that SOX9 may have a very critical role in the

endothelium as endothelial cells with *Sox9* deletion were never detected as SOX9 negative mesenchyme in the heart valves. This indicates that EMT may have never occurred in the *VE-Cre* or the *Sox9* deleted cells perished immediately following EMT. This leads to the question: why do the *Sox9* cKO valves have such a different phenotype from the *Sox9* mutant valves? One possibility is that in the *Tie2-Cre* driver strain, *Cre* is still expressed in the endothelium and early mesenchyme cells that have just undergone EMT whereas the *VE-Cre* expression is more restricted to the endothelium. Thus, *Tie2-Cre* allows for a longer time for *Sox9* to be deleted in the AVC mesenchyme thus giving a more severe embryonic phenotype.

The *Tie2-Cre* driver strains was not completely efficient in *Sox9* deletion as SOX9 positive mesenchyme was detected in the *Sox9* cKO heart valves and suggests some cells escaped deletion by *Cre* and were able to populate the heart valves. This is a major caveat in using these *Sox9* cKO mice to understand the role of SOX9 in the developing heart valves and therefore careful analyses of the extent of *Sox9* deletion in the heart valves is required. For downstream analyses, the *Sox9* cKO valves were evaluated for SOX9 protein or *Sox9* transcript levels to determine which *Sox9* cKOs had efficient loss of SOX9.

Before proceeding onto additional analyses, I confirmed that the *Sox9* cKO heart valves had a decrease in cell proliferation as was seen in the previous publication (46). I observed that the number of phospho histone H3 positive cells was reduced in the AVC region of the *Sox9* cKO hearts when compared to WT. I next looked at a cell cycle marker, cyclin D1. To progress through cell cycle appropriately and to continue to proliferate quickly, cyclin D1 must be rapidly moved between the nucleus and cytoplasm and subsequently degraded (reviewed in (161)). Interestingly, cyclin D1 was found in a subset of SOX9 negative mesenchymal cells and cyclin D1 was localized within the cytoplasm in the *Sox9* cKO heart valve. Similar to our findings,

another study published that knockdown of SOX9 in rat mesenchymal stem cells caused reduced proliferation and increased levels and stability of cyclin D1 (60). Cyclin D1 is not a target of SOX9 in the AVC however it could be that one of its downstream regulators are affected by loss of SOX9, such as the F-box proteins (such as *Fbxw8* that is targeted by SOX9) that are known to degrade cyclin D1 in the cytoplasm. Also, the lack of cyclin D1 degradation could account in part for the slowed/reduced proliferation in the *Sox9* cKO heart valves.

7.5 Identification and regulation of SOX9 target genes in the developing heart valves

Although many studies have alluded to the role of SOX9 in proliferation and other cellular processes, there has been little progress in understanding the downstream targets of SOX9 and how gene expression is altered in the absence of SOX9. Therefore, I generated transcriptome profiles from the WT and *Sox9* cKO heart valves to determine which transcripts were altered upon loss of *Sox9* in the E12.5 heart valves. Transcriptome analysis on E12.5 WT and *Sox9* cKO valves revealed that down-regulated genes in the *Sox9* cKO valves were heavily involved in processes critical for heart development such as mesenchymal cell proliferation, EMT, and endocardial cushion morphogenesis whereas up-regulated genes were mostly involved in stress related functions. The down-regulated category of genes had the most heart valve specific functions and correlates nicely with the fact that SOX9 is known to be an activator more than a repressor of transcription. To rule out any bias in the RNA-Seq libraries, I compared the RNA-Seq data to a published list of AV-enriched genes (142) and found that approximately 60% of these genes did not substantially change in expression levels and supports that there is not an overall loss of valve specific genes in the *Sox9* cKO valves. Housekeeping genes are also not drastically altered in the *Sox9* cKO valves.

To discover critical targets of SOX9 in the heart valves, I compared genes with altered expression in the *Sox9* cKO (>1.5 fold change) with the gene targets identified in the SOX9 AVC ChIP-Seq library. This analysis revealed 139 genes that were both a SOX9 target in the AVC and have altered expression in the *Sox9* cKO valves. Of these, three quarters were down-regulated and one quarter up-regulated in gene expression. In general, the changes in gene expression of SOX9 targets in the *Sox9* cKO AVC were not substantial. This suggests that SOX9 is involved in fine tuning gene expression rather than acting as an on/off switch. It is also possible that SOX9 may have another unknown role other than regulating transcriptional activity of its targets. For example, SOX9 has been suggested in other systems to alter chromatin dynamics near regions densely populated with enhancers termed super enhancers (63). Additionally, SOXE factors like SOX10 have been shown to have DNA bending capabilities (162) and it could be that SOX9 also bends DNA to bring complexes of transcription factors together to regulate gene expression.

7.6 SOX9 directly controls genes associated with proliferation across cell types

To better understand SOX9's context independent roles in multiple cells types, I compared three SOX9 ChIP-Seq data sets (AVC, Limb, and HF-SCs) and showed that nearly 300 SOX9 binding sites were located at the exact same genomic location across these three different tissues. Nearly a third of these shared SOX9 binding sites are associated with genes that are involved in proliferation, which supports the potential role for SOX9 in maintaining a proliferative state during embryonic development. Numerous publications over the years have drawn links between SOX9 and proliferation. However, a direct mechanistic connection via its transcriptional targets has remained elusive. In AVC, limb and HF-SCs, SOX9 directly targets the TFs: *Fos*, *FosL1*,

and *FosL2* suggesting that SOX9 can regulate their mRNA expression levels. FOS and JUN family members heterodimerize, to form the AP-1 complex, which is known to regulate cell proliferation and cell survival, in part via cyclin D1 expression (163). In mesenchymal stem cells, a stable SOX9 knockdown caused reduced proliferation, delayed S-phase progression, and increased cyclin D1 protein stability (60). I also observed that cyclin D1 protein was increased in SOX9-deficient heart valves, suggesting that SOX9 may play a role in the progression through S-phase via regulation of cyclin D1. Of note; *Junb* is occupied by SOX9 in its regulatory regions. JUNB is best known to inhibit cell growth by antagonizing c-JUN activity although this is highly context dependent (163). In this study, *Fos* and *Junb* transcripts were up-regulated in SOX9-deficient AVCs, suggesting that their uncontrolled and altered mRNA expression levels may in part contribute to organ hypoplasia seen in *Sox9* mutants.

In addition to AP-1 factors, several other genes known to have roles in cell proliferation have SOX9 binding within their regulatory regions, including *Cops5*, *Srpk2*, *Akt2*, *Eed*, *Hdac1*, *Hdac2*, *p53* (*Trp53*) and *protein kinase A* (*Prkaca,* PKA) in all three tissues examined. COPS5 associates with JUN proteins to increase binding specificity and can degrade the cell cycle inhibitor p27Kip1 (164). Loss of *Cops5* in embryonic limb results in shortened limbs due to impaired chondrogenesis and *Sox9* levels were decreased in mutant long bones (165) suggesting a potential feedback loop between SOX9 and COPS5. Additionally the kinase, SRPK2 can promote proliferation and cell cycle progression by enhancing Cyclin D1 levels (166). While AKT2, another kinase targeted by SOX9, regulates progression of cell cycle via phosphorylation of its targets. These phosphorylation targets of AKT2 include the cyclin-dependent kinase inhibitors. Additionally, AKT2 maintains protein stability of important cell cycle regulators such as c-MYC and D-type cyclins via Gsk3β during cell cycle (167).

Interestingly, several epigenetic regulators, EED, HDAC1 and HDAC2 were identified as commonly targeted by SOX9 and are associated with cell proliferation (168,169). Although HDACs are classically known for their roles in deaceylation and transcriptional repression, there is evidence that points to a more general role in proliferation. In both *Hdac1/2* knockout and knockdown experiments, proliferation was decreased and inhibitors of HDACs exhibit similar anti-proliferative effects (reviewed in (169)). Altered proliferation levels associated with *Hdac1/2* loss or inhibition may be attributable to the requirement of a fine balance between transcriptional activation and repression within cells. *Eed* is part of the Polycomb repressive complex (PRC) 2 complex that is involved in trimethylation of histone H3 lysine 27 (H3K27me3) leading to transcriptional repression. PRC2 members, EZH2 and EED, are controlled by E2F transcription factors and are required for cell proliferation (168). Together, E2F and the PRC2 members, EZH2 and EED, mediate the functions of the pRB-E2F growth control pathway. Of interest, inactivation of EZH2 in the developing heart causes major congenital heart defects such as defects of the ventricular septum, hypertrabeculation, and hypoplasia of the myocardium (170).

Although not identified as a common target in the HF-SCs, SOX9 occupied the regulatory regions associated with p53 (TRP53) and protein kinase A (*Prkaca*) in the AVC and limb, of which both of these factors have known roles in cell proliferation. p53 activates DNA repair and arrests proliferation by pausing cell cycle to fix DNA damage and if the damage is severe, p53 initiates cell death (171). PKA is induced by cyclic adenosine monophosphate (cAMP) and regulates cellular growth and proliferation through a variety of mechanisms (172). Of note, PKA phosphorylates SOX9 and increases its activity during chondrogenesis (173). The activities of

p53 and PKA in cell proliferation may be specific to mesenchyme as SOX9 binding sites are only found in AVC and limb.

A major caveat of my work demonstrating that SOX9 activates and promotes cell cycle as a common role of SOX9 across many cell types is that SOX9 has also previously been shown to be involved in suppression of proliferation and cell cycle in other cell types such as the intestinal epithelial cells of the crypt (174). This could be related to the fact that SOX9 may play an important role in the switch between proliferation and differentiation. In general cells must exit cell cycle and stop proliferating to differentiate, however there are always exceptions to the rule. In the intestinal epithelial stem/progenitor cells it has been shown that different levels of SOX9 promote (low level) or suppress proliferation (high levels) (174). This highlights the importance of understanding the level of SOX9 expression and in which context you are examining for the function of SOX9. Another situation where SOX9 has been shown opposing roles in proliferation is in cancers. For example, in some colorectal cancers high levels of SOX9 have been associated with more aggressive and proliferative subtypes while at the same time it has been shown to decrease the tumorigenicity in other colorectal cancer cells (64). This discrepancy for the role of SOX9 in colorectal cancers is likely due to the origins of the cancer initiating cells in these cancer subtypes and emphasizes that it is crucial to understand the context in which the functions of SOX9 are studied.

Taken together, our data suggests that SOX9 promotes proliferation across heart valve and limb mesenchyme cell types during development via binding to promoters and enhancers of critical regulators like AP1 proteins, kinases, and histone modifiers.

7.7 SOX9 is a master regulator of a core network of TFs in heart valve development

By comparing transcriptome analysis in *Sox9* mutant mice with genome wide SOX9 binding sites in the AVC, I have identified many potential SOX9 target genes that may be critical for valve formation, including ECM related genes and transcription factors. Interestingly, SOX9 targets that were down-regulated in the *Sox9* cKO valves included numerous critical transcription factors known to be involved in heart development, such as *Lef1*, *Pitx2* and *Hand2*. Loss of *Lef1* (via TBX20 deletion), *Pitx2* and *Hand2* are all known to be associated with heart valve defects (175-177). The most highly down-regulated, SOX9-targetted TFs in *Sox9* cKO valves were *Twist1*, *Sox4*, and *Mecom/Evi1*. Similar to SOX9, TWIST1, SOX4 and Mecom/EVI1 are highly expressed in the cardiac cushions during development and mutation of these factors leads to major valve abnormalities which are embryonic lethal (130,131,178).

SOX proteins are known to regulate other transcription factors that will function as their future co-factors (47). For instance, SOX9 regulates and cooperates with SOX5/6 to regulate target genes in the developing limb (48) and corroborating this, both SOX5/6 were targeted by SOX9 in the SOX9 limb ChIP-Seq library. Similarly, SOX9 may activate SOX4 in the heart to help co-regulate heart valve-specific genes. Motif analysis on SOX9 bound regions in the AVC revealed EVI1 as another potential co-factor for SOX9 and comparison of EVI1 bound regions in cancer cells (128) with SOX9 AVC bound regions identified hundreds of potentially overlapping target genes (Hoodless lab, unpublished). This supports a model in which EVI1 is a co-factor of SOX9 in the developing heart valves.

TWIST1 is well known to be associated with EMT in many different systems (reviewed in (179)). Here, I have shown that SOX9 can modulate the level of *Twist1* expression in the developing valves via qRT-PCR. In the SOX9-deficient heart valves, *Twist1* transcript levels

were reduced by approximately 3 fold in the valve mesenchyme by qRT-PCR. TWIST1 has been previously shown to have important roles in the developing heart valves. For example, TWIST1 can induce proliferation and migration of valve mesenchyme during early valve formation (180,181) and following EMT, TWIST1 plays a role in regulating differentiation of the AVC mesenchyme (182). Additionally, when TWIST1 persists at later stages of valve development, it leads to increased mesenchyme proliferation, increased TBX20 expression, and more primitive ECM composition (181) resembling a more early embryonic valve phenotype. Of interest, it has been shown that TWIST1 directly regulates *Tbx20* (183). Our study found that TBX20 was a SOX9 target with down-regulated transcript levels in the *Sox9* cKO valves. This suggests that TWIST1 and SOX9 may cooperate to regulate *Tbx20* in developing heart valves.

Taken together, the correlation of transcriptome analysis and ChIP-Seq analysis reveals that SOX9 regulates a core regulatory network of transcription factors that are required at various steps of heart valve development. It should be noted that loss of SOX9 in the heart valves alters transcript expression levels modestly. Thus the role of SOX9 may be to modulate the level of gene regulation rather than to absolutely activate or repress gene expression. Nevertheless, the number of critical TFs that are known to be involved in heart valve development targeted by SOX9 and have reduced mRNA expression in the *Sox9* cKO heart valves is remarkable and suggests that their combined loss of expression may explain the lethal phenotype observed in the *Sox9* cKO embryos. Intriguingly, many of the TFs regulated by SOX9 also have been suggested to regulate each other's expression such as TWIST1, which has been shown to regulate *Tbx20* (183) and TBX20 in turn has been shown to regulate LEF1 (177). EVI1 can regulate SOX4 and alters its expression (131) and EVI1 and SOX4 can collaborate together

to regulate gene expression in myeloid leukemia (184). This illustrates how networks of transcription factors are working together to generate the heart valves during development.

Recently, SOX9 has been show to regulate chromatin dynamics near super enhancers in HF-SCs (63). Super enhancers are a cluster of enhancers that have been shown to be connected to genes that are associated with tissue identity. It is possible that binding of SOX9 to locations near many essential heart transcription factors to allows for activation of these regions and promote further valve cell differentiation. This illustrates the complex interactions that occur at multiple levels in heart valve development and suggests that these essential TFs are regulated in numerous ways to ensure proper valve formation. This work establishes that SOX9 and its transcriptional target TFs form a critical gene regulatory network to drive valve morphogenesis. In humans, aberrant expression of SOX9 and its transcriptional targets have been associated with adult heart valve disease (31). Thus, understanding the SOX9 initiated transcriptional networks in heart valve development may provide additional insights into adult heart valve disease.

7.8 Examination of other defined roles of SOX9 in EMT and ECM generation

Although SOX9 has been implicated in the process of EMT in neural crest cells, this study did not find any overt differences in EMT markers at the transcript level or at the protein level in the E12.5 *Sox9* cKO heart valves. This suggests that perhaps in the developing heart valves that SOX9 is not essential for EMT but may necessary for the maintenance and survival of the AVC mesenchyme cells. In contrast, the phenotype of the *Sox9fl/fl;VE-Cre* mice indicates there may be an early role for SOX9 in EMT and that *Sox9*-deficient endocardial cells may never undergo EMT. Another study where *Sox9* null embryos were generated by crossing mice where they conditionally deleted one allele of *Sox9* in oocytes and one *Sox9* allele in spermatids lead to

embryonic death at E11.5-12 due to congestive heart failure and embryos had severely hypoplastic cardiac cushions (69). Further analysis of the *Sox9*-deficient heart valves revealed that SOX9 inhibits EMT following the delamination and preliminary migration of the cells away from the endocardium before they become definitive mesenchyme (69). Of note, I did not detect any SOX9 negative mesenchyme even at the earliest stages of EMT starting at E9.5. Since there is conflicting evidence on the role of SOX9 in EMT, more in depth studies are required to discover the exact role of SOX9 in the heart valves.

SOX9 is well known for its role in regulating ECM production in the successive steps of cartilage formation in the developing limb (reviewed in (41)). Since the limb and heart valves share many similarities in composition and structure, expression of ECM components were analyzed in *Sox9* cKO heart valves. In the absence of *Sox9, Periostin*, *Elastin*, and *Matrix Gla protein* transcripts were reduced as identified by qRT-PCR and RNA-Seq analysis. Additional ECM components such as *Col9a1*, *Col9a3*, *Prelp*, *Col6a6*, *Mfap4*, *Matn4*, etc were also reduced in the *Sox9* cKO AVC RNA-Seq library. All of the aforementioned ECM components are all targets of SOX9 in the AVC ChIP-Seq library. PERIOSTIN has been shown to have a critical role in AV valve development by binding integrins and linking intracellular kinase dependent signalling (185) and is required for AVC mesenchyme maturation and ECM compaction (186). However, analysis of PERIOSTIN protein levels in WT and *Sox9* cKO valves demonstrated that PERIOSTIN was not reduced in the *Sox9* cKO AVC and almost seemed up-regulated compared to overall valve area. However, a small number of SOX9 positive mesenchyme remained in the *Sox9* cKO valves that could be secreting higher levels of PERIOSTIN to compensate for decreased transcript levels in the SOX9 negative mesenchyme. *Elastin* is another interesting molecule as it is required to maintain the elasticity of the adult heart valves and would be

appealing to investigate further. Future analyses of the relationship between SOX9 and ECM would be focused on developing a better understanding of heart valve ECM composition during development and how it is altered upon loss of *Sox9* in the heart valves.

7.9 Concluding remarks

In this work, I have analyzed the global *in vivo* transcriptional targets of SOX9 in the embryonic heart valves and limb generated from ChIP-Seq libraries previously made in our lab (R. Cullum for ChIP and GSC for sequencing). For the first time, thousands of SOX9 binding sites have been revealed in the heart valves and limb and will provide an excellent resource for future research by our lab and others upon publication (Garside et al., accepted). Understanding of the downstream transcriptional targets of SOX9 in embryonic tissues is extremely limited and to my current knowledge the only embryonic SOX9 ChIP-Seq library was performed on the vertebral column (125) as was discussed earlier in this study. Surprisingly, the minority of studies are composed of ChIP-Seq from embryonic tissues while the majority of ChIP-Seq is performed on cell lines or embryonic stem cells and thus making this data even more valuable to the field. Future analyses should be focused on further understanding the transcriptional targets of SOX9 in a given tissue and how SOX9 transcriptional targets change throughout the development of a tissue. In this study, I have shown that SOX9 is expressed throughout heart valve development. It has been proposed by us and others that SOX9 likely changes its roles during tissue formation and this change in roles is highly dependent on its co-factors. Therefore, SOX9 binding should be analyzed dynamically over time within an embryonic tissue with a specific focus on identifying its binding partners as they are likely guiding the change in the role of SOX9 over time.

To gain a better understanding of the function of SOX9 it is extremely valuable to generate a *Sox9*-deficient mouse model to analyze the changes that occur upon the loss of *Sox9* in the heart valves. Therefore, in this study I had generated two *Sox9* mutant models using the Cre/Lox system: *Sox9fl/fl;VE-Cre* and *Sox9fl/f;Tie2-Cre* mutant mice which deletes *Sox9* specifically in endothelial cells and subsequently the heart valve mesenchyme. Since the goal of this investigation was to analyze the heart valves in absence of *Sox9,* the *Sox9fl/fl;VE-Cre* mice were not suitable for this purpose as SOX9 negative mesenchyme could not be detected in the embryonic heart valves. Examination of the *Sox9fl/fl;VE-Cre* mice revealed an unexpected phenotype and future analysis should be focused on teasing out the role of SOX9 in the endothelium itself or within the early EMT stages before becoming fully mesenchymal. Fortunately, SOX9 negative mesenchyme could be detected in the *Sox9fl/fl;Tie2-Cre* (*Sox9* cKO) mutant heart valves and could be used for our downstream analyses. Furthermore, proliferation defects were confirmed in the *Sox9* cKO heart valves, which is a common feature of many organs in which *Sox9* is deleted. This suggests that a common role of SOX9 may be involved in proliferation. To examine this further, I compared SOX9 binding sites from other tissues with our data and identified a subset of commonly targeted genes that were involved in proliferation. Taken together this data suggests that SOX9 has both context independent and context dependent roles. Future work should focus on how exactly SOX9 regulates each of the different processes that occur during proliferation and cell cycle and focus in on critical regulators like the AP1 proteins like *Junb* and *Fos* and as well as critical factors like p53. Additionally, although SOX9 has been generally shown to be an activator of transcription, my work has also shown that SOX9 can act as repressor for factors such as *Junb*. Understanding how SOX9 represses its targets could also be an interesting avenue to follow up in the future.

To uncover the context dependent and critical targets of SOX9 in the heart valves, I generated transcriptome profiles from WT and *Sox9fl/fl;Tie2-Cre* mutant heart valves using RNA-Seq and compared them with the SOX9 binding sites in the heart valves. This analysis generated a short list of 139 critical genes were both SOX9 targets in the heart valves and have altered expression in the *Sox9* cKO heart valves. Strikingly, a high number of these were transcription factors that had known roles in the developing heart and suggest that SOX9 regulates a heart specific transcriptional network to guide heart valve formation. Further studies should focus on how all of these critical transcription factors work together to form the heart valves. Taken together, there are many avenues to be followed up to get a better handle on the function of SOX9 and this is only just touching on the vast interactions and processes that SOX9 is involved in during development. This data has identified a number of key factors involved in early valve formation that are regulated by SOX9 and hopefully in turn, these could be used as predictive factors of heart disease, or as targets for new therapeutic strategies for heart valve disease and congenital heart valve defects. As SOX9 is involved in development of many different organ systems as well as implicated in a variety of diseases, this data may provide new insights on the role of SOX9 and its transcriptional network within a diverse group of organs and diseases.

REFERENCES

1. Miquerol, L. and Kelly, R.G. (2013) Organogenesis of the vertebrate heart. *Wiley Interdiscip Rev Dev Biol*, **2**, 17-29.
2. Abu-Issa, R. and Kirby, M.L. (2007) Heart field: from mesoderm to heart tube. *Annu Rev Cell Dev Biol*, **23**, 45-68.
3. Hinton, R.B. and Yutzey, K.E. (2011) Heart valve structure and function in development and disease. *Annu Rev Physiol*, **73**, 29-46.
4. Combs, M.D. and Yutzey, K.E. (2009) Heart valve development: regulatory networks in development and disease. *Circ Res*, **105**, 408-421.
5. Snarr, B.S., Kern, C.B. and Wessels, A. (2008) Origin and fate of cardiac mesenchyme. *Dev. Dyn.*, **237**, 2804-2819.
6. Person, A.D., Klewer, S.E. and Runyan, R.B. (2005) Cell biology of cardiac cushion development. *Int Rev Cytol*, **243**, 287-335.
7. Camenisch, T.D., Molin, D.G., Person, A., Runyan, R.B., Gittenberger-de Groot, A.C., McDonald, J.A. and Klewer, S.E. (2002) Temporal and distinct TGFbeta ligand requirements during mouse and avian endocardial cushion morphogenesis. *Dev Biol*, **248**, 170-181.
8. Schroeder, J.A., Jackson, L.F., Lee, D.C. and Camenisch, T.D. (2003) Form and function of developing heart valves: coordination by extracellular matrix and growth factor signaling. *J Mol Med (Berl)*, **81**, 392-403.
9. Markwald, R.R., Fitzharris, T.P. and Manasek, F.J. (1977) Structural development of endocardial cushions. *Am J Anat*, **148**, 85-119.
10. Restivo, A., Piacentini, G., Placidi, S., Saffirio, C. and Marino, B. (2006) Cardiac outflow tract: a review of some embryogenetic aspects of the conotruncal region of the heart. *Anat Rec A Discov Mol Cell Evol Biol*, **288**, 936-943.
11. Hinton, R.B., Jr., Lincoln, J., Deutsch, G.H., Osinska, H., Manning, P.B., Benson, D.W. and Yutzey, K.E. (2006) Extracellular matrix remodeling and organization in developing and diseased aortic valves. *Circ Res*, **98**, 1431-1438.
12. Hinton, R.B., Jr., Alfieri, C.M., Witt, S.A., Glascock, B.J., Khoury, P.R., Benson, D.W. and Yutzey, K.E. (2008) Mouse heart valve structure and function: echocardiographic and morphometric analyses from the fetus through the aged adult. *Am J Physiol Heart Circ Physiol*, **294**, H2480-2488.
13. Aikawa, E., Whittaker, P., Farber, M., Mendelson, K., Padera, R.F., Aikawa, M. and Schoen, F.J. (2006) Human semilunar cardiac valve remodeling by activated cells from fetus to adult: implications for postnatal adaptation, pathology, and tissue engineering. *Circulation*, **113**, 1344-1352.
14. Butcher, J.T. and Markwald, R.R. (2007) Valvulogenesis: the moving target. *Philos Trans R Soc Lond B Biol Sci*, **362**, 1489-1503.
15. Kruithof, B.P., Krawitz, S.A. and Gaussin, V. (2007) Atrioventricular valve development during late embryonic and postnatal stages involves condensation and extracellular matrix remodeling. *Dev Biol*, **302**, 208-217.
16. Sacks, M.S. and Yoganathan, A.P. (2007) Heart valve function: a biomechanical perspective. *Philos Trans R Soc Lond B Biol Sci*, **362**, 1369-1391.
17. Vesely, I. (1998) The role of elastin in aortic valve mechanics. *J Biomech*, **31**, 115-123.

18. de Lange, F.J., Moorman, A.F., Anderson, R.H., Manner, J., Soufan, A.T., de Gier-de Vries, C., Schneider, M.D., Webb, S., van den Hoff, M.J. and Christoffels, V.M. (2004) Lineage and morphogenetic analysis of the cardiac valves. *Circ Res*, **95**, 645-654.
19. Lincoln, J., Alfieri, C.M. and Yutzey, K.E. (2004) Development of heart valve leaflets and supporting apparatus in chicken and mouse embryos. *Dev Dyn*, **230**, 239-250.
20. Wessels, A., van den Hoff, M.J., Adamo, R.F., Phelps, A.L., Lockhart, M.M., Sauls, K., Briggs, L.E., Norris, R.A., van Wijk, B., Perez-Pomares, J.M. *et al.* (2012) Epicardially derived fibroblasts preferentially contribute to the parietal leaflets of the atrioventricular valves in the murine heart. *Developmental biology*, **366**, 111-124.
21. Liu, A.C., Joag, V.R. and Gotlieb, A.I. (2007) The emerging role of valve interstitial cell phenotypes in regulating heart valve pathobiology. *Am J Pathol*, **171**, 1407-1418.
22. Garside, V.C., Chang, A.C., Karsan, A. and Hoodless, P.A. (2013) Co-ordinating Notch, BMP, and TGF-beta signaling during heart valve development. *Cellular and molecular life sciences : CMLS*, **70**, 2899-2917.
23. Xiao, H. and Zhang, Y.Y. (2008) Understanding the role of transforming growth factor-beta signalling in the heart: overview of studies using genetic mouse models. *Clin Exp Pharmacol Physiol*, **35**, 335-341.
24. Conway, S.J., Doetschman, T. and Azhar, M. (2011) The inter-relationship of periostin, TGF beta, and BMP in heart valve development and valvular heart diseases. *ScientificWorldJournal*, **11**, 1509-1524.
25. Mohler, E.R., 3rd, Gannon, F., Reynolds, C., Zimmerman, R., Keane, M.G. and Kaplan, F.S. (2001) Bone formation and inflammation in cardiac valves. *Circulation*, **103**, 1522-1528.
26. Kaden, J.J., Bickelhaupt, S., Grobholz, R., Vahl, C.F., Hagl, S., Brueckmann, M., Haase, K.K., Dempfle, C.E. and Borggrefe, M. (2004) Expression of bone sialoprotein and bone morphogenetic protein-2 in calcific aortic stenosis. *J Heart Valve Dis*, **13**, 560-566.
27. Ankeny, R.F., Thourani, V.H., Weiss, D., Vega, J.D., Taylor, W.R., Nerem, R.M. and Jo, H. (2011) Preferential activation of SMAD1/5/8 on the fibrosa endothelium in calcified human aortic valves--association with low BMP antagonists and SMAD6. *PLoS One*, **6**, e20969.
28. Rosenkranz, S. (2004) TGF-beta1 and angiotensin networking in cardiac remodeling. *Cardiovasc Res*, **63**, 423-432.
29. Walker, G.A., Masters, K.S., Shah, D.N., Anseth, K.S. and Leinwand, L.A. (2004) Valvular myofibroblast activation by transforming growth factor-beta: implications for pathological extracellular matrix remodeling in heart valve disease. *Circ Res*, **95**, 253-260.
30. Liu, A.C. and Gotlieb, A.I. (2008) Transforming growth factor-beta regulates in vitro heart valve repair by activated valve interstitial cells. *Am J Pathol*, **173**, 1275-1285.
31. Hulin, A., Deroanne, C.F., Lambert, C.A., Dumont, B., Castronovo, V., Defraigne, J.O., Nusgens, B.V., Radermecker, M.A. and Colige, A.C. (2012) Metallothionein-dependent up-regulation of TGF-beta2 participates in the remodelling of the myxomatous mitral valve. *Cardiovasc Res*, **93**, 480-489.
32. Girdauskas, E., Schulz, S., Borger, M.A., Mierzwa, M. and Kuntze, T. (2011) Transforming growth factor-beta receptor type II mutation in a patient with bicuspid aortic valve disease and intraoperative aortic dissection. *Ann Thorac Surg*, **91**, e70-71.

33. Attaran, S., Sherwood, R., Dastidar, M.G. and El-Gamel, A. (2010) Identification of low circulatory transforming growth factor beta-1 in patients with degenerative heart valve disease. *Interact Cardiovasc Thorac Surg*, **11**, 791-793.
34. Luna-Zurita, L., Prados, B., Grego-Bessa, J., Luxan, G., del Monte, G., Benguria, A., Adams, R.H., Perez-Pomares, J.M. and de la Pompa, J.L. (2010) Integration of a Notch-dependent mesenchymal gene program and Bmp2-driven cell invasiveness regulates murine cardiac valve formation. *J Clin Invest*, **120**, 3493-3507.
35. Timmerman, L.A., Grego-Bessa, J., Raya, A., Bertran, E., Perez-Pomares, J.M., Diez, J., Aranda, S., Palomo, S., McCormick, F., Izpisua-Belmonte, J.C. *et al.* (2004) Notch promotes epithelial-mesenchymal transition during cardiac development and oncogenic transformation. *Genes Dev*, **18**, 99-115.
36. Acharya, A., Hans, C.P., Koenig, S.N., Nichols, H.A., Galindo, C.L., Garner, H.R., Merrill, W.H., Hinton, R.B. and Garg, V. (2011) Inhibitory role of Notch1 in calcific aortic valve disease. *PLoS One*, **6**, e27743.
37. Lincoln, J., Lange, A.W. and Yutzey, K.E. (2006) Hearts and bones: shared regulatory mechanisms in heart valve, cartilage, tendon, and bone development. *Dev Biol*, **294**, 292-302.
38. Chakraborty, S., Cheek, J., Sakthivel, B., Aronow, B.J. and Yutzey, K.E. (2008) Shared gene expression profiles in developing heart valves and osteoblast progenitor cells. *Physiol Genomics*, **35**, 75-85.
39. Long, F. and Ornitz, D.M. (2013) Development of the endochondral skeleton. *Cold Spring Harb Perspect Biol*, **5**, a008334.
40. Mackie, E.J., Tatarczuch, L. and Mirams, M. (2011) The skeleton: a multi-functional complex organ. The growth plate chondrocyte and endochondral ossification. *J Endocrinol*, **211**, 109-121.
41. DeLise, A.M., Fischer, L. and Tuan, R.S. (2000) Cellular interactions and signaling in cartilage development. *Osteoarthritis Cartilage*, **8**, 309-334.
42. Zuscik, M.J., Hilton, M.J., Zhang, X., Chen, D. and O'Keefe, R.J. (2008) Regulation of chondrogenesis and chondrocyte differentiation by stress. *J Clin Invest*, **118**, 429-438.
43. Chakraborty, S., Combs, M.D. and Yutzey, K.E. (2010) Transcriptional regulation of heart valve progenitor cells. *Pediatr Cardiol*, **31**, 414-421.
44. Lange, A.W. and Yutzey, K.E. (2006) NFATc1 expression in the developing heart valves is responsive to the RANKL pathway and is required for endocardial expression of cathepsin K. *Dev Biol*, **292**, 407-417.
45. Akiyama, H., Chaboissier, M.C., Martin, J.F., Schedl, A. and de Crombrugghe, B. (2002) The transcription factor Sox9 has essential roles in successive steps of the chondrocyte differentiation pathway and is required for expression of Sox5 and Sox6. *Genes Dev*, **16**, 2813-2828.
46. Lincoln, J., Kist, R., Scherer, G. and Yutzey, K.E. (2007) Sox9 is required for precursor cell expansion and extracellular matrix organization during mouse heart valve development. *Dev Biol*, **305**, 120-132.
47. Kamachi, Y. and Kondoh, H. (2013) Sox proteins: regulators of cell fate specification and differentiation. *Development*, **140**, 4129-4144.

48. Han, Y. and Lefebvre, V. (2008) L-Sox5 and Sox6 drive expression of the aggrecan gene in cartilage by securing binding of Sox9 to a far-upstream enhancer. *Mol Cell Biol*, **28**, 4999-5013.
49. Bondurand, N., Pingault, V., Goerich, D.E., Lemort, N., Sock, E., Le Caignec, C., Wegner, M. and Goossens, M. (2000) Interaction among SOX10, PAX3 and MITF, three genes altered in Waardenburg syndrome. *Hum Mol Genet*, **9**, 1907-1917.
50. Ludwig, A., Rehberg, S. and Wegner, M. (2004) Melanocyte-specific expression of dopachrome tautomerase is dependent on synergistic gene activation by the Sox10 and Mitf transcription factors. *FEBS Lett*, **556**, 236-244.
51. Barrionuevo, F. and Scherer, G. (2010) SOX E genes: SOX9 and SOX8 in mammalian testis development. *Int J Biochem Cell Biol*, **42**, 433-436.
52. Haldin, C.E. and LaBonne, C. (2010) SoxE factors as multifunctional neural crest regulatory factors. *Int J Biochem Cell Biol*, **42**, 441-444.
53. Pritchett, J., Athwal, V., Roberts, N., Hanley, N.A. and Hanley, K.P. (2011) Understanding the role of SOX9 in acquired diseases: lessons from development. *Trends Mol Med*, **17**, 166-174.
54. Wagner, T., Wirth, J., Meyer, J., Zabel, B., Held, M., Zimmer, J., Pasantes, J., Bricarelli, F.D., Keutel, J., Hustert, E. *et al.* (1994) Autosomal sex reversal and campomelic dysplasia are caused by mutations in and around the SRY-related gene SOX9. *Cell*, **79**, 1111-1120.
55. Piper, K., Ball, S.G., Keeling, J.W., Mansoor, S., Wilson, D.I. and Hanley, N.A. (2002) Novel SOX9 expression during human pancreas development correlates to abnormalities in Campomelic dysplasia. *Mech Dev*, **116**, 223-226.
56. Seymour, P.A., Freude, K.K., Tran, M.N., Mayes, E.E., Jensen, J., Kist, R., Scherer, G. and Sander, M. (2007) SOX9 is required for maintenance of the pancreatic progenitor cell pool. *Proc Natl Acad Sci U S A*, **104**, 1865-1870.
57. Rockich, B.E., Hrycaj, S.M., Shih, H.P., Nagy, M.S., Ferguson, M.A., Kopp, J.L., Sander, M., Wellik, D.M. and Spence, J.R. (2013) Sox9 plays multiple roles in the lung epithelium during branching morphogenesis. *Proc Natl Acad Sci U S A*, **110**, E4456-4464.
58. Thomsen, M.K., Butler, C.M., Shen, M.M. and Swain, A. (2008) Sox9 is required for prostate development. *Dev Biol*, **316**, 302-311.
59. Trowe, M.O., Shah, S., Petry, M., Airik, R., Schuster-Gossler, K., Kist, R. and Kispert, A. (2010) Loss of Sox9 in the periotic mesenchyme affects mesenchymal expansion and differentiation, and epithelial morphogenesis during cochlea development in the mouse. *Dev Biol*, **342**, 51-62.
60. Stockl, S., Bauer, R.J., Bosserhoff, A.K., Gottl, C., Grifka, J. and Grassel, S. (2013) Sox9 modulates cell survival and adipogenic differentiation of multipotent adult rat mesenchymal stem cells. *J Cell Sci*, **126**, 2890-2902.
61. Guo, W., Keckesova, Z., Donaher, J.L., Shibue, T., Tischler, V., Reinhardt, F., Itzkovitz, S., Noske, A., Zurrer-Hardi, U., Bell, G. *et al.* (2012) Slug and Sox9 cooperatively determine the mammary stem cell state. *Cell*, **148**, 1015-1028.
62. Kadaja, M., Keyes, B.E., Lin, M., Pasolli, H.A., Genander, M., Polak, L., Stokes, N., Zheng, D. and Fuchs, E. (2014) SOX9: a stem cell transcriptional regulator of secreted niche signaling factors. *Genes & development*, **28**, 328-341.

63. Adam, R.C., Yang, H., Rockowitz, S., Larsen, S.B., Nikolova, M., Oristian, D.S., Polak, L., Kadaja, M., Asare, A., Zheng, D. *et al.* (2015) Pioneer factors govern super-enhancer dynamics in stem cell plasticity and lineage choice. *Nature*.
64. Matheu, A., Collado, M., Wise, C., Manterola, L., Cekaite, L., Tye, A.J., Canamero, M., Bujanda, L., Schedl, A., Cheah, K.S. *et al.* (2012) Oncogenicity of the developmental transcription factor Sox9. *Cancer Res*, **72**, 1301-1315.
65. Wang, H., He, L., Ma, F., Regan, M.M., Balk, S.P., Richardson, A.L. and Yuan, X. (2013) SOX9 regulates low density lipoprotein receptor-related protein 6 (LRP6) and T-cell factor 4 (TCF4) expression and Wnt/beta-catenin activation in breast cancer. *J Biol Chem*, **288**, 6478-6487.
66. Shi, Z., Chiang, C.I., Mistretta, T.A., Major, A. and Mori-Akiyama, Y. (2013) SOX9 directly regulates IGFBP-4 in the intestinal epithelium. *Am J Physiol Gastrointest Liver Physiol*, **305**, G74-83.
67. Sakai, D., Suzuki, T., Osumi, N. and Wakamatsu, Y. (2006) Cooperative action of Sox9, Snail2 and PKA signaling in early neural crest development. *Development*, **133**, 1323-1333.
68. Akiyama, H. (2008) Control of chondrogenesis by the transcription factor Sox9. *Mod Rheumatol*, **18**, 213-219.
69. Akiyama, H., Chaboissier, M.C., Behringer, R.R., Rowitch, D.H., Schedl, A., Epstein, J.A. and de Crombrugghe, B. (2004) Essential role of Sox9 in the pathway that controls formation of cardiac valves and septa. *Proc Natl Acad Sci U S A*, **101**, 6502-6507.
70. Ng, L.J., Wheatley, S., Muscat, G.E., Conway-Campbell, J., Bowles, J., Wright, E., Bell, D.M., Tam, P.P., Cheah, K.S. and Koopman, P. (1997) SOX9 binds DNA, activates transcription, and coexpresses with type II collagen during chondrogenesis in the mouse. *Dev Biol*, **183**, 108-121.
71. Rahkonen, O., Savontaus, M., Abdelwahid, E., Vuorio, E. and Jokinen, E. (2003) Expression patterns of cartilage collagens and Sox9 during mouse heart development. *Histochem Cell Biol*, **120**, 103-110.
72. Peacock, J.D., Levay, A.K., Gillaspie, D.B., Tao, G. and Lincoln, J. (2010) Reduced sox9 function promotes heart valve calcification phenotypes in vivo. *Circ Res*, **106**, 712-719.
73. Chang, A.C., Garside, V.C., Fournier, M., Smrz, J., Vrljicak, P., Umlandt, P., Fuller, M., Robertson, G., Zhao, Y., Tam, A. *et al.* (2014) A Notch-dependent transcriptional hierarchy promotes mesenchymal transdifferentiation in the cardiac cushion. *Dev Dyn*, **243**, 894-905.
74. Wirrig, E.E., Hinton, R.B. and Yutzey, K.E. (2011) Differential expression of cartilage and bone-related proteins in pediatric and adult diseased aortic valves. *J Mol Cell Cardiol*, **50**, 561-569.
75. Alexopoulos, A., Bravou, V., Peroukides, S., Kaklamanis, L., Varakis, J., Alexopoulos, D. and Papadaki, H. (2010) Bone regulatory factors NFATc1 and Osterix in human calcific aortic valves. *Int J Cardiol*, **139**, 142-149.
76. Caira, F.C., Stock, S.R., Gleason, T.G., McGee, E.C., Huang, J., Bonow, R.O., Spelsberg, T.C., McCarthy, P.M., Rahimtoola, S.H. and Rajamannan, N.M. (2006) Human degenerative valve disease is associated with up-regulation of low-density

lipoprotein receptor-related protein 5 receptor-mediated bone formation. *J Am Coll Cardiol*, **47**, 1707-1712.
77. Cheek, J.D., Wirrig, E.E., Alfieri, C.M., James, J.F. and Yutzey, K.E. (2012) Differential activation of valvulogenic, chondrogenic, and osteogenic pathways in mouse models of myxomatous and calcific aortic valve disease. *J Mol Cell Cardiol*, **52**, 689-700.
78. Bi, W., Deng, J.M., Zhang, Z., Behringer, R.R. and de Crombrugghe, B. (1999) Sox9 is required for cartilage formation. *Nat Genet*, **22**, 85-89.
79. Bell, D.M., Leung, K.K., Wheatley, S.C., Ng, L.J., Zhou, S., Ling, K.W., Sham, M.H., Koopman, P., Tam, P.P. and Cheah, K.S. (1997) SOX9 directly regulates the type-II collagen gene. *Nat Genet*, **16**, 174-178.
80. Bridgewater, L.C., Lefebvre, V. and de Crombrugghe, B. (1998) Chondrocyte-specific enhancer elements in the Col11a2 gene resemble the Col2a1 tissue-specific enhancer. *J Biol Chem*, **273**, 14998-15006.
81. Xie, W.F., Zhang, X., Sakano, S., Lefebvre, V. and Sandell, L.J. (1999) Trans-activation of the mouse cartilage-derived retinoic acid-sensitive protein gene by Sox9. *J Bone Miner Res*, **14**, 757-763.
82. Sekiya, I., Tsuji, K., Koopman, P., Watanabe, H., Yamada, Y., Shinomiya, K., Nifuji, A. and Noda, M. (2000) SOX9 enhances aggrecan gene promoter/enhancer activity and is up-regulated by retinoic acid in a cartilage-derived cell line, TC6. *J Biol Chem*, **275**, 10738-10744.
83. Kou, I. and Ikegawa, S. (2004) SOX9-dependent and -independent transcriptional regulation of human cartilage link protein. *J Biol Chem*, **279**, 50942-50948.
84. Liu, C.J., Zhang, Y., Xu, K., Parsons, D., Alfonso, D. and Di Cesare, P.E. (2007) Transcriptional activation of cartilage oligomeric matrix protein by Sox9, Sox5, and Sox6 transcription factors and CBP/p300 coactivators. *Front Biosci*, **12**, 3899-3910.
85. Bernard, P., Tang, P., Liu, S., Dewing, P., Harley, V.R. and Vilain, E. (2003) Dimerization of SOX9 is required for chondrogenesis, but not for sex determination. *Hum Mol Genet*, **12**, 1755-1765.
86. Coustry, F., Oh, C.D., Hattori, T., Maity, S.N., de Crombrugghe, B. and Yasuda, H. (2010) The dimerization domain of SOX9 is required for transcription activation of a chondrocyte-specific chromatin DNA template. *Nucleic Acids Res*, **38**, 6018-6028.
87. Genzer, M.A. and Bridgewater, L.C. (2007) A Col9a1 enhancer element activated by two interdependent SOX9 dimers. *Nucleic Acids Res*, **35**, 1178-1186.
88. Zhang, P., Jimenez, S.A. and Stokes, D.G. (2003) Regulation of human COL9A1 gene expression. Activation of the proximal promoter region by SOX9. *J Biol Chem*, **278**, 117-123.
89. Peacock, J.D., Huk, D.J., Ediriweera, H.N. and Lincoln, J. (2011) Sox9 transcriptionally represses Spp1 to prevent matrix mineralization in maturing heart valves and chondrocytes. *PLoS One*, **6**, e26769.
90. Bi, W., Huang, W., Whitworth, D.J., Deng, J.M., Zhang, Z., Behringer, R.R. and de Crombrugghe, B. (2001) Haploinsufficiency of Sox9 results in defective cartilage primordia and premature skeletal mineralization. *Proc Natl Acad Sci U S A*, **98**, 6698-6703.
91. Hoffman, J.I. and Kaplan, S. (2002) The incidence of congenital heart disease. *J Am Coll Cardiol*, **39**, 1890-1900.

92. Pierpont, M.E., Basson, C.T., Benson, D.W., Jr., Gelb, B.D., Giglia, T.M., Goldmuntz, E., McGee, G., Sable, C.A., Srivastava, D. and Webb, C.L. (2007) Genetic basis for congenital heart defects: current knowledge: a scientific statement from the American Heart Association Congenital Cardiac Defects Committee, Council on Cardiovascular Disease in the Young: endorsed by the American Academy of Pediatrics. *Circulation*, **115**, 3015-3038.
93. Roger, V.L., Go, A.S., Lloyd-Jones, D.M., Adams, R.J., Berry, J.D., Brown, T.M., Carnethon, M.R., Dai, S., de Simone, G., Ford, E.S. *et al.* (2011) Heart disease and stroke statistics--2011 update: a report from the American Heart Association. *Circulation*, **123**, e18-e209.
94. Rabkin, E., Aikawa, M., Stone, J.R., Fukumoto, Y., Libby, P. and Schoen, F.J. (2001) Activated interstitial myofibroblasts express catabolic enzymes and mediate matrix remodeling in myxomatous heart valves. *Circulation*, **104**, 2525-2532.
95. Rabkin-Aikawa, E., Farber, M., Aikawa, M. and Schoen, F.J. (2004) Dynamic and reversible changes of interstitial cell phenotype during remodeling of cardiac valves. *J Heart Valve Dis*, **13**, 841-847.
96. Pomerance, A. (1972) Pathogenesis of aortic stenosis and its relation to age. *Br Heart J*, **34**, 569-574.
97. Passik, C.S., Ackermann, D.M., Pluth, J.R. and Edwards, W.D. (1987) Temporal changes in the causes of aortic stenosis: a surgical pathologic study of 646 cases. *Mayo Clin Proc*, **62**, 119-123.
98. Peterson, M.D., Roach, R.M. and Edwards, J.E. (1985) Types of aortic stenosis in surgically removed valves. *Arch Pathol Lab Med*, **109**, 829-832.
99. Stephan, P.J., Henry, A.C., 3rd, Hebeler, R.F., Jr., Whiddon, L. and Roberts, W.C. (1997) Comparison of age, gender, number of aortic valve cusps, concomitant coronary artery bypass grafting, and magnitude of left ventricular-systemic arterial peak systolic gradient in adults having aortic valve replacement for isolated aortic valve stenosis. *Am J Cardiol*, **79**, 166-172.
100. Sheikh, A.M. and Livesey, S.A. (2010) Surgical management of valve disease in the early 21st century. *Clin Med*, **10**, 177-181.
101. Levay, A.K., Peacock, J.D., Lu, Y., Koch, M., Hinton, R.B., Jr., Kadler, K.E. and Lincoln, J. (2008) Scleraxis is required for cell lineage differentiation and extracellular matrix remodeling during murine heart valve formation in vivo. *Circ Res*, **103**, 948-956.
102. Garg, V., Muth, A.N., Ransom, J.F., Schluterman, M.K., Barnes, R., King, I.N., Grossfeld, P.D. and Srivastava, D. (2005) Mutations in NOTCH1 cause aortic valve disease. *Nature*, **437**, 270-274.
103. Nigam, V. and Srivastava, D. (2009) Notch1 represses osteogenic pathways in aortic valve cells. *J Mol Cell Cardiol*, **47**, 828-834.
104. Nus, M., MacGrogan, D., Martinez-Poveda, B., Benito, Y., Casanova, J.C., Fernandez-Aviles, F., Bermejo, J. and de la Pompa, J.L. (2011) Diet-induced aortic valve disease in mice haploinsufficient for the Notch pathway effector RBPJK/CSL. *Arterioscler Thromb Vasc Biol*, **31**, 1580-1588.
105. Impey, S., McCorkle, S.R., Cha-Molstad, H., Dwyer, J.M., Yochum, G.S., Boss, J.M., McWeeney, S., Dunn, J.J., Mandel, G. and Goodman, R.H. (2004) Defining the CREB

regulon: a genome-wide analysis of transcription factor regulatory regions. *Cell*, **119**, 1041-1054.
106. Kim, J., Bhinge, A.A., Morgan, X.C. and Iyer, V.R. (2005) Mapping DNA-protein interactions in large genomes by sequence tag analysis of genomic enrichment. *Nat Methods*, **2**, 47-53.
107. Hou, J., Charters, A.M., Lee, S.C., Zhao, Y., Wu, M.K., Jones, S.J., Marra, M.A. and Hoodless, P.A. (2007) A systematic screen for genes expressed in definitive endoderm by Serial Analysis of Gene Expression (SAGE). *BMC Dev Biol*, **7**, 92.
108. McKnight, K.D., Hou, J. and Hoodless, P.A. (2007) Dynamic expression of thyrotropin-releasing hormone in the mouse definitive endoderm. *Dev Dyn*, **236**, 2909-2917.
109. Hassan, A.S., Hou, J., Wei, W. and Hoodless, P.A. (2010) Expression of two novel transcripts in the mouse definitive endoderm. *Gene Expr Patterns*, **10**, 127-134.
110. Robertson, G., Hirst, M., Bainbridge, M., Bilenky, M., Zhao, Y., Zeng, T., Euskirchen, G., Bernier, B., Varhol, R., Delaney, A. *et al.* (2007) Genome-wide profiles of STAT1 DNA association using chromatin immunoprecipitation and massively parallel sequencing. *Nat Methods*, **4**, 651-657.
111. Li, H. and Durbin, R. (2009) Fast and accurate short read alignment with Burrows-Wheeler transform. *Bioinformatics (Oxford, England)*, **25**, 1754-1760.
112. Fejes, A.P., Robertson, G., Bilenky, M., Varhol, R., Bainbridge, M. and Jones, S.J. (2008) FindPeaks 3.1: a tool for identifying areas of enrichment from massively parallel short-read sequencing technology. *Bioinformatics*, **24**, 1729-1730.
113. Robertson, A.G., Bilenky, M., Tam, A., Zhao, Y., Zeng, T., Thiessen, N., Cezard, T., Fejes, A.P., Wederell, E.D., Cullum, R. *et al.* (2008) Genome-wide relationship between histone H3 lysine 4 mono- and tri-methylation and transcription factor binding. *Genome Res*, **18**, 1906-1917.
114. Kent, W.J., Sugnet, C.W., Furey, T.S., Roskin, K.M., Pringle, T.H., Zahler, A.M. and Haussler, D. (2002) The human genome browser at UCSC. *Genome Res*, **12**, 996-1006.
115. Blankenberg, D., Von Kuster, G., Coraor, N., Ananda, G., Lazarus, R., Mangan, M., Nekrutenko, A. and Taylor, J. (2010) Galaxy: a web-based genome analysis tool for experimentalists. *Curr Protoc Mol Biol*, **Chapter 19**, Unit 19 10 11-21.
116. Liu, T., Ortiz, J.A., Taing, L., Meyer, C.A., Lee, B., Zhang, Y., Shin, H., Wong, S.S., Ma, J., Lei, Y. *et al.* (2011) Cistrome: an integrative platform for transcriptional regulation studies. *Genome Biol*, **12**, R83.
117. Eden, E., Navon, R., Steinfeld, I., Lipson, D. and Yakhini, Z. (2009) GOrilla: a tool for discovery and visualization of enriched GO terms in ranked gene lists. *BMC Bioinformatics*, **10**, 48.
118. Kwon, A.T., Arenillas, D.J., Worsley Hunt, R. and Wasserman, W.W. (2012) oPOSSUM-3: advanced analysis of regulatory motif over-representation across genes or ChIP-Seq datasets. *G3 (Bethesda)*, **2**, 987-1002.
119. Kim, D., Pertea, G., Trapnell, C., Pimentel, H., Kelley, R. and Salzberg, S.L. (2013) TopHat2: accurate alignment of transcriptomes in the presence of insertions, deletions and gene fusions. *Genome Biol*, **14**, R36.
120. Trapnell, C., Williams, B.A., Pertea, G., Mortazavi, A., Kwan, G., van Baren, M.J., Salzberg, S.L., Wold, B.J. and Pachter, L. (2010) Transcript assembly and quantification

by RNA-Seq reveals unannotated transcripts and isoform switching during cell differentiation. *Nat Biotechnol*, **28**, 511-515.
121. Baker, A., Saltik, M., Lehrmann, H., Killisch, I., Mautner, V., Lamm, G., Christofori, G. and Cotten, M. (1997) Polyethylenimine (PEI) is a simple, inexpensive and effective reagent for condensing and linking plasmid DNA to adenovirus for gene delivery. *Gene Ther*, **4**, 773-782.
122. Wheatley, S., Wright, E., Jeske, Y., A, M.C., Bowles, J. and Koopman, P. (1996) Aetiology of the skeletal dysmorphology syndrome campomelic dysplasia: expression of the Sox9 gene during chondrogenesis in mouse embryos. *Ann N Y Acad Sci*, **785**, 350-352.
123. Winter, E.M. and Gittenberger-de Groot, A.C. (2007) Epicardium-derived cells in cardiogenesis and cardiac regeneration. *Cell Mol Life Sci*, **64**, 692-703.
124. Snarr, B.S., Kern, C.B. and Wessels, A. (2008) Origin and fate of cardiac mesenchyme. *Dev Dyn*, **237**, 2804-2819.
125. Chatterjee, S., Sivakamasundari, V., Yap, S.P., Kraus, P., Kumar, V., Xing, X., Lim, S.L., Sng, J., Prabhakar, S. and Lufkin, T. (2014) In vivo genome-wide analysis of multiple tissues identifies gene regulatory networks, novel functions and downstream regulatory genes for Bapx1 and its co-regulation with Sox9 in the mammalian vertebral column. *BMC Genomics*, **15**, 1072.
126. Kadaja, M., Keyes, B.E., Lin, M., Pasolli, H.A., Genander, M., Polak, L., Stokes, N., Zheng, D. and Fuchs, E. (2014) SOX9: a stem cell transcriptional regulator of secreted niche signaling factors. *Genes & development*, **28**, 328-341.
127. Ramezani-Rad, P., Geng, H., Hurtz, C., Chan, L.N., Chen, Z., Jumaa, H., Melnick, A., Paietta, E., Carroll, W.L., Willman, C.L. *et al.* (2013) SOX4 enables oncogenic survival signals in acute lymphoblastic leukemia. *Blood*, **121**, 148-155.
128. Bard-Chapeau, E.A., Jeyakani, J., Kok, C.H., Muller, J., Chua, B.Q., Gunaratne, J., Batagov, A., Jenjaroenpun, P., Kuznetsov, V.A., Wei, C.L. *et al.* (2012) Ecotopic viral integration site 1 (EVI1) regulates multiple cellular processes important for cancer and is a synergistic partner for FOS protein in invasive tumors. *Proc Natl Acad Sci U S A*, **109**, 2168-2173.
129. Oh, C.D., Lu, Y., Liang, S., Mori-Akiyama, Y., Chen, D., de Crombrugghe, B. and Yasuda, H. (2014) SOX9 Regulates Multiple Genes in Chondrocytes, Including Genes Encoding ECM Proteins, ECM Modification Enzymes, Receptors, and Transporters. *PLoS One*, **9**, e107577.
130. Ya, J., Schilham, M.W., de Boer, P.A., Moorman, A.F., Clevers, H. and Lamers, W.H. (1998) Sox4-deficiency syndrome in mice is an animal model for common trunk. *Circ Res*, **83**, 986-994.
131. Bard-Chapeau, E.A., Szumska, D., Jacob, B., Chua, B.Q., Chatterjee, G.C., Zhang, Y., Ward, J.M., Urun, F., Kinameri, E., Vincent, S.D. *et al.* (2014) Mice carrying a hypomorphic Evi1 allele are embryonic viable but exhibit severe congenital heart defects. *PLoS One*, **9**, e89397.
132. Furumatsu, T. and Asahara, H. (2010) Histone acetylation influences the activity of Sox9-related transcriptional complex. *Acta Med Okayama*, **64**, 351-357.
133. Furumatsu, T., Ozaki, T. and Asahara, H. (2009) Smad3 activates the Sox9-dependent transcription on chromatin. *Int J Biochem Cell Biol*, **41**, 1198-1204.

134. Gu, S., Boyer, T.G. and Naski, M.C. (2012) Basic helix-loop-helix transcription factor Twist1 inhibits transactivator function of master chondrogenic regulator Sox9. *J Biol Chem*, **287**, 21082-21092.
135. Goodnough, L.H., Chang, A.T., Treloar, C., Yang, J., Scacheri, P.C. and Atit, R.P. (2012) Twist1 mediates repression of chondrogenesis by beta-catenin to promote cranial bone progenitor specification. *Development*, **139**, 4428-4438.
136. Alva, J.A., Zovein, A.C., Monvoisin, A., Murphy, T., Salazar, A., Harvey, N.L., Carmeliet, P. and Iruela-Arispe, M.L. (2006) VE-Cadherin-Cre-recombinase transgenic mouse: a tool for lineage analysis and gene deletion in endothelial cells. *Dev Dyn*, **235**, 759-767.
137. Vincent, S.D. and Robertson, E.J. (2003) Highly efficient transgene-independent recombination directed by a maternally derived SOX2CRE transgene. *Genesis*, **37**, 54-56.
138. Dy, P., Wang, W., Bhattaram, P., Wang, Q., Wang, L., Ballock, R.T. and Lefebvre, V. (2012) Sox9 directs hypertrophic maturation and blocks osteoblast differentiation of growth plate chondrocytes. *Dev Cell*, **22**, 597-609.
139. Maganti, K., Rigolin, V.H., Sarano, M.E. and Bonow, R.O. (2010) Valvular heart disease: diagnosis and management. *Mayo Clin Proc*, **85**, 483-500.
140. Kisanuki, Y.Y., Hammer, R.E., Miyazaki, J., Williams, S.C., Richardson, J.A. and Yanagisawa, M. (2001) Tie2-Cre transgenic mice: a new model for endothelial cell-lineage analysis in vivo. *Developmental biology*, **230**, 230-242.
141. Sarikas, A., Xu, X., Field, L.J. and Pan, Z.Q. (2008) The cullin7 E3 ubiquitin ligase: a novel player in growth control. *Cell Cycle*, **7**, 3154-3161.
142. DeLaughter, D.M., Christodoulou, D.C., Robinson, J.Y., Seidman, C.E., Baldwin, H.S., Seidman, J.G. and Barnett, J.V. (2013) Spatial transcriptional profile of the chick and mouse endocardial cushions identify novel regulators of endocardial EMT in vitro. *J Mol Cell Cardiol*, **59**, 196-204.
143. Vokes, S.A., Ji, H., Wong, W.H. and McMahon, A.P. (2008) A genome-scale analysis of the cis-regulatory circuitry underlying sonic hedgehog-mediated patterning of the mammalian limb. *Genes Dev*, **22**, 2651-2663.
144. Visel, A., Blow, M.J., Li, Z., Zhang, T., Akiyama, J.A., Holt, A., Plajzer-Frick, I., Shoukry, M., Wright, C., Chen, F. *et al.* (2009) ChIP-seq accurately predicts tissue-specific activity of enhancers. *Nature*, **457**, 854-858.
145. Blow, M.J., McCulley, D.J., Li, Z., Zhang, T., Akiyama, J.A., Holt, A., Plajzer-Frick, I., Shoukry, M., Wright, C., Chen, F. *et al.* (2010) ChIP-Seq identification of weakly conserved heart enhancers. *Nat Genet*, **42**, 806-810.
146. Liu, C.F. and Lefebvre, V. (2015) The transcription factors SOX9 and SOX5/SOX6 cooperate genome-wide through super-enhancers to drive chondrogenesis. *Nucleic acids research*.
147. Ohba, S., He, X., Hojo, H. and McMahon, A.P. (2015) Distinct Transcriptional Programs Underlie Sox9 Regulation of the Mammalian Chondrocyte. *Cell Rep*, **12**, 229-243.
148. Meech, R., Edelman, D.B., Jones, F.S. and Makarenkova, H.P. (2005) The homeobox transcription factor Barx2 regulates chondrogenesis during limb development. *Development*, **132**, 2135-2146.

149. Takigawa, Y., Hata, K., Muramatsu, S., Amano, K., Ono, K., Wakabayashi, M., Matsuda, A., Takada, K., Nishimura, R. and Yoneda, T. (2010) The transcription factor Znf219 regulates chondrocyte differentiation by assembling a transcription factory with Sox9. *J Cell Sci*, **123**, 3780-3788.
150. Yoon, B.S., Ovchinnikov, D.A., Yoshii, I., Mishina, Y., Behringer, R.R. and Lyons, K.M. (2005) Bmpr1a and Bmpr1b have overlapping functions and are essential for chondrogenesis in vivo. *Proc Natl Acad Sci U S A*, **102**, 5062-5067.
151. Haller, R., Schwanbeck, R., Martini, S., Bernoth, K., Kramer, J., Just, U. and Rohwedel, J. (2011) Notch1 signaling regulates chondrogenic lineage determination through Sox9 activation. *Cell Death Differ*.
152. Dolfini, D., Gatta, R. and Mantovani, R. (2012) NF-Y and the transcriptional activation of CCAAT promoters. *Crit Rev Biochem Mol Biol*, **47**, 29-49.
153. Semenza, G.L. (1998) Hypoxia-inducible factor 1: master regulator of O2 homeostasis. *Curr Opin Genet Dev*, **8**, 588-594.
154. Amarilio, R., Viukov, S.V., Sharir, A., Eshkar-Oren, I., Johnson, R.S. and Zelzer, E. (2007) HIF1alpha regulation of Sox9 is necessary to maintain differentiation of hypoxic prechondrogenic cells during early skeletogenesis. *Development*, **134**, 3917-3928.
155. Liu, H. and Fisher, S.A. (2008) Hypoxia-inducible transcription factor-1alpha triggers an autocrine survival pathway during embryonic cardiac outflow tract remodeling. *Circ Res*, **102**, 1331-1339.
156. Kato, K., Bhattaram, P., Penzo-Mendez, A., Gadi, A. and Lefebvre, V. (2015) SOXC Transcription Factors Induce Cartilage Growth Plate Formation in Mouse Embryos by Promoting Noncanonical WNT Signaling. *Journal of bone and mineral research : the official journal of the American Society for Bone and Mineral Research*.
157. Neeb, Z., Lajiness, J.D., Bolanis, E. and Conway, S.J. (2013) Cardiac outflow tract anomalies. *Wiley Interdiscip Rev Dev Biol*, **2**, 499-530.
158. Zhou, B., von Gise, A., Ma, Q., Rivera-Feliciano, J. and Pu, W.T. (2008) Nkx2-5- and Isl1-expressing cardiac progenitors contribute to proepicardium. *Biochemical and biophysical research communications*, **375**, 450-453.
159. Cai, C.L., Martin, J.C., Sun, Y., Cui, L., Wang, L., Ouyang, K., Yang, L., Bu, L., Liang, X., Zhang, X. *et al.* (2008) A myocardial lineage derives from Tbx18 epicardial cells. *Nature*, **454**, 104-108.
160. Wessels, A., van den Hoff, M.J., Adamo, R.F., Phelps, A.L., Lockhart, M.M., Sauls, K., Briggs, L.E., Norris, R.A., van Wijk, B., Perez-Pomares, J.M. *et al.* (2012) Epicardially derived fibroblasts preferentially contribute to the parietal leaflets of the atrioventricular valves in the murine heart. *Developmental biology*, **366**, 111-124.
161. Alao, J.P. (2007) The regulation of cyclin D1 degradation: roles in cancer development and the potential for therapeutic invention. *Mol Cancer*, **6**, 24.
162. Peirano, R.I. and Wegner, M. (2000) The glial transcription factor Sox10 binds to DNA both as monomer and dimer with different functional consequences. *Nucleic Acids Res*, **28**, 3047-3055.
163. Shaulian, E. (2010) AP-1--The Jun proteins: Oncogenes or tumor suppressors in disguise? *Cell Signal*, **22**, 894-899.

164. Claret, F.X., Hibi, M., Dhut, S., Toda, T. and Karin, M. (1996) A new group of conserved coactivators that increase the specificity of AP-1 transcription factors. *Nature*, **383**, 453-457.
165. Bashur, L.A., Chen, D., Chen, Z., Liang, B., Pardi, R., Murakami, S. and Zhou, G. (2014) Loss of jab1 in osteochondral progenitor cells severely impairs embryonic limb development in mice. *J Cell Physiol*, **229**, 1607-1617.
166. Jang, S.W., Liu, X., Fu, H., Rees, H., Yepes, M., Levey, A. and Ye, K. (2009) Interaction of Akt-phosphorylated SRPK2 with 14-3-3 mediates cell cycle and cell death in neurons. *J Biol Chem*, **284**, 24512-24525.
167. Xu, N., Lao, Y., Zhang, Y. and Gillespie, D.A. (2012) Akt: a double-edged sword in cell proliferation and genome stability. *J Oncol*, **2012**, 951724.
168. Bracken, A.P., Pasini, D., Capra, M., Prosperini, E., Colli, E. and Helin, K. (2003) EZH2 is downstream of the pRB-E2F pathway, essential for proliferation and amplified in cancer. *EMBO J*, **22**, 5323-5335.
169. Kelly, R.D. and Cowley, S.M. (2013) The physiological roles of histone deacetylase (HDAC) 1 and 2: complex co-stars with multiple leading parts. *Biochem Soc Trans*, **41**, 741-749.
170. He, A., Ma, Q., Cao, J., von Gise, A., Zhou, P., Xie, H., Zhang, B., Hsing, M., Christodoulou, D.C., Cahan, P. *et al.* (2012) Polycomb repressive complex 2 regulates normal development of the mouse heart. *Circ Res*, **110**, 406-415.
171. Giono, L.E. and Manfredi, J.J. (2006) The p53 tumor suppressor participates in multiple cell cycle checkpoints. *J Cell Physiol*, **209**, 13-20.
172. Stork, P.J. and Schmitt, J.M. (2002) Crosstalk between cAMP and MAP kinase signaling in the regulation of cell proliferation. *Trends Cell Biol*, **12**, 258-266.
173. Huang, W., Zhou, X., Lefebvre, V. and de Crombrugghe, B. (2000) Phosphorylation of SOX9 by cyclic AMP-dependent protein kinase A enhances SOX9's ability to transactivate a Col2a1 chondrocyte-specific enhancer. *Mol Cell Biol*, **20**, 4149-4158.
174. Formeister, E.J., Sionas, A.L., Lorance, D.K., Barkley, C.L., Lee, G.H. and Magness, S.T. (2009) Distinct SOX9 levels differentially mark stem/progenitor populations and enteroendocrine cells of the small intestine epithelium. *Am J Physiol Gastrointest Liver Physiol*, **296**, G1108-1118.
175. Liu, C., Liu, W., Palie, J., Lu, M.F., Brown, N.A. and Martin, J.F. (2002) Pitx2c patterns anterior myocardium and aortic arch vessels and is required for local cell movement into atrioventricular cushions. *Development*, **129**, 5081-5091.
176. Holler, K.L., Hendershot, T.J., Troy, S.E., Vincentz, J.W., Firulli, A.B. and Howard, M.J. (2010) Targeted deletion of Hand2 in cardiac neural crest-derived cells influences cardiac gene expression and outflow tract development. *Dev Biol*, **341**, 291-304.
177. Cai, X., Zhang, W., Hu, J., Zhang, L., Sultana, N., Wu, B., Cai, W., Zhou, B. and Cai, C.L. (2013) Tbx20 acts upstream of Wnt signaling to regulate endocardial cushion formation and valve remodeling during mouse cardiogenesis. *Development*, **140**, 3176-3187.
178. Vincentz, J.W., Barnes, R.M., Rodgers, R., Firulli, B.A., Conway, S.J. and Firulli, A.B. (2008) An absence of Twist1 results in aberrant cardiac neural crest morphogenesis. *Dev Biol*, **320**, 131-139.

179. Teng, Y. and Li, X. (2014) The roles of HLH transcription factors in epithelial mesenchymal transition and multiple molecular mechanisms. *Clin Exp Metastasis*, **31**, 367-377.
180. Shelton, E.L. and Yutzey, K.E. (2008) Twist1 function in endocardial cushion cell proliferation, migration, and differentiation during heart valve development. *Dev Biol*, **317**, 282-295.
181. Chakraborty, S., Wirrig, E.E., Hinton, R.B., Merrill, W.H., Spicer, D.B. and Yutzey, K.E. (2010) Twist1 promotes heart valve cell proliferation and extracellular matrix gene expression during development in vivo and is expressed in human diseased aortic valves. *Dev Biol*, **347**, 167-179.
182. Vrljicak, P., Cullum, R., Xu, E., Chang, A.C., Wederell, E.D., Bilenky, M., Jones, S.J., Marra, M.A., Karsan, A. and Hoodless, P.A. (2012) Twist1 transcriptional targets in the developing atrio-ventricular canal of the mouse. *PLoS One*, **7**, e40815.
183. Lee, M.P. and Yutzey, K.E. (2011) Twist1 directly regulates genes that promote cell proliferation and migration in developing heart valves. *PLoS One*, **6**, e29758.
184. Boyd, K.E., Xiao, Y.Y., Fan, K., Poholek, A., Copeland, N.G., Jenkins, N.A. and Perkins, A.S. (2006) Sox4 cooperates with Evi1 in AKXD-23 myeloid tumors via transactivation of proviral LTR. *Blood*, **107**, 733-741.
185. Ghatak, S., Misra, S., Norris, R.A., Moreno-Rodriguez, R.A., Hoffman, S., Levine, R.A., Hascall, V.C. and Markwald, R.R. (2014) Periostin induces intracellular cross-talk between kinases and hyaluronan in atrioventricular valvulogenesis. *J Biol Chem*, **289**, 8545-8561.
186. Snider, P., Hinton, R.B., Moreno-Rodriguez, R.A., Wang, J., Rogers, R., Lindsley, A., Li, F., Ingram, D.A., Menick, D., Field, L. *et al.* (2008) Periostin is required for maturation and extracellular matrix stabilization of noncardiomyocyte lineages of the heart. *Circ Res*, **102**, 752-760.

APPENDIX I SOX9 immunostaining on E12.5 whole embryo (A, B, E) and E10.5 heart (C, D, F).

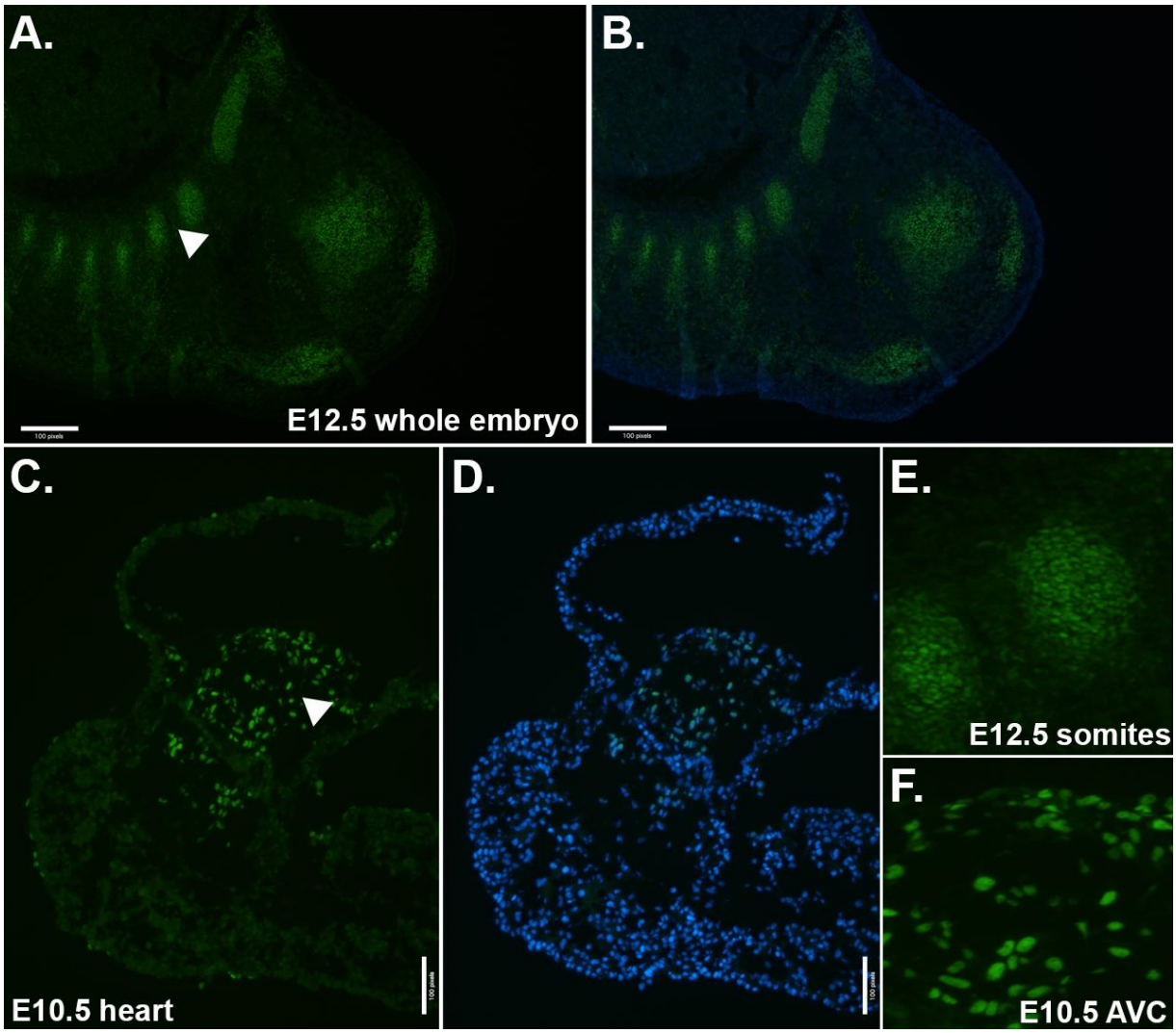

SOX9 is labeled in green and DAPI (to label nuclei) is labeled in blue. E. and F. Show nuclear staining in tissues know to express SOX9. Arrowheads indicate SOX9 positive regions.

APPENDIX II Quality verification of the SOX9 ChIP-Seq libraries and gene associations. Part A and B were generated by M. Bilenky and Part C was generated by R. Cullum.

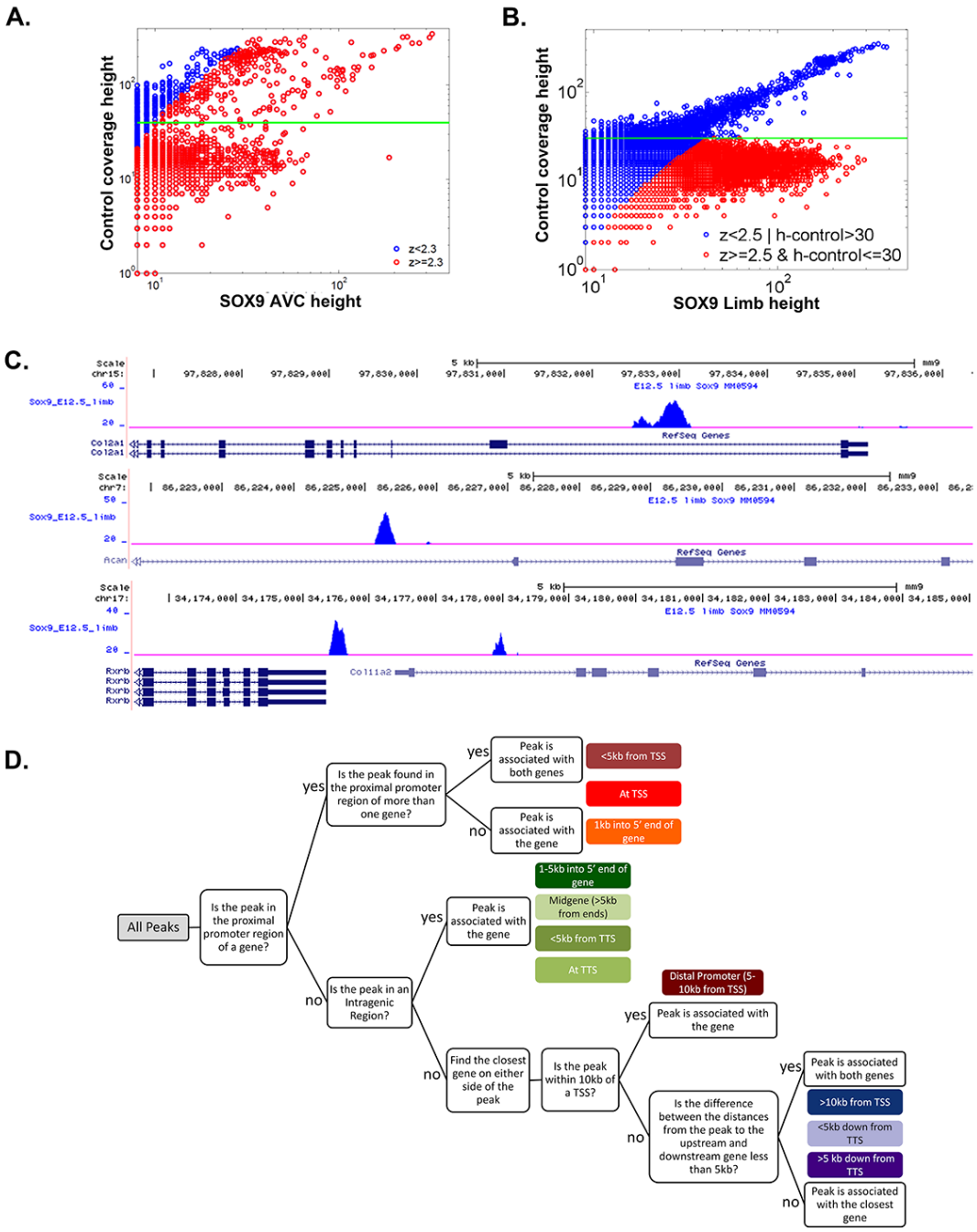

A. Comparison of control coverage peak height versus SOX9 E12.5 AVC or **B.** E12.5 limb peak height to determine a local z-score threshold for peak inclusion in downstream analysis. **C.** UCSC genome browser screenshots of known SOX9 target genes in the limb: *Col2a1*, *Acan*, *Col11a2* in the SOX9 E12.5 limb ChIP-Seq library. **D.** A schematic of how SOX9 peaks were associated with different genomic regions at or near the target gene.

APPENDIX III Characteristics of the SOX9 ChIP-Seq libraries

ChIP-Seq Library	Mapped Reads (M)	Reads into Peaks	Height Threshold	Width of peaks	Peak Criteria	Number of Peaks	Number of Genes
SOX9 E12.5 AVC	6.84	39,847	8	307.3 bp (+/- 86.0 bp)	Height 8+, control 30 subtracted, z-score 2.3, sub0.3	2602	2453
SOX9 E12.5 Limb	76.4	181,294	28	321.5 bp (+/- 90.3 bp)	Height 28+, control 30 subtracted, z-score 2.5, sub0.5	9087	5750

APPENDIX IV Gene Ontology (GO) analysis on the E12.5 AVC and limb overlapping SOX9 peaks using GOrilla

GO term description	P-value	Enrichment	-10*(LOG10 (p-value))
regulation of Rab protein signal transduction	8.50E-05	22.72	40.70581
immunoglobulin V(D)J recombination	1.80E-05	18.18	47.44727
B cell lineage commitment	7.95E-04	13.63	30.99633
pyramidal neuron development	7.95E-04	13.63	30.99633
mRNA splice site selection	6.49E-04	6.68	31.87755
demethylation	8.04E-04	3.95	30.94744
negative regulation of protein localization to nucleus	9.11E-04	3.53	30.40482
regulation of organelle assembly	5.84E-04	3.44	32.33587
cellular response to nutrient levels	6.98E-04	2.96	31.56145
cellular response to extracellular stimulus	3.67E-04	2.87	34.35334
cofactor biosynthetic process	7.04E-04	2.81	31.52427
positive regulation of cytoskeleton organization	1.58E-04	2.74	38.01343
positive regulation of protein complex assembly	6.04E-04	2.62	32.18963
positive regulation of cellular component biogenesis	1.23E-05	2.45	49.10095
response to extracellular stimulus	7.83E-04	2.32	31.06238
mRNA processing	1.59E-05	2.26	47.98603
regulation of cell cycle process	2.73E-06	2.25	55.63837
mitotic nuclear division	1.52E-04	2.24	38.18156
positive regulation of organelle organization	2.76E-05	2.2	45.59091
chordate embryonic development	1.71E-04	2.18	37.67004
response to oxidative stress	4.28E-04	2.17	33.68556
in utero embryonic development	3.11E-04	2.14	35.0724
embryo development ending in birth or egg hatching	2.43E-04	2.13	36.14394
modification-dependent protein catabolic process	2.95E-04	2.07	35.30178
DNA metabolic process	4.32E-07	2.06	63.64516
ubiquitin-dependent protein catabolic process	4.21E-04	2.06	33.75718
modification-dependent macromolecule catabolic process	3.84E-04	2.04	34.15669
mRNA metabolic process	7.95E-05	2.03	40.99633
DNA repair	2.62E-04	2	35.81699
histone modification	8.17E-04	2	30.87778
RNA processing	3.24E-06	1.99	54.89455
regulation of nervous system development	5.41E-07	1.98	62.66803
covalent chromatin modification	9.49E-04	1.98	30.22734
positive regulation of nervous system development	1.38E-04	1.97	38.60121
chromatin modification	4.01E-05	1.96	43.96856
chromatin organization	1.80E-05	1.94	47.44727
regulation of neurogenesis	5.45E-06	1.93	52.63603
regulation of cell cycle	1.54E-06	1.92	58.12479

GO term description	P-value	Enrichment	-10*(LOG10 (p-value))
nervous system development	9.22E-04	1.9	30.35269
regulation of neuron differentiation	1.06E-04	1.88	39.74694
positive regulation of apoptotic process	1.18E-04	1.85	39.28118
regulation of cellular component biogenesis	1.18E-04	1.85	39.28118
cell division	9.63E-04	1.85	30.16374
regulation of organelle organization	7.48E-06	1.83	51.26098
positive regulation of programmed cell death	1.45E-04	1.83	38.38632
mitotic cell cycle process	3.09E-04	1.83	35.10042
negative regulation of transcription from RNA polymerase II promoter	1.96E-05	1.81	47.07744
regulation of cell development	1.74E-05	1.77	47.59451
positive regulation of cell death	2.68E-04	1.77	35.71865
cellular macromolecule catabolic process	9.41E-04	1.74	30.2641
nucleic acid metabolic process	2.58E-17	1.72	165.8838
negative regulation of RNA metabolic process	3.84E-06	1.72	54.15669
cellular response to DNA damage stimulus	6.48E-04	1.72	31.88425
positive regulation of cellular component organization	6.18E-05	1.7	42.09012
RNA metabolic process	1.43E-13	1.69	128.4466
negative regulation of nitrogen compound metabolic process	1.52E-06	1.69	58.18156
negative regulation of cellular macromolecule biosynthetic process	6.75E-06	1.68	51.70696
negative regulation of RNA biosynthetic process	1.44E-05	1.68	48.41638
negative regulation of nucleic acid-templated transcription	1.63E-05	1.68	47.87812
negative regulation of transcription, DNA-templated	1.85E-05	1.68	47.32828
negative regulation of nucleobase-containing compound metabolic process	4.61E-06	1.67	53.36299
negative regulation of macromolecule biosynthetic process	6.71E-06	1.66	51.73277
RNA biosynthetic process	2.04E-09	1.65	86.9037
regulation of cell differentiation	4.20E-07	1.65	63.76751
transcription from RNA polymerase II promoter	3.79E-04	1.65	34.21361
negative regulation of cell differentiation	8.53E-04	1.65	30.69051
nucleobase-containing compound metabolic process	8.34E-18	1.64	170.7883
transcription, DNA-templated	3.91E-09	1.64	84.07823
nucleic acid-templated transcription	3.91E-09	1.64	84.07823
cellular response to stress	3.02E-05	1.64	45.19993
system development	6.74E-04	1.63	31.7134
heterocycle metabolic process	3.15E-17	1.62	165.0169
macromolecule biosynthetic process	8.35E-11	1.62	100.7831
heterocycle biosynthetic process	6.07E-10	1.62	92.16811
nucleobase-containing compound biosynthetic process	1.66E-09	1.62	87.79892
macromolecular complex subunit organization	1.65E-07	1.62	67.82516

GO term description	P-value	Enrichment	-10*(LOG10 (p-value))
positive regulation of cell differentiation	4.25E-04	1.61	33.71611
cellular aromatic compound metabolic process	1.69E-16	1.6	157.7211
cellular macromolecule biosynthetic process	6.06E-10	1.6	92.17527
aromatic compound biosynthetic process	2.44E-09	1.6	86.1261
cellular nitrogen compound biosynthetic process	2.60E-09	1.59	85.85027
negative regulation of gene expression	2.06E-05	1.59	46.86133
cellular nitrogen compound metabolic process	2.05E-16	1.58	156.8825
organic cyclic compound biosynthetic process	2.99E-09	1.58	85.24329
regulation of transcription from RNA polymerase II promoter	1.06E-06	1.58	59.74694
cellular biosynthetic process	5.65E-12	1.57	112.4795
negative regulation of cellular biosynthetic process	4.62E-05	1.57	43.35358
negative regulation of biosynthetic process	4.86E-05	1.57	43.13364
positive regulation of developmental process	1.11E-04	1.57	39.54677
organic cyclic compound metabolic process	1.77E-15	1.56	147.5203
cellular macromolecule metabolic process	4.60E-20	1.55	193.3724
nitrogen compound metabolic process	5.68E-16	1.54	152.4565
biosynthetic process	4.61E-11	1.52	103.363
positive regulation of transcription from RNA polymerase II promoter	6.11E-04	1.52	32.13959
organic substance biosynthetic process	1.92E-10	1.51	97.16699
cellular component organization or biogenesis	3.39E-12	1.5	114.698
cellular component organization	7.67E-12	1.5	111.152
regulation of multicellular organismal development	5.81E-05	1.49	42.35824
positive regulation of RNA metabolic process	2.12E-04	1.49	36.73664
macromolecule modification	3.46E-06	1.48	54.60924
regulation of developmental process	6.07E-06	1.47	52.16811
protein localization	3.42E-04	1.47	34.65974
regulation of RNA metabolic process	2.99E-08	1.46	75.24329
regulation of transcription, DNA-templated	7.24E-08	1.46	71.40261
organelle organization	1.01E-05	1.46	49.95679
regulation of cellular component organization	3.93E-05	1.46	44.05607
cellular component assembly	1.96E-04	1.46	37.07744
positive regulation of transcription, DNA-templated	5.28E-04	1.46	32.77366
positive regulation of nucleic acid-templated transcription	5.28E-04	1.46	32.77366
positive regulation of RNA biosynthetic process	5.54E-04	1.46	32.5649
macromolecule metabolic process	2.45E-16	1.45	156.1083
regulation of nucleobase-containing compound metabolic process	1.97E-08	1.45	77.05534
regulation of cellular macromolecule biosynthetic process	2.10E-08	1.45	76.77781
regulation of nucleic acid-templated transcription	1.03E-07	1.45	69.87163

GO term description	P-value	Enrichment	-10*(LOG10 (p-value))
positive regulation of gene expression	2.10E-04	1.45	36.77781
cellular catabolic process	2.31E-04	1.45	36.36388
macromolecule localization	4.57E-04	1.45	33.40084
cellular protein modification process	3.03E-05	1.44	45.18557
protein modification process	3.03E-05	1.44	45.18557
negative regulation of macromolecule metabolic process	4.54E-05	1.44	43.42944
single-organism organelle organization	2.42E-04	1.44	36.16185
establishment of localization in cell	7.33E-04	1.44	31.34896
regulation of macromolecule biosynthetic process	6.46E-08	1.43	71.89767
positive regulation of nucleobase-containing compound metabolic process	4.57E-04	1.43	33.40084
cellular metabolic process	6.76E-19	1.42	181.7005
regulation of nitrogen compound metabolic process	3.18E-08	1.42	74.97573
cellular protein metabolic process	9.94E-06	1.42	50.02614
regulation of gene expression	5.39E-08	1.41	72.68411
regulation of cellular biosynthetic process	1.82E-07	1.4	67.39929
regulation of biosynthetic process	1.92E-07	1.4	67.16699
negative regulation of cellular metabolic process	1.64E-04	1.4	37.85156
positive regulation of cellular process	1.42E-07	1.37	68.47712
negative regulation of metabolic process	1.38E-04	1.37	38.60121
positive regulation of macromolecule metabolic process	1.25E-04	1.36	39.0309
cellular response to stimulus	5.91E-04	1.36	32.28413
anatomical structure development	8.37E-05	1.35	40.77275
primary metabolic process	6.43E-14	1.34	131.9179
regulation of macromolecule metabolic process	5.23E-08	1.34	72.81498
organic substance metabolic process	3.03E-14	1.33	135.1856
regulation of primary metabolic process	1.07E-07	1.33	69.70616
metabolic process	6.49E-14	1.31	131.8776
regulation of cellular metabolic process	9.69E-07	1.3	60.13676
regulation of metabolic process	1.03E-06	1.27	59.87163
positive regulation of biological process	1.29E-05	1.27	48.8941
developmental process	2.53E-05	1.27	45.96879
single-organism metabolic process	1.91E-04	1.26	37.18967
single-organism developmental process	1.74E-04	1.25	37.59451
cellular process	9.73E-14	1.23	130.1189
negative regulation of biological process	5.73E-04	1.23	32.41845
single-organism cellular process	1.16E-05	1.18	49.35542

APPENDIX V GO analysis on the E12.5 AVC SOX9 peaks (>2 fold enrichment)

GO term description	P-value	Enrichment	-10*(LOG10 (p-value))
atrioventricular valve development	1.95E-04	8.46	37.09965
fat pad development	1.24E-04	7.05	39.06578
neutrophil homeostasis	8.82E-04	6.77	30.54531
immunoglobulin V(D)J recombination	8.82E-04	6.77	30.54531
pyramidal neuron development	8.82E-04	6.77	30.54531
branching morphogenesis of a nerve	8.82E-04	6.77	30.54531
histone H4-K20 methylation	3.93E-04	6.04	34.05607
presynaptic membrane assembly	3.93E-04	6.04	34.05607
radial glia guided migration of Purkinje cell	3.93E-04	6.04	34.05607
presynaptic membrane organization	1.66E-04	5.64	37.79892
receptor localization to synapse	9.44E-04	5.29	30.25028
chorio-allantoic fusion	9.44E-04	5.29	30.25028
cell migration in hindbrain	2.86E-04	4.56	35.43634
regulation of cardiac muscle cell contraction	1.12E-04	4.51	39.50782
positive regulation of oligodendrocyte differentiation	2.01E-04	4.23	36.96804
mitotic metaphase plate congression	3.41E-04	3.98	34.67246
atrial septum morphogenesis	8.66E-04	3.95	30.62482
regulation of actin filament-based movement	5.50E-04	3.76	32.59637
metaphase plate congression	3.44E-04	3.63	34.63442
membrane assembly	8.52E-04	3.56	30.6956
positive regulation of glial cell differentiation	1.38E-05	3.48	48.60121
regulation of oligodendrocyte differentiation	1.38E-05	3.48	48.60121
positive regulation of transforming growth factor beta receptor signaling pathway	5.21E-04	3.46	32.83162
regulation of neuron migration	1.31E-04	3.45	38.82729
adipose tissue development	1.93E-04	3.32	37.14443
heterophilic cell-cell adhesion via plasma membrane cell adhesion molecules	7.10E-05	3.23	41.48742
positive regulation of gliogenesis	1.12E-05	2.99	49.50782
regulation of myelination	5.90E-04	2.82	32.29148
regulation of cardiac muscle contraction	7.80E-04	2.74	31.07905
regulation of glial cell differentiation	1.04E-05	2.73	49.82967
negative regulation of Ras protein signal transduction	6.08E-04	2.68	32.16096
regulation of synaptic transmission, glutamatergic	2.83E-04	2.64	35.48214
cell-cell adhesion via plasma-membrane adhesion molecules	9.55E-08	2.63	70.19997
negative regulation of small GTPase mediated signal transduction	7.87E-04	2.62	31.04025
cell-cell adhesion	1.23E-07	2.61	69.10095
regulation of gliogenesis	1.87E-06	2.6	57.28158
negative regulation of osteoblast differentiation	7.69E-04	2.52	31.14074

GO term description	P-value	Enrichment	-10*(LOG10 (p-value))
homophilic cell adhesion via plasma membrane adhesion molecules	9.09E-05	2.4	40.41436
regulation of cation channel activity	4.21E-04	2.4	33.75718
regulation of DNA binding	8.51E-05	2.36	40.7007
regulation of transforming growth factor beta receptor signaling pathway	4.82E-04	2.2	33.16953
regulation of dendrite development	8.30E-05	2.12	40.80922
negative regulation of cytoplasmic transport	8.17E-04	2.12	30.87778
negative regulation of cell migration	1.69E-06	2.09	57.72113
negative regulation of neuron projection development	4.08E-04	2.09	33.8934
striated muscle tissue development	7.25E-04	2.09	31.39662
muscle tissue development	2.71E-04	2.07	35.67031
negative regulation of neuron differentiation	7.17E-06	2.06	51.44481
positive regulation of cell cycle process	3.62E-06	2.05	54.41291
central nervous system neuron differentiation	4.24E-04	2.05	33.72634
negative regulation of canonical Wnt signaling pathway	7.52E-04	2.05	31.23782
negative regulation of cell motility	3.74E-06	2.03	54.27128
regulation of cellular response to growth factor stimulus	2.28E-05	2.03	46.42065
positive regulation of transmembrane receptor protein serine/threonine kinase signaling pathway	6.60E-04	2.03	31.80456
nervous system development	4.20E-10	2.02	93.76751
regulation of muscle tissue development	4.36E-04	2.01	33.60514
negative regulation of cell projection organization	4.36E-04	2.01	33.60514
negative regulation of neurogenesis	9.74E-07	2	60.11441
blood vessel development	5.07E-04	2	32.94992

APPENDIX VI GO analysis on the E12.5 Limb SOX9 ChIP-Seq peaks (>2fold enrichment)

GO term description	P-value	Enrichment	-10*(LOG10 (p-value))
endocardial cushion development	3.53E-05	3.6	44.52225
positive regulation of Wnt signaling pathway, planar cell polarity pathway	1.27E-04	3.6	38.96196
regulation of Wnt signaling pathway, planar cell polarity pathway	6.75E-06	3.3	51.70696
chondrocyte development	3.19E-08	3.22	74.96209
positive regulation of non-canonical Wnt signaling pathway	2.39E-04	3.2	36.21602
negative regulation of transcription by competitive promoter binding	7.71E-04	3.15	31.12946
axon regeneration	7.71E-04	3.15	31.12946
chorio-allantoic fusion	7.71E-04	3.15	31.12946
negative regulation of retinoic acid receptor signaling pathway	7.71E-04	3.15	31.12946
spinal cord dorsal/ventral patterning	7.71E-04	3.15	31.12946
cardiac chamber formation	3.04E-04	2.95	35.17126
face development	3.04E-04	2.95	35.17126
negative regulation of fibroblast growth factor receptor signaling pathway	3.93E-05	2.88	44.05607
regulation of non-canonical Wnt signaling pathway	3.93E-05	2.88	44.05607
cardiac right ventricle morphogenesis	9.03E-04	2.88	30.44312
cardiac ventricle formation	9.03E-04	2.88	30.44312
cerebellar Purkinje cell layer development	3.26E-04	2.77	34.86782
heart valve morphogenesis	7.49E-07	2.74	61.25518
chondrocyte differentiation	5.28E-09	2.7	82.77366
lens morphogenesis in camera-type eye	1.17E-04	2.7	39.31814
embryonic digestive tract development	1.17E-04	2.7	39.31814
body morphogenesis	9.13E-04	2.7	30.39529
embryonic camera-type eye development	9.13E-04	2.7	30.39529
positive regulation of myelination	9.13E-04	2.7	30.39529
mesenchyme development	2.76E-10	2.68	95.59091
ventricular septum development	4.21E-05	2.65	43.75718
outflow tract septum morphogenesis	3.20E-04	2.64	34.9485
regulation of cardiac muscle cell contraction	3.20E-04	2.64	34.9485
negative regulation of smoothened signaling pathway	2.05E-06	2.63	56.88246
axonal fasciculation	1.13E-04	2.6	39.46922
sialylation	1.13E-04	2.6	39.46922
negative chemotaxis	4.01E-05	2.57	43.96856
negative regulation of anoikis	8.56E-04	2.57	30.67526
regulation of p38MAPK cascade	8.56E-04	2.57	30.67526
atrioventricular valve morphogenesis	8.56E-04	2.57	30.67526
mitotic G2/M transition checkpoint	8.56E-04	2.57	30.67526
negative regulation of oligodendrocyte differentiation	8.56E-04	2.57	30.67526

GO term description	P-value	Enrichment	-10*(LOG10 (p-value))
dendrite morphogenesis	3.64E-08	2.56	74.38899
cartilage development involved in endochondral bone morphogenesis	2.97E-04	2.54	35.27244
cardiac septum morphogenesis	9.29E-11	2.53	100.3198
negative regulation of embryonic development	5.12E-06	2.53	52.9073
regulation of fibroblast growth factor receptor signaling pathway	5.12E-06	2.53	52.9073
ureteric bud development	1.84E-06	2.52	57.35182
neural crest cell development	1.04E-04	2.52	39.82967
negative regulation of canonical Wnt signaling pathway	2.23E-16	2.49	156.517
protein hydroxylation	7.66E-04	2.48	31.15771
regulation of cell proliferation involved in heart morphogenesis	7.66E-04	2.48	31.15771
mesenchyme morphogenesis	7.66E-04	2.48	31.15771
establishment of epithelial cell polarity	7.66E-04	2.48	31.15771
regulation of axon extension involved in axon guidance	7.66E-04	2.48	31.15771
neural tube development	2.18E-07	2.46	66.61544
cranial nerve development	2.66E-04	2.46	35.75118
negative regulation of cartilage development	9.35E-05	2.45	40.29188
positive regulation of epithelial to mesenchymal transition	1.18E-05	2.44	49.28118
positive regulation of mesenchymal cell proliferation	1.34E-06	2.4	58.72895
cardiac ventricle morphogenesis	2.91E-05	2.4	45.36107
tight junction assembly	6.66E-04	2.4	31.76526
regulation of extracellular matrix organization	6.66E-04	2.4	31.76526
regulation of actin filament-based movement	6.66E-04	2.4	31.76526
positive regulation of neurological system process	6.66E-04	2.4	31.76526
regulation of smoothened signaling pathway	3.54E-10	2.38	94.50997
neuron recognition	2.52E-05	2.36	45.98599
ventricular septum morphogenesis	2.52E-05	2.36	45.98599
mesenchymal cell development	7.08E-05	2.35	41.49967
cardiac septum development	2.00E-04	2.35	36.9897
positive regulation of stem cell differentiation	3.66E-07	2.34	64.36519
positive regulation of cardiac muscle hypertrophy	5.67E-04	2.34	32.46417
melanocyte differentiation	5.67E-04	2.34	32.46417
cell differentiation involved in kidney development	5.67E-04	2.34	32.46417
camera-type eye morphogenesis	5.67E-04	2.34	32.46417
embryonic digestive tract morphogenesis	5.67E-04	2.34	32.46417
positive regulation of muscle hypertrophy	5.67E-04	2.34	32.46417
positive regulation of cardiac muscle cell proliferation	5.67E-04	2.34	32.46417
regulation of cartilage development	1.52E-08	2.33	78.18156
mesonephric epithelium development	7.77E-06	2.33	51.09579
negative regulation of Wnt signaling pathway	4.58E-17	2.33	163.3913
regulation of mesenchymal cell proliferation	8.69E-07	2.31	60.6098

GO term description	P-value	Enrichment	-10*(LOG10 (p-value))
ephrin receptor signaling pathway	1.83E-05	2.29	47.37549
mesonephric tubule development	1.83E-05	2.29	47.37549
pigment cell differentiation	4.76E-04	2.29	33.22393
mesenchymal cell differentiation	4.76E-04	2.29	33.22393
regulation of chondrocyte differentiation	2.03E-06	2.28	56.92504
collagen fibril organization	5.60E-06	2.27	52.51812
connective tissue development	1.94E-07	2.26	67.12198
cardiac muscle cell differentiation	1.54E-05	2.26	48.12479
embryonic digit morphogenesis	6.00E-08	2.25	72.21849
digestive tract development	4.70E-06	2.25	53.27902
appendage development	4.26E-05	2.25	43.7059
regulation of cardiac muscle cell proliferation	4.26E-05	2.25	43.7059
limb development	4.26E-05	2.25	43.7059
embryonic eye morphogenesis	3.96E-04	2.25	34.02305
positive regulation of cartilage development	3.96E-04	2.25	34.02305
cell differentiation in hindbrain	3.96E-04	2.25	34.02305
cellular response to transforming growth factor beta stimulus	1.18E-04	2.23	39.28118
somatic stem cell maintenance	1.20E-06	2.22	59.20819
regulation of oligodendrocyte differentiation	3.54E-05	2.22	44.50997
positive regulation of cardiac muscle tissue growth	3.26E-04	2.22	34.86782
negative regulation of glial cell differentiation	9.72E-05	2.21	40.12334
cardiac chamber morphogenesis	9.72E-05	2.21	40.12334
regulation of myelination	2.92E-05	2.2	45.34617
regulation of catenin import into nucleus	9.06E-04	2.19	30.42872
mesoderm development	2.41E-05	2.18	46.17983
positive regulation of BMP signaling pathway	7.98E-05	2.18	40.97997
cartilage development	4.96E-10	2.16	93.04518
central nervous system neuron axonogenesis	2.18E-04	2.16	36.61544
lung cell differentiation	2.18E-04	2.16	36.61544
establishment or maintenance of bipolar cell polarity	7.36E-04	2.16	31.33122
oligodendrocyte differentiation	7.36E-04	2.16	31.33122
establishment or maintenance of apical/basal cell polarity	7.36E-04	2.16	31.33122
regulation of epithelial to mesenchymal transition	1.51E-06	2.15	58.21023
eye morphogenesis	1.51E-06	2.15	58.21023
epithelial to mesenchymal transition	1.61E-05	2.14	47.93174
response to transforming growth factor beta	1.77E-04	2.14	37.52027
mammary gland development	1.77E-04	2.14	37.52027
regulation of organ formation	1.77E-04	2.14	37.52027
regulation of keratinocyte proliferation	5.95E-04	2.13	32.25483
positive regulation of smoothened signaling pathway	5.95E-04	2.13	32.25483

GO term description	P-value	Enrichment	-10*(LOG10 (p-value))
regulation of neuron migration	5.95E-04	2.13	32.25483
synapse assembly	1.43E-04	2.12	38.44664
outflow tract morphogenesis	1.07E-05	2.11	49.70616
positive regulation of heart growth	4.79E-04	2.11	33.19664
lung epithelial cell differentiation	4.79E-04	2.11	33.19664
adipose tissue development	4.79E-04	2.11	33.19664
regulation of canonical Wnt signaling pathway	1.95E-15	2.11	147.0997
neural tube closure	1.08E-08	2.09	79.66576
negative regulation of cellular carbohydrate metabolic process	3.85E-04	2.09	34.14539
nerve development	3.85E-04	2.09	34.14539
proteoglycan metabolic process	9.33E-05	2.08	40.30118
negative regulation of carbohydrate metabolic process	9.33E-05	2.08	40.30118
sensory organ morphogenesis	1.15E-06	2.07	59.39302
kidney epithelium development	7.51E-05	2.07	41.2436
regulation of cardiac muscle hypertrophy	3.09E-04	2.07	35.10042
positive regulation of cardiac muscle tissue development	3.09E-04	2.07	35.10042
embryonic hindlimb morphogenesis	3.09E-04	2.07	35.10042
stem cell development	3.09E-04	2.07	35.10042
tube closure	1.84E-08	2.06	77.35182
regulation of cardiac muscle tissue growth	6.04E-05	2.06	42.18963
regulation of stem cell differentiation	2.48E-09	2.05	86.05548
glial cell differentiation	7.49E-07	2.05	61.25518
hindlimb morphogenesis	4.84E-05	2.05	43.15155
embryonic skeletal system development	4.84E-05	2.05	43.15155
regulation of astrocyte differentiation	8.21E-04	2.04	30.85657
developmental growth involved in morphogenesis	2.51E-08	2.03	76.00326
negative regulation of cellular response to growth factor stimulus	7.97E-08	2.03	70.98542
regulation of heart growth	3.11E-05	2.03	45.0724
neuroepithelial cell differentiation	6.53E-04	2.03	31.85087
appendage morphogenesis	8.48E-11	2.03	100.716
limb morphogenesis	8.48E-11	2.03	100.716
peptidyl-tyrosine dephosphorylation	2.49E-05	2.02	46.03801
actin filament bundle organization	1.26E-04	2.02	38.99629
tube formation	3.59E-11	2.02	104.4491
regulation of BMP signaling pathway	1.63E-07	2.01	67.87812
regulation of morphogenesis of a branching structure	4.98E-06	2.01	53.02771
cardiocyte differentiation	1.99E-05	2.01	47.01147
positive regulation of axon extension	5.19E-04	2.01	32.84833
heterophilic cell-cell adhesion via plasma membrane cell adhesion molecules	5.19E-04	2.01	32.84833
regulation of muscle hypertrophy	5.19E-04	2.01	32.84833

GO term description	P-value	Enrichment	-10*(LOG10 (p-value))
regulation of embryonic development	5.48E-09	2	82.61219
establishment or maintenance of cell polarity	2.68E-08	2	75.71865
negative regulation of stem cell differentiation	4.12E-04	2	33.85103
regulation of Wnt signaling pathway	2.55E-17	2	165.9346

APPENDIX VII Co-factor analysis on E12.5 AVC SOX9 peaks using oPOSSUM

TF Name	Family	Z-score	Fisher score	KS score
NFYA	NFY CCAAT-binding	198.475	39.548	1.06
Foxd3	Forkhead	38.57	0	10.733
ELK4	Ets	31.851	0.092	1.841
GABPA	Ets	31.781	0	9.582
Arnt::Ahr	Helix-Loop-Helix	28.338	0	12.047
ELK1	Ets	27.371	0	3.325
E2F1	E2F	25.698	0.038	2.588
MZF1_5-13	BetaBetaAlpha-zinc finger	22.501	0	2.384
MIZF	BetaBetaAlpha-zinc finger	20.69	1.115	0.857
RREB1	BetaBetaAlpha-zinc finger	19.293	0.077	1.279
Sox17	High Mobility Group	18.322	0	2.194
znf143	BetaBetaAlpha-zinc finger	16.135	0.394	3.373
Gfi	BetaBetaAlpha-zinc finger	14.88	0	3.395
Pax4	Homeo	12.267	0.91	0.337
Egr1	BetaBetaAlpha-zinc finger	10.597	0	5.781
Myb	Myb	10.562	0	1.161
Arnt	Helix-Loop-Helix	9.454	0	3.251
SOX9	High Mobility Group	8.339	0	3.356
Pax5	Homeo	6.826	0.101	1.02
Pax6	Homeo	6.498	0.241	0.382
HIF1A::ARNT	Helix-Loop-Helix	5.448	0	3.784
SRF	MADS	5.162	0.164	1.222
Myc	Helix-Loop-Helix	5.006	0	7.057
STAT1	Stat	4.411	0	3.3
USF1	Helix-Loop-Helix	4.239	0	7.264
Stat3	Stat	4.154	0	2.299
SP1	BetaBetaAlpha-zinc finger	3.791	0	16.503
Gata1	GATA	3.617	0	2.903
TAL1::TCF3	Helix-Loop-Helix	3.081	0	1.921
Tal1::Gata1	Helix-Loop-Helix	2.982	0	2.236
TLX1::NFIC	Homeo::Nuclear Factor I-CCAAT-binding	2.977	0.037	0.269
Klf4	BetaBetaAlpha-zinc finger	2.619	0	16.978
Mycn	Helix-Loop-Helix	2.369	0	6.218
CREB1	Leucine Zipper	1.899	0	1.753
Ar	Hormone-nuclear Receptor	1.759	0.097	0.377
Hand1::Tcfe2a	Helix-Loop-Helix	1.163	0	0.764
YY1	BetaBetaAlpha-zinc finger	0.86	0	1.79
MYC::MAX	Helix-Loop-Helix	0.061	0	6.456

TF Name	Family	Z-score	Fisher score	KS score
Nr2e3	Hormone-nuclear Receptor	-0.291	0	0.336
SPIB	Ets	-0.765	0	1.333
PBX1	Homeo	-2.132	0	5.21
Spz1	Other	-2.207	0	1.678
T	T	-2.275	0	1.145
NFATC2	Rel	-2.319	0	8.571
IRF2	IRF	-2.424	0.013	0.924
TBP	TATA-binding	-2.454	0	1.693
RXRA::VDR	Hormone-nuclear Receptor	-3.107	0.01	2.188
NR3C1/glucocorticoid receptor	Hormone-nuclear Receptor	-3.139	0	1.29
FOXI1	Forkhead	-3.324	0	1.81
EWSR1-FLI1	Ets	-3.539	0.026	3.024
TP53	Loop-Sheet-Helix	-3.658	0	NA
NR2F1	Hormone-nuclear Receptor	-4.251	0	2.986
RUNX1	Runt	-4.789	0	4.038
Evi1	BetaBetaAlpha-zinc finger	-5.29	0	0
SRY	High Mobility Group	-5.933	0	6.734
IRF1	IRF	-6.826	0	1.044
RELA	Rel	-6.829	0	0.848
TEAD1	Homeo	-7.2	0	0.945
PPARG	Hormone-nuclear Receptor	-7.925	0	NA
REL	Rel	-8.643	0	1.707
NR1H2::RXRA	Hormone-nuclear Receptor	-9.215	0	0.833
MAX	Helix-Loop-Helix	-10.207	0	3.379
ESR1 estrogen receptor	Hormone-nuclear Receptor	-10.391	0	0.298
REST	BetaBetaAlpha-zinc finger	-10.395	0	4.182
PLAG1	BetaBetaAlpha-zinc finger	-10.405	0	1.142
FOXA1	Forkhead	-10.416	0	1.502
SPI1	Ets	-10.973	0	5.005
Zfp423	BetaBetaAlpha-zinc finger	-11.668	0	2.002
Sox2	High Mobility Group	-11.798	0	0.358
Tcfcp2l1	CP2	-12.09	0	0.711
FEV	Ets	-12.355	0	1.916
RORA_2	Hormone-nuclear Receptor	-12.449	0	3.055
RXR::RAR_DR5	Hormone-nuclear Receptor	-12.614	0	0.679
ELF5	Ets	-12.781	0	0.445
FOXF2	Forkhead	-13.08	0	0.705
FOXO3	Forkhead	-13.195	0	1.016
FOXD1	Forkhead	-13.33	0	0.815

TF Name	Family	Z-score	Fisher score	KS score
HNF4A	Hormone-nuclear Receptor	-14.244	0	6.243
NFKB1	Rel	-14.302	0	0.607
NF-kappaB	Rel	-14.45	0	0.731
ZNF354C	BetaBetaAlpha-zinc finger	-15.125	0	2.976
HLF	Leucine Zipper	-15.155	0	1.383
ESR2	Hormone-nuclear Receptor	-15.313	0	4.212
Myf	Helix-Loop-Helix	-15.41	0	4.787
Nobox	Homeo	-15.741	0	3.037
Nkx3-2	Homeo	-16.487	0	2.24
Foxq1	Forkhead	-16.879	0	1.355
Ddit3::Cebpa	Leucine Zipper	-17.045	0	5.092
NR4A2	Hormone-nuclear Receptor	-17.765	0	1.421
NHLH1	Helix-Loop-Helix	-17.806	0	0.814
Sox5	High Mobility Group	-18.321	0	6.668
NFE2L2	Leucine Zipper	-18.347	0	2.082
EBF1	Helix-Loop-Helix	-18.387	0	2.684
RORA_1	Hormone-nuclear Receptor	-18.965	0	0.495
CEBPA	Leucine Zipper	-19.414	0	1.749
NKX3-1	Homeo	-19.869	0	6.957
MEF2A	MADS	-20.129	0	0.448
ARID3A	Arid	-20.208	0	13.33
HNF1B	Homeo	-20.221	0	0.311
HNF1A	Homeo	-20.293	0	0.018
INSM1	BetaBetaAlpha-zinc finger	-20.383	0	0.431
AP1	Leucine Zipper	-20.659	0	1.066
NFIL3	Leucine Zipper	-20.784	0	0.842
MZF1_1-4	BetaBetaAlpha-zinc finger	-21.086	0	4.195
Pou5f1	Homeo	-21.101	0	7.828
Esrrb	Hormone-nuclear Receptor	-21.905	0	0.565
PPARG::RXRA	Hormone-nuclear Receptor	-24.086	0	0.976
Foxa2	Forkhead	-24.433	0	0.62
Nkx2-5	Homeo	-25.019	0	15.005
CTCF	BetaBetaAlpha-zinc finger	-25.447	0	7.839
Lhx3	Homeo	-26.743	0	2.374
Pdx1	Homeo	-31.159	0	13.441
ZEB1	BetaBetaAlpha-zinc finger	-32.138	0	4.17
Prrx2	Homeo	-32.235	0	10.028
Zfx	BetaBetaAlpha-zinc finger	-36.939	0	2.924
HOXA5	Homeo	-38.02	0	8.106

APPENDIX VIII Co-factor analysis on E12.5 Limb SOX9 ChIP-Seq peaks using oPOSSUM

TF Name	Family	Z-score	Fisher score	KS score
NFYA	NFY CCAAT-binding	158.069	12.692	9.07
SOX9	High Mobility Group	126.862	23.474	inf
Arnt::Ahr	Helix-Loop-Helix	107.402	0	10.71
Sox17	High Mobility Group	84.886	0	inf
SRY	High Mobility Group	79.23	0	inf
Nobox	Homeo	51.933	0	26.905
FOXO3	Forkhead	48.618	0	13.324
Sox5	High Mobility Group	42.458	0	inf
NFATC2	Rel	40.316	0	19.607
TBP	TATA-binding	39.536	0	22.72
FOXD1	Forkhead	37.307	0	13.622
ELK4	Ets	33.496	0	3.971
FOXA1	Forkhead	31.86	0	6.198
ELK1	Ets	29.737	0	7.474
znf143	BetaBetaAlpha-zinc finger	24.473	0.255	1.102
E2F1	E2F	24.222	0	2.799
TAL1::TCF3	Helix-Loop-Helix	21.905	0	2.354
RUNX1	Runt	21.887	0	11.594
Myb	Myb	20.083	0	4.638
RREB1	BetaBetaAlpha-zinc finger	20.006	0.006	1.512
Sox2	High Mobility Group	17.821	0.001	5.323
Nr2e3	Hormone-nuclear Receptor	16.391	0	1.054
ARID3A	Arid	16.313	0	inf
REST	BetaBetaAlpha-zinc finger	15.684	0	17.27
Foxa2	Forkhead	15.307	0	2.252
GABPA	Ets	13.726	0	17.468
MIZF	BetaBetaAlpha-zinc finger	13.56	0	2.097
Foxq1	Forkhead	11.655	0	14.274
TLX1::NFIC	Homeo::Nuclear Factor I-CCAAT-binding	11.432	0.022	0.503
Arnt	Helix-Loop-Helix	9.015	0	15.301
Pdx1	Homeo	8.98	0	29.36
Myf	Helix-Loop-Helix	8.732	0	12.504
NR3C1	Hormone-nuclear Receptor	8.428	0	4.618
NFIL3	Leucine Zipper	8.306	0	1.583
TP53	Loop-Sheet-Helix	7.438	0.693	0.405
Ar	Hormone-nuclear Receptor	6.944	0.027	5.734
Stat3	Stat	6.376	0	0.723
T	T	5.47	0	0.413
Hand1::Tcfe2a	Helix-Loop-Helix	5.015	0	2.47
Egr1	BetaBetaAlpha-zinc finger	4.831	0	2.551

TF Name	Family	Z-score	Fisher score	KS score
TEAD1	Homeo	4.751	0	0.474
Pax4	Homeo	4.579	0.191	0.722
FOXI1	Forkhead	4.299	0	20.282
STAT1	Stat	2.854	0	1.349
PBX1	Homeo	2.478	0	1.979
SPIB	Ets	1.959	0	1.37
Nkx2-5	Homeo	1.69	0	inf
HIF1A::ARNT	Helix-Loop-Helix	0.688	0	8.938
FOXF2	Forkhead	0.519	0	2.212
CEBPA	Leucine Zipper	0.24	0	14.912
HNF1B	Homeo	0.223	0	2.913
ELF5	Ets	0.131	0	3.574
CREB1	Leucine Zipper	-0.404	0	0.737
NHLH1	Helix-Loop-Helix	-1.791	0	3.673
Pax6	Homeo	-2.146	0	0.317
Pax5	Homeo	-2.214	0	0.628
Gfi	BetaBetaAlpha-zinc finger	-2.869	0	5.289
MYC::MAX	Helix-Loop-Helix	-2.941	0	6.58
FEV	Ets	-3.018	0	16.956
HNF1A	Homeo	-3.02	0	2.607
Myc	Helix-Loop-Helix	-3.796	0	8.464
NR1H2::RXRA	Hormone-nuclear Receptor	-5.658	0.005	2.565
REL	Rel	-6.14	0	2.427
HOXA5	Homeo	-6.463	0	26.411
Tcfcp2l1	CP2	-6.666	0	11.518
USF1	Helix-Loop-Helix	-7.045	0	22.988
RELA	Rel	-7.601	0	5.184
PLAG1	BetaBetaAlpha-zinc finger	-8.018	0	0.219
Mycn	Helix-Loop-Helix	-8.085	0	11.659
RXRA::VDR	Hormone-nuclear Receptor	-9.307	0	0.55
CTCF	BetaBetaAlpha-zinc finger	-10.641	0	inf
RORA_2	Hormone-nuclear Receptor	-10.729	0	0.183
MZF1_5-13	BetaBetaAlpha-zinc finger	-10.77	0	3.058
PPARG	Hormone-nuclear Receptor	-11.813	0	0.485
SPI1	Ets	-11.905	0	18.301
RXR::RAR_DR5	Hormone-nuclear Receptor	-12.632	0	0.151
SP1	BetaBetaAlpha-zinc finger	-13.081	0	15.687
SRF	MADS	-13.32	0	0.514
Lhx3	Homeo	-14.774	0	3.375
NKX3-1	Homeo	-16.276	0	4.105
Spz1	Other	-16.922	0	1.57

TF Name	Family	Z-score	Fisher score	KS score
Foxd3	Forkhead	-17.417	0	24.447
HLF	Leucine Zipper	-17.471	0	1.01
EWSR1-FLI1	Ets	-19.461	0	1.946
Pou5f1	Homeo	-19.626	0	6.752
ESR1	Hormone-nuclear Receptor	-19.944	0	2.899
YY1	BetaBetaAlpha-zinc finger	-20.346	0	11.262
IRF1	IRF	-20.689	0	0.406
IRF2	IRF	-21.023	0	1.204
INSM1	BetaBetaAlpha-zinc finger	-24.527	0	2.253
MEF2A	MADS	-24.844	0	14.004
RORA_1	Hormone-nuclear Receptor	-24.911	0	16.866
Zfp423	BetaBetaAlpha-zinc finger	-24.935	0	2.117
NF-kappaB	Rel	-26.889	0	2.164
ESR2	Hormone-nuclear Receptor	-27.728	0	5.333
Klf4	BetaBetaAlpha-zinc finger	-28.154	0	25.153
EBF1	Helix-Loop-Helix	-28.941	0	3.851
MAX	Helix-Loop-Helix	-29.2	0	8.283
NR2F1	Hormone-nuclear Receptor	-29.349	0	13.531
Evi1	BetaBetaAlpha-zinc finger	-30.224	0	2.405
NFE2L2	Leucine Zipper	-30.379	0	13.965
Prrx2	Homeo	-30.551	0	14.077
NFKB1	Rel	-31.456	0	2.732
PPARG::RXRA	Hormone-nuclear Receptor	-33.146	0	5.169
Ddit3::Cebpa	Leucine Zipper	-34.676	0	0.776
AP1	Leucine Zipper	-36.486	0	3.356
HNF4A	Hormone-nuclear Receptor	-37.596	0	7.214
ZNF354C	BetaBetaAlpha-zinc finger	-37.804	0	15.248
NR4A2	Hormone-nuclear Receptor	-41.454	0	8.67
Nkx3-2	Homeo	-43.266	0	3.417
Esrrb	Hormone-nuclear Receptor	-47.361	0	21.754
MZF1_1-4	BetaBetaAlpha-zinc finger	-50.975	0	5.293
ZEB1	BetaBetaAlpha-zinc finger	-57.591	0	15.323
Zfx	BetaBetaAlpha-zinc finger	-65.478	0	2.103
Tal1::Gata1	Helix-Loop-Helix	-86.39	0	18.036
Gata1	GATA	-90.866	0	12.197

APPENDIX IX Co-factor analysis on E12.5 AVC and Limb overlapping SOX9 peaks using oPOSSUM

TF Name	Family	Z-score	Fisher score	KS score
NFYA	NFY CCAAT-binding	230.391	36.368	7.472
SOX9	High Mobility Group	114.989	2.762	inf
Arnt::Ahr	Helix-Loop-Helix	108.149	0	4.151
Sox17	High Mobility Group	83.192	0	inf
SRY	High Mobility Group	64.902	0	inf
ELK4	Ets	44.534	0	6.128
ELK1	Ets	39.113	0	9.663
Nobox	Homeo	36.639	0	28.151
FOXO3	Forkhead	36.064	0	14.221
NFATC2	Rel	34.236	0	28.366
E2F1	E2F	33.365	0	3.659
TBP	TATA-binding	32.724	0	22.547
znf143	BetaBetaAlpha-zinc finger	29.187	0.225	3.196
RREB1	BetaBetaAlpha-zinc finger	26.91	0.002	0.598
Sox5	High Mobility Group	26.815	0	inf
GABPA	Ets	26.637	0	26.61
FOXD1	Forkhead	25.686	0	13.686
Myb	Myb	22.756	0	5.986
FOXA1	Forkhead	22.445	0	4.374
MIZF	BetaBetaAlpha-zinc finger	21.525	0.003	3.054
TAL1::TCF3	Helix-Loop-Helix	20.773	0	1.596
RUNX1	Runt	17.368	0	14.43
Nr2e3	Hormone-nuclear Receptor	14.197	0	0.49
Arnt	Helix-Loop-Helix	12.404	0	17.215
TLX1::NFIC	Homeo::Nuclear Factor I-CCAAT-binding	11.639	0.005	0.276
Pax4	Homeo	9.88	0.354	0.44
REST	BetaBetaAlpha-zinc finger	9.53	0	18.768
Sox2	High Mobility Group	9.324	0	4.348
Egr1	BetaBetaAlpha-zinc finger	9.259	0	5.81
Stat3	Stat	7.655	0	0.62
Ar	Hormone-nuclear Receptor	7.121	0.013	4.855
NR3C1	Hormone-nuclear Receptor	5.884	0	4.918
Hand1::Tcfe2a	Helix-Loop-Helix	4.962	0	2.597
STAT1	Stat	4.622	0	2.174
Gfi	BetaBetaAlpha-zinc finger	4.53	0	7.787
Foxd3	Forkhead	4.306	0	28.679
T	T	3.902	0	0.067
HIF1A::ARNT	Helix-Loop-Helix	3.179	0	11.859
ARID3A	Arid	3.027	0	inf

TF Name	Family	Z-score	Fisher score	KS score
TP53	Loop-Sheet-Helix	2.781	0.375	1.099
FOXI1	Forkhead	1.618	0	20.268
SPIB	Ets	1.402	0	2.973
Pax5	Homeo	1.219	0	0.762
TEAD1	Homeo	1.039	0	0.568
PBX1	Homeo	0.907	0	4.661
MZF1_5-13	BetaBetaAlpha-zinc finger	0.82	0	3.638
Pax6	Homeo	0.81	0	0.052
Foxq1	Forkhead	0.694	0	13.617
Foxa2	Forkhead	0.628	0	1.024
Myf	Helix-Loop-Helix	0.607	0	16.752
CREB1	Leucine Zipper	0.593	0	2.212
Myc	Helix-Loop-Helix	-1.015	0	11.258
MYC::MAX	Helix-Loop-Helix	-2.531	0	11.206
NFIL3	Leucine Zipper	-3.987	0	0.687
USF1	Helix-Loop-Helix	-4.261	0	23.441
FOXF2	Forkhead	-5.805	0	2.39
ELF5	Ets	-5.994	0	3.914
Mycn	Helix-Loop-Helix	-6.03	0	14.956
Pdx1	Homeo	-8.166	0	inf
FEV	Ets	-8.469	0	16.07
REL	Rel	-9.294	0	0.618
SRF	MADS	-9.549	0	1.638
RXRA::VDR	Hormone-nuclear Receptor	-9.667	0	0.751
CEBPA	Leucine Zipper	-9.667	0	15.168
SP1	BetaBetaAlpha-zinc finger	-9.756	0	25.403
RELA	Rel	-9.849	0	2.747
NHLH1	Helix-Loop-Helix	-9.874	0	2.696
NR1H2::RXRA	Hormone-nuclear Receptor	-9.931	0	4.079
HNF1B	Homeo	-10.556	0	3.164
Tcfcp2l1	CP2	-11.49	0	10.385
Nkx2-5	Homeo	-11.654	0	inf
PLAG1	BetaBetaAlpha-zinc finger	-12.044	0	0.011
HNF1A	Homeo	-13.587	0	1.837
PPARG	Hormone-nuclear Receptor	-14.079	0	0.835
RORA_2	Hormone-nuclear Receptor	-15.548	0	0.366
SPI1	Ets	-15.597	0	23.064
Spz1	Other	-15.998	0	2.814
RXR::RAR_DR5	Hormone-nuclear Receptor	-17.09	0	0.107
YY1	BetaBetaAlpha-zinc finger	-17.53	0	10.936
EWSR1-FLI1	Ets	-19.215	0	1.774

TF Name	Family	Z-score	Fisher score	KS score
IRF2	IRF	-20.07	0	1.118
CTCF	BetaBetaAlpha-zinc finger	-21.33	0	inf
IRF1	IRF	-21.469	0	1.341
ESR1	Hormone-nuclear Receptor	-22.396	0	1.753
HLF	Leucine Zipper	-22.662	0	0.854
Klf4	BetaBetaAlpha-zinc finger	-23.679	0	inf
HOXA5	Homeo	-24.581	0	34.252
NKX3-1	Homeo	-24.614	0	8.469
Lhx3	Homeo	-27.367	0	4.691
Zfp423	BetaBetaAlpha-zinc finger	-27.394	0	1.259
Pou5f1	Homeo	-27.74	0	9.828
NR2F1	Hormone-nuclear Receptor	-27.889	0	13.979
Evi1	BetaBetaAlpha-zinc finger	-28.83	0	1.495
NF-kappaB	Rel	-30.428	0	1.466
MAX	Helix-Loop-Helix	-30.549	0	7.222
RORA_1	Hormone-nuclear Receptor	-30.998	0	12.518
INSM1	BetaBetaAlpha-zinc finger	-31.084	0	2.862
ESR2	Hormone-nuclear Receptor	-31.593	0	6.775
MEF2A	MADS	-31.916	0	11.244
EBF1	Helix-Loop-Helix	-34.008	0	3.41
NFKB1	Rel	-34.469	0	1.314
NFE2L2	Leucine Zipper	-35.357	0	15.804
Ddit3::Cebpa	Leucine Zipper	-38.586	0	2.868
HNF4A	Hormone-nuclear Receptor	-39.885	0	9.767
PPARG::RXRA	Hormone-nuclear Receptor	-40.293	0	3.076
ZNF354C	BetaBetaAlpha-zinc finger	-40.302	0	17.371
AP1	Leucine Zipper	-41.801	0	4.691
Prrx2	Homeo	-42.856	0	21.505
NR4A2	Hormone-nuclear Receptor	-44.91	0	5.274
Nkx3-2	Homeo	-45.861	0	3.077
Esrrb	Hormone-nuclear Receptor	-52.043	0	17.442
MZF1_1-4	BetaBetaAlpha-zinc finger	-54.772	0	8.3
ZEB1	BetaBetaAlpha-zinc finger	-65.784	0	18.683
Zfx	BetaBetaAlpha-zinc finger	-75.099	0	3.942
Tal1::Gata1	Helix-Loop-Helix	-75.525	0	9.895
Gata1	GATA	-78.193	0	5.479

APPENDIX X Comparisons of SOX9 peaks in the AVC and limb with SMAD3 (A.) and TWIST1 (B.) peaks in the E11.5 and E10.5 AVC respectively.

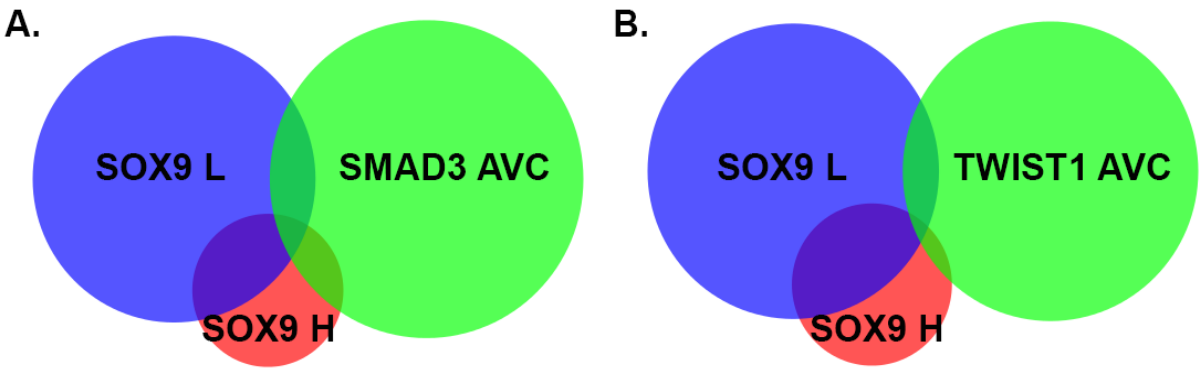

APPENDIX XI Top 100 differentially expressed genes in the *Sox9* cKO AVC RNA-Seq

Gene symbol	WT FPKM	*Sox9*cKO FPKM	p-value	Fold change down in cKO	Fold change up in cKO
Egr1	10.22	47.26	5.00E-05	0.218	4.590
Bhlhe40	12.17	56.04	5.00E-05	0.219	4.575
Shisa2	30.94	8.33	5.00E-05	3.681	0.272
Lum	75.59	18.94	5.00E-05	3.976	0.252
Col9a1	12.62	1.44	5.00E-05	8.239	0.121
Col9a3	12.10	1.35	5.00E-05	8.406	0.119
Papss2	29.53	3.01	5.00E-05	9.533	0.105
Mstn	9.79	0.84	5.00E-05	10.465	0.096
Btn1a1	6.92	0.29	5.00E-05	18.197	0.055
Fos	2.45	13.97	0.00015	0.181	5.522
Prelp	3.97	0.32	0.00015	9.701	0.103
Hmgcs2	9.68	2.52	0.0002	3.726	0.268
Ndrg1	5.81	19.15	0.00025	0.307	3.256
Ier3	20.74	76.65	0.00035	0.272	3.682
Tnrc6b	66.09	13.91	0.00035	4.724	0.212
Mir208a	1248.83	0.00	0.00045	1248.830	0.000
Dct	3.90	0.47	0.00055	6.970	0.143
Ctnna2	3.30	0.56	0.0006	5.141	0.195
Kdm5d	0.62	4.73	0.00065	0.148	6.742
Col6a6	4.10	1.19	0.001	3.246	0.308
Iigp1	5.39	1.40	0.001	3.665	0.273
Ddx3y	1.81	9.76	0.0012	0.194	5.160
Uty	0.72	4.90	0.0015	0.164	6.111
Shroom1	3.70	0.92	0.0015	3.718	0.269
Stc2	2.58	9.35	0.0017	0.284	3.523
Dpysl4	3.17	0.60	0.0018	4.664	0.214
Nppb	121.27	346.05	0.0021	0.351	2.852
Slc17a7	3.49	0.77	0.0021	4.138	0.242
Serpine1	2.91	8.96	0.0023	0.332	3.013
Ntsr1	2.59	0.61	0.0023	3.803	0.263
Hbb-bh1	556.69	1682.09	0.0024	0.331	3.021
2610203C20Rik	25.89	8.92	0.0025	2.881	0.347
Car3	11.84	2.90	0.0025	3.983	0.251
Ntn4	9.84	3.24	0.0026	2.975	0.336
Adcy2	0.96	3.65	0.0026	0.284	3.527
Pitx2	19.54	7.02	0.0028	2.758	0.363
Sox5	4.33	1.43	0.0028	2.902	0.345
Derl3	0.77	5.65	0.0029	0.152	6.597
Col9a2	6.08	1.80	0.0030	3.259	0.307

Gene symbol	WT FPKM	*Sox9*cKO FPKM	p-value	Fold change down in cKO	Fold change up in cKO
Fdx1l	185.14	48.86	0.0030	3.783	0.264
AI646023	1.74	0.41	0.0031	3.580	0.279
Mfap4	60.79	22.22	0.0032	2.729	0.366
Vsnl1	14.24	4.45	0.0034	3.148	0.318
Twist1	37.16	13.38	0.0035	2.765	0.362
Matn4	4.16	0.26	0.0035	11.711	0.085
Fgfr2	19.88	7.65	0.0035	2.577	0.388
Rtn1	8.40	2.47	0.0041	3.309	0.302
Serpinb9b	0.72	3.42	0.0044	0.233	4.285
Shox2	8.56	2.38	0.0044	3.496	0.286
Sfrp2	24.36	8.74	0.0047	2.767	0.361
Eif2s3y	2.32	11.09	0.0048	0.217	4.617
Mt1	32.99	93.26	0.0048	0.354	2.821
9030425E11Rik	17.83	7.00	0.0058	2.527	0.396
Rn45s	2519.92	3336.26	0.0060	0.755	1.324
Oprl1	6.71	2.40	0.0063	2.728	0.367
Btn2a2	1.51	0.37	0.0065	3.441	0.291
Slc2a3	16.24	39.24	0.0065	0.415	2.408
Nr4a1	8.16	20.72	0.0067	0.397	2.519
Dlg2	6.99	2.68	0.0067	2.550	0.392
Dusp4	9.16	22.42	0.0072	0.411	2.431
Baalc	2.89	0.94	0.0073	2.877	0.348
Nr2f1	9.44	3.08	0.0075	3.000	0.333
Islr	5.72	1.87	0.0080	2.957	0.338
Hsd3b6	29.81	67.14	0.0087	0.445	2.248
Figf	6.52	2.08	0.0087	3.042	0.329
Eln	28.80	12.92	0.0093	2.219	0.451
Crabp1	12.24	3.97	0.0094	3.036	0.329
Rd3	1.50	0.46	0.0104	2.865	0.349
Lims2	1.43	5.66	0.0112	0.265	3.773
Meox1	23.20	9.76	0.0112	2.364	0.423
Aqp3	0.46	2.42	0.0113	0.223	4.476
Hemgn	1.52	4.52	0.0116	0.351	2.850
Gpr50	4.64	1.42	0.0120	3.109	0.322
Dnm1	7.66	3.13	0.0124	2.400	0.417
Snai3	0.51	2.63	0.0125	0.222	4.502
Eya4	2.50	0.88	0.0125	2.641	0.379
Shisa6	3.05	1.04	0.0125	2.758	0.363
Irx6	1.54	4.11	0.0129	0.390	2.567
Foxp2	6.99	2.97	0.0130	2.306	0.434

Gene symbol	WT FPKM	*Sox9*cKO FPKM	p-value	Fold change down in cKO	Fold change up in cKO
Scube1	10.11	4.47	0.0133	2.233	0.448
Zfp503	4.16	1.47	0.0134	2.719	0.368
Thsd7b	4.73	1.98	0.0135	2.318	0.431
Epha3	12.45	5.51	0.0137	2.238	0.447
Chst3	1.68	0.61	0.0139	2.515	0.398
Rassf2	6.12	2.58	0.0142	2.320	0.431
Krt19	22.93	52.14	0.0144	0.441	2.268
Sox9	18.23	7.34	0.0144	2.464	0.406
Bmp10	29.69	65.56	0.0149	0.454	2.204
Guca2b	18.79	4.99	0.0151	3.715	0.269
Prss35	43.84	20.39	0.0154	2.145	0.466
Hba-a2	689.57	1585.85	0.0155	0.435	2.300
Prap1	46.11	14.51	0.0156	3.162	0.316
Per1	6.32	14.58	0.0159	0.438	2.285
Aplnr	14.16	6.22	0.0161	2.256	0.443
Prl8a2	0.44	6.03	0.0163	0.088	11.315
Lmod1	0.63	1.79	0.0183	0.387	2.583
Prrx1	9.20	3.94	0.0191	2.300	0.435
Rarg	7.64	3.18	0.0194	2.362	0.423
Nfatc4	13.78	6.36	0.0199	2.150	0.465

*≧1FPKM in the WT or *Sox9* cKO library.

** Combined set of differentially expressed genesgenerated from duplicate libraries for each genotype as determined by the Cufflinks program.

APPENDIX XII Genes with altered expression (>1.5FC down) with a SOX9 peak in the AVC

Gene symbol	Full Gene Name	WT FPKM	cKO FPKM	p-value	FC down
Btn1a1	butyrophilin, subfamily 1, member A1	6.92	0.29	0.0001	18.197
Prelp	proline/arginine-rich end leucine-rich repeat protein	3.97	0.32	0.0002	9.701
Tnrc6b	trinucleotide repeat containing 6B	66.09	13.91	0.0004	4.724
Ctnna2	catenin (cadherin-associated protein), alpha 2	3.30	0.56	0.0006	5.141
Col6a6	collagen, type VI, alpha 6	4.10	1.19	0.0010	3.246
Ntn4	netrin 4	9.84	3.24	0.0026	2.975
Pitx2	paired-like homeodomain 2	19.54	7.02	0.0028	2.758
Twist1	twist family bHLH transcription factor 1	37.16	13.38	0.0035	2.765
Fgfr2	fibroblast growth factor receptor 2	19.88	7.65	0.0035	2.577
Clmp/ 9030425E11Rik	CXADR-like membrane protein	17.83	7.00	0.0058	2.527
Dlg2	discs, large homolog 2 (Drosophila)	6.99	2.68	0.0067	2.550
Nr2f1	nuclear receptor subfamily 2, group F, member 1	9.44	3.08	0.0075	3.000
Eln	elastin	28.80	12.92	0.0093	2.219
Eya4	eyes absent homolog 4 (Drosophila)	2.50	0.88	0.0125	2.641
Foxp2	forkhead box P2	6.99	2.97	0.0130	2.306
Scube1	signal peptide, CUB domain, EGF-like 1	10.11	4.47	0.0133	2.233
Thsd7b	thrombospondin, type I, domain containing 7B	4.73	1.98	0.0135	2.318
Chst3	carbohydrate (chondroitin 6) sulfotransferase 3	1.68	0.61	0.0139	2.515
Nfatc4	nuclear factor of activated T-cells, cytoplasmic, calcineurin-dependent 4	13.78	6.36	0.0199	2.150
Mecom	MDS1 and EVI1 complex locus	21.24	10.72	0.0280	1.973
Osr1	odd-skipped related transciption factor 1	4.16	1.58	0.0311	2.532
Negr1	neuronal growth regulator 1	3.79	1.69	0.0316	2.172
Plcb1	phospholipase C, beta 1 (phosphoinositide-specific)	4.47	2.12	0.0329	2.055
Gria1	glutamate receptor, ionotropic, AMPA 1	2.32	1.03	0.0368	2.132
Ptx3	pentraxin 3, long	7.57	2.89	0.0386	2.568
Acvr1c	activin A receptor, type IC	1.95	0.91	0.0462	2.023
Antxr1	anthrax toxin receptor 1	13.24	7.02	0.0496	1.873
Garnl3	GTPase activating Rap/RanGAP domain-like 3	7.35	3.67	0.0496	1.975
Msx1	msh homeobox 1	10.41	4.84	0.0559	2.130
Spint2	serine peptidase inhibitor, Kunitz type, 2	17.41	8.65	0.0561	2.002

Gene symbol	Full Gene Name	WT FPKM	cKO FPKM	p-value	FC down
Cpne5	copine V	14.08	7.43	0.0580	1.884
Ly86	lymphocyte antigen 86	3.50	1.33	0.0597	2.515
Postn	periostin, osteoblast specific factor	402.15	200.48	0.0625	2.005
Bmf	Bcl2 modifying factor	10.88	5.91	0.0650	1.829
Klhl29	kelch-like family member 29	1.41	0.67	0.0676	1.951
Tmem26	transmembrane protein 26	3.68	1.88	0.0685	1.914
Phactr1	phosphatase and actin regulator 1	2.80	1.40	0.0706	1.937
Plce1	phospholipase C, epsilon 1	10.50	6.00	0.0711	1.739
Nfix	nuclear factor I/X (CCAAT-binding transcription factor)	15.16	7.16	0.0741	2.103
1700084E18Rik	1700084E18Rik	2.82	0.49	0.0827	4.916
Inhba	inhibin, beta A	10.28	5.29	0.0842	1.925
Gfra1	GDNF family receptor alpha 1	4.79	2.57	0.0853	1.829
Grm7	glutamate receptor, metabotropic 7	1.39	0.60	0.0964	2.122
Mapk8ip1	mitogen-activated protein kinase 8 interacting protein 1	5.26	2.83	0.0976	1.825
Rasl11a	RAS-like, family 11, member A	3.40	1.46	0.0977	2.243
Sox4	SRY (sex determining region Y)-box 4	74.78	44.61	0.0980	1.675
Hexim1	hexamethylene bis-acetamide inducible 1	13.00	7.62	0.1005	1.696
Olfm1	olfactomedin 1	6.68	3.55	0.1069	1.860
Ociad2	OCIA domain containing 2	10.40	5.83	0.1103	1.772
Odz4/Tenm4	teneurin transmembrane protein 4	6.78	4.07	0.1107	1.652
Slc24a3	solute carrier family 24 (sodium/potassium/calcium exchanger), member 3	5.33	2.97	0.1140	1.769
Sncaip	synuclein, alpha interacting protein	10.65	6.39	0.1203	1.657
Axin2	axin 2	9.08	5.43	0.1238	1.660
Clstn2	calsyntenin 2	3.30	1.87	0.1241	1.731
Id4	inhibitor of DNA binding 4, dominant negative helix-loop-helix protein	4.68	2.43	0.1251	1.891
Id2	inhibitor of DNA binding 2, dominant negative helix-loop-helix protein	118.92	73.04	0.1254	1.627
Efna4	ephrin-A4	6.90	3.75	0.1307	1.820
Kcnab2	potassium voltage-gated channel, shaker-related subfamily, beta member 2	2.46	1.36	0.1327	1.754
Rbm34	RNA binding motif protein 34	4.68	2.76	0.1446	1.673
Asb13	ankyrin repeat and SOCS box containing 13	3.77	2.14	0.1489	1.727
Kitl	KIT ligand	19.78	12.60	0.1526	1.565
Tpbg	Trophoblast glycoprotein	5.53	3.33	0.1557	1.645
Odz3	Teneurin transmembrane protein 3 (Tenm3)	16.66	10.77	0.1571	1.543

Gene symbol	Full Gene Name	WT FPKM	cKO FPKM	p-value	FC down
3000002C10Rik	3000002C10Rik	3.01	1.58	0.1580	1.850
Clip3	CAP-GLY Domain containing linker protein	20.10	11.85	0.1612	1.690
Rftn2	raftlin family member 2	4.71	2.89	0.1699	1.606
Abcb1b	ATP-binding cassette, sub-family B (MDR/TAP), member 1	1.62	0.86	0.1707	1.783
Mylip	myosin regulatory light chain interacting protein	5.56	3.37	0.1713	1.633
Hand2	heart and neural crest derivatives expressed 2	46.27	30.34	0.1741	1.523
Epha7	EPH receptor A7	30.86	19.95	0.1752	1.544
Cbx3	chromobox homolog 3	2.06	1.09	0.1774	1.812
Nap1l3	nucleosome assembly protein 1-like 3	1.68	0.93	0.1807	1.716
Fbln2	fibulin 2	91.25	59.80	0.1835	1.525
Zdhhc14	zinc finger, DHHC-type containing 14	1.68	0.94	0.1855	1.718
Arrdc4	arrestin domain containing 4	10.13	6.35	0.1868	1.588
Rbfox1	RNA binding protein, fox-1 homolog (C. elegans) 1	1.47	0.84	0.1872	1.673
2610035D17Rik	2610035D17Rik	4.56	2.67	0.1885	1.682
Msrb2	methionine sulfoxide reductase B2	14.29	8.67	0.1936	1.640
Tusc1	tumor suppressor candidate 1	2.68	1.39	0.1947	1.863
Txnip	thioredoxin interacting protein	115.03	75.79	0.2031	1.517
Angptl4	angiopoietin-like 4	7.53	4.70	0.2032	1.590
Tbcc	tubulin folding cofactor C	8.76	5.54	0.2073	1.570
Rab7l1	RAB7, member RAS oncogene family-like 1	4.29	2.46	0.2082	1.711
Mecom	MDS1 and EVI1 complex locus	2.85	1.52	0.2284	1.824
Foxp4	forkhead box P4	28.89	18.54	0.2343	1.555
Gpr173	G protein-coupled receptor 173	3.05	1.88	0.2373	1.590
Efcab1	EF-hand calcium binding domain 1	1.47	0.75	0.2393	1.843
Fam174a	family with sequence similarity 174, member A	6.29	4.04	0.2444	1.545
Ehd3	EH-domain containing 3	3.70	2.43	0.2535	1.500
Prox2	prospero homeobox 2	1.35	0.80	0.2630	1.599
Mafb	v-maf avian musculoaponeurotic fibrosarcoma oncogene homolog B	3.08	1.96	0.2637	1.540
Zfp185	zinc finger protein 185 (LIM domain)	2.64	1.71	0.2647	1.512
Xrcc4	X-ray repair complementing defective repair in Chinese hamster cells 4	10.83	7.17	0.2674	1.503
Acrbp	acrosin binding protein	3.90	2.42	0.2740	1.589
Tiam2	T-cell lymphoma invasion and metastasis 2	4.43	2.74	0.2741	1.593
Nr4a2	nuclear receptor subfamily 4, group A, member 2	2.27	1.44	0.2759	1.535
B230217C12Rik	B230217C12Rik	2.99	1.93	0.3526	1.527

Gene symbol	Full Gene Name	WT FPKM	cKO FPKM	p-value	FC down
Rbp7	retinol binding protein 7, cellular	2.01	1.12	0.3740	1.730
C230052I12Rik	C230052I12Rik	5.38	3.35	0.4240	1.588
Mpv17l2	MPV17 mitochondrial membrane protein-like 2	12.63	7.90	0.4455	1.592
Psd	pleckstrin and Sec7 domain containing	2.18	1.29	0.4741	1.635
Dnajb11	DnaJ (Hsp40) homolog, subfamily B, member 11	1.37	0.55	0.6987	2.254
Stat4	signal transducer and activator of transcription 4	1.16	0.62	1.0000	1.757
Htr1b	5-hydroxytryptamine (serotonin) receptor 1B, G protein-coupled	1.15	0.34	1.0000	2.861
Col4a4	collagen, type IV, alpha 4	1.14	0.55	1.0000	1.923
4930572J05Rik/Them6	thioesterase superfamily member 6	1.05	0.65	1.0000	1.533
Lrrn1	leucine rich repeat neuronal 1	1.05	0.21	1.0000	3.752

*FC = Fold change

APPENDIX XIII Genes with altered expression (>1.5FC up) with a SOX9 peak in the AVC

Gene symbol	Full Gene Name	WT FPKM	cKO FPKM	p-value	FC up in cKO
Bhlhe40	Basic Helix-Loop-Helix Family, Member E40	12.17	56.04	5.00E-05	4.575
Fos	FBJ murine osteosarcoma viral oncogene homolog	2.45	13.97	0.0002	5.522
Dusp4	Dual specificity phosphatase 4	9.16	22.42	0.0072	2.431
Stc1	Stanniocalcin 1	4.32	9.66	0.0227	2.206
Ddit3	DNA-damage-inducible transcript 3	11.93	72.50	0.0461	6.036
Nrg1	Neuregulin 1	2.98	6.50	0.0466	2.140
Junb	Jun B proto-oncogene	2.40	5.41	0.0510	2.201
Fhdc1	FH2 domain containing 1	1.06	2.05	0.0801	1.859
Gramd1b	GRAM domain containing 1B	10.72	18.23	0.1035	1.694
Gm14005	Gm14005 predicted gene 14005	1.07	3.18	0.1101	2.803
1700026D08Rik	1700026D08Rik	0.92	2.12	0.1105	2.178
Fam46c	Family with sequence similarity 46, member C	22.75	35.72	0.1494	1.568
Edn1	Endothelin 1	7.25	11.75	0.1629	1.613
Lama1	Laminin, alpha 1	1.79	2.87	0.1685	1.576
Snora28	Small nucleolar RNA, H/ACA box 28	0.00	78.38	0.1711	78.484
Nrn1	Neuritin 1	3.43	5.90	0.1774	1.698
Map3k13	Mitogen-activated protein kinase kinase kinase 13	0.78	1.32	0.1836	1.610
St8sia1	ST8 alpha-N-acetyl-neuraminide alpha-2,8-sialyltransferase 1	2.14	3.44	0.1989	1.581
Zfp97	Zinc finger protein 97	1.18	2.04	0.2002	1.673
Nampt	Nicotinamide phosphoribosyltransferase	10.04	15.21	0.2161	1.509
Sgca	Sarcoglycan, alpha (50kDa dystrophin-associated glycoprotein)	6.56	10.15	0.2277	1.539
Abra	Actin-binding Rho activating protein	6.49	10.00	0.2441	1.533
Cox7c	Cytochrome c oxidase subunit VIIc	25.46	39.16	0.2538	1.536
Snord49a	Small nucleolar RNA, C/D box 49A	0.00	12066.80	0.2543	12066.900
Fah	Fumarylacetoacetate hydrolase (fumarylacetoacetase)	2.07	3.34	0.2577	1.587
Dgat2	Diacylglycerol O-acyltransferase 2	3.12	4.80	0.2664	1.525
Dbp	albumin D-box binding protein	2.63	4.13	0.6176	1.549
6430411K18Rik	6430411K18Rik	2.47	4.32	0.6789	1.722
Steap1	Six transmembrane epithelial antigen of the prostate 1	0.58	1.46	1.0000	2.294
1700092M07Rik	1700092M07Rik	0.58	1.11	1.0000	1.769
Hspa1a	Heat shock 70kDa protein 1A	0.57	1.04	1.0000	1.706
Adamtsl3	ADAMTS-like 3	0.66	1.19	1.0000	1.694

*FC = Fold change